

Mapping Cortical Alteration Patterns in Transdiagnostic Psychopathology: A Systems Framework Integrating Cortical Architecture and Developmental Susceptibility

Inaugural-Dissertation

zur Erlangung des Doktorgrades
der Mathematisch-Naturwissenschaftlichen Fakultät
der Heinrich-Heine-Universität Düsseldorf

vorgelegt von

Meike Dorothee Hettwer
aus Göttingen

Düsseldorf, Dezember 2024

aus dem Institut für Systemische Neurowissenschaften
Heinrich-Heine-Universität Düsseldorf

Gedruckt mit der Genehmigung der
Mathematisch-Naturwissenschaftlichen Fakultät der
Heinrich-Heine-Universität Düsseldorf

Berichterstatter:

1. Prof. Dr. Simon B. Eickhoff
2. Prof. Dr. Tobias Kalenscher

Tag der mündlichen Prüfung:

Table of Contents

1	<i>Summary.....</i>	<i>I</i>
2	<i>Zusammenfassung.....</i>	<i>II</i>
3	<i>List of Abbreviations.....</i>	<i>IV</i>
4	<i>Introduction.....</i>	<i>1</i>
4.1	Transdiagnostic concepts in psychiatric research.....	1
4.1.1	Toward a systems-level understanding of transdiagnostic brain alterations.....	2
4.2	Linking cortical architecture and developmental trajectories to vulnerability.....	3
4.2.1	Topographic heterogeneity across the cortical landscape.....	3
4.2.2	Cortical architecture confers differential neurobiological susceptibility.....	5
4.2.3	Neurodevelopmental perspectives on psychiatric vulnerability.....	5
4.3	Susceptibility and resilience to psychosocial adversity.....	6
4.4	Neuroimaging systems-level cortical organization and maturational consolidation.....	8
4.4.1	Systems-level approaches to capturing global cortical patterns.....	8
4.4.2	Intra-cortical myelin mapping to capture cortical consolidation.....	9
4.5	Open science facilitates new routes for psychiatric neuroimaging.....	10
4.6	Aims of this thesis.....	11
5	<i>Empirical work.....</i>	<i>12</i>
5.1	Study 1: Coordinated cortical thickness alterations across six neurodevelopmental and psychiatric disorders.....	12
5.2	Study 2: Longitudinal variation in resilient psychosocial functioning is associated with ongoing cortical myelination and functional reorganization during adolescence.....	27
6	<i>Summary and Conclusion.....</i>	<i>43</i>
6.1	Overall synopsis.....	43
6.2	Integration with the literature.....	45
6.2.1	Cortical alterations in mental disorders recapitulate cortical topography.....	45
6.2.2	Adolescent susceptibility to adversity links to asynchronous cortical consolidation.....	46
6.3	Broader implications, future directions, and further considerations.....	47
6.3.1	Integrating transdiagnostic perspectives and psychiatric variability.....	48
6.3.2	Supporting youth mental health through neurodevelopmentally informed interventions.....	49
6.4	Conclusion.....	50

7	<i>References</i>	51
8	<i>Publications</i>	62
9	<i>Conference Contributions</i>	64
10	<i>Acknowledgements</i>	65
11	<i>Author Declaration</i>	67
12	<i>Appendix</i>	68
12.1	Supplementary Material for: Coordinated cortical thickness alterations across six neurodevelopmental and psychiatric disorders	69
12.2	Supplementary Material for: Longitudinal variation in resilient psychosocial functioning is associated with ongoing cortical myelination and functional reorganization during adolescence	90

1 Summary

Transdiagnostic research in psychiatry indicates substantial commonalities between mental disorders. The high prevalence of psychiatric comorbidity has been attributed to shared etiologies and overlapping alterations in brain structure and function. Yet, it remains unclear whether overlapping brain alterations arise from shared constraints imposed by underlying neurobiology. This thesis provides insights into how brain organization, particularly the spatial architecture and developmental trajectories of the cortex, may constrain transdiagnostic cortical alterations and susceptibility during vulnerable developmental periods.

A population-level model aimed to uncover systematically co-occurring cortical thickness (CT) alterations across six mental disorders (*Study 1*). Identified transdiagnostic co-alterations reflected elements of underlying connectome organization, particularly lateral prefrontal and medial-temporal connectivity profiles. Moreover, they were spatially organized, with prefrontal vs. temporal and sensory-limbic vs. occipitoparietal regions exhibiting distinct co-alteration profiles. Overall, the extent to which any two regions exhibited similar CT alterations across disorders reflected their similarity in cytoarchitecture, gene expression profile, and functional task engagement. *Study 1* thus provides insights into the spatial organization of transdiagnostic CT alterations and how the cortex's heterogeneous neurobiology may guide these recurrent patterns.

A longitudinal neurodevelopmental model was applied in adolescents and young adults to study susceptibility in a period during which first psychiatric symptoms often emerge (*Study 2*). The model investigated how variation in mental well-being in response to psychosocial adversity relates to ongoing cortical maturation, particularly focusing on the asynchronous progression of plasticity and consolidation. Nuanced intracortical myelin mapping revealed that a higher rate of anterolateral prefrontal myelination and widespread association cortex reorganization were associated with positive changes in adolescents' resilience to psychosocial adversity. Conversely, increasing susceptibility was related to weaker myeloarchitectonic consolidation and decreased stability of prefrontal functional networks. *Study 2* thus revealed that the efficacy with which adolescents navigate psychosocial challenges varies in relation to ongoing cortical refinement processes at multiple scales.

The current work advances our understanding of how the cortex's spatial and developmental architecture shapes the systematic organization of transdiagnostic cortical alterations. As such, cortical alterations relevant to dimensional psychopathology may be embedded in an intrinsic cortical coordinate system defined by multiple axes of neurobiological heterogeneity and protracted development. Further research is needed to understand potentially synchronized spatiotemporal progressions along observed co-alteration patterns. Moreover, findings can inspire neurodevelopmentally informed interventions tailored to the timing of plastic periods of brain circuits involved in navigating psychosocial challenges.

2 Zusammenfassung

Transdiagnostische Forschungsansätze zeigen beträchtliche Gemeinsamkeiten zwischen psychiatrischen Erkrankungen auf. Die hohe Prävalenz von Komorbidität wird dabei auf gemeinsame Ätiologie und überlappende Veränderungen in der Gehirnstruktur und -funktion zurückgeführt. Die vorliegende Arbeit untersucht, wie die Organisation des Gehirns transdiagnostische Muster kortikaler Veränderungen und Variabilität während vulnerabler Entwicklungsphasen hervorbringen könnte, insbesondere im Hinblick auf die neurobiologische Architektur und Entwicklung des Kortex.

Ein populationsbasiertes Modell wurde verwendet, um systematische Zusammenhänge zwischen regionalen Veränderungen der kortikalen Dicke bei sechs psychiatrischen Erkrankungen zu erfassen (*Studie 1*). Regionale Veränderungen waren in ein transdiagnostisches Kovarianznetzwerk eingebettet. Dieses spiegelte die räumliche Organisation funktioneller Netzwerke wider, insbesondere lateral präfrontale und medial-temporale Konnektivität. Eine Dimensionsreduktion zeigte zudem unterschiedliche Kovarianzprofile zwischen präfrontalen und temporalen sowie zwischen sensorisch/limbischen und okzipitoparietalen Regionen auf. Generell schien der Grad, zu dem zwei Regionen über verschiedene Erkrankungen hinweg ähnlich betroffen waren, mit ihrer Ähnlichkeit in der Zytoarchitektur, im Genexpressionsprofil und in der Beteiligung an funktionellen Prozessen zusammenzuhängen. Ergebnisse aus *Studie 1* legen deshalb nahe, dass transdiagnostische Veränderungen der kortikalen Dicke räumlich organisiert sind und die heterogene Neurobiologie des Kortex reflektieren.

Ein längsschnittliches Modell untersuchte den Zusammenhang zwischen der Anfälligkeit gegenüber psychosozialen Risikofaktoren und kortikaler Reifung während eines Zeitraums, in dem psychiatrische Symptome oft zum ersten Mal auftreten - die Adoleszenz bis zum jungen Erwachsenenalter (*Studie 2*). Das Modell untersuchte dabei spezifisch die asynchronen Entwicklungsverläufe kortikaler Plastizität und Konsolidierung. Die bildgebungsbasierte Analyse intrakortikaler Myelinprofile zeigte, dass eine stärkere Myelinisierung im anterolateralen präfrontalen Kortex sowie eine myeloarchitektonische Reorganisation von Assoziationskortex mit positiven Veränderungen in der Resilienz von Jugendlichen assoziiert waren. Umgekehrt ging eine zunehmende Anfälligkeit mit einer abgeschwächten myeloarchitektonischen Konsolidierung und einer geringeren Stabilität präfrontaler funktioneller Netzwerke einher. *Studie 2* zeigt daher eine dynamische Variabilität in der Bewältigung psychosozialer Herausforderungen auf, die im Zusammenhang mit vielschichtigen kortikalen Reifungsprozessen steht.

Die Ergebnisse deuten darauf hin, dass transdiagnostische kortikale Veränderungen einem gemeinsamen, systematischen Organisationsprinzip unterliegen. Dabei scheinen kortikale Veränderungen in ein intrinsisches kortikales Koordinatensystem eingebettet zu sein, dessen Achsen durch verschiedene Skalen neurobiologischer Heterogenität und asynchroner Entwicklungsverläufe definiert werden. Zukünftige Forschung kann Aufschluss darüber geben, ob räumliche Muster

transdiagnostischer Kortexveränderungen auch zeitlich synchronisierte Prozesse widerspiegeln. Darüber hinaus regen die Ergebnisse Interventionen an, die bereits im Jugendalter an individuelle Phasen der kortikalen Plastizität angepasst werden - insbesondere in Netzwerken, die in der Bewältigung psychosozialer Herausforderungen involviert sind.

3 List of Abbreviations

ADHD	Attention-deficit/hyperactivity disorder
Agr	Agranular cortex
APQ	Alabama parenting questionnaire
ASD	Autism spectrum disorder
BD	Bipolar disorder
CT	Cortical thickness
CTQ	Childhood trauma questionnaire
DAN	Dorsal attention network
DMN	Default mode network
Dys	Dysgranular cortex
ENIGMA	Enhancing NeuroImaging Genetics through Meta-Analysis
Eu-(I-III)	Eulaminar cortex I-III
FC	Functional connectivity
FPN	Frontoparietal network
GMV	Grey matter volume
HiTOP	Hierarchical Taxonomy of Psychopathology
IFG	Inferior frontal gyrus
Koni	Konicortex
LEQ	Life events questionnaire
LIM	Limbic network
MDD	Major depressive disorder
MI	Maturation index
MOPS	Measure of parenting style
MPC	Microstructural profile covariance
MRI	Magnetic resonance imaging
MT	Magnetization transfer
NSPN	NeuroScience in Psychiatry Network
OCD	Obsessive compulsive disorder
P-factor	General psychopathology factor
PFC	Prefrontal cortex
RDoC	Research Domain Criteria
ResPSF	Resilient psychosocial functioning
SCZ	Schizophrenia
SES	Socio-economic status
SM	Sensorimotor network
VAN	Ventral attention network
VIS	Visual network

4 Introduction

Mental illness is one of the leading causes of global disease burden (Arias et al., 2022). According to the World Health Organization, one in eight individuals currently lives with a mental disorder, placing a significant burden on individuals' quality of life, societal welfare, and economic productivity (Arias et al., 2022; WHO, 2022). Mental health issues often surface during adolescence and young adulthood, a period of pronounced biopsychosocial change that prepares young individuals to live independent lives (Paus et al., 2008; Solmi et al., 2022). Concerningly, the morbidity and mortality burden of mental illness is rising across most sociodemographic groups (Kieling et al., 2024; Patel et al., 2018), emphasizing the current need for effective prevention and treatment strategies. A major factor impeding the diagnosis and etiological understanding of psychopathology is the pronounced phenomenological overlap between mental disorders, which can be observed across genetic, neurobiological, and clinical levels (Lee et al., 2019; Newson et al., 2021; Radonjic et al., 2021), as well as in epidemiological comorbidity (Caspi et al., 2020; Plana-Ripoll et al., 2019). Therefore, transdiagnostic research in psychiatry approaches the complex pathophysiology of mental disorders by identifying core mechanisms relevant to multiple disorders (Fusar-Poli et al., 2019). These efforts aim to elucidate pathways for integrative prevention and treatment strategies and may guide educational and healthcare practices to meet the pressing demands of today's society.

This thesis addresses transdiagnostic phenomena at the level of shared brain alterations. Specifically, I investigated how the cortex's heterogeneous neurobiological architecture and protracted development may give rise to individual variability in susceptibility and transdiagnostic pathology.

4.1 Transdiagnostic concepts in psychiatric research

Vulnerability to mental illness reflects a complex interaction between biological, psychological, and environmental risk and protective factors (Hankin & Abela, 2005). This multifactorial etiology of mental illness substantially overlaps between different psychiatric diagnoses. Approximately 75% of genetic risk variants confer liability to more than one mental disorder (Anttila et al., 2018; Lee et al., 2019). Similarly, environmental adversity is often more predictive of overall psychopathology than discrete symptom domains (Keyes et al., 2012; McLaughlin et al., 2020). Shared genetic and environmental risk factors may contribute to and interact with deviations from normative neurodevelopment, conferring vulnerability to psychopathology (Buckholtz & Meyer-Lindenberg, 2012; Parkes et al., 2021). At the epidemiological level, the categorization of mental disorders is further challenged by high rates of psychiatric comorbidity and heterogeneity within diagnostic categories (Newson et al., 2021; Plana-Ripoll et al., 2019). Ultimately, having any mental disorder increases the risk of developing another disorder throughout the lifespan (Caspi et al., 2020). A growing research

avenue thus points toward unifying and parsimonious constructs of psychopathology (Caspi et al., 2014; Dell’Osso et al., 2019; Lahey et al., 2012). Such constructs propose continuous and dimensional symptom profiles, whose expression can vary in severity and cut across diagnostic categories. The Hierarchical Taxonomy of Psychopathology (HiTOP; Kotov et al., 2017), for instance, identifies hierarchically organized dimensions with families of symptoms that predictably co-occur, such as internalizing (e.g., depression and anxiety), externalizing (e.g., drug use and antisocial behavior), and thought disorder symptoms (e.g., psychosis). Moreover, a general psychopathology (p -) factor has been proposed to reflect an individual's propensity to develop any form of psychopathology (Caspi et al., 2014). Such dimensional approaches suggest that each disorder may reflect a combination of graded expressions of disorder-specific features and a generalized, transdiagnostic vulnerability. Research addressing such transdiagnostic phenomena has been guided by the Research Domain Criteria (RDoC; Insel et al., 2010), which emphasize the integrative study of genetic, neuroscientific, and cognitive domains beyond symptomatic presentation.

4.1.1 Toward a systems-level understanding of transdiagnostic brain alterations

Efforts to elucidate the neurobiological basis of transdiagnostic phenomena have reported both shared and distinct brain alterations across disorders (Gandal et al., 2018; Repple et al., 2023; Taylor et al., 2023). Meta-analytic evidence indicates shared grey matter volume (GMV) loss in the insula and dorsal anterior cingulate (Goodkind et al., 2015; Taylor et al., 2023), and cortical thickness (CT) reductions in the ventral temporal cortex (Patel et al., 2021) across adult patients with schizophrenia (SCZ), bipolar disorder (BD), obsessive-compulsive disorder (OCD), major depressive disorder (MDD), autism spectrum disorder (ASD), and attention-deficit/hyperactivity disorder (ADHD). Developmental studies further link dimensional psychopathology scores to alterations in the late-maturing association cortex. These include GMV deviations in the dorsal anterior cingulate, ventromedial prefrontal, and inferior temporal cortex (Parkes et al., 2021), and connectivity changes in salience and frontoparietal networks (Xie et al., 2023). In sum, alterations in several brain regions are implicated in multiple mental disorders.

Transdiagnostic alterations generally appear to map better to networks than to discrete regions (Segal et al., 2023; Taylor et al., 2023). Specifically, alterations are concentrated in networks that mature later and are involved in abstract cognitive functions, such as cognitive control and flexibility (Barch, 2017; McTeague et al., 2017; Segal et al., 2023). These systematic patterns likely reflect that individual brain regions do not operate in isolation and mature in a partly synchronized or network-like fashion (Raznahan et al., 2011; Segal et al., 2024). Correspondingly, systematic co-alteration patterns have been proposed in several disorder-specific studies. For instance, regions exhibiting cortical thinning in SCZ also show alterations in adjacent white matter integrity (Di Biase et al., 2019). In ASD, mutual relationships between morphological alterations in different regions have been proposed to represent shared vulnerabilities and potentially shared neurodevelopmental aberrations (Liloia et al., 2021; Sha

et al., 2022). Mass-univariate analyses thus likely paint an incomplete picture by neglecting the interrelationships between regional effects. To address this, recent studies have described transdiagnostic similarities in whole-brain patterns, complementing regionally discrete findings (Opel et al., 2020; Patel et al., 2021; Radonjic et al., 2021). It emerged that SCZ, BD, OCD, MDD, and, to some extent, ASD show similarities in the spatial patterns of structural cortical alterations, which were stronger in genetically correlated disorders (Bourque et al., 2024; Radonjic et al., 2021). These findings raise the question of why certain sets of brain regions are more frequently implicated in psychopathology than others, resulting in synchronized alterations that are systematically represented across several mental disorders. Identifying such systematic patterns is crucial to understanding the spatiotemporal trajectory of pathological processes, their neurobiological and developmental origins, and systematic targets for early interventions relevant to a broad range of mental disorders.

4.2 Linking cortical architecture and developmental trajectories to vulnerability

It remains unclear to which degree overlaps in cortical alterations across mental disorders may arise from systematic constraints imposed by intrinsic cortical organization. Our understanding of transdiagnostic phenomena may thus be advanced by recognizing how cortical vulnerability to psychopathological alterations is shaped by the cortex's spatially heterogeneous neurobiology and temporally asynchronous maturation. Here, I refer to cortical vulnerability as the intrinsic neurobiological characteristics that may render a brain region more susceptible to intrinsic or extrinsic risk factors. As such, I highlight a neurobiological perspective that interacts with a range of biopsychosocial factors influencing psychiatric vulnerability.

4.2.1 Topographic heterogeneity across the cortical landscape

Over a century of brain cartography has underscored the cortex's remarkable heterogeneity that gives rise to functional diversity (Amunts et al., 2020; Vogt & Vogt, 1919; Zilles et al., 2002). Cortical architecture varies between regions and across multiple neurobiological scales. Here, variations in local microstructure (e.g., cyto- and myeloarchitecture, gene expression, and receptor distribution), are closely intertwined with macroscale network organization, facilitating global integration and local specialization (Zilles et al., 2002; Zilles & Amunts, 2015). This variation defines microstructurally and functionally diverse areas whose borders vary across neurobiological scales (Eickhoff et al., 2018; Vogt & Vogt, 1919). According to the structural model (García-Cabezas et al., 2019), the extent to which cortical areas exhibit analogous microarchitecture predicts the strength of their interconnectivity and the cortical layers involved in these connections. Moreover, variation in their layer differentiation distinguishes types of information processing and enhances processing hierarchies. As such, layer differentiation gradually decreases from externally focused sensory and motor cortices toward

transmodal association cortices (Mesulam, 1998). This shows how the spatial arrangement of cortical regions relative to their neighbors yields insights into their neurobiology.

The cortex's complex architecture, from micro- to macroscale, is organized along multiple spatial axes (**Figure 1**). A dominant organizational principle is the differentiation of unimodal and transmodal association cortices, with the latter comprising (para)limbic and heteromodal regions (Mesulam, 1998). Functionally, such segregation of unimodal sensorimotor from transmodal default mode networks (DMN) is thought to optimize flexible human cognition by balancing externally and internally oriented processing (Margulies et al., 2016; Mesulam, 1998). Structurally, variation in cytoarchitectonic complexity confers a plasticity-stability continuum (García-Cabezas et al., 2017). Elevated potential for plasticity is found in the less differentiated (para)limbic cortex and transmodal regions with complex dendritic arborization, which is enhanced by protracted development and synaptic plasticity. Conversely, stability increases toward the eulaminate (e.g., primary sensory) cortex with increasing laminar differentiation and myelin content (Barbas, 1995; García-Cabezas et al., 2019; Nieuwenhuys & Broere, 2017). Such structural and functional hierarchies are closely intertwined. According to Mesulam's (1998) seminal work, constrained synaptic plasticity in sensory cortices facilitates the reliable registration of inputs, whereas plasticity in hierarchically segregated transmodal cortices allows the generation and adaptation of abstract representations. This organization is integrated into network topology (van den Heuvel et al., 2012; van den Heuvel & Sporns, 2013). Densely connected network hubs that mediate integrative processes across distant regions are typically found in transmodal cortices. These central nodes facilitate efficient communication throughout the brain but are metabolically demanding and biologically costly (Liang et al., 2013; Tomasi et al., 2013). Ultimately, it is assumed that the complex and multiscale topography of the cortex gives rise to flexible cognition and diversity across individuals (Kong et al., 2019; Mesulam, 1998).

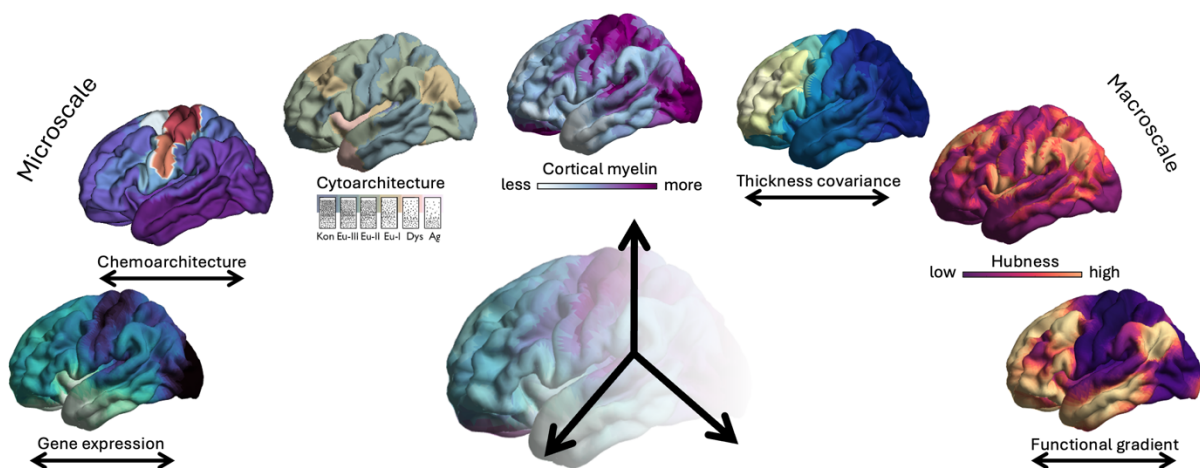


Figure 1. The human cortex is spatially organized along multiple spatial axes and across multiple neurobiological scales. Arrows indicate feature variation along unitless axes. Generated plots are based on openly accessible data from: (left to right: Markello et al., 2022; Hänisch et al., 2023; Paquola et al., 2024; Hettwer et al., 2024; Valk et al., 2020; Xu et al., 2022; Margulies et al., 2016).

4.2.2 *Cortical architecture confers differential neurobiological susceptibility*

The various neurobiological features characterizing cortical architecture have differentially been linked to susceptibility to psychopathological changes (Fornito et al., 2015; García-Cabezas et al., 2019). This suggests that the spatial arrangement of differentially susceptible regions may give rise to pathological patterns that reflect aspects of cortical organization. *At the microscale*, regional variation in risk gene expression has been shown to influence patterns of GMV alterations (van der Meer et al., 2022) and functional circuit disbalance by affecting neurotransmitter systems (Cioli et al., 2014; Zhou et al., 2012). *At the mesoscale*, similar cyto- and myeloarchitectural features in spatially distant regions can result in synchronized vulnerability due to shared plasticity and strong interconnectivity (García-Cabezas et al., 2019). Indeed, meta-analyses that report transdiagnostic GMV reductions in the anterior cingulate cortex and the insula (Forte et al., 2024; Goodkind et al., 2015) highlight regions that are microstructurally similar (paralimbic) and situated closer to the more plastic pole of a plasticity-stability axis. *At the macroscale*, patterns of structural alterations appear to be constrained by global connectome organization (Cauda et al., 2018; Fornito et al., 2015; Vanasse et al., 2021). Alterations are more frequently observed in densely connected network hubs and are thought to recapitulate their metabolic demands and physiological stress (Cauda et al., 2018; Crossley et al., 2014; Fornito et al., 2015; Vanasse et al., 2021). Some regions may particularly contribute to the interregional synchronization of pathology through their connections. This results in patterns of alterations reminiscent of their connectivity profile and may characterize them as disease epicenters (Zhou et al., 2012). For instance, network-based spreading models have highlighted the anterior cingulate cortex and widespread frontoparietal regions as putative SCZ epicenters (Georgiadis et al., 2024; Shafiei et al., 2020).

Overall, the cortex's topographic heterogeneity indicates that pathological alterations in mental illness do not affect all brain regions equally but may follow a systematic, network-like pattern. Examining the spatial co-occurrence of cortical alterations in relation to the cortex's neurobiology may thus uncover organizational principles that explain common patterns across different mental disorders.

4.2.3 *Neurodevelopmental perspectives on psychiatric vulnerability*

The intrinsic architecture of the cortex is refined throughout typical neurodevelopment (Baum et al., 2017; Larsen et al., 2023). Such refinement processes are protracted, unfolding asynchronously across the cortex into early adulthood (Norbom et al., 2021; Sydnor et al., 2023). Maturation programs creating periods of plasticity and consolidation appear to progress from the unimodal sensorimotor cortex to the transmodal association cortex. The extended maturation of the association cortex implies sustained malleability, conferred by the protracted development of stability-promoting features. These may involve the modulation of excitation/inhibition balance, the formation of perineuronal nets which stabilize synaptic architecture, and an increase in plasticity-restricting intracortical myelination that

limits structural rewiring beyond critical periods (Carceller et al., 2023; Larsen et al., 2023; McGee et al., 2005; Takesian & Hensch, 2013). In normative development, prolonged developmental programs are thought to facilitate the refinement of cognitive, emotional, and social processes through learning and adaptation (Giedd & Denker, 2015). However, plastic periods also render neural structures more susceptible to adverse environmental impacts. The protracted plasticity and reorganization of association cortices during adolescence and early adulthood has thus been considered a vulnerable period for developmental psychopathology (Paus et al., 2008).

The influence of developmental timing and the progression pattern of cortical malleability adds a *spatiotemporal* dimension to capturing susceptibility. From a neurobiological perspective, susceptibility is putatively highest when risk factor exposure temporally coincides with enhanced plasticity in regions engaged in processing or responding to risk factor exposure (Cooper & Mackey, 2016; Paus et al., 2008). Intriguingly, developmental plasticity may thus convey windows of both risk and opportunity. On the one hand, prolonged periods of plasticity give more room for aberrations in the magnitude and timing of neural system refinement (Paus et al., 2008). Correspondingly, the influence of environmental impact on cortical development appears to follow the unimodal-transmodal maturational axis, whereby psychosocial risk factor exposure during adolescence predominantly affects the late-maturing transmodal pole (Keller et al., 2024; Sydnor et al., 2023). This concentration of structural and functional alterations in association cortices is also observed in nearly every major mental disorder (Fortea et al., 2024; McTeague et al., 2017; Romer et al., 2021). On the other hand, developmental plasticity yields the necessary opportunity to adapt and mature, and for enriched environments to leave beneficial traces on malleable brain structures (Giedd & Denker, 2015; Hüttenrauch et al., 2016). Maturational trajectories are thus likely intertwined with psychiatric vulnerability through several mechanisms, influencing neurobiological susceptibility as well as cognitive and affective development. Here, the asynchronous progression of maturational processes across the cortical landscape further suggests variability in susceptibility with age. This underscores the need to address both inter- and intra-individual variation in psychiatric susceptibility with neurodevelopmentally informed models.

4.3 Susceptibility and resilience to psychosocial adversity

Humans do not exist and mature in a vacuum, and genetic variation alone cannot fully explain mental health outcomes (Krug et al., 2024; Lynch et al., 2021). The environment in which individuals grow up, along with significant life events they may encounter, can impact neurodevelopmental trajectories and contribute to the pathogenesis of mental illness (Holz et al., 2023; Pollok et al., 2022). As such, psychosocial adversity and trauma represent major transdiagnostic risk factors for most mental disorders and sub-clinical well-being (Copeland et al., 2018; Green et al., 2010; Hogg et al., 2023; Scrimin et al., 2018). Experiencing familial adversity, such as emotional and physical abuse or neglect,

or facing traumatic life events, such as the death of a loved one, are not rare phenomena. Epidemiological studies indicate that 25-40% of youth experience some form of maltreatment, and more than half of adolescents in the USA report traumatic life events (Lippard & Nemeroff, 2020; McLaughlin et al., 2013). Identifying factors that influence an individual's susceptibility to mental health challenges in the face of adversity is thus relevant to large parts of the global population.

The breadth of mental health impairments that psychosocial adversity has been linked to has partly been attributed to its influence on key cognitive functions, such as executive functions, which are commonly affected in mental illness (Etkin et al., 2013; Lynch et al., 2021). Especially when experienced early in life, exposure to psychosocial adversity can shift neurodevelopmental timings (Sisk & Gee, 2024; Tooley et al., 2021) and induce brain alterations that persist into adulthood (Holz et al., 2023). At the same time, it is increasingly recognized that many individuals retain mental well-being despite considerable exposure to psychiatric risk factors, a concept termed resilience. Outcome-oriented definitions regard resilience, or resilient psychosocial functioning, as a dynamic construct involving the adaptation to risk factors rather than a stable trait (Kalisch et al., 2017; Masten et al., 2021). Analogous to identifying risk pathways, ongoing resilience research elucidates biopsychosocial resilience factors that reduce the likelihood of negative outcomes. For instance, psychological traits, such as positive appraisal tendencies (Kalisch et al., 2024), and protective genetic variants (Hess et al., 2024) may reduce the likelihood of lifetime psychiatric disorders. Enriched environments with parental and friendship support can further mitigate the impact of negative childhood experiences on mental well-being (McLaughlin et al., 2020; Van Harmelen et al., 2017; VanBronkhorst et al., 2024).

Yet, a holistic understanding of biobehavioral adaptation to the ever-changing environment also requires a brain-centric perspective. This perspective aims to identify neurobiological factors associated with the (un)successful navigation of psychosocial challenges. Previous neuroimaging research has highlighted the role of circuits involved in emotion regulation and stress reactivity for resilience, such as orbitofrontal and subcortical limbic volumes and connectivity. Notably, individual differences in these circuits have been reported both as correlates of adversity exposure (Brieant et al., 2021; Holz et al., 2023) and mental health outcomes relative to adversity exposure, i.e., resilience and susceptibility (Eaton et al., 2022; van der Werff et al., 2013). Concepts of the neurobiology of resilience further highlight circuits involved in regulatory flexibility and cognitive control, which may facilitate the selection of adaptive cognitive strategies to cope with adversity (Kalisch et al., 2024). Overall, current resilience research aims to identify neural circuits that support specific psychological and cognitive functions, which in turn may influence how individuals respond to adversity.

Complementary to this angle, neurodevelopmentally informed models that integrate concepts of neurobiological susceptibility hold great potential for elucidating a brain-centric understanding of navigating psychosocial challenges. Particularly during vulnerable developmental periods, leveraging nuanced estimates of ongoing cortical refinement may offer a better understanding of the interplay between asynchronous cortical malleability and the effects of environmental adversity on mental health.

4.4 Neuroimaging systems-level cortical organization and maturational consolidation

4.4.1 Systems-level approaches to capturing global cortical patterns

In vivo neuroimaging and systems-level analytical techniques have provided comprehensive insights into the integration of regional pathological alterations with the broader network architecture (Fornito et al., 2015; Vanasse et al., 2021). Two common approaches to capture this integration are: (1) Examining how regional features are spatially aligned with connectome organization, and (2) analyzing inter-regional similarities in cortical features to identify network-like patterns of those features (Hansen et al., 2023; Lerch et al., 2006; Vanasse et al., 2021). The former (1) may be achieved using *in vivo* structural and functional connectivity estimates. For instance, diffusion tensor imaging maps structural connections by quantifying the directional movement of water molecules along white matter tracts (Pierpaoli et al., 1996). Functional connectivity (FC), on the other hand, assumes interactions indirectly through temporally synchronized co-activation, as indicated by correlated blood oxygen level-dependent signal fluctuations (Biswal et al., 1995). The latter (2) is typically based on correlation or covariance approaches that capture inter-regional similarities of cortical features. Here, post-mortem analyses have provided insights into topological patterns of covarying gene expression patterns, laminar differentiation, and neurotransmitter distributions (Hansen et al., 2022a; Saberi et al., 2023). *In vivo*, this approach has been applied predominantly to cortical morphology such as CT. CT can be estimated with sub-millimetric precision as the distance between an inner white surface and its corresponding point on an outer grey matter (pial) surface, taking cortical folding into account (Fischl (2012); **Figure 2A**). Covariance of CT between regions has been proposed to reflect synchronized and genetically coupled maturation (Alexander-Bloch et al., 2019; Raznahan et al., 2011) and co-occurring alterations in illness (Sha et al., 2022; Wannan et al., 2019).

In recent years, the gradient framework has emerged as a popular approach to capturing dominant axes of feature variation across the cortex (Huntenburg et al., 2018; Margulies et al., 2016). By compressing measures of inter-regional similarities to a single dimension, derived gradients provide fundamental insights into macroscale principles of cortical organization and can be visualized on a cortical map. Essentially, gradients order brain regions in terms of their variation in a feature of interest (Huntenburg et al., 2018). Regions that show high similarity are situated more closely together, whereas maximally different regions constitute the apices of a gradient. This approach has successfully captured organizational principles across anatomical, functional, developmental, and evolutionary scales (Luo et al., 2024; Margulies et al., 2016; Paquola et al., 2019a; Valk et al., 2020). In the context of identifying systematic motifs underlying cortical alterations in mental illness, the gradient approach holds promise to uncover synchronized vs. independent cortical alteration patterns by placing similarly affected regions closer together in a low-dimensional space - independent from their cortical location.

4.4.2 Intra-cortical myelin mapping to capture cortical consolidation

Nuanced analytical approaches may shine light on the mechanistic links between developmental susceptibility and cortical maturation, such as cortical malleability and consolidation. By insulating neural connections to enhance circuit efficiency, myelin modulates adaptive maturation. However, it also limits structural plasticity by consolidating existing connections (Mount & Monje, 2017; Xin & Chan, 2020). How this balance mediates developmental susceptibility is currently unclear. Recent advances in intra-cortical myelin mapping have provided mesoscale, *in vivo* proxies of the progression of maturational refinement and consolidation across cortical development (Paquola et al., 2019a; Whitaker et al., 2016). These approaches utilize quantitative neuroimaging contrasts dominated by myelin-related molecules, such as magnetization transfer (MT). Briefly, MT captures the magnetization exchange between hydrogen nuclei that are bound to water and those bound to macromolecules, which are primarily found in myelin (Sled, 2018; Weiskopf et al., 2021). Although MT-derived myelin measures are indirect proxies, they show good convergence with histological measures (Mancini et al., 2020; Paquola & Hong, 2023) and sensitivity to individual differences (Ziegler et al., 2019). Intriguingly, myelin mapping allows the study of the cortical depth dimension *in vivo*, inspired by histological microstructural profiling (Eickhoff et al., 2005; Schleicher et al., 1999). In neuroimaging, such depth-wise profiling typically entails (1) the reconstruction of multiple intracortical surfaces between inner (white) and outer (pial) grey matter surfaces, and (2) the sampling of myelin-sensitive image intensity values at each cortical depth surface (**Figure 2B**). This approach has captured high estimated myelin content that increases gradually with cortical depth in unimodal sensorimotor regions, in contrast to lower and less variable myelin content in the paralimbic cingulate and ventral temporal cortex (Paquola & Hong, 2023).

In addition to a nuanced regional characterization, the inter-regional similarity of derived profiles, termed microstructural profile covariance (MPC; Paquola et al., 2019b), enables the study of synchronized changes in myeloarchitecture. One core assumption underlying the MPC approach is that

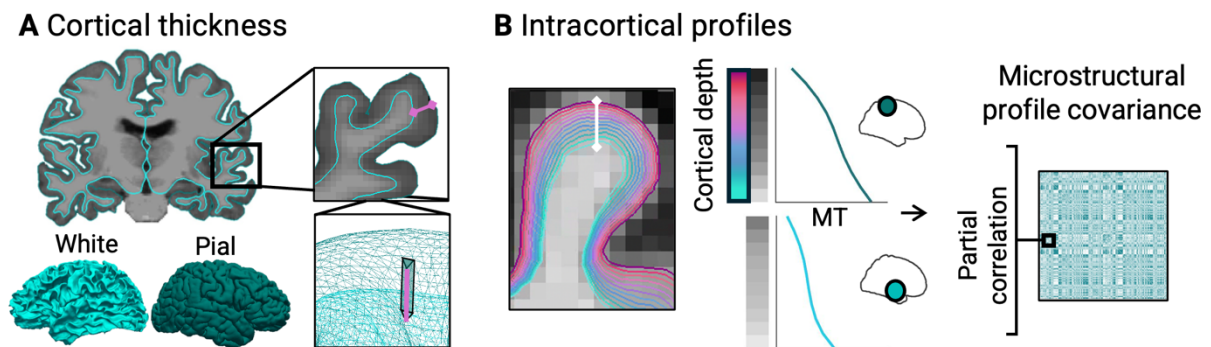


Figure 2. Schematic presentation of *in vivo* estimations of cortical thickness (**A**) and intracortical surfaces used to extract intracortical microstructural profiles (**B**). Images were self-generated. MT = Magnetization transfer.

inter-regional similarities in cortical microstructure predict their structural connectivity (García-Cabezas et al., 2019). Here, developmental changes in similarity suggest structural segregation and integration. Studies on intracortical myelin development have successfully captured the protracted consolidation of connectivity hubs and spatially synchronized cortical differentiation throughout adolescence (Paquola et al., 2019a; Whitaker et al., 2016). Overall, leveraging intra-cortical proxies of myelin maturation promises to deliver nuanced insights into cortical refinement during vulnerable developmental periods.

4.5 Open science facilitates new routes for psychiatric neuroimaging

In recent years, international collaborative efforts have reshaped psychiatric neuroimaging through the formation of multicenter consortia and open science initiatives. To increase reliability, complementary sampling designs have promoted ‘big data’ approaches with higher between-person generalizability, and ‘deep phenotyping’ yielding individual-level precision (Gell et al., 2024; Gratton et al., 2022). The Enhancing NeuroImaging Genetics through Meta-Analysis (ENIGMA; Thompson et al., 2014) consortium has spearheaded the meta-analytic integration of data on pathological brain alterations from around the globe. This collaborative approach aims to enhance statistical power, increase demographic and genetic diversity, and reduce site-specific biases, to collectively reveal more generalizable insights. Concurrently, ‘deep data’ approaches emphasize richer sample characterization of comparatively smaller samples, often involving longitudinal and multimodal data (Gell et al., 2024). This depth of information allows for the study of interactions between mental health, environmental influences, and multiscale brain features. Together, the two approaches provide complementary insights into generalizable principles in representative samples, and multifactorial processes at the individual level.

The increasing accessibility of digitized brain atlases further aids in contextualizing neuroimaging findings with, e.g., cytoarchitectonic atlases, gene expression patterns, and functional task engagement (Hawrylycz et al., 2015; Larivière et al., 2021; Triarhou, 2007; Yarkoni et al., 2011). By revealing systematic associations with certain neurobiological profiles, such contextualization provides insights into the potential etiology of pathological patterns. In sum, international collaborative efforts have paved the way for large-scale, nuanced, and comprehensive research, creating unprecedented opportunities for studying the neurobiology of psychiatric vulnerability.

4.6 Aims of this thesis

Converging evidence suggests that various mental health impairments are linked to shared brain alterations. This thesis aims to provide insights into how brain organization, in particular the spatial architecture and developmental trajectories of the cerebral cortex, may guide transdiagnostic cortical alterations and susceptibility during adolescence. To this end, I took two complementary perspectives on dimensional psychopathology: Using a population-level cross-disorder model (*Study 1*), I examined neurobiological features associated with the spatial organization of shared CT alterations. Using a longitudinal model (*Study 2*), I then studied how developmental variability in cortical consolidation may underpin variation in resilience or susceptibility to psychosocial adversity during adolescence.

In *Study 1*, I took a systems-level approach to reveal co-occurring CT alterations across mental disorders. Specifically, I investigated whether transdiagnostic co-alterations are organized in a network-like fashion that systematically reflects elements of underlying cortical architecture. This approach assumes that overlaps in pathological patterns arise because sets of brain regions share their neurobiology and susceptibility. This may lead to alteration patterns that are systematically represented across disorders. To address this, I used a structural covariance approach capturing CT co-alteration networks across six mental disorders (ADHD, ASD, BD, MDD, SCZ, and OCD) based on ENIGMA summary statistics (12,024 patients and 18,969 unaffected individuals). I further identified neurobiological features reflected in co-alteration patterns by integrating ENIGMA effect size maps with normative connectivity data, as well as cytoarchitectonic, transcriptomic, and task-based functional cortical maps.

In *Study 2*, I investigated how variations in adolescents' resilience or susceptibility to psychosocial adversity are tied to ongoing cortical consolidation at the individual level. I focused specifically on myelination due to its modulatory role both in limiting plasticity through consolidation and in adjusting circuit efficiency as part of maturation and responding to the environment. In a longitudinal study, I defined resilient and susceptible outcomes as lower or higher levels of psychosocial distress than expected based on adversity exposure levels. I further employed intra-cortical myelin mapping in combination with functional connectivity to capture systems-level cortical reorganization and consolidation. By linking variation in resilience/ susceptibility to maturational variability, *Study 2* aimed to provide nuanced insights into biobehavioral adaptation to psychosocial adversity.

In sum, this thesis aimed to establish a systematic framework linking cortical alteration patterns in dimensional psychopathology to the spatial layout and protracted maturation of the cerebral cortex.

5 Empirical work

5.1 Study 1: Coordinated cortical thickness alterations across six neurodevelopmental and psychiatric disorders

Hettwer, M. D., Larivière, S., Park, B. Y., van den Heuvel, O. A., Schmaal, L., Andreassen, O. A., Ching, C. R. K., Hoogman, M., Buitelaar, J., van Rooij, D., Veltman, D. J., Stein, D. J., Franke, B., van Erp, T. G. M., ENIGMA ADHD Working Group, ENIGMA Autism Working Group, ENIGMA Bipolar Disorder Working Group, ENIGMA Major Depression Working Group, ENIGMA OCD Working Group, ENIGMA Schizophrenia Working Group, Jahanshad, N., Thompson, P. M., Thomopoulos, S. I., Bethlehem, R. A. I., Bernhardt, B. C., Eickhoff, S. B., Valk, S. L. (2022). Coordinated cortical thickness alterations across six neurodevelopmental and psychiatric disorders. *Nature communications*, 13(1), 6851.

Impact Factor (2023): 14.7

5-year Impact Factor (2023): 16.1

This is an open access article licensed under a Creative Commons Attribution 4.0 International License (<https://creativecommons.org/licenses/by/4.0/>).

Authorship Attribution Statement

I conceptualized the study, analyzed the data, prepared the figures, interpreted the findings, and wrote the drafts of the manuscript under the supervision of S. L. Valk and S. B. Eickhoff. Data acquisition, aggregation, and processing was performed by the ENIGMA ADHD Working Group, ENIGMA Autism Working Group, ENIGMA Bipolar Disorder Working Group, ENIGMA Major Depression Working Group, ENIGMA OCD Working Group, ENIGMA Schizophrenia Working Group, under the guidance of O. A. van den Heuvel, L. Schmaal, O. A. Andreassen, C. R. K. Ching, M. Hoogman, J. Buitelaar, D. van Rooij, D. J. Veltman, D. J. Stein, B. Franke, T. G. M. van Erp, N. Jahanshad, P. M. Thompson, and S. I. Thomopoulos. All authors reviewed the results and approved the final version of the attached paper.

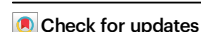


Coordinated cortical thickness alterations across six neurodevelopmental and psychiatric disorders

Received: 16 February 2022

Accepted: 24 October 2022

Published online: 11 November 2022



A list of authors and their affiliations appears at the end of the paper

Neuropsychiatric disorders are increasingly conceptualized as overlapping spectra sharing multi-level neurobiological alterations. However, whether transdiagnostic cortical alterations covary in a biologically meaningful way is currently unknown. Here, we studied co-alteration networks across six neurodevelopmental and psychiatric disorders, reflecting pathological structural covariance. In 12,024 patients and 18,969 controls from the ENIGMA consortium, we observed that co-alteration patterns followed normative connectome organization and were anchored to prefrontal and temporal disease epicenters. Manifold learning revealed frontal-to-temporal and sensory/limbic-to-occipitoparietal transdiagnostic gradients, differentiating shared illness effects on cortical thickness along these axes. The principal gradient aligned with a normative cortical thickness covariance gradient and established a transcriptomic link to cortico-cerebello-thalamic circuits. Moreover, transdiagnostic gradients segregated functional networks involved in basic sensory, attentional/perceptual, and domain-general cognitive processes, and distinguished between regional cytoarchitectonic profiles. Together, our findings indicate that shared illness effects occur in a synchronized fashion and along multiple levels of hierarchical cortical organization.

The conceptualization of neurodevelopmental and psychiatric disorders has undergone several transformations toward overlapping spectra of psychopathology^{1,2} associated with underlying polygenicity, neurodevelopmental etiology, and epidemiological comorbidity^{1,3,4}. Efforts to empirically understand their dimensional structure has linked the general liability for mental illness to shared risk factors and common alterations in neurodevelopmental processes, predisposing to the clinical conditions ultimately manifested^{5–8}. Coordinated multi-level brain alterations across disorders may explain these phenomenological overlaps and common etiology.

Big-data neuroscience initiatives such as the Enhancing Neuroimaging Genetics through Meta-Analysis (ENIGMA) consortium have facilitated large-scale transdiagnostic investigations to identify shared and disorder-specific brain alterations⁹. These studies consistently report cortical thickness alterations in neurodevelopmental and psychiatric disorders^{10–15}, which serves as a proxy measure for neuronal

density, cytoarchitecture, and intracortical myelination^{16–18}. Crucially, previous ENIGMA findings suggest that regional morphological alterations are not only shared between disorders^{19–22}, but also in part associated with shared genetic etiology²⁰, regional pyramidal-cell gene expression²¹, microstructure, and neurotransmitter system organization²². While these findings highlight regional overlaps as shared effects between disorders, the current study aims to address inter-regional dependencies capturing coordinated transdiagnostic patterns of illness effects. That is, differences in brain morphology and function observed in psychiatric patients appear to follow network-like patterns constricted by underlying connectome organization^{23–25}. According to the nodal stress hypothesis, highly interconnected regions ('hubs') show increased susceptibility to pathological processes due to shared metabolic alterations, spread of pathogens, or similar gene expression profiles^{25,26}. In addition, regional disruptions can act as 'disease epicenters' by promoting pathological processes in

✉ e-mail: m.hettwer@fz-juelich.de; s.valk@fz-juelich.de

areas they connect to, thus constituting anchors of network-like alterations²⁷. Although the role of network characteristics for cortical alterations in psychopathology is well established^{25,28,29}, it remains unknown how cross-disorder morphological alterations are embedded in a joint co-alteration network, and whether organizational principles shaping such a network link to underlying neurobiology.

An intuitive approach capturing inter-regional dependencies of illness effects is structural covariance of cortical thickness alterations, which forms cortex-wide co-alteration networks. While structural covariance partly reflects synchronized and genetically coupled maturation during healthy neurodevelopment^{30–32}, consolidated atrophy in illness also occurs more frequently in regions with high structural covariance^{33,34}. Moreover, inter-regional similarities in cortical features tend to be hierarchically organized: Previous mappings of low-dimensional cortex-wide gradients have described continua of cytoarchitectural complexity, long- versus short-distance connectivity, cell density, transcriptomic expression, and phylogenetic and ontogenetic timing^{35–38}. Such gradients (or ‘axes’) compactly summarize covariance patterns via connectome decomposition techniques^{35,39}, and place brain regions with similar covariance profiles closer together in a common coordinate-frame, regardless of their position on the cortex. These axes offer insights into the global arrangements of cortical features and appear to be distorted in several neuropsychiatric conditions^{22,40–42}. Together, previous research highlights the role of convergent hierarchical neurobiological profiles as a central feature of healthy brain organization. Yet, it is currently unknown whether the global arrangement of regional vulnerability to mental illness follows a hierarchical organization as well.

In this study, we identified hubs of transdiagnostic co-alteration networks and disease epicenters using meta-analytical maps for six neurodevelopmental and psychiatric disorders (autism spectrum disorder (ASD), attention-deficit/hyperactivity disorder (ADHD), major depressive disorder (MDD), schizophrenia spectrum disorders (SCZ), bipolar disorder (BD), and obsessive-compulsive disorder (OCD)), provided by the ENIGMA consortium^{10–15}. We further employed a cortex-wide gradient mapping approach to identify hierarchical cortical arrangements of transdiagnostic illness effects. Last, we contextualized derived gradients with cytoarchitectonic and functional cortical profiles for multi-level evaluation and studied the embedding of individual disorder impact maps within our framework. We performed multiple robustness checks to evaluate the stability of our findings.

Results

Transdiagnostic co-alteration hubs inform disease epicenters

Consistent with previous work^{19,21,22}, we selected six neurodevelopmental and psychiatric disorders for which illness effects have been studied in large samples in collaborative international meta-analyses by the ENIGMA consortium. To study coordinated transdiagnostic effects of illness on cortical thickness, we accessed summary statistics from 12,024 patients with ASD¹⁰, ADHD¹¹, MDD¹², SCZ¹³, BD¹⁴, or OCD¹⁵, and 18,969 unaffected individuals from previously published ENIGMA studies (see Table S1). Analyses were restricted to adult samples, except for ASD for which available summary statistics included all age groups. See Table S2 for information on sample demographics. For each condition, we retrieved a Cohen's *d* map via the ENIGMA Toolbox⁴³ reflecting case-control differences in cortical thickness for 68 Desikan-Killiany parcels⁴⁴ (Fig. 1A). Cohen's *d* maps were corrected for different combinations of covariates including age, sex, site, and intelligence quotient (Table S2). For contextualization with normative network properties, we further accessed healthy control cortico-cortical structural (diffusion-weighted tractography; DTI) and functional (resting-state functional magnetic resonance imaging; rs-fMRI) connectivity data from an independent sample of healthy young adults from the

Human Connectome Project (HCP⁴⁵) through the ENIGMA Toolbox⁴³ (Fig. 1B).

First, we computed a transdiagnostic co-alteration matrix by correlating Cohen's *d* values between regions and across disorders. Regions showing a high sum of strong connections (i.e., correlations) were identified as co-alteration hubs (Fig. 1C). Transdiagnostic hub regions predominated in bilateral medial temporal gyrus and ventral temporal cortex, and more widespread in temporal and frontal regions. When studying which regions are most strongly and consistently affected across disorders via the sum of normalized illness effect maps ('hit map'; see Fig. S1), we observed a significant correlation with transdiagnostic co-alteration hubs ($r = 0.42$, $p_{\text{spin}} < 0.0001$), suggesting that hubs are placed in regions with shared impact. This effect predominated for shared thickness reductions ($r = 0.334$; $p_{\text{spin}} = 0.01$) rather than relative increases ($r = -0.30$; $p_{\text{spin}} = 0.02$). Furthermore, the spatial pattern of co-alteration hubs correlated with normative functional connectivity hubs ($r = 0.50$, $p_{\text{spin}} < 0.0001$), but less so with structural hubs ($r = 0.18$, $p_{\text{spin}} = 0.08$). Co-alteration hubs were comparable at different thresholds and when correcting for sample size (see Fig. S2).

Having confirmed a general convergence between hubs of coordinated cortical thickness alterations and normative connectome organization, we next investigated whether these patterns are anchored to potential disease epicenters. As previous work has indicated, epicenter mapping aids to understand how the normative connectivity profile associated with a specific region may play a central role in the manifestation of a disorder^{27,46,47}. Here, we identified transdiagnostic epicenters as regions whose connectivity profile may underlie illness effects that are consistently organized across disorders, i.e., regions whose network embedding correlates significantly with co-alteration hubs. Thus, the epicenter mapping approach highlights the role of regions that do not necessarily constitute hubs themselves⁴⁸ but may contribute to shaping shared patterns of illness effects through strong or distributed connections with co-alteration hubs. Systematically investigating connectivity profiles of 68 cortical seeds revealed primarily temporal and prefrontal regions as potential transdiagnostic disease epicenters (Fig. 1D). This finding held true when computing epicenters based on the 'hit map' (Fig. S1E, F). Highest ranked functional disease epicenters were observed in the left entorhinal cortex, left pars orbitalis, right banks of the superior temporal sulcus (STS), left pars triangularis, and left STS ($r = 0.55–0.59$; all $p_{\text{spin}} < 0.05$). Top five structural disease epicenters were present in left pars opercularis and triangularis, inferior parietal lobe, STS bank, and caudal middle frontal gyrus ($r = 0.28–0.42$; all $p_{\text{spin}} < 0.05$).

Macroscale gradients of transdiagnostic co-alteration networks

So far, our analyses suggest that the cortex-wide network of transdiagnostic illness effects is non-randomly organized, with hubs of prominent covariance and epicenters shaping the co-alteration network. Next, via manifold learning, we sought to study the embedding of these features within low-dimensional organizational gradients^{39,49}. This analysis was based on the same co-alteration matrix used to derive transdiagnostic hubs (Figs. 1C and 2A). We applied diffusion map embedding⁴⁹ to project regional and long-range connections within covariance networks into a common space. This yielded unitless components, each of which denotes the position of nodes on a continuum describing similarities in regions' structural covariance profiles (Fig. 2A). Thus, opposing apices of a gradient reflect maximally divergent covariance patterns.

The principal gradient of transdiagnostic covariance (G1) captured a dominant dissociation between frontal and temporal lobes and accounted for 36% of variance in transdiagnostic co-alteration (Fig. 2B). The secondary gradient (G2) spanned from occipito-parietal regions to temporo-limbic structures, explaining 21% of variance. Findings were comparable at different thresholds and robust

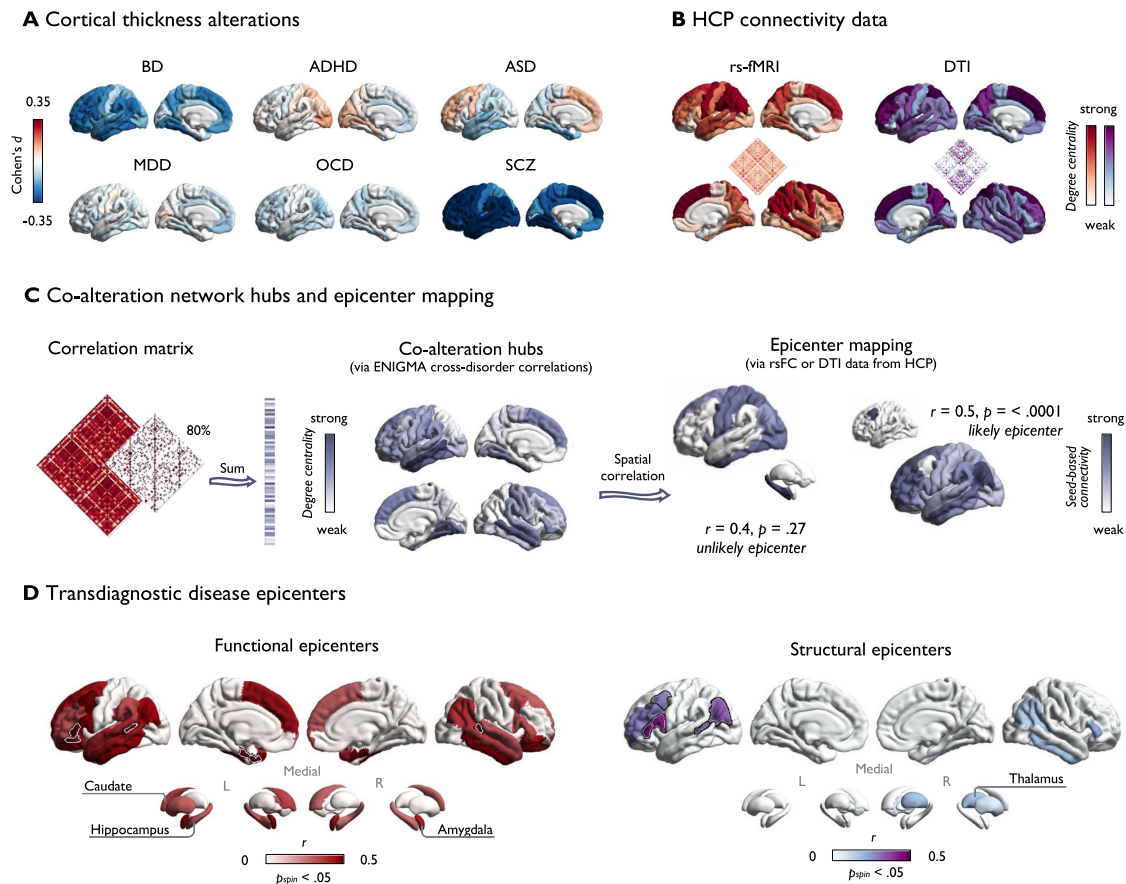


Fig. 1 | Hubs and epicenters shaping transdiagnostic co-alteration patterns.

A Disorder-specific Cohen's d maps indicating case-control differences in cortical thickness. **B** Normative connectivity matrices derived from resting-state functional magnetic resonance imaging (rs-fMRI) and diffusion-weighted tensor imaging (DTI) from the Human Connectome Project (HCP⁴⁵) and hubs (degree centrality). **C** Left: Computation of co-alteration hubs. Degree centrality was computed as the sum of above-threshold (80%) connections at each parcel using disorder maps from the Enhancing Neuroimaging Genetics through Meta-analyses (ENIGMA) consortium. Right: Visualization of the epicenter mapping approach using resting state functional connectivity (rsFC) or DTI. Seed-based connectivity profiles were systematically correlated with co-alteration hubs (using Pearson's r and assessing

significance via two-sided spin-tests, correcting for spatial auto-correlation, without further correction for multiple comparisons). **D** Transdiagnostic disease epicenters are depicted as correlations between co-alteration hubs and HCP normative seed-based connectivity profiles (rs-fMRI or diffusion tensor imaging (DTI)), thresholded at $p_{spin} < 0.05$ (this panel shows DTI examples). High correlations imply high likelihood of a structure constituting a disease epicenter. Top five functional and structural disease epicenters are framed in white/black. Source data are provided as a Source Data file. ADHD = Attention-deficit/hyperactivity disorder; ASD = Autism spectrum disorder, BD = Bipolar disorder, MDD = Major depressive disorder, OCD = Obsessive-compulsive disorder, SCZ = Schizophrenia spectrum disorders.

against parameter manipulation, sample size correction, and selection of diagnoses (see Fig. S2). An overview of all computed gradients is presented in Fig. S3. Investigating the correspondence between the disease epicenters and the transdiagnostic gradients, we found that the apices of G1 captured previously identified functional disease epicenters (Fig. S4). This implies that frontal and temporal epicenters each contribute to the overall pattern of co-alterations but do so in a maximally distinct manner (Fig. S5).

Since previous studies have shown that cortical thickness alterations in psychopathology are more prominent in regions with high structural covariance⁵⁰, we assessed whether the disease-related relative changes in cortical thickness align with normative organization of absolute cortical thickness. Indeed, we observed a correlation between the principal cortical thickness covariance gradient (anterior-posterior; Fig. 2C)³⁶ and G1 ($r = -0.74$, $p_{spin} = 0.0015$) but not G2 ($r = -0.11$, $p_{spin} = 0.27$). The second cortical thickness covariance gradient (inferior-superior) was not related to G1 ($r = 0.32$, $p_{spin} = 0.21$) or G2 ($r = -0.25$, $p_{spin} = 0.07$).

Microstructural and transcriptomic contextualization

After capturing macroscale organization of disease effects, we contextualized identified gradients with microscale cytoarchitecture to gain a multi-level understanding of neurobiological cortical profiles in shaping transdiagnostic co-alteration networks. To this end, we stratified our gradients according to von Economo-Koskinas cytoarchitectonic classes⁵¹. We observed a prominent distinction between granular and agranular cortices across our principal transdiagnostic gradient (Fig. 2D), whereas G2 distinguished between granular and parietal cytoarchitectonic classes.

Using post-mortem gene expression data from the Allen Human Brain Atlas (AHBA) as a reference⁵², we next identified genes for which spatial expression patterns significantly correlated with G1 (see Table S3). This approach has previously revealed genetic links to normative brain development and organization^{52–54} as well as structural abnormalities in disease^{42,55,56}. We generated null models to assess spatial specificity (including spatially autocorrelated phenotype maps⁵⁷) and gene specificity (including (i) genes with similar levels of

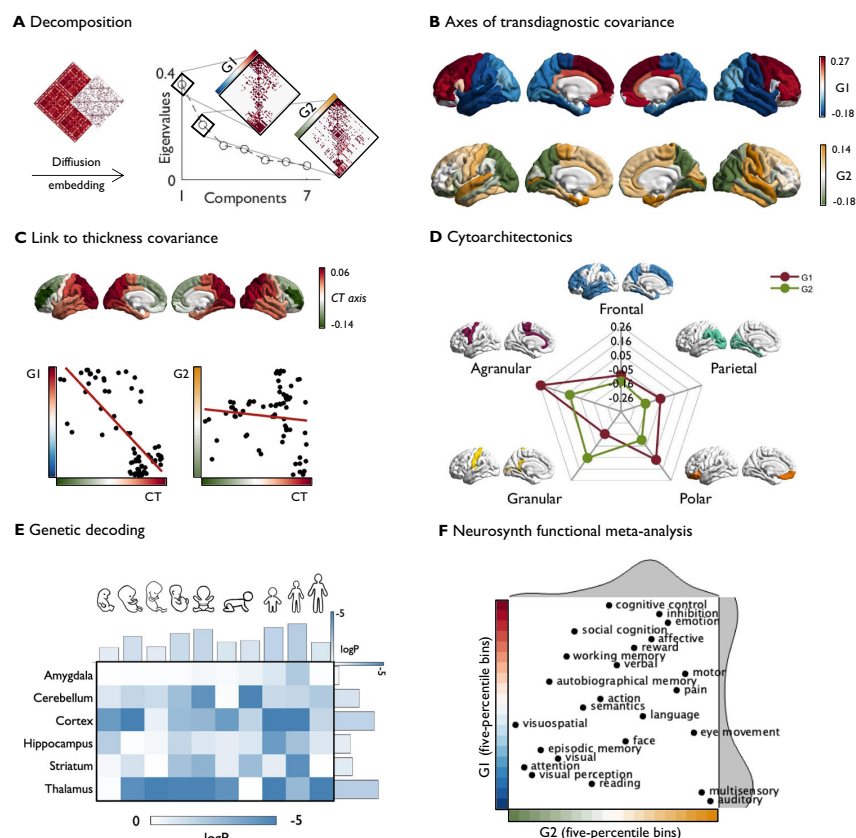


Fig. 2 | Macroscale organization of transdiagnostic covariance in cortical thickness alterations. **A** A cross-disorder structural covariance matrix was thresholded at 80% and decomposed using diffusion map embedding. Covariance along the principal (G1) and second (G2) gradients is depicted on the right. **B** Transdiagnostic gradients G1 and G2. **C** Correlation between a normative axis of cortical thickness (CT) covariance³⁶ and transdiagnostic gradients. **D** Cross-condition gradients stratified according to von Economo-Koskinas cytoarchitectonic classes⁵¹. **E** Developmental gene enrichment analysis based on 232 genes for

which spatial expression patterns correlated with G1 (of which 146 showed a positive correlation, i.e., were overexpressed in prefrontal compared to temporal regions). **F** Meta-analysis for diverse cognitive functions obtained from NeuroSynth⁶⁰. We computed parcel-wise z-statistics, capturing node-function associations, and calculated the center of gravity of each function along 20 five-percentile bins of G1 and G2. Function terms are ordered by the weighted mean of their location along the gradients. Source data are provided as a Source Data file.

coexpression and (ii) genes overexpressed in the brain compared to the rest of the body³⁸ of the identified gene set. Out of 232 genes for which expression patterns correlated significantly with G1, 146 showed a positive correlation with G1, i.e., they were more strongly expressed in the PFC than in temporal regions. Developmental gene enrichment analysis⁵⁹ revealed that next to the cortex, identified genes were most prominently expressed in the thalamus and cerebellum across various developmental windows (Fig. 2E). In a combined assessment of all brain structures, genes appeared to be enriched most strongly during neonatal early infancy, mid/late childhood, and adolescence. G2 was not significantly associated with genes included in the AHBA after correcting for spatial and gene specificity.

Associations with task-based functional activations

Next, we aimed to identify potential functional implications by investigating whether transdiagnostic gradients dissociate regions associated with distinct functional engagement. To this end, we conducted a meta-analysis on task-specific functional activations for 24 cognitive terms using the NeuroSynth database⁶⁰. We binned each gradient into five-percentile bins and defined regions of the same bin as a region of interest (ROI). Resulting 20 ROIs for each gradient were then tested for their overlap with meta-analytic ROIs associated with each of the 24

cognitive terms via z-statistics. The magnitude of an average z-value at a ROI (i.e., a position along the gradient) reflects the strength of its association with a certain functional task activation. We sorted the topic terms by their weighted mean position along both gradients, revealing systematic shifts in functional networks along transdiagnostic axes of co-alteration. In a combined 2D space framed by both gradients, we could distinguish between different co-alteration patterns in primary (e.g., 'auditory') and 'multisensory' regions at the temporal apex, higher-order perceptual structures (e.g., 'visual perception' and 'attention') at the occipito-parietal apex, and complex cognitive functions (e.g., 'cognitive control' and 'inhibition') at the frontal apex (Fig. 2F and Fig. S6).

Embedding of individual disorders within a transdiagnostic co-alteration space

Having established several features guiding a transdiagnostic co-alteration network, we last aimed to evaluate the positioning of individual disorders within this continuous transdiagnostic space. To this end, we first studied the correspondence between a parcel's whole-brain transdiagnostic covariance profile and a parcel's whole-brain disorder-specific covariance profile (see Fig. 3A, B). While associations with the transdiagnostic pattern vary between

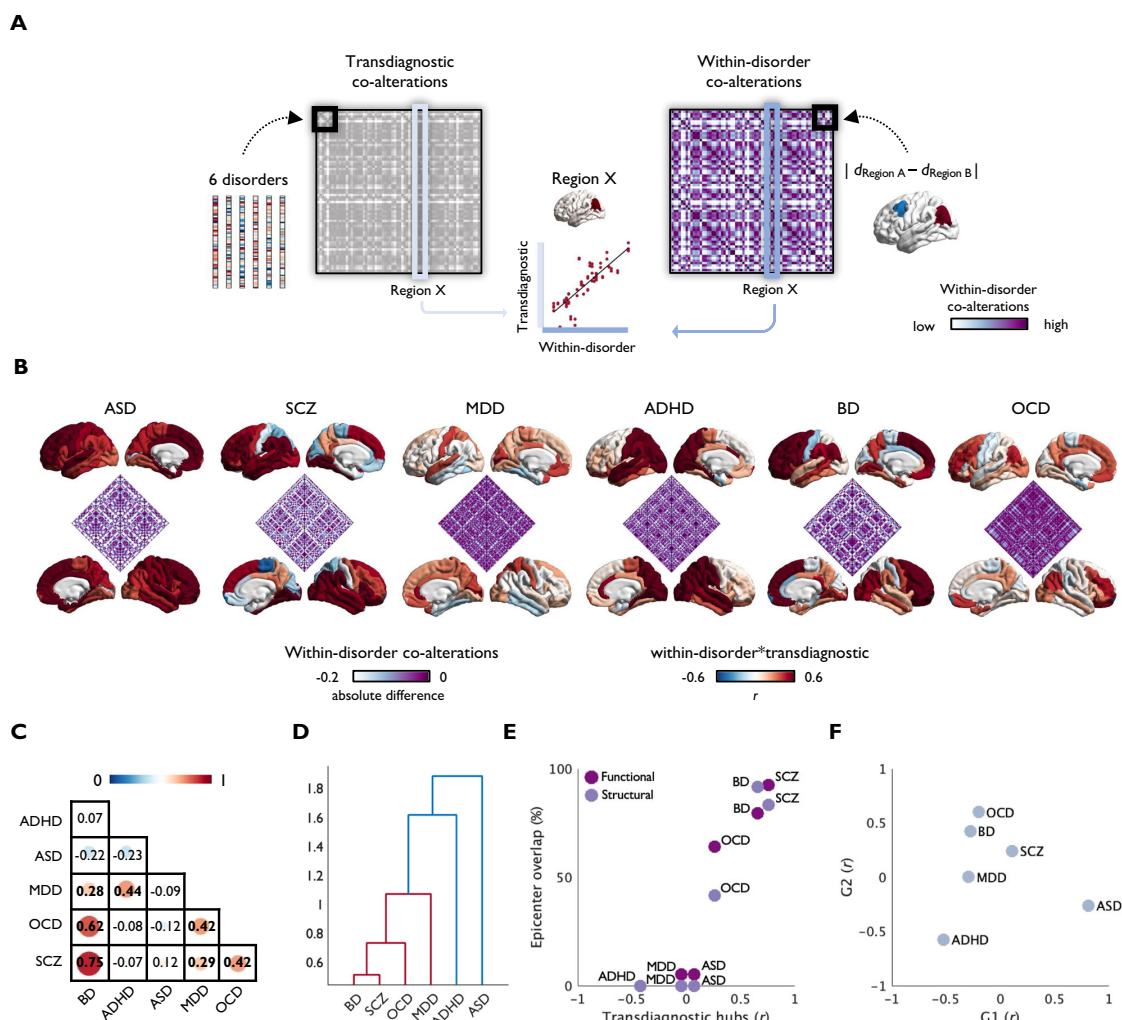


Fig. 3 | Embedding of six disorders within transdiagnostic co-alteration networks. **A** Computation of transdiagnostic and within-disorder co-alteration matrices. **B** Region-wise correspondence between disorder-specific and transdiagnostic co-alteration profiles. Disorder-specific inter-regional difference scores were inverted so that higher correlations with transdiagnostic patterns indicate higher coupling. **C** Similarity of illness effects between disorders, i.e., correlations of Cohen's d maps, and how they cluster together in a two-cluster solution (**D**). Position of individual disorders within a transdiagnostic co-alteration space based

on **E** the correlation between transdiagnostic hubs and Cohen's d maps (x-axis) and the overlap between transdiagnostic and disorder-specific epicenters (y-axis); and **F** the correlation between the principal (G1) and secondary (G2) transdiagnostic gradients with Cohen's d maps. Source data are provided as a Source Data file. ASD = Autism spectrum disorder, SCZ = Schizophrenia spectrum diagnoses, MDD = Major depressive disorder, ADHD = Attention-deficit/hyperactivity disorder, BD = Bipolar disorder, OCD = Obsessive-compulsive disorder.

disorders and across the cortex, most disorders showed highest similarity to shared patterns in heteromodal cortices. This mirrors other findings presented here which suggest heteromodal cortices as regions that not only tend to be affected, but also tend to be affected similarly across disorders and in a synchronized manner across the cortex. Next, we compared the degree of similarity between disorders and their embedding within the transdiagnostic co-alteration space. Replicating what previous transdiagnostic studies have shown^{19,20}, we observed a cluster composed of SCZ, BD, and OCD, while ADHD and ASD stayed separate (Fig. 3C, D). In contrast to clustering approaches, our cross-disorder covariance approach aimed to describe a transdiagnostic organizational space in which disorder effects occur. Indeed, we found that disorders that cluster together, such as SCZ, BD, and OCD showed a similar placement within this transdiagnostic co-alteration framework (see

Fig. 3D–F). While transdiagnostic hubs correlated with illness effect maps in SCZ ($r = 0.76$, $p_{\text{spin}} < 0.0001$), BD ($r = 0.66$, $p_{\text{spin}} = 0.001$), and OCD ($r = 0.26$, $p_{\text{spin}} = 0.03$), this was not the case for ASD ($r = 0.07$, $p_{\text{spin}} = 0.31$) and MDD ($r = -0.05$, $p_{\text{spin}} = 0.41$), and ADHD showed a negative correlation ($r = -0.42$, $p_{\text{spin}} = 0.003$). Similarly, disorder-specific epicenters overlapped with transdiagnostic epicenters in SCZ, BD, and OCD, and in part in MDD (see Fig. 3E and Fig. S7), whereas ADHD and ASD showed no significant disorder-specific epicenters in the first place. Together, these analyses indicate that similar illness effect maps relate to similar degrees to transdiagnostic co-alteration hubs, are linked to epicenters that overlap to similar degrees with transdiagnostic epicenters (Fig. 3E), and are positioned more closely together in a transdiagnostic covariance space framed by G1 and G2 (Fig. 3F and Table S4). However, we also observe that disorders which show some similarity but are

allocated to different clusters, such as MDD and ADHD, are positioned closer to each other in our continuous transdiagnostic space, crossing cluster boundaries.

Discussion

Our study reports coordinated effects of six major mental disorders (SCZ, BD, OCD, ASD, ADHD, and MDD) on cortical thickness and their association with functionally relevant neurobiological patterns across multiple scales of analysis. Thus, we extended previous investigations of shared regional effects^{19–22} toward a network-based approach that embeds regional alterations within cortical hierarchies of transdiagnostic covariance of illness effects.

We identified hubs of transdiagnostic co-alteration predominantly in lateral and ventral temporal lobes, with some impact on post-central and medial frontal regions. Importantly, these hubs overlapped with regions showing shared thickness alterations, indicating especially pronounced coordination within co-alteration networks between consistently affected regions. Observing an interrelationship of pathological cortical thickness alterations between temporal and prefrontal heteromodal cortices, but less so in unimodal and paralimbic cortices, indicates distinguishable processes shared between disorders and across the cortex. Furthermore, co-alteration hubs followed the spatial pattern of normative functional connectivity hubs, suggesting that captured variability in susceptibility may link to nodal stress^{25,26,61}. Indeed, in vivo markers of e.g., aberrant energy metabolism and post-mortem proteomic analyses have revealed overlaps between MDD, SCZ, and BD^{62–64}. As hubs are more strongly influenced by genes than non-hubs⁶⁵, hub regions may exhibit increased shared vulnerability for atypical neurodevelopment, supported by both the polygenicity and genetic overlaps in psychiatric diagnoses. Thus, nodal stress, along with other potential factors such as shared genetic susceptibility, appears to be a strong candidate explanation for the irregular topographic distribution of covarying illness effects^{28,66}.

Present results further indicate that large-scale patterns of shared illness effects are shaped by both structural and functional epicenters. That is, transdiagnostic epicenters suggest a central role of prefrontal and temporal cortex in the manifestation of mental illness, indicating how transdiagnostic cortical alterations are anchored in the connectivity of identified regions. Notably, influences of functional epicenters emerged above and beyond hard-wired tracts. Such a divergence is likely⁶⁷, as functional connectivity reflects a temporal correlation of activity which may be driven by distant input into a spatially distributed polysynaptic network^{68,69}. The high concordance of prefrontal and temporal connectivity profiles with co-alteration hubs indicates that epicenters preferentially emerged in regions known to extend long-range connections⁷⁰, facilitating their contribution to cortex-wide organizational patterns. Structures in the mediotemporal lobe and ventrolateral PFC were identified as most likely epicenters. Both regions have been implicated in cognitive impairments and developmental susceptibility across neurodevelopmental and psychiatric disorders^{53,71,72}. Mediotemporal structures further act as nodal points between multimodal cortical association areas and the sub-cortex, and feature transitions in cytoarchitecture from iso- to allocortical regions³⁷. These features may increase both vulnerability to nodal stress and the spread of pathological alterations through wide-ranging connections. At the same time, the vIPFC shows protracted plasticity throughout multiple neurodevelopmental stages⁷³. While allowing for continuous refinement of complex cognitive abilities, protracted plasticity gives room for aberrant maturational processes leaving the individual more susceptible to developmental aberrations. Overall, the epicenter mapping approach thus identified anchors of large-scale transdiagnostic co-alteration networks in regions that both have the

potential to spread illness effects through long-range connections and are susceptible to maturational aberration.

Further investigating transdiagnostic covariance via manifold learning, we recapitulated cortex-wide gradients along which co-alteration patterns were organized. The principal transdiagnostic gradient captured a cortex-wide segregation of frontal and temporal structures, indicating that cortical thickness alterations in both regions are embedded in maximally distinct covariance networks. The concordance of G1 with the normative organizational axis of cortical thickness covariance³⁶ mirrors previous findings indicating increased susceptibility to cortical atrophy in regions that exert high structural covariance^{33,74}. As cortical thickness covariance is assumed to reflect common maturational trajectories³⁰, atypical neurodevelopment likely contributes to shaping cortical gradients of co-alteration networks. The process of shaping transdiagnostic gradients throughout development may further be influenced by subcortico-cortical circuits^{75–78}, as suggested by our transcriptomic decoding findings. Here, we observed that genes whose expression pattern aligns with G1 are also enriched in the cerebellum and thalamus in early developmental phases. Notably, studies on subcortical interactions have linked impaired functional coordination within cerebello-thalamo-cortical circuits to a general liability for psychopathology^{79,80}. It is thus possible that the organization of transdiagnostic co-alterations observed in the cortex partly builds upon alterations in subcortical circuits. The secondary gradient was restricted to uni- and heteromodal sensory cortices in the posterior cortex, segregating regions that hold primary sensory (pericalcarine cortex, post-central and superior temporal gyrus) and paralimbic (entorhinal) cortices from multimodal association regions in the occipito-parietal cortex. Both axes described segregations along different cytoarchitectural classes. Whereas G1 traversed between agranular, paralimbic, versus granular, primary cortices, G2 showed a cytoarchitectural divergence between granular and frontal/parietal cortices. Variable susceptibility to disease impact thus suggests that areas with shared cytoarchitecture are more likely embedded similarly within pathological networks. This may be due to similar local computational strategies supported by cell count and wiring strategies⁷, development⁸¹, and the degree of plasticity associated with different degrees of cortical lamination⁵³. Future work may further investigate the specific neurobiological mechanism linking cytoarchitecture, function, and mental illness.

We further contextualized our findings with respect to functional processes through meta-analytical task-based activations. Combining G1 and G2 in a two-dimensional space revealed distinct co-alteration profiles at three levels of information processing, i.e., primary/multi-sensory, perception/attention, and domain-general cognitive control. Interestingly, all three levels show various processing impairments in different neuropsychiatric conditions which are in part interrelated: Firstly; atypical early development of sensory cortices can contribute to social cognitive deficits through impaired social cue perception^{82,83} and, more generally, deficits in multisensory binding^{83,84}. Secondly; at an intermediary level, aberrant functional involvement and structural integrity of attention networks have been identified as a prominent transdiagnostic feature of neuropsychiatric conditions^{28,85}. Thirdly; upstream consequences of dysregulated attention networks ultimately contribute to impaired higher-order cognitive functions such as executive control. Impaired executive control does not only constitute a transdiagnostic feature in mental illness⁸⁶, but is also a predictor of cognitive and socio-occupational impairment^{86–88}. Despite inter-related deficits within functional networks, the observation that multiple processing levels are associated with distinct structural co-alteration patterns indicates independent maturational causes and distinct vulnerability. In line with findings from cytoarchitectonic contextualization, levels of functional engagement of cortices involved in similar tasks appear to leave brain regions processing similar types of information with shared susceptibility. Given that

sensory regions develop earlier than association regions in the cortical maturational sequence⁸⁹, differences in pathological covariance profiles may link to the degree to which their developmental peaks overlap with vulnerable periods for neurodevelopmental and psychiatric disorders. This raises the question whether identified cortical gradients also reflect a spatiotemporal gradient of atypical neurodevelopment and inspire respective investigations in longitudinal/prospective studies. Overall, our findings indicate that the degree to which regional alterations may be linked to and potentially facilitate alterations in other brain regions (i.e., potential epicenters), and the degree to which such interrelations pose a general feature of the neurodevelopmental and psychiatric disorders included (i.e., co-alteration hubs) appears to vary across the cortex and follows general neurobiological principles of brain organization (i.e., cortex-wide axes).

Last, we aimed to investigate how the proposed transdiagnostic co-alteration space, framed by both transdiagnostic covariance gradients, compares to previous descriptions of cross-disorder similarities and disorder clusters. That is, our cross-disorder covariance approach generates a continuous space within which disorders vary with respect to their topography of similarity to transdiagnostic patterns across the cortex. While we indeed found that positions of disorders within this space converge with their allocation to disorder clusters, the co-alteration framework captures both similarities within and between clusters in a continuous manner. By embedding illness effects within a space shaped by genetic and maturational processes, we gain further insight in differentiable neurobiological mechanisms underlying individual disorders. Indeed, the first gradient, stretching between frontal and temporal regions showed similarities with a previously described anterior-posterior axis along the cortical mantle⁹⁰. Previous work has indicated differentiable spatial patterns of co-maturation and development along several spatial axes, indicating the interplay of multiple neurodevelopmental mechanisms across the cortex^{86,90,91}. The observed systematic alterations along such axes across disorders may reflect differential disruptions in pre- and post-natal neurodevelopment. Moreover, we observed that, for most disorders, overlap between disorder-specific and transdiagnostic covariance is highest in heteromodal cortices. This convergence may be linked to their placement within these neurodevelopmental axes^{53,92}, supporting these regions as targets of transdiagnostic investigations. Future work may evaluate potential causes and critical time windows of development within this framework, enhancing our understanding of the ontogeny of cortical organization in health and disorder.

It is of note that, although disorder impact generally converged in heteromodal regions and linked to transdiagnostic covariance gradients, each disorder showed a unique embedding within our framework. For example, though we observed widespread coupling between transdiagnostic and disorder specific covariance networks in ASD and ADHD, and marked association with the principal transdiagnostic covariance gradient, there was only reduced correspondence with the epicenter framework, indicating disrupted relationship between disorder hubs and connectivity profiles. Conversely, MDD showed in particular correspondence with transdiagnostic patterns in ventral PFC, subgenual anterior cingulate, somatosensory cortex and nucleus accumbens, but showed reduced correspondence with transdiagnostic epicenters and the transdiagnostic gradients. It is possible that MDD, being at the center of the 2D gradient space and showing highest similarities with both ADHD and OCD, can be best described by yet another axis not captured in the current framework which is dominated by neurodevelopmental patterning. The future work expanding our framework to more disorders as well as atlases with higher granularity may be able to further pin-point differential axes of embedding for different disorders.

While our findings underline the relevance of transdiagnostic approaches, they do not contradict the existence of etiological and phenomenological differences within and between psychiatric

diagnoses. Our transdiagnostic approach does not capture heterogeneity within and between highly related diagnostic categories, as expected to be present e.g., within the included SCZ (schizophrenia spectrum disorders) and BD (type I and II combined) samples. However, shared features crossing diagnostic boundaries are likely also an important factor contributing to within-disorder heterogeneity. Moreover, individuals may be diagnosed with multiple different disorders across their lifespan⁴. Understanding which neurobiological principles drive the spectrum of varying neurodevelopmental and psychiatric disorders is a crucial piece of the puzzle of the biological origin of disorder variability. Yet, investigating both disorder-specific phenomena and heterogeneity within (spectrum-)diagnoses forms a crucial line of research that will continue to complement our transdiagnostic findings. Presented cortex-wide co-alteration features shall facilitate and provide a transdiagnostic coordinate frame for such insights.

Although we mostly included adult samples and age-corrected summary statistics, there are some offsets among mean ages of ENIGMA maps and between ENIGMA maps and the reference data from other sources (e.g., HCP). These offsets potentially influenced parameters known to change during development and aging, such as hub organization⁸⁹. In addition, neurodevelopmental conditions have different mean ages of onset so that patients included have certainly experienced different lengths of disease and medication histories. It should further be noted that also other disorders such as substance abuse or anxiety disorders tend to co-occur with some of the disorders included here, but could not be included in the analyses as ENIGMA cortical thickness summary statistics have not yet been published. Further work including a wider range of disorders will help to evaluate the generalizability of our transdiagnostic model. ENIGMA summary statistics used here are based on the Desikan-Killiany atlas⁴⁴. They thus contain comparatively sparse data points across the cortex and summarize data from broader areas that contain a mosaic of neurobiological regions that may be differentially affected by disease. Moreover, differences in parcel size⁹³, measurement error, subject motion and scanner/site effects^{94,95} may slightly influence spatial covariance analyses. Last, the lack of subject-level clinical information impeded the direct assessment of clinical implications of current findings. However, understanding the principles according to which cortical alteration patterns are organized across diagnoses will provide a fruitful basis for further investigations on the interrelationship between network organization and symptoms shared across disorders, as well as variations within categorical diagnoses.

In sum, our findings highlight the value of linking multiple neurobiological levels of information—from macroscale neuroimaging to microscale transcriptomic data—to identify systematic transdiagnostic patterns of illness effects. Investigating these patterns revealed coordinated cortical alterations across conditions that are shaped by connectomic, cytoarchitectonic, and functional characteristics. As such, we provide a cortical coordinate system in line with concepts of dimensional psychiatry and network-based pathology, to which future clinical neuroscience findings can be aligned and integrated. Future work may further expand on this approach not only to include different modalities and neuroimaging metrics (e.g., surface area and subcortical structures), but also to consider a much wider range of conditions and age ranges, which is now becoming increasingly possible due to the availability of multi-disease consortia and datasets^{96,97}. This may provide a crucial step toward understanding the neuroetiology of neuropsychiatric conditions.

Methods

ENIGMA neuroimaging summary statistics

For our transdiagnostic analyses, we used publicly available multi-site summary statistics published by the ENIGMA Consortium, and available within the ENIGMA Toolbox (<https://github.com/MICA-MNI/>)

ENIGMA⁴³). Included neurodevelopmental and psychiatric disorders comprised ADHD¹¹ ($n_{\text{cases}} = 733$, $n_{\text{controls}} = 539$), ASD¹⁰ ($n_{\text{cases}} = 1571$, $n_{\text{controls}} = 1651$), BD (type I and II, cumulated)¹⁴ ($n_{\text{cases}} = 1837$, $n_{\text{controls}} = 2582$), MDD¹² ($n_{\text{cases}} = 1911$, $n_{\text{controls}} = 7663$), OCD¹⁵ ($n_{\text{cases}} = 1498$, $n_{\text{controls}} = 1436$), and SCZ (including schizophrenia spectrum diagnoses)¹³ ($n_{\text{cases}} = 4474$, $n_{\text{controls}} = 5098$). Except for ASD for which available summary statistics included all age groups, we restricted our analyses to adult samples. This decision may increase the variance in disease duration due to differences in typical ages of onset associated with the six diagnoses. However, we aimed to match adults to minimize effects that are linked to development and aging, which are potentially larger than the effects of disease duration. We based our analyses on covariate-adjusted case-control differences denoted by across-site random-effects meta-analyses of Cohen's d -values for cortical thickness. Age, sex, and site information was fitted to cortical thickness measures via multiple linear regression analyses. As previous studies have shown associations between IQ and brain structure as well as alterations of this association in ASD⁹⁸, IQ was included as a covariate in the ASD sample. See Table S2 for an overview on demographics and study-specific covariates. Preceding the computation of summary statistics, raw data was pre-processed, segmented and parcellated according to the Desikan-Killiany atlas⁴⁴ in FreeSurfer (<http://surfer.nmr.mgh.harvard.edu>) at each site and according to standard ENIGMA quality control protocols (see <http://enigma.ini.usc.edu/protocols/imaging-protocols>). Sample sizes ranged from 1272 (ADHD) to 9572 (SCZ). We redirect the reader to the original publications^{10–15} for more details on age matching and controlling for medication or comorbidities. Ethics approval and subjects' informed consent was obtained by individual cohort investigators.

Population connectivity data

Functional and structural connectivity matrices were based on 1 h of rs-fMRI and diffusion MRI from healthy adults ($n = 207$, 83 males, mean age = 28.73 ± 3.73 years), respectively. The data were acquired through the HCP⁴⁵, minimally pre-processed according to HCP guidelines⁹⁹ and made publicly available as group-average structural and functional connectivity matrices in the ENIGMA Toolbox⁴³. See Supplementary Material for more information about the computation of connectivity matrices.

Structural covariance of disease effects on local brain structure

We derived a 68×68 cross-condition correlation matrix by computing inter-regional Pearson's correlations of cortical thickness Cohen's d values across the six conditions.

Covariance hubs and transdiagnostic disease epicenters

In order to derive co-alteration network hubs using a degree centrality approach, we first identified which connections (i.e., correlations) of the previously derived cross-condition correlation matrix belong to the top 20% of strong connections. We then computed the sum of these connections for each parcel, where regions with many strong connections represent hubs of high transdiagnostic covariance of illness effects (Fig. 2A). Next, we accessed whole-brain functional (rs-fMRI) and structural (DTI) connectivity matrices from a healthy adult HCP dataset⁴⁵ via the ENIGMA Toolbox⁴³, which we also thresholded at 80%. Normative connectivity hub maps based on HCP data was computed using the same degree centrality approach (i.e., the sum of all strong connections) and spatially correlated with the transdiagnostic structural co-alteration hub map. Significance was assessed via spin tests (see Supplementary Material and ref. [57]). This analysis aimed to assess whether co-alteration hub regions align with the normative underlying connectome and may thus be linked to nodal stress.

To identify transdiagnostic disease epicenters, we systematically assessed spatial similarity of each parcel's normative whole-brain connectivity profile with our map of co-alteration hubs using spatial

permutation tests. To do so, we collected seed-based functional (rs-fMRI) and structural (DTI) connectivity matrices for each parcel and 14 subcortical structures from the same HCP dataset⁴⁵. We then spatially correlated each structure's connectivity profile with the co-alteration hub map. The higher the spatial similarity between an epicenter's connectivity profile and co-alteration hubs, the more likely this structure represents a disease epicenter (at $p < 0.05$ after spin tests). Resulting likelihoods were ranked to identify the top five structural and functional transdiagnostic disease epicenters.

Gradient decomposition

We computed macroscale organizational gradients using BrainSpace⁴⁹ (<https://github.com/MICA-MNI/BrainSpace>) in Matlab 2020b. The 68×68 structural covariance matrix was thresholded at 80% and transformed into a non-negative square symmetric affinity matrix by using a normalized angle similarity kernel. We then applied diffusion mapping as a nonlinear dimensionality reduction method^{39,49} to estimate the low-dimensional embedding of our previously derived high-dimensional affinity matrix. Here, cortical nodes that are close together reflect nodes that are inter-connected by either many supra-threshold or few very strong edges, whereas nodes that are farther apart reflect little or no covariance. We set α , a parameter which controls the impact of sampling density (where 0–1 = maximal to no influence), to 0.5. This α value retains global relations in the low-dimensional space and is assumed to be comparatively robust to noise in the input matrix. Lastly, we assessed the amount of information explained by received gradients, selected the first two gradients for further analyses and projected them onto a cortical mesh using BrainStat (<https://github.com/MICA-MNI/BrainStat>).

Link to normative axes of cortical thickness organization

An association with normative cortical thickness organization was studied by correlating derived transdiagnostic gradients with previously established gradients of cortical thickness covariance in healthy adults. These two normative gradients were based on cortical thickness data from individuals in the S1200 HCP sample and were derived using the same diffusion embedding approach as described above (see ref. [36]). Spatial associations were evaluated using spin tests⁵⁷.

Cytoarchitectonic contextualization

To determine whether transdiagnostic gradients recapitulate cytoarchitectonic variation evidenced by post-mortem histological assessments, we further stratified our gradients according to the five von Economo-Koskinas cytoarchitectonic classes⁵¹. This atlas subdivides the cortex into five categories: agranular (thick cortex housing large cells but scarce layers II and IV), frontal (thick cortex, large but sparse cells, layers II and IV are present), parietal (thick cortex that is rich in cells, dense layers II and IV, slender pyramidal cells), polar (thin cortex, rich in cells, particularly granular cells) and granular/koni-cortex (very thin cortex with highest density of small cells).

Genetic decoding

Having established macro- and microscale contextualization of our findings, we finally aimed to understand its association with gene transcriptomic data provided by the Allen Institute for Brain Science (AIBS)⁵². Microarray expression data was processed in abagen¹⁰⁰, including intensity-based filtering, normalization and aggregation within Desikan-Killiany parcels and across donors. Only genes with a similarity of $r > 0.2$ across donors were included, resulting in 12,668 genes for the analysis⁴³. We correlated transdiagnostic gradients with the post-mortem gene expression maps and tested for spatial and gene specificity using several null models: First, we generated a set of random spatially autocorrelated phenotype maps⁵⁷ to test the spatial specificity of associations observed

between gene transcriptomic profiles and transdiagnostic gradients. Genes with an expression profile significantly correlated with G1 or G2 ($p_{\text{spin}} < 0.01$) were defined as gene set for following gene specificity tests. Next, using the Gene Annotation using Macroscale Brain-imaging Association (GAMBA) Toolbox⁵⁸, we tested this gene set against two types of null models: The null-coexpressed-gene model and the null-brain-gene model. The null-coexpressed-gene model includes genes with a similar co-expression level as the gene set of interest to generate null distributions. The null-brain-gene model generates null models exclusively from genes over-expressed in brain tissue and is thus more conservative than classical random-gene models. If a gene set was identified as significantly associated with a transdiagnostic gradient in both linear regressions and described permutation tests, it was next used as input for a developmental enrichment analysis via the cell-type specific expression analysis (CSEA) developmental expression tool (<http://genetics.wustl.edu/jdlab/csea-tool-2>)⁵⁹. This allowed us to compare genes identified with respect to the AIBS repository with developmental expression profiles from the BrainSpan dataset (<http://www.brainspan.org>), yielding more detailed, yet indirect, information about brain structures and developmental windows in which identified genes are enriched.

Functional decoding

To assess whether transdiagnostic gradients capture differential impact on cognitive networks, we assessed the distribution of various cognitive functions along transdiagnostic gradients^{35,53}. To this end, we conducted a meta-analysis using the NeuroSynth⁶⁰ database. Briefly, we derived 20 ROI maps by decomposing G1 and G2 into five-percentile bins and combining regions of the same bin to a joint ROI. The granularity of five-percentile bins is assumed to capture subtle variations along cortical axes. We then examined the association of each ROI with 24 cognitive topic terms via z-statistics. Topic terms were then sorted based on their center of gravity and arranged in a two-dimensional space that was created by merging G1 and G2, for visualization.

Association between disorder-specific illness effect patterns with transdiagnostic findings

Last, we aimed to understand the degree to which cortical alterations observed in individual disorders are reflected in described transdiagnostic features. To this end, we first examined cross-cortical similarities of illness effects within disorders^{101,102}, via absolute differences in Cohen's d values between regions. We then correlated each parcel's disorder-specific whole-brain covariance profile with the previously described transdiagnostic covariance profile of the same parcel. This allowed us to investigate disorder-specific cortical topographies of varying regional associations with transdiagnostic patterns. Second, we examined the similarity of illness effect maps among disorders via pair-wise correlations and applied hierarchical clustering to the resulting cross-disorder correlation matrix. These steps allowed us to investigate how disorders with varying similarity to each other and to transdiagnostic features described in this study are positioned in the proposed transdiagnostic covariance space. To this end, we correlated the transdiagnostic co-alteration hub map with disorder-specific Cohen's d maps, and computed disorder-specific epicenters by systematically correlating each region's normative connectivity profile (rs-fMRI and DTI) to disorder-specific Cohen's d maps. We then assessed the overlap between disorder-specific and transdiagnostic epicenters in percent, and combined this with the association to transdiagnostic hubs in a 2D space. Similarly, we examined the correlation between transdiagnostic gradients and disorder-specific Cohen's d maps in a 2D space framed by G1 and G2. Together, these analyses revealed

how individual disorders are embedded in relation to each other within a transdiagnostic coordinate frame.

Reporting summary

Further information on research design is available in the Nature Research Reporting Summary linked to this article.

Data availability

All data analyzed in this paper were obtained from open-access sources. Disorder-specific Cohen's d maps derived from ENIGMA meta-analyses were accessed via the ENIGMA Toolbox (v. 1.1.3; <https://enigma-toolbox.readthedocs.io/en/latest/>; ⁴³). Through the toolbox, we also accessed normative connectivity data from a Human Connectome Project young adult sample (HCP; <http://www.humanconnectome.org/>; ⁴⁵), the von Economo-Koskinas cytoarchitectonic atlas⁵¹, and gene transcriptomic data from the Allen human brain atlas (<https://human.brain-map.org/>) as accessible through Abagen (<https://doi.org/10.5281/zenodo.4984124>). The functional meta-analysis was based on the NeuroSynth database (<https://neurosynth.org/>). Developmental enrichment analyses were based on the Brainspan dataset (<https://www.brainspan.org/static/download.html>). Data generated for this study were made publicly available under https://github.com/CNG-LAB/cngopen/tree/main/transdiagnostic_gradients and <https://doi.org/10.5281/zenodo.7180120>. Raw imaging data supporting our findings are not publicly available as they contain information that could compromise the privacy of study participants. There are data sharing restrictions imposed by (i) ethical review boards of the participating sites, and consent documents; (ii) national and trans-national data sharing law, such as GDPR; and (iii) institutional processes, some of which require a signed MTA for limited and predefined data use. However, we welcome sharing data with researchers, requiring only that they submit an analysis plan for a secondary project to the leading team of the Working Group (<http://enigma.ini.usc.edu>). Once this analysis plan is approved, access to the relevant data will be provided contingent on data availability and local PI approval and compliance with all supervening regulations. If applicable, distribution of analysis protocols to sites will be facilitated. Source data are provided with this paper. Source data are provided with this paper (Supplementary Material). Source data are provided with this paper.

Code availability

Custom code generated for this project was made publicly available under https://github.com/CNG-LAB/cngopen/tree/main/transdiagnostic_gradients and <https://doi.org/10.5281/zenodo.7180120>. Our analysis code makes use of open software: Gradient mapping analyses were carried out using BrainSpace (v. 0.1.2; <https://brainspace.readthedocs.io/en/latest/>) and epicenters were computed using code from the ENIGMA Toolbox (v. 1.1.3; <https://enigma-toolbox.readthedocs.io/en/latest/>; ⁴³). Visualizations were carried out using BrainStat (v. 0.3.6; <https://github.com/MICA-MNI/BrainStat>) in combination with ColorBrewer (v. 1.0.0; <https://github.com/scottclowe/cbrewer2>). Genetic analyses were performed using the GAMBA Toolbox (2021; <https://github.com/dutchconnectomelab/GAMBA-MATLAB>) and the cell-specific enrichment analysis tool (v. 1.1; <http://genetics.wustl.edu/jdlab/csea-tool-2/>).

References

1. Dell'Osso, L., Lorenzi, P. & Carpita, B. The neurodevelopmental continuum towards a neurodevelopmental gradient hypothesis. *J. Psychopathol.* **25**, 179–182 (2019).
2. Insel, T. et al. Research Domain Criteria (RDoC): Toward a New Classification Framework for Research on Mental Disorders. *Am. J. Psychiatry* **167**, 748–751 (2010).
3. Wendt, F. R., Pathak, G. A., Tylee, D. S., Goswami, A. & Polimanti, R. Heterogeneity and Polygenicity in Psychiatric Disorders: A

- Genome-Wide Perspective. *Chronic Stress* **4**, 247054702092484 (2020).
4. Plana-Ripoll, O. et al. Exploring comorbidity within mental disorders among a Danish national population. *JAMA Psychiatry* **76**, 259–270 (2019).
 5. Paus, T., Keshavan, M. & Giedd, J. N. Why do many psychiatric disorders emerge during adolescence? *Nat. Rev. Neurosci.* **9**, 947–957 (2008).
 6. Lahey, B. B. et al. Is there a general factor of prevalent psychopathology during adulthood? *J. Abnorm. Psychol.* **121**, 971 (2012).
 7. Marshall, M. The hidden links between mental disorders. *Nature* **581**, 19–21 (2020).
 8. Pettersson, E., Larsson, H., D’Onofrio, B. M., Bolte, S. & Lichtenstein, P. The general factor of psychopathology: a comparison with the general factor of intelligence with respect to magnitude and predictive validity. *World Psychiatry* **19**, 206–213 (2020).
 9. Thompson, P. M. et al. ENIGMA and global neuroscience: a decade of large-scale studies of the brain in health and disease across more than 40 countries. *Transl. Psychiatry* **10**, 1–28 (2020).
 10. van Rooij, D. et al. Cortical and Subcortical Brain Morphometry Differences Between Patients With Autism Spectrum Disorder and Healthy Individuals Across the Lifespan: Results From the ENIGMA ASD Working Group. *Am. J. Psychiatry* **175**, 359–369 (2018).
 11. Hoogman, M. et al. Brain Imaging of the Cortex in ADHD: A Coordinated Analysis of Large-Scale Clinical and Population-Based Samples. *Am. J. Psychiatry* **176**, 531–542 (2019).
 12. Schmaal, L. et al. Cortical abnormalities in adults and adolescents with major depression based on brain scans from 20 cohorts worldwide in the ENIGMA Major Depressive Disorder Working Group. *Mol. Psychiatry* **22**, 900–909 (2017).
 13. van Erp, T. G. M. et al. Cortical Brain Abnormalities in 4474 Individuals With Schizophrenia and 5098 Control Subjects via the Enhancing Neuro Imaging Genetics Through Meta Analysis (ENIGMA) Consortium. *Biol. Psychiatry* **84**, 644–654 (2018).
 14. Hibar, D. P. et al. Cortical abnormalities in bipolar disorder: an MRI analysis of 6503 individuals from the ENIGMA Bipolar Disorder Working Group. *Mol. Psychiatry* **23**, 932–942 (2018).
 15. Boedhoe, P. S. W. et al. Cortical Abnormalities Associated With Pediatric and Adult Obsessive-Compulsive Disorder: Findings From the ENIGMA Obsessive-Compulsive Disorder Working Group. *Am. J. Psychiatry* **175**, 453–462 (2018).
 16. Natu, V. S. et al. Apparent thinning of human visual cortex during childhood is associated with myelination. *Proc. Natl Acad. Sci.* **116**, 20750 (2019).
 17. Cahalane, D. J., Charvet, C. J. & Finlay, B. L. Systematic, balancing gradients in neuron density and number across the primate isocortex. *Front. Neuroanat.* **6**, 28 (2012).
 18. Wagstyl, K., Ronan, L., Goodyer, I. M. & Fletcher, P. C. Cortical thickness gradients in structural hierarchies. *Neuroimage* **111**, 241–250 (2015).
 19. Opel, N. et al. Cross-Disorder Analysis of Brain Structural Abnormalities in Six Major Psychiatric Disorders: A Secondary Analysis of Mega- and Meta-analytical Findings From the ENIGMA Consortium. *Biol. Psychiatry* **88**, 678–686 (2020).
 20. Radonjic, N. V. et al. Structural brain imaging studies offer clues about the effects of the shared genetic etiology among neuropsychiatric disorders. *Mol. Psychiatry* <https://doi.org/10.1038/s41380-020-01002-z> (2021).
 21. Patel, Y. et al. Virtual Histology of Cortical Thickness and Shared Neurobiology in 6 Psychiatric Disorders. *JAMA Psychiatry* **78**, 47 (2021).
 22. Park, B. et al. Multilevel neural gradients reflect transdiagnostic effects of major psychiatric conditions on cortical morphology. 2021.10.29.466434 <https://www.biorxiv.org/content/10.1101/2021.10.29.466434v1> (2021) <https://doi.org/10.1101/2021.10.29.466434>.
 23. Menon, V. Large-scale brain networks and psychopathology: a unifying triple network model. *Trends Cogn. Sci.* **15**, 483–506 (2011).
 24. Cauda, F. et al. Brain structural alterations are distributed following functional, anatomic and genetic connectivity. *Brain* **141**, 3211–3232 (2018).
 25. Fornito, A., Zalesky, A. & Breakspear, M. The connectomics of brain disorders. *Nat. Rev. Neurosci.* **16**, 159–172 (2015).
 26. Crossley, N. A. et al. The hubs of the human connectome are generally implicated in the anatomy of brain disorders. *Brain* **137**, 2382–2395 (2014).
 27. Larivière, S. et al. Network-based atrophy modeling in the common epilepsies: A worldwide ENIGMA study. *Sci. Adv.* **6**, eabc6457 (2020).
 28. Vanasse, T. J. et al. Brain pathology recapitulates physiology: a network meta-analysis. *Commun. Biol.* **4**, 1–11 (2021).
 29. Cauda, F. et al. The morphometric co-atrophy networking of schizophrenia, autistic and obsessive spectrum disorders. *Hum. Brain Mapp.* **39**, 1898–1928 (2018).
 30. Raznahan, A. et al. Patterns of Coordinated Anatomical Change in Human Cortical Development: A Longitudinal Neuroimaging Study of Maturation Coupling. *Neuron* **72**, 873–884 (2011).
 31. Chen, C.-H. et al. Genetic topography of brain morphology. *Proc. Natl Acad. Sci.* **110**, 17089–17094 (2013).
 32. Alexander-Bloch, A. F. et al. Human Cortical Thickness Organized into Genetically-determined Communities across Spatial Resolutions. *Cereb. Cortex* **29**, 106–118 (2019).
 33. Wannan, C. M. J. et al. Evidence for Network-Based Cortical Thickness Reductions in Schizophrenia. *Am. J. Psychiatry* **176**, 552–563 (2019).
 34. Seeley, W. W., Crawford, R. K., Zhou, J., Miller, B. L. & Greicius, M. D. Neurodegenerative Diseases Target Large-Scale Human Brain Networks. *Neuron* **62**, 42–52 (2009).
 35. Margulies, D. S. et al. Situating the default-mode network along a principal gradient of macroscale cortical organization. *Proc. Natl Acad. Sci.* **113**, 12574–12579 (2016).
 36. Valk, S. L. et al. Shaping brain structure: Genetic and phylogenetic axes of macroscale organization of cortical thickness. *Sci. Adv.* **6**, eabb3417 (2020).
 37. Paquola, C. et al. A multi-scale cortical wiring space links cellular architecture and functional dynamics in the human brain. *PLOS Biol.* **18**, e3000979 (2020).
 38. Burt, J. B. et al. Hierarchy of transcriptomic specialization across human cortex captured by structural neuroimaging topography. *Nat. Neurosci.* **21**, 1251–1259 (2018).
 39. Coifman, R. R. & Lafon, S. Diffusion maps. *Appl. Comput. Harmon. Anal.* **21**, 5–30 (2006).
 40. Hong, S.-J., Valk, S. L., Di Martino, A., Milham, M. P. & Bernhardt, B. C. Multidimensional Neuroanatomical Subtyping of Autism Spectrum Disorder. *Cereb. Cortex* **28**, 3578–3588 (2018).
 41. Dong, D. et al. Compression of Cerebellar Functional Gradients in Schizophrenia. *Schizophr. Bull.* <https://doi.org/10.1093/schbul/sbaa016> (2020).
 42. Park, B. et al. Differences in subcortico-cortical interactions identified from connectome and microcircuit models in autism. *Nat. Commun.* **12**, 2225 (2021).
 43. Larivière, S. et al. The ENIGMA Toolbox: multiscale neural contextualization of multisite neuroimaging datasets. *Nat. Methods* **18**, 698–700 (2021).
 44. Desikan, R. S. et al. An automated labeling system for subdividing the human cerebral cortex on MRI scans into gyral based regions of interest. *Neuroimage* **31**, 968–980 (2006).

45. Van Essen, D. C. et al. The Human Connectome Project: a data acquisition perspective. *Neuroimage* **62**, 2222–2231 (2012).
46. Zhou, J., Gennatas, E. D., Kramer, J. H., Miller, B. L. & Seeley, W. W. Predicting regional neurodegeneration from the healthy brain functional connectome. *Neuron* **73**, 1216–1227 (2012).
47. Shafiei, G. et al. Spatial Patterning of Tissue Volume Loss in Schizophrenia Reflects Brain Network Architecture. *Biol. Psychiatry* **87**, 727–735 (2020).
48. van den Heuvel, M. P., Kahn, R. S., Goñi, J. & Sporns, O. High-cost, high-capacity backbone for global brain communication. *Proc. Natl Acad. Sci. U. S. A* **109**, 11372–11377 (2012).
49. Vos de Wael, R. et al. BrainSpace: a toolbox for the analysis of macroscale gradients in neuroimaging and connectomics datasets. *Commun. Biol.* **3**, 103 (2020).
50. Romer, A. L. et al. Pervasively Thinner Neocortex as a Transdiagnostic Feature of General Psychopathology. *Am. J. Psychiatry* **178**, 174–182 (2021).
51. Triarhou, L. C. The Economo-Koskinas atlas revisited: cytoarchitectonics and functional context. *Stereotact. Funct. Neurosurg.* **85**, 195–203 (2007).
52. Hawrylycz, M. et al. Canonical genetic signatures of the adult human brain. *Nat. Neurosci.* **18**, 1832 (2015).
53. Paquola, C. et al. Shifts in myeloarchitecture characterise adolescent development of cortical gradients. *eLife* **8**, e50482 (2019).
54. Bertolero, M. A. et al. The human brain's network architecture is genetically encoded by modular pleiotropy. *ArXiv Prepr. ArXiv190507606* (2019).
55. Altmann, A. et al. A systems-level analysis highlights microglial activation as a modifying factor in common epilepsies. *Neuropathol. Appl. Neurobiol.* **48**, e12758 (2022).
56. Fornito, A., Arnatkevičiūtė, A. & Fulcher, B. D. Bridging the gap between connectome and transcriptome. *Trends Cogn. Sci.* **23**, 34–50 (2019).
57. Alexander-Bloch, A. F. et al. On testing for spatial correspondence between maps of human brain structure and function. *Neuroimage* **178**, 540–551 (2018).
58. Wei, Y. et al. Statistical testing in transcriptomic-neuroimaging studies: a how-to and evaluation of methods assessing spatial and gene specificity. *Hum. Brain Mapp.* **43**, 885–901 (2022).
59. Dougherty, J. D., Schmidt, E. F., Nakajima, M. & Heintz, N. Analytical approaches to RNA profiling data for the identification of genes enriched in specific cells. *Nucleic Acids Res.* **38**, 4218–4230 (2010).
60. Yarkoni, T., Poldrack, R. A., Nichols, T. E., Van Essen, D. C. & Wager, T. D. Large-scale automated synthesis of human functional neuroimaging data. *Nat. Methods* **8**, 665–670 (2011).
61. Buckner, R. L. et al. Cortical hubs revealed by intrinsic functional connectivity: mapping, assessment of stability, and relation to Alzheimer's disease. *J. Neurosci.* **29**, 1860–1873 (2009).
62. Volz, H.-P. et al. Reduced phosphodiesterases and high-energy phosphates in the frontal lobe of schizophrenic patients: a 31P chemical shift spectroscopic-imaging study. *Biol. Psychiatry* **47**, 954–961 (2000).
63. Mohamed, M. A. & Sheikh, A. S. F. Magnetic resonance spectroscopy in major depressive disorder. *Int J. Emerg. Ment. Health* **17**, 167–187 (2015).
64. Zuccoli, G. S., Saia-Cereda, V. M., Nascimento, J. M. & Martins-de-Souza, D. The energy metabolism dysfunction in psychiatric disorders postmortem brains: focus on proteomic evidence. *Front. Neurosci.* **11**, 493 (2017).
65. Arnatkevičiūtė, A. et al. Genetic influences on hub connectivity of the human connectome. *Nat. Commun.* **12**, 1–14 (2021).
66. Cioli, C., Abdi, H., Beaton, D., Burnod, Y. & Mesmoudi, S. Differences in human cortical gene expression match the temporal properties of large-scale functional networks. *PLoS ONE* **9**, e115913 (2014).
67. Suárez, L. E., Markello, R. D., Betzel, R. F. & Misisic, B. Linking Structure and Function in Macroscale Brain Networks. *Trends Cogn. Sci.* **24**, 302–315 (2020).
68. Damoiseaux, J. S. & Greicius, M. D. Greater than the sum of its parts: a review of studies combining structural connectivity and resting-state functional connectivity. *Brain Struct. Funct.* **213**, 525–533 (2009).
69. Honey, C. J. et al. Predicting human resting-state functional connectivity from structural connectivity. *Proc. Natl Acad. Sci.* **106**, 2035–2040 (2009).
70. Wang, Y. et al. Long-range connections mirror and link micro-architectural and cognitive hierarchies in the human brain. 2021.10.25.465692 <https://www.biorxiv.org/content/10.1101/2021.10.25.465692v1> (2021) <https://doi.org/10.1101/2021.10.25.465692>.
71. Hiser, J. & Koenigs, M. The Multifaceted Role of the Ventromedial Prefrontal Cortex in Emotion, Decision Making, Social Cognition, and Psychopathology. *Biol. Psychiatry* **83**, 638–647 (2018).
72. Takei, Y. et al. Temporal lobe and inferior frontal gyrus dysfunction in patients with schizophrenia during face-to-face conversation: A near-infrared spectroscopy study. *J. Psychiatr. Res.* **47**, 1581–1589 (2013).
73. Sydnor, V. J. et al. Neurodevelopment of the association cortices: Patterns, mechanisms, and implications for psychopathology. *Neuron* **109**, 2820–2846 (2021).
74. Valk, S. L., Di Martino, A., Milham, M. P. & Bernhardt, B. C. Multi-center mapping of structural network alterations in autism. *Hum. Brain Mapp.* **36**, 2364–2373 (2015).
75. Wang, S.-H., Kloth, D. & Badura, A. The Cerebellum, Sensitive Periods, and Autism. *Neuron* **83**, 518–532 (2014).
76. Hwang, K., Bertolero, M. A., Liu, W. B. & D'Esposito, M. The Human Thalamus Is an Integrative Hub for Functional Brain Networks. *J. Neurosci.* **37**, 5594–5607 (2017).
77. Krol, A., Wimmer, R. D., Halassa, M. M. & Feng, G. Thalamic Reticular Dysfunction as a Circuit Endophenotype in Neurodevelopmental Disorders. *Neuron* **98**, 282–295 (2018).
78. Wang, Z. G. et al. Community-informed connectomics of the thalamocortical system in generalized epilepsy. *Neurology* **93**, E1112–E1122 (2019).
79. Romer, A. L. et al. Structural alterations within cerebellar circuitry are associated with general liability for common mental disorders. *Mol. Psychiatry* **23**, 1084–1090 (2018).
80. Hariri, A. R. The Emerging Importance of the Cerebellum in Broad Risk for Psychopathology. *Neuron* **102**, 17–20 (2019).
81. Llorca, A. et al. A stochastic framework of neurogenesis underlies the assembly of neocortical cytoarchitecture. *eLife* **8**, e51381 (2019).
82. Javitt, D. C. When doors of perception close: bottom-up models of disrupted cognition in schizophrenia. *Annu. Rev. Clin. Psychol.* **5**, 249–275 (2009).
83. Robertson, C. E. & Baron-Cohen, S. Sensory perception in autism. *Nat. Rev. Neurosci.* **18**, 671–684 (2017).
84. de Gelder, B. et al. Multisensory integration of emotional faces and voices in schizophrenics. *Schizophr. Res.* **72**, 195–203 (2005).
85. Goodkind, M. et al. Identification of a common neurobiological substrate for mental illness. *JAMA Psychiatry* **72**, 305–315 (2015).
86. Etkin, A., Gyurak, A. & O'Hara, R. A neurobiological approach to the cognitive deficits of psychiatric disorders. *Dialogues Clin. Neurosci.* **15**, 419 (2013).
87. Depp, C. A. et al. Meta-analysis of the association between cognitive abilities and everyday functioning in bipolar disorder. *Bipolar Disord.* **14**, 217–226 (2012).

88. Harvey, P. D. & Strassnig, M. Predicting the severity of everyday functional disability in people with schizophrenia: cognitive deficits, functional capacity, symptoms, and health status. *World Psychiatry* **11**, 73–79 (2012).
89. Ouyang, M., Kang, H., Detre, J. A., Roberts, T. P. L. & Huang, H. Short-range connections in the developmental connectome during typical and atypical brain maturation. *Neurosci. Biobehav. Rev.* **83**, 109–122 (2017).
90. Valk, S. et al. Shaping brain structure: genetic and phylogenetic axes of macroscale organization of cortical thickness. *Sci. Adv.* **6**, eabb3417 (2020).
91. Zhu, Y. et al. Spatiotemporal transcriptomic divergence across human and macaque brain development. *Science* **362**, eaat8077 (2018).
92. Baum, G.L. et al. Graded Variation in T1w/T2w Ratio during Adolescence: Measurement, Caveats, and Implications for Development of Cortical Myelin. *J Neurosci* **42**, 5681–5694 (2022).
93. Bryce, N. V. et al. Brain parcellation selection: an overlooked decision point with meaningful effects on individual differences in resting-state functional connectivity. *NeuroImage* **243**, 118487 (2021).
94. Eshaghzadeh Torbati, M. et al. A multi-scanner neuroimaging data harmonization using RAVEL and ComBat. *NeuroImage* **245**, 118703 (2021).
95. Chen, A.A. et al. Mitigating site effects in covariance for machine learning in neuroimaging data. *Hum. Brain Mapp.* **43**, 1179–1195 (2022).
96. Cross-Disorder Group of the Psychiatric Genomics Consortium. Genomic relationships, novel loci, and pleiotropic mechanisms across eight psychiatric disorders. *Cell* **179**, 1469–1482 (2019).
97. Di Martino, A. et al. The autism brain imaging data exchange: towards a large-scale evaluation of the intrinsic brain architecture in autism. *Mol. Psychiatry* **19**, 659–667 (2014).
98. Misaki, M., Wallace, G. L., Dankner, N., Martin, A. & Bandettini, P. A. Characteristic cortical thickness patterns in adolescents with autism spectrum disorders: Interactions with age and intellectual ability revealed by canonical correlation analysis. *NeuroImage* **60**, 1890–1901 (2012).
99. Glasser, M. F. et al. The minimal preprocessing pipelines for the Human Connectome Project. *Neuroimage* **80**, 105–124 (2013).
100. Arnatkevičiūtė, A., Fulcher, B. D. & Fornito, A. A practical guide to linking brain-wide gene expression and neuroimaging data. *Neuroimage* **189**, 353–367 (2019).
101. Sha, Z. et al. Subtly altered topological asymmetry of brain structural covariance networks in autism spectrum disorder across 43 datasets from the ENIGMA consortium. *Mol. Psychiatry* **27**, 2114–2125 (2022).
102. Huntenburg, J. M. et al. A Systematic Relationship Between Functional Connectivity and Intracortical Myelin in the Human Cerebral Cortex. *Cereb. Cortex N. Y. N.* **1991** **27**, 981–997 (2017).

Acknowledgements

Many scientists around the world contributed to ENIGMA but did not take part in the writing of this report. A full list of contributors to ENIGMA is available at <http://enigma.ini.usc.edu/about-2/consortium/members/>. The authors would like to express their gratitude to the open science initiatives that made this work possible: (i) the ENIGMA Consortium (core funding for ENIGMA was provided by the NIH Big Data to Knowledge (BD2K) program under consortium grant U54 EB020403 to P.M.T.), (ii)

The Allen Human Brain Atlas and the abagen toolbox (<https://doi.org/10.5281/zenodo.4984124>), and (iii) the Human Connectome Project (principal investigators David Van Essen and Kamil Ugurbil; U54 MH091657), funded by the 16 NIH institutes and centers that support the NIH Blueprint for Neuroscience Research and by the McDonnell Center for Systems Neuroscience at Washington University. MDH was funded by the German Federal Ministry of Education and Research (BMBF) and the Max Planck Society. S.L. acknowledges funding from Fonds de la Recherche du Québec – Santé (FRQ-S) and the Canadian Institutes of Health Research (CIHR). B.Y.P. was funded by the National Research Foundation of Korea (NRF-2021R1F1A1052303; NRF-2022R1A5A7033499), Institute for Information and Communications Technology Planning and Evaluation (IITP) funded by the Korea Government (MSIT) (No. 2022-O-00448, Deep Total Recall: Continual Learning for Human-Like Recall of Artificial Neural Networks; No. 2020-O-01389, Artificial Intelligence Convergence Research Center (Inha University); No. RS-2022-00155915, Artificial Intelligence Convergence Innovation Human Resources Development (Inha University); No. 2021-O-02068, Artificial Intelligence Innovation Hub), and Institute for Basic Science (IBS-R015-D1). M.H. is supported by a personal Veni grant from the Netherlands Organization for Scientific Research (NWO, grant number 91619115). J.B. is supported by the EU-AIMS (European Autism Interventions) and AIMS-2-TRIALS programmes which receive support from Innovative Medicines Initiative Joint Undertaking Grant No. 115300 and 777394, the resources of which are composed of financial contributions from the European Union's FP7 and Horizon2020 Programmes, and from the European Federation of Pharmaceutical Industries and Associations (EFPIA) companies' in-kind contributions, and AUTISM SPEAKS, Autistica and SFARI; and by the Horizon2020 supported programme CANDY Grant No. 847818). B.B. acknowledges research funding from the SickKids Foundation (N17-039), the Natural Sciences and Engineering Research Council of Canada (NSERC; Discovery-1304413), CIHR (FDN-154298, PJT-174995), the Azrieli Center for Autism Research (ACAR), an MNI-Cambridge collaboration grant, salary support from FRQ-S (Chercheur-Boursier), Brain-Canada, the Helmholtz International BigBrain Analytics and Learning Laboratory (Hiball) and the Canada Research Chairs (CRC) Program. S.L.V. was supported by the Max Planck Society through the Otto Hahn Award and the Helmholtz International BigBrain Analytics and Learning Laboratory (Hiball).

Author contributions

The authors confirm contribution to the paper as follows: Study conception and design: M.D.H., S.L.V.; Data collection: O.A.C.D.H., L.S., O.A.A., C.R.K.C., M.H., K.B., D.V.R., D.J.V., D.J.S., B.F., T.G.M.V.E., N.J., P.M.T., S.I.T., ENIGMA ADHD Working Group, ENIGMA Autism Working Group, ENIGMA Bipolar Disorder Working Group, ENIGMA Major Depression Working Group, ENIGMA OCD Working Group, ENIGMA Schizophrenia Working Group; Analysis and interpretation of results: M.D.H., S.L.V.; Draft paper preparation: M.D.H., S.L.V.; Draft paper revision: M.D.H., S.B.E., B.C.B., P.M.T., S.I.T., R.A.I.B., S.L., B.Y.P., S.L.V.; All authors reviewed the results and approved the final version of the paper.

Funding

Open Access funding enabled and organized by Projekt DEAL.

Competing interests

O.A.A. received speaker's honorarium from Lundbeck and Sunovion, Consultant to HealthLytix. Jan Buitelaar has been a consultant to/member of advisory board of and/or speaker for Takeda/Shire, Roche, Medice, Angelini, Janssen, and Servier. P.M.T. received grant support from Biogen, Inc., and consulting payments from Kairos Venture Capital, for work unrelated to the current paper. Other authors declare no competing interests.

Additional information

Supplementary information The online version contains supplementary material available at <https://doi.org/10.1038/s41467-022-34367-6>.

Correspondence and requests for materials should be addressed to M. D. Hettwer or S. L. Valk.

Peer review information *Nature Communications* thanks Wei Liao and the other, anonymous, reviewer(s) for their contribution to the peer review of this work. Peer reviewer reports are available.

Reprints and permissions information is available at <http://www.nature.com/reprints>

Publisher's note Springer Nature remains neutral with regard to jurisdictional claims in published maps and institutional affiliations.

Open Access This article is licensed under a Creative Commons Attribution 4.0 International License, which permits use, sharing, adaptation, distribution and reproduction in any medium or format, as long as you give appropriate credit to the original author(s) and the source, provide a link to the Creative Commons license, and indicate if changes were made. The images or other third party material in this article are included in the article's Creative Commons license, unless indicated otherwise in a credit line to the material. If material is not included in the article's Creative Commons license and your intended use is not permitted by statutory regulation or exceeds the permitted use, you will need to obtain permission directly from the copyright holder. To view a copy of this license, visit <http://creativecommons.org/licenses/by/4.0/>.

© The Author(s) 2022

M.D. Hettwer^{1,2,3,4}✉, S. Larivière⁵, B. Y. Park^{6,5,6,7}, O. A. van den Heuvel⁸, L. Schmaal^{9,10}, O. A. Andreassen¹¹, C. R. K. Ching¹², M. Hoogman¹³, J. Buitelaar¹⁴, D. van Rooij¹⁴, D. J. Veltman⁸, D. J. Stein¹⁵, B. Franke¹³, T. G. M. van Erp^{16,17}, ENIGMA ADHD Working Group*, ENIGMA Autism Working Group*, ENIGMA Bipolar Disorder Working Group*, ENIGMA Major Depression Working Group*, ENIGMA OCD Working Group*, ENIGMA Schizophrenia Working Group*, N. Jahanshad¹², P. M. Thompson¹², S. I. Thomopoulos¹², R. A. I. Bethlehem^{18,19}, B. C. Bernhardt⁵, S. B. Eickhoff^{1,3} & S. L. Valk^{1,3,4}✉

¹Institute of Systems Neuroscience, Medical Faculty, Heinrich Heine University Düsseldorf, Düsseldorf, Germany. ²Max Planck School of Cognition, Max Planck Institute for Human Cognitive and Brain Sciences, Leipzig, Germany. ³Institute of Neuroscience and Medicine, Brain & Behavior (INM-7), Research Centre Jülich, Jülich, Germany. ⁴Max Planck Institute for Human Cognitive and Brain Sciences, Leipzig, Germany. ⁵Multimodal Imaging and Connectome Analysis Lab, McConnell Brain Imaging Centre, Montreal Neurological Institute, McGill University, Montreal, QC, Canada. ⁶Department of Data Science, Inha University, Incheon, Republic of Korea. ⁷Center for Neuroscience Imaging Research, Institute for Basic Science, Suwon, Republic of Korea. ⁸Amsterdam UMC, Vrije Universiteit Amsterdam, Department of Anatomy and Neuroscience and Psychiatry, Amsterdam Neuroscience, Amsterdam, The Netherlands. ⁹Centre for Youth Mental Health, The University of Melbourne, Melbourne, VIC, Australia. ¹⁰Orygen, Parkville, VIC, Australia. ¹¹NORMENT Centre, Division of Mental Health and Addiction, University of Oslo and Oslo University Hospital, Oslo, Norway. ¹²Imaging Genetics Center, Mark & Mary Stevens Neuroimaging and Informatics Institute, Keck School of Medicine, University of Southern California, Marina del Rey, CA, USA. ¹³Departments of Psychiatry and Human Genetics, Donders Institute for Brain, Cognition and Behaviour, Radboud University Medical Center, Nijmegen, The Netherlands. ¹⁴Department of Cognitive Neuroscience, Donders Institute for Brain, Cognition and Behaviour, Radboud University Medical Center, Nijmegen, The Netherlands. ¹⁵South African Medical Research Council Unit on Risk & Resilience in Mental Disorders, Department of Psychiatry & Neuroscience Institute, University of Cape Town, Cape Town, South Africa. ¹⁶Clinical Translational Neuroscience Laboratory, Department of Psychiatry and Human Behavior, University of California Irvine, Irvine Hall, Irvine, CA, USA. ¹⁷Center for the Neurobiology of Learning and Memory, University of California Irvine, Irvine, CA, USA. ¹⁸Autism Research Centre, Department of Psychiatry, University of Cambridge, Cambridge, UK. ¹⁹Brain Mapping Unit, Department of Psychiatry, University of Cambridge, Cambridge, UK. *Lists of authors and their affiliations appear at the end of the paper ✉e-mail: m.hettwer@fz-juelich.de; s.valk@fz-juelich.de

ENIGMA ADHD Working Group

M. Hoogman¹³ & B. Franke¹³

ENIGMA Autism Working Group

J. Buitelaar¹⁴ & D. van Rooij¹⁴

ENIGMA Bipolar Disorder Working Group

O. A. Andreassen¹¹ & C. R. K. Ching¹²

ENIGMA Major Depression Working Group

D. J. Veltman⁸ & L. Schmaal^{9,10}

ENIGMA OCD Working Group

O. A. van den Heuvel⁸ & D. J. Stein ¹⁵

ENIGMA Schizophrenia Working Group

T. G. M. van Erp^{16,17}

5.2 Study 2: Longitudinal variation in resilient psychosocial functioning is associated with ongoing cortical myelination and functional reorganization during adolescence

Hettwer, M. D., Dorfschmidt, L., Puhlmann, L., Jacob, L. M., Paquola, C., Bethlehem, R. A., NSPN Consortium, Bullmore, E. T., Eickhoff, S. B., Valk, S. L. (2024). Longitudinal variation in resilient psychosocial functioning is associated with ongoing cortical myelination and functional reorganization during adolescence. *Nature Communications*, 15(1), 1-15.

Impact Factor (2023): 14.7

5-year Impact Factor (2023): 16.1

This is an open access article licensed under a Creative Commons Attribution 4.0 International License (<https://creativecommons.org/licenses/by/4.0/>).

Authorship Attribution Statement


I designed the study, analyzed the data, prepared the figures, interpreted the findings, and wrote the drafts of the manuscript under the supervision of S. L. Valk and S. B. Eickhoff. Data was acquired by the NSPN Consortium headed by E. T. Bullmore and processed by L. Dorfschmidt, R. A. Bethlehem, and me. All authors reviewed the results and revised and approved the final version of the attached paper.

Longitudinal variation in resilient psychosocial functioning is associated with ongoing cortical myelination and functional reorganization during adolescence

Received: 9 February 2024

Accepted: 3 July 2024

Published online: 29 July 2024

 Check for updates

Meike D. Hettwer^{1,2,3,4}✉, Lena Dorfschmidt^{5,6,7}, Lara M. C. Puhlmann^{4,8}, Linda M. Jacob⁴, Casey Paquola¹, Richard A. I. Bethlehem⁹, NSPN Consortium*, Edward T. Bullmore⁵, Simon B. Eickhoff^{1,2,3} & Sofie L. Valk^{1,2,3,4}✉

Adolescence is a period of dynamic brain remodeling and susceptibility to psychiatric risk factors, mediated by the protracted consolidation of association cortices. Here, we investigated whether longitudinal variation in adolescents' resilience to psychosocial stressors during this vulnerable period is associated with ongoing myeloarchitectural maturation and consolidation of functional networks. We used repeated myelin-sensitive Magnetic Transfer (MT) and resting-state functional neuroimaging ($n = 141$), and captured adversity exposure by adverse life events, dysfunctional family settings, and socio-economic status at two timepoints, one to two years apart. Development toward more resilient psychosocial functioning was associated with increasing myelination in the anterolateral prefrontal cortex, which showed stabilized functional connectivity. Studying depth-specific intracortical MT profiles and the cortex-wide synchronization of myeloarchitectural maturation, we further observed wide-spread myeloarchitectural reconfiguration of association cortices paralleled by attenuated functional reorganization with increasingly resilient outcomes. Together, resilient/susceptible psychosocial functioning showed considerable intra-individual change associated with multi-modal cortical refinement processes at the local and system-level.

Adolescence is a period of pronounced brain remodeling that mediates biological and psychosocial maturation, but also heightened susceptibility to environmental adversity that may influence developmental trajectories^{1,2}. The study of longitudinal trajectories in the

presence of adversity exposure³ and psychiatric symptoms^{2,4,5} has thus been fundamental to advancing our understanding of inter- and intra-individual differences in psychiatric susceptibility. At the same time, there is a growing recognition that many individuals maintain good

¹Institute of Neuroscience and Medicine, Brain & Behavior (INM-7), Research Centre Jülich, Jülich, Germany. ²Max Planck School of Cognition, Leipzig, Germany. ³Institute of Systems Neuroscience, Medical Faculty and University Hospital Düsseldorf, Heinrich Heine University Düsseldorf, Düsseldorf, Germany. ⁴Max Planck Institute for Human Cognitive and Brain Sciences, Leipzig, Germany. ⁵Department of Psychiatry, University of Cambridge, Cambridge, UK. ⁶Lifespan Brain Institute, The Children's Hospital of Philadelphia and Penn Medicine, Philadelphia, PA, USA. ⁷Department of Child and Adolescent Psychiatry and Behavioral Sciences, Children's Hospital of Philadelphia, Philadelphia, PA, USA. ⁸Leibniz Institute for Resilience Research, Mainz, Germany. ⁹Department of Psychology, University of Cambridge, Cambridge, UK. *A list of authors and their affiliations appears at the end of the paper. ✉e-mail: m.hettwer@fz-juelich.de; valk@cbs.mpg.de

mental well-being despite adversity, i.e., show resilient adaptation^{6–8}. To comprehend bio-behavioral adaptation to an ever-changing environment, it has been vital to integrate neurodevelopmental assessments, complementary to inter-personal and physiological factors. Converging evidence from cross-sectional studies has highlighted brain regions involved in emotion regulation and stress reactivity in relation to adolescent susceptibility or resilience to environmental adversity. Specifically, resilient adaptation has been linked to larger prefrontal and hippocampal volumes, increased prefrontal regulation of amygdala activity, attenuated amygdala responses to adverse stimuli, and increased structural connectivity of the corpus callosum^{9,10}. In the past decade, however, psychosocial conceptualizations have increasingly highlighted the dynamic nature of resilience^{7,9,11–14}. Correspondingly, the ability to adapt to environmental adversity may show considerable intra-individual changes tied to plastic neurodevelopment. However, longitudinal studies exploring this notion, especially during periods of heightened susceptibility to psychopathology, remain scarce^{1,9,15}.

Insights into adolescent brain development have recently expanded from analyses of cortical size metrics (such as volume and thickness) to more fine-grained proxies of intra-cortical myelin maturation^{5,16,17}. This line of research highlights the continuous myelination of intra- and inter-regional connections, enhancing circuit efficiency as a central feature of adolescent cortical maturation^{18,19}. While myelination restricts structural plasticity by consolidating established connections, it has also been found to continuously modulate network dynamics to adapt to ever-changing environmental circumstances^{19,20}. Rates of myelin maturation are heterochronous across the cortex and are particularly protracted in highly interconnected association cortices^{16,21,22}. This protracted maturation, implying longer periods of developmental plasticity, likely reflects later refinement of functional networks associated with abstract cognitive functions, such as cognitive control. However, it also renders them more susceptible to environmental impact and psychopathological alterations^{16,21,22}. Thus, the dual role of myelin in structural consolidation and dynamic functional adaptation makes the study of ongoing adolescent myelination a compelling focus to address the question of whether the maturation of behavioral capacities for psychosocial adaptation is tied to ongoing cortical consolidation.

Recent advances in *in vivo* imaging of cortical myelin have improved our understanding of myeloarchitectural maturation. One promising imaging contrast is magnetic transfer saturation (MT)²³, which is dominated by myelin-related molecules in the brain, as has been confirmed by several histological validation studies^{24–26}. It has also been demonstrated to be sensitive to both developmental processes^{5,16,17} and pathological alterations in myelin content²⁷. Aiming at more nuanced insights into age-related changes in intracortical myeloarchitecture, several studies have sampled myelin-proxies across intra-cortical depths perpendicular to the cortical mantle, commonly referred to as “cortical profiling”^{5,16}. Such depth-dependent profiling allows analysis of synchronized, large-scale patterns of cortical myeloarchitectural development by quantifying changes in inter-regional similarities (microstructural profile covariance; MPC). Previous work suggests that microstructural similarity predicts cortico-cortical connectivity^{28,29}. Thus, studying changes in MPC with age yields valuable insights into system-level microstructural integration and differentiation, and its potential link to functional reorganization^{30,31}. Association areas, in particular, represent a nexus of mixed intra-cortical profiles^{32,33} that show marked and partly synchronized refinement well into early adulthood¹⁶. This microstructural refinement may be central to supporting the maturation of the intrinsic functional organization of the default and frontal parietal networks, supporting continued cognitive development of functions such as cognitive control and emotional flexibility^{34,35}. In sum, leveraging multi-modal, system-level approaches is imperative to unravel

the complex role of cortical refinement in mental health and aligns with the broader understanding that maturational and psychopathological cortical alterations occur in a network-like fashion^{36,37}.

Together, previous research suggests that (1) understanding the development of psychosocial resilience requires complementary longitudinal studies, (2) the protracted consolidation of association cortices by myelination throughout adolescence likely confers increased susceptibility to adverse environmental influences, and (3) *in vivo* myelin mapping has facilitated multi-modal and multi-scale insights into cortical development. On this basis, the current study investigated whether intra-individual change in susceptibility and resilience to environmental adversity exposure is tied to differential rates of local and global myeloarchitectural consolidation, and accompanying functional maturation during adolescence and young adulthood (age range: 14–26 yrs). Environmental stressors included dysfunctional family environments, significant adverse life events, and low socioeconomic status, at two consecutive time points, one to two years apart. For each time point, we quantified a continuous resilient psychosocial functioning (RES_{PSF}) score, reflecting psychosocial functioning adjusted for individual stressor exposure. That is, RES_{PSF} scores reflect residual variance in psychosocial distress that is not explained by the normative response to the stressor load an individual faced^{7,38}. Thus, lower-than-expected distress reflects resilient adaptation, whereas higher-than-expected distress reflects greater susceptibility to environmental stressors³⁸. We then investigated associations between intra-individual changes in resilient psychosocial functioning and brain maturation, specifically focusing on the role of ongoing myelination^{18,21} and the impact on intrinsic function. We observed that longitudinal development towards more susceptible or resilient outcomes was associated with differential rates of prefrontal myelination, prefrontal functional network maturation, and cortex-wide myeloarchitectural reorganization of association cortices. Thus, extending cross-sectional studies suggesting increased susceptibility of association cortices to environmental impact^{16,21,22}, we conclude that adolescent cortical maturation of areas typically implicated in psychopathology is tied to dynamic intra-individual changes in psychosocial functioning relative to adversity.

Results

Resilient psychosocial functioning (RES_{PSF}) scores (Fig. 1)

We quantified continuous RES_{PSF} scores by predicting psychosocial distress from measures of environmental adversity (Fig. 1A). Briefly, we derived a latent factor (Supplementary Table S1; $\chi^2 = 34293$, $p < 0.001$), reflecting levels of psychosocial distress across domains of anxiety, depression, antisocial and compulsive-obsessive behavior, self-esteem, psychotic-like experiences, and mental well-being (similar to refs. 38,39). In a supervised random forest prediction, we then predicted psychosocial distress scores from adverse life events, childhood trauma, parenting style, family situation, and socioeconomic status ($R^2 = 0.21$, MAE = 15.15, correlation between true and predicted distress scores: $r = 0.46$). The inverse deviations between true and predicted distress, i.e., the model residuals, were extracted to quantify resilient psychosocial functioning. RES_{PSF} scores thus reflect a spectrum ranging from susceptible to resilient outcomes, i.e., the extent to which an individual shows higher or lower distress levels than expected given their stressor exposure (for similar approaches, see refs. 38,40–43). For parsimony, we will refer to this spectrum as resilient psychosocial functioning, which shall include the susceptible (negative) end of the spectrum. See Supplementary Table S2 for links to demographic data.

Different sub-samples were included across analyses in this study (Fig. 1A; see Supplementary Methods for details): The computation of distress score loadings ($n = 1533$) and the prediction from adversity measures ($n = 712$; subsample with additional NSPN U-change questionnaires) were conducted in independent samples to avoid leakage

effects. From the $n = 712$ sub-sample, we studied general patterns of MT maturation in $n = 199$ for whom longitudinal imaging data were available. We then linked longitudinal imaging patterns to change in resilient psychosocial functioning in $n = 141$ individuals who additionally completed all included questionnaires at repeated time points.

Fundamental patterns of MT maturation

We started our investigations by evaluating fundamental myeloarchitectural patterns in the entire imaging sample ($n = 199$; 18.83 ± 2.84 y; 96 female), before addressing individual differences with respect to developing resilient psychosocial functioning. We visualized the group-averaged regional MT change between first and last imaging sessions (Δ MT) and observed a widespread intra-individual increase in MT (Fig. 1B; 1.26 ± 0.34 y apart). Δ MT was highest towards frontal and temporal poles with strongest inter-individual variability (std) in the

ventral prefrontal cortex. Systematic sampling of myelin-sensitive MT intensities along 10 equivolumetric surfaces perpendicular to the cortical mantle further revealed generally highest mean and inter-individual variability in Δ MT in mid-to-deep layers.

Intra-individual changes in resilient psychosocial functioning

To study longitudinal variation in resilient psychosocial functioning, we assessed the change (Δ) in Res_{PSF} scores between the first and last measurement timepoint (on average 1.14 (SD 0.32) years apart) in $n = 141$ individuals for whom both repeated imaging and behavioral assessments were available (Fig. 1A). 57% of individuals showed a positive change in resilient psychosocial functioning with age (mean $\Delta = 2.40$; SD = 16.35). We did not observe sex differences or age effects on changes in Res_{PSF} scores in either this subsample or in the larger behavioral prediction sample in which Res_{PSF} scores were calculated

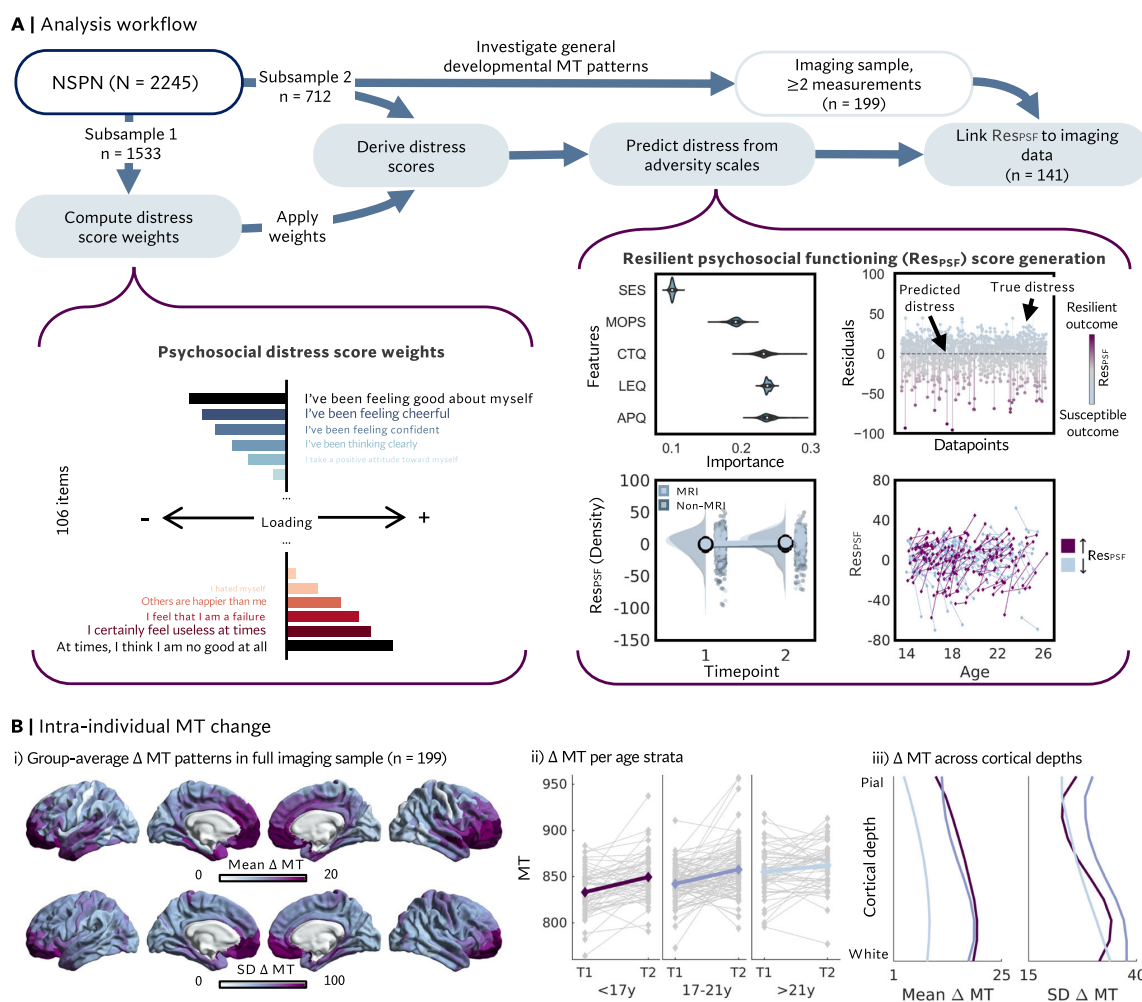


Fig. 1 | Behavioral analysis workflow and group-average longitudinal change in myelin-sensitive Magnetic Transfer (MT). **A** Based on the Neuroscience in Psychiatry Network (NSPN) cohort, resilient psychosocial functioning (Res_{PSF}) scores were computed for each subject at each available time point by predicting psychosocial distress (left) from adversity assessments (Alabama parenting questionnaire (APQ), Life events questionnaire (LEQ), Childhood trauma questionnaire (CTQ), Measure of Parenting style (MOPS), and socio-economic status (SES)). Res_{PSF} scores were defined as the difference between observed and predicted

distress, i.e., showing higher (i.e., more susceptible) or lower (i.e., more resilient) than expected psychosocial distress. Longitudinal changes in Res_{PSF} are depicted in the bottom panel for participants that are part of the neuroimaging (MRI) or solely behavioral (non-MRI) analyses. **B** (i) Mean and standard deviation (SD) of intra-individual change in myelin-sensitive Magnetic Transfer (Δ MT) in the full imaging sample ($n = 199$). (ii) Δ MT averaged across the cortex and visualized for three age strata. (iii) Mean and SD of Δ MT across 10 intracortical depths and across the cortex. Line colors for (ii) and (iii) reflect age strata defined in the Middle panel.

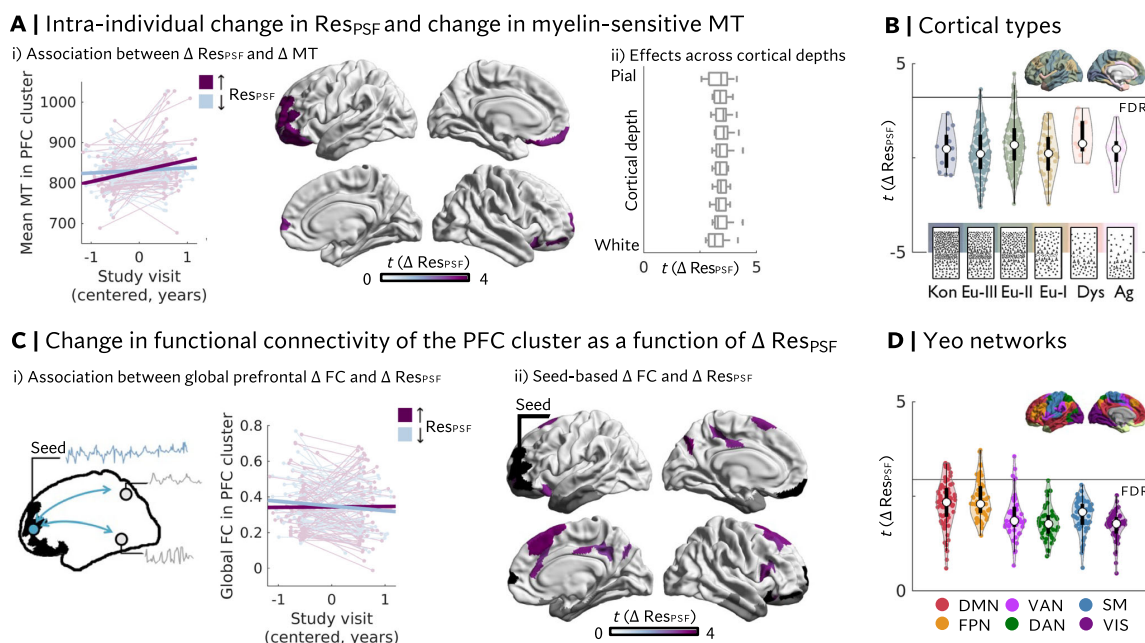


Fig. 2 | Development of resilient psychosocial functioning is associated with changes in anterolateral prefrontal myelin-sensitive Magnetic Transfer (MT) and functional connectivity (FC). **A** (i) A general linear model testing the association between change in resilient psychosocial functioning scores (Res_{PSF}) and change in MT (Δ MT) revealed that adolescents who showed increasingly resilient responses to psychosocial stressors with age showed a higher rate of myelin-sensitive MT change in the anterolateral prefrontal cortex (PFC; $p < 0.05$, FDR corrected, 10,000 permutations; two-sided test). (ii) This effect was on average homogeneous across cortical depths. Box plots for each intra-cortical surface include t -values derived for significant regions depicted in (i), where the box is defined by minima = 25% and maxima = 75%, lines depict medians, and whiskers are defined by values 1.5 times the interquartile range. Effects were predominantly located in eulamine cortex II and III (**B**). Defining the cluster identified in (**A**) as a

seed (**C**), we further observed that prefrontal FC was more globally maintained (i) with increasing Res_{PSF}. Across the cortex (ii), this effect was most prominent in default mode (DMN) and frontoparietal (FPN) networks (**D**; $p < 0.05$, FDR corrected, 10,000 permutations; two-sided test). Gray masks in functional data reflect parcels that were excluded due to low signal-to-noise ratios. In (**B**) and (**D**), white dots reflect medians, violins depict vertical kernel density plots, the minima and maxima of black boxes are defined by 25% and 75% quartiles. All results depicted here are based on $n = 141$ individuals. Note that line plots in (A) and (C) are colored with respect to increasing vs. decreasing Res_{PSF} for visualization, but analyses were performed on continuous Res_{PSF} scores. Kon = Konicortex, Eu-I-III = Eulamine I-III, Dys = Dysgranular, Ag = Agranular; VAN = Ventral attention network, DAN = Dorsal attention network, SM = Sensorimotor, VIS = Visual.

($n = 455$ out of $n = 712$ individuals with at least two measurement time points) (Supplementary Table S2). Longitudinal changes in resilient psychosocial functioning were not related to changes in stressor exposure (Supplementary Fig. S1) and showed comparable distributions in individuals included in the imaging analyses and individuals included in the behavioral analyses only (Supplementary Fig. S2).

Intra-individual variation in resilient psychosocial functioning and myelin-sensitive MT (Fig. 2)

Once longitudinal MT patterns and Res_{PSF} scores were determined, we aimed to elucidate the association between ongoing myelination during adolescence and changes in resilient psychosocial functioning ($n = 141$). We observed a positive association between developing toward more resilient functioning (i.e., an intra-individual increase in Res_{PSF} scores) and Δ MT in the predominantly left-lateralized anterolateral prefrontal cortex (PFC; $t_{\max}(134) = 4.51$; $\beta_{\text{standardized}} = 0.36$; $CI_{\text{standardized } \beta} = [0.20, 0.52]$ (medium effect); $p_{10,000 \text{ permutations}} \& \text{FDR} < 0.05$; Fig. 2A). This effect was robust to several analytical choices and sub-sampling (see Supplementary Fig. S3). Given that myelination rates are not homogeneous across cortical depths (see Fig. 1B iii), we further tested for intracortical differentiability of the observed effect within the prefrontal cluster. The positive association between longitudinal variation in resilient psychosocial functioning and Δ MT was homogeneous across 10 intra-cortical sampling depths (Fig. 2A ii).

We next assessed whether the effects of longitudinal variation in resilient psychosocial functioning were concentrated in regions characterized by a specific cytoarchitecture, and associated duration of developmental plasticity, using cortical types. The five cortical types included agranular, dysgranular, eulamine I, II and III, and konicortex and have been proposed to represent a hierarchy of cortical architectonics, ranging from highly differentiated and myelinated konicortex to less differentiated and more plastic agranular cortex^{28,44}. We stratified the unthresholded t -map according to this prior categorization of cortical types and identified which cortical types overlapped with the significant prefrontal cluster. We observed that parcels showing a significant effect of changes in Res_{PSF} scores were located in eulamine cortex II & III (Fig. 2B), which contain regions of comparatively high cytoarchitectural complexity and layer differentiation. Overall, the cortical topology of the unthresholded t -map followed a general posterior-to-anterior pattern, aligning with a cortex-wide axis of MT development (Supplementary Fig. S4).

Probing whether observed longitudinal effects might be related to cross-sectional differences at baseline, we observed no cross-sectional association between Res_{PSF} scores and MT. One medial frontal gyrus parcel showed lower baseline MT in individuals with lower Res_{PSF} scores at baseline compared to follow-up (see Supplementary Fig. S5).

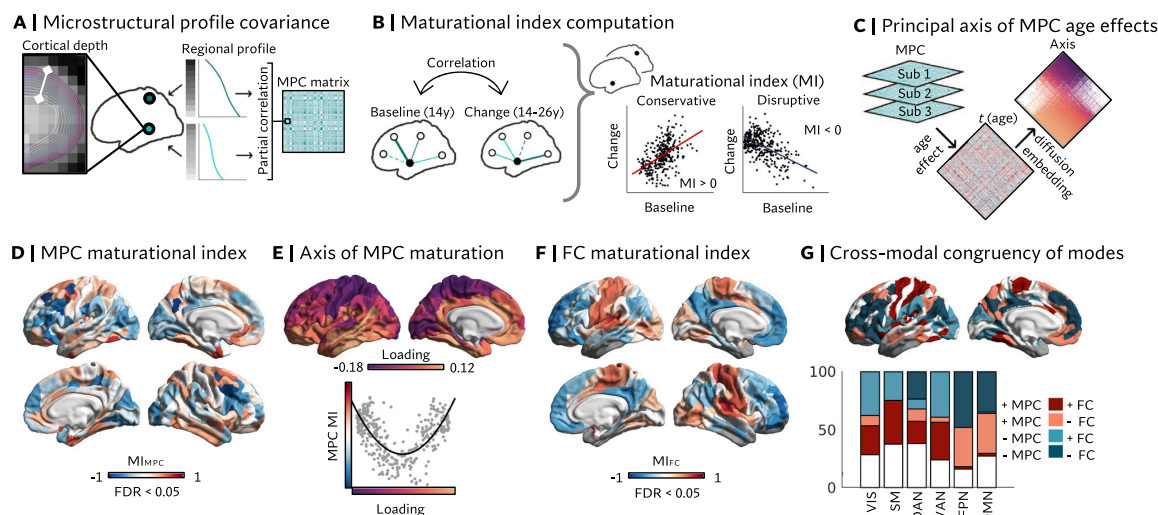


Fig. 3 | Systems-level cortical maturation in the full imaging sample (n = 199), capturing multi-modal reorganization in association cortices. **A–C** Depict analytical approaches. **A** MT intensities were sampled along 10 equi-volumetric surfaces between gray matter (pial) and gray matter/white matter boundaries to derive microstructural profiles and a microstructural profile covariance (MPC) matrix. **B** The maturational index (MI) captures correlations between baseline (i.e., a pattern predicted for age 14 by a mixed effects general linear model) and change patterns (i.e., the age effect estimated by that model) in a region's network. **C** A low-dimensional axis of MPC age effects was derived by applying diffusion map embedding to order regions according to their similarity in synchronized microstructural differentiation with age. **D–G** depict derived maturational patterns. **D** MI of MPC (MI_{MPC}; pFDR < 0.05), showing conservative development in ventral

temporal and dorsal regions, and disruptive reorganization in fronto-parietal association cortex. **E** Relationship between the MI_{MPC} and the principal axis of MPC maturation. The non-linear relationship indicates that conservatively developing ventral and dorsal regions follow maximally different developmental patterns. **F** MI of functional connectivity (MI_{FC}; pFDR < 0.05), showing conservative development in sensorimotor cortex and disruptive reorganization in heteromodal association cortex. **G** Maturational categories: Overlaps between MI_{MPC} and MI_{FC} per Yeo network. + = conservative, - = disruptive. VIS Visual, SM Sensorimotor, DAN Dorsal attention network, VAN Ventral attention network, FPN Frontoparietal network, DMN Default mode network. Gray masks in functional connectivity (FC) data reflect parcels that were excluded due to low signal-to-noise ratios.

Intra-individual change in intrinsic functional connectivity of the anterolateral prefrontal cortex

Having established a positive association between myelin-sensitive MT increase and intra-individual increases in resilient psychosocial functioning, we next investigated concordant changes in the prefrontal cluster's intrinsic functional connectivity (Fig. 2C). To this end, we defined the identified prefrontal parcels exhibiting a significant effect in MT analyses as a seed and assessed both global (i.e., degree centrality) and network-level effects of changes in Res_{PSF} scores on intrinsic functional connectivity (Δ FC). Globally, we observed more maintained levels of cortex-wide functional connectivity with increasingly resilient outcomes, whereas increasingly susceptible outcomes were associated with a segregation (small global effect: $t(134) = 2.45$; $\beta_{\text{standardized}} = 0.21$; $CI_{\text{standardized}} \beta = [0.04, 0.37]$, $p = 0.02$). Studying the cortex-wide pattern of associations between changes in Res_{PSF} scores and prefrontal Δ FC revealed that effects were concentrated in regions of the default mode, frontoparietal and ventral attention networks (medium regional effect: $t_{\text{max}}(134) = 3.78$; $\beta_{\text{standardized}} = 0.31$; $CI_{\text{standardized}} \beta = [0.14, 0.46]$, $p_{10,000} \text{ permutations} \text{ \& } FDR < 0.05$; Fig. 2C, D) and were driven by sub-regions of the PFC cluster that are part of the default mode network (see Supplementary Fig. S6).

System-level cortical maturation (Fig. 3)

Thus far, our analyses suggest a role of local prefrontal myeloarchitectural and inter-regional functional network maturation for developmental changes in susceptible/resilient psychosocial functioning. This suggests that local microstructural alterations may also reflect system-level cortical refinement. Therefore, we next aimed to study system-level myeloarchitectural and parallel functional reorganization. To this end, we computed a microstructural profile covariance (MPC) network reflecting interregional similarities of

myeloarchitectural profiles. The MPC matrix was generated by first probing MT intensities at ten equally spaced intra-cortical depth coordinates, yielding cortical depth profiles of regional MT from the pial surface to the white matter boundary of each cortical area. We then calculated the pairwise Pearson correlation between regional profiles while controlling for average MT intensity to derive the MPC matrix (Fig. 3A). This allowed us to examine the topology of synchronized effects of age on depth-specific changes in approximated myelin content, which are reflected in changes in regional intra-cortical profiles and thus their inter-regional similarity. Next, we computed a maturational index (MI_{MPC}; Fig. 3B), which captures the age-related change of all MPC edges of a node as a function of their respective baseline patterns (estimated for age 14⁴⁵). The MI_{MPC} revealed a topologically heterogeneous pattern of reorganization ($p < 0.05$, FDR) with strongest reorganization in frontoparietal association cortices (Fig. 3D). This pattern was robust to sub-sampling (Supplementary Fig. S7). The MI_{MPC} was spatially aligned with a previously established cortical axis of age-related MPC change (Fig. 3C). Regions closer on this axis exhibit more similar patterns of age-related change in MPC, whereas distant regions undergo dissimilar development¹⁶. The axis captures a differentiation of frontoparietal association cortices that we found to exhibit disruptive reorganization, to resemble either idiopathic sensory or paralimbic/temporal cortex maturational patterns (Fig. 3E). At the same time, we observed a U-shaped association between the MI_{MPC} and the main axis of age effects, where regions at the extremes of the axis exhibited a positive MI_{MPC}, i.e., a positive correlation between baseline and change patterns. A positive MI_{MPC} reflects an integration of regions that showed higher myeloarchitectural similarity at baseline and/or a differentiation of regions that were already dissimilar at baseline. This strengthening of existing patterns has been termed 'conservative' development⁴⁵. Conversely,

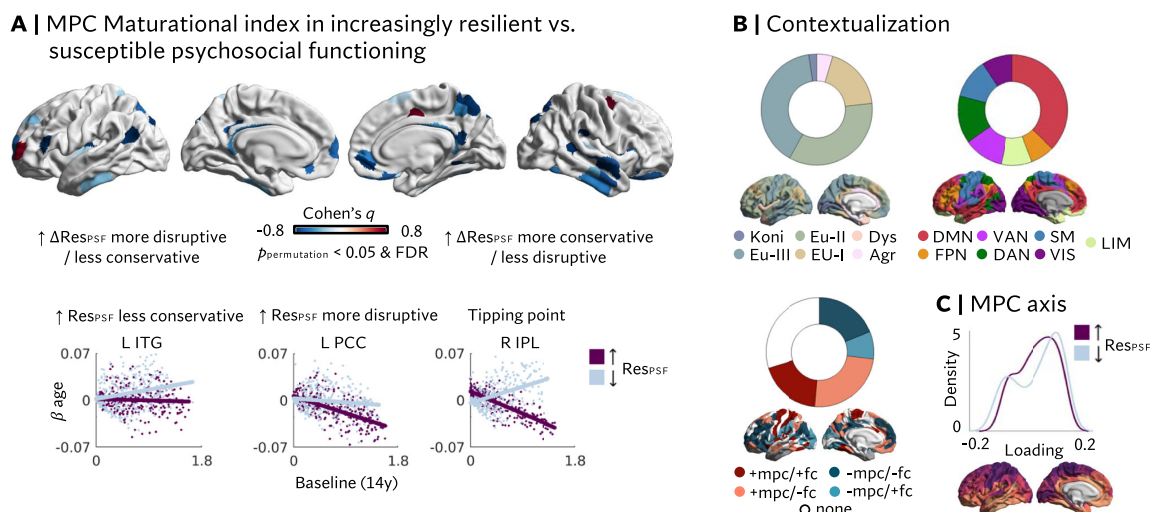


Fig. 4 | More disruptive reorganization of microstructural profile covariance (MPC) networks with increasingly resilient mental health outcomes. **A** Top; Cohen's q for group differences in the microstructural Maturation Index (MI_{MPC} ; FDR $p < 0.05$ & 10,000 permutations, $p < 0.05$) indicating a widespread negative shift (i.e., more disruptive reorganization or less conservative MPC development) in the group of individuals who developed towards more resilient outcomes ($\uparrow \Delta \text{Res}_{\text{PSF}}$). Group differences were computed via z-tests and significance was assessed based on both $p < 0.05$ FDR and non-parametric permutation testing (10,000 permutations; $p < 0.05$). Tests were two-sided. Bottom; A negative shift for the $\uparrow \Delta \text{Res}_{\text{PSF}}$ group can reflect three main scenarios: Less conservative development (left), more disruptive development (middle), or disruptive development in a region that exhibits neither disruptive nor conservative development in the full

sample (right; tipping point). **B** Contextualization of regions with a significant group difference (in any direction), revealing that differences in MI_{MPC} are more frequently located in Eulaminar cortex II & III, default mode areas, and regions exhibiting decoupled microstructural compared to functional development. **C** Density plot of axis loadings per group, reflecting a more compressed axis in the group of individuals who developed towards more resilient outcomes. For scatter and density plots, the $\uparrow \Delta \text{Res}_{\text{PSF}}$ group is depicted in purple and the $\downarrow \Delta \text{Res}_{\text{PSF}}$ group in blue. Statistical tests were two-sided. Kon Konicortex, Eu-I-III Eulaminar I-III, Dys Dysgranular, Ag Agranular, DMN Default mode network, FPN Frontoparietal network, VAN Ventral attention network, DAN Dorsal attention network, SM Sensorimotor, VIS Visual, LIM Limbic.

towards the center of the axis, we observed a negative MI_{MPC} , indicating a reorganization of MPC embedding. Here, regions that were more dissimilar at baseline became more integrated with each other and/or regions with higher myeloarchitectural similarity became more differentiated. This is termed 'disruptive' reorganization (which does not imply pathological disruption, but rather a disruption of baseline patterns during development).

Given the complex relationship between system-level structural and functional development^{34,46}, we studied the convergence of myeloarchitectural and functional maturational modes. The MI based on functional connectivity (MI_{FC}) is characterized by a clear differentiation of 'conservative' development in unimodal regions and 'disruptive' reorganization in heteromodal association areas (Fig. 3F⁴⁵). We found parallel conservative development as well as MPC-reorganization co-occurring with conservative FC development in regions involved in sensory- and attention-related processes (visual, sensorimotor, and ventral attention network). Regions of the default mode and frontoparietal networks showed both cross-modal reorganization and structure-function divergence, with MPC showing conservative but FC disruptive developmental patterns (Fig. 3G). Together, this shows that microstructural and intrinsic functional organization show both convergent and divergent system-level maturational patterns.

System-level maturation and intra-individual change in resilient psychosocial functioning (Fig. 4)

Last, we investigated whether longitudinal changes in resilient psychosocial functioning are associated with different degrees of system-level reorganization between the ages of 14 and 26. Because both the MI and the main axis of age-related MPC change are derived from group-level statistics, it was required to form groups for these analyses

by dichotomizing behavioral changes reflecting increasingly resilient ($\uparrow \Delta \text{Res}_{\text{PSF}}$) vs. increasingly susceptible ($\downarrow \Delta \text{Res}_{\text{PSF}}$) outcomes. We observed significant group differences between $\uparrow \Delta \text{Res}_{\text{PSF}}$ and $\downarrow \Delta \text{Res}_{\text{PSF}}$ individuals in the MI_{MPC} in 43 predominantly heteromodal regions (Fig. 4A; $p < 0.05$ FDR & 10,000 permutations). 93% of these regions showed a negative shift in MI_{MPC} in individuals developing towards more resilient outcomes, mostly reflecting less conservative development (58%; Fig. 4B; Supplementary Table S3), but also more disruptive reorganization (19%). A further 16% of these reflected regions that generally showed no significant association between baseline and age-related change patterns in the full imaging sample, that is, in regions that followed neither conservative nor disruptive developmental patterns. The observations were robust to alternative modeling approaches (Supplementary Fig. S8).

Contextualizing these findings with existing atlases of cortical types²⁸ and intrinsic functional networks⁴⁷ revealed that group differences were concentrated in Eulaminar-II (35%) and -III (40%) cortex, defined anatomically, and the default mode network (DMN; 37%), defined functionally (Fig. 4B). In a complementary approach, we investigated MPC maturation along a low-dimensional cortical axis. We observed a more pronounced bimodal distribution of loadings along the principal axis in the group of individuals who developed toward higher susceptibility. That is, regions were situated toward the differentiated apices rather than the middle of the axis, reflecting increasing microstructural similarity to the axis' anchors. Conversely, the axis was slightly compressed in the group of individuals who developed toward more resilient outcomes. Here, more parcels loaded on the middle of the axis reflecting less synchronization with the anchor profiles (Fig. 4C).

Throughout this study, functional connectivity data were used to contextualize the myeloarchitectural results. Considering the

topology of cross-modal congruency of MIs (Fig. 3G), we observed that group differences in MI_{MPC} were largely located in regions where MPC and FC did not follow convergent MI patterns (see Fig. 4B). That is, group differences were most frequently located in regions exhibiting conservative MPC but decoupled, disruptive FC development (35%). The MI_{FC} itself showed subtle group differences in eight confined, primarily prefrontal regions (Supplementary Fig. S9). Five of these regions showed less disruptive, three exhibited less conservative development in the group of individuals who became more resilient with age.

Together, this suggests that both myeloarchitecture and functional connectivity show marked maturational reorganization tied to resilient/susceptible changes in psychosocial functioning, establishing the brain as a key feature of adaptive development.

Discussion

In the current study, we report that intra-individual variation in adolescent psychosocial functioning relative to environmental adversity is tied to ongoing myeloarchitectural and functional maturation of association cortices. Here, resilient and susceptible outcomes were operationalized as comparatively lower or higher levels of psychosocial distress in the face of psychosocial stressors, resulting in a continuous score that adjusts for variations in stressor exposure at different time points. We used a dimensional approach aligning with previous studies that underscore psychosocial adversity as a pivotal transdiagnostic risk factor that is more predictive of overall psychopathology than discrete symptom domains^{48,49}. In addition, our longitudinal design puts emphasis on the dynamic nature of resilient functioning, combined with myeloarchitectural brain phenotypes that account for regional variations along cortical depth. Thus, we provide nuanced and multimodal evidence that protracted maturation of association cortices is associated with changing abilities to adapt to psychosocial stressors during adolescence.

Enhanced anterolateral prefrontal myelination links to increasingly resilient psychosocial functioning

Investigating longitudinal changes in myelin revealed a positive association between ΔMT in anterolateral and orbitofrontal cortex and changes in resilient psychosocial functioning at medium effect size. This finding is consistent with previous cross-sectional reports suggesting a particular susceptibility of the ventral prefrontal cortex to environmental adversity^{3,22,50} and central role in resilient adaptation^{10,48}. Here, we extend previous findings on cortical volumes and functional connectivity toward longitudinal myelin plasticity. A beneficial effect of enhanced prefrontal myelination may directly be linked to the optimization of adaptive cognitive strategies facilitating successful navigation in an ever-changing environment⁵¹. That is, ongoing plasticity of myelination fosters circuit modification and synchronization through a multitude of parallel mechanisms²⁰. These may include regulatory influences on axon conductance to optimize the synchronization of spike arrivals^{52,53}, neuronal metabolism and excitability^{54,55}, and structural plasticity^{14,56}. In the prefrontal cortex, the optimization of circuit efficiency is closely linked to the maturation of cognitive functions such as executive functions, including emotion regulation, and enhanced social and cognitive flexibility required for adaptation^{57,58}. Thus, prefrontal maturation may directly facilitate resilient psychosocial functioning by fostering cognitive strategies such as cognitive reappraisal, self-awareness about potential maladaptive cognitive biases, or decision making/ problem solving to evaluate the impact of adverse experiences and, for example, seek social support. Thus, the acquisition of beneficial cognitive strategies may therefore mediate the positive association between prefrontal maturation and resilient psychosocial functioning. Conversely, attenuated prefrontal myelination and impaired executive control have been linked to transdiagnostic mental health impairments^{59–61}.

Schizophrenia rat models further suggest links between interneuron hypomyelination and cognitive inflexibility⁶². It is noteworthy that adolescents exhibiting increasingly susceptible outcomes in the present study did not surpass clinical thresholds. However, current findings indicate that cross-sectional associations between susceptibility to psychopathological spectra and prefrontal myeloarchitectural development described in patient and animal data can already be observed at the level of intra-individual variation in susceptibility. Lastly, in addition to potential cognitive effects, psychosocial adversity is likely to elicit a physiological stress response activating the Hypothalamus-Pituitary-Adrenal axis. The ventral PFC is involved in and can recursively be affected by physiological stress responses through glucocorticoid-induced structural remodeling^{63,64}. While the current data do not allow to test protective effects at the molecular level, it is possible that increased consolidation of connections through myelination may enhance physiological resistance to adverse stressor-induced PFC remodeling.

We probed whether varying levels of myeloarchitectural consolidation coincided with differences in functional network maturation of the identified anterolateral prefrontal region, indirectly suggesting a potential resistance to stressor-induced remodeling. Indeed, we observed greater stability of PFC connectivity among individuals who developed toward more resilient psychosocial functioning. Conversely, increasingly susceptible mental health outcomes were associated not only with a reduced rate of prefrontal myelination, but also with a segregation of prefrontal connectivity within abstract cognitive networks (small global effect, medium regional effects). In normative development, most prefrontal sub-regions show decreases in global network embedding during childhood followed by a plateau in early adulthood^{65–67}. This pattern reflects a combination of increasing integration within networks of which they are part, such as the DMN and FPN, but a segregation from other networks such as the dorsal attention network. Here, the segregation of the anterolateral PFC region both globally and within the DMN and FPN in individuals manifesting increasingly susceptible outcomes suggests a closer tie to patterns reminiscent of earlier developmental stages in both prefrontal connectivity and mean myelin-sensitive MT. Together, increased longitudinal myelination of anterolateral prefrontal regions may link to facilitated adaptation to adversity by optimizing the efficiency of prefrontal cognitive circuits relevant to flexible adaptation and resistance to adverse remodeling.

Synchronized reorganization of regions higher up the cytoarchitectonic and functional hierarchies are implicated in developing resilient psychosocial functioning

Brain alterations linked to both maturational and psychopathological cortical alterations have been proposed to occur in a network-like fashion rather than in isolation^{36,37}, underlining the importance of considering the embedding of local changes in a globally changing system. Therefore, we studied the cortical topology of synchronized maturation of intracortical profiles, to then probe whether areas exhibiting most pronounced reorganization during adolescence are more strongly implicated in the development of resilient psychosocial functioning. We described a maturational index reflecting age-related change as a function of baseline patterns and observed the most profound reorganization in frontoparietal association cortices. The MI_{MPC} pattern aligned with a previously established principal axis of age-related MPC change that suggests fronto-parietal association cortices to differentiate most profoundly in synchronization with either dorsal/unimodal or ventral/paralimbic anchors¹⁶. Importantly, the microstructural maturational topology differs to some extent from the maturational topology that has been previously described for functional networks⁴⁵. In particular, cognitive networks such as the FPN and DMN exhibited not only congruent disruptive development, but also a structure-function de-coupling marked by conservative MPC

but disruptive FC development. The partially independent remodeling of functional and structural connectivity has been suggested to shape functional specialization in transmodal association cortex critical for executive functions³⁴. At the same time, it underscores the importance of multimodal studies in understanding the consequences of system-level maturation.

We observed associations between MI and changes in resilient psychosocial functioning in microstructural, and regionally confined effects in intrinsic functional data. Compared to individuals developing toward higher stressor susceptibility, adolescents developing toward more resilient outcomes exhibited a negative-shift in the microstructural MI_{MPC} across heteromodal association cortices. This negative-shift reflected both less conservative and more disruptive development. The observed reduction in conservative development was further highlighted by a compressed axis of MPC change, with fewer regions loading toward the apices/anchors of the axis. In contrast to the ΔRes_{PSF} effects observed in MI_{MPC} , MI_{FC} effects were more locally concentrated in the bilateral prefrontal cortex and presented a positive rather than negative shift in MI_{FC} in individuals who became more resilient with age. That is, the $+\Delta Res_{PSF}$ group exhibited less disruptive development in the PFC. This finding is complementary to microstructural maturational patterns associated with longitudinal change in resilient functioning and converges with the observation that increasingly resilient outcomes were associated with more maintained prefrontal functional connectivity (see Fig. 2C). Previous work suggests that regions that are most developmentally active during adolescence, primarily association cortices, are most strongly implicated in mental health¹. While we generally observed effects in association cortices, this was not exclusive to regions exhibiting disruptive reorganization. In particular for the microstructural MI_{MPC} , effects associated with changes in resilient psychosocial functioning were marked in the temporal cortex, which in turn exhibited largely conservative development. Our results thus indicate that longitudinal variation in resilient psychosocial functioning is linked to altered degrees of myeloarchitectural reorganization, but this was independent from whether a region generally developed conservatively or disruptively.

Across the analytical scales and imaging modalities included in this study, regions implicated in longitudinal change in resilient psychosocial functioning were characterized by their high position along cortical hierarchies of cytoarchitectonic complexity and functional network abstraction. That is, findings emerged predominantly in the cytoarchitecturally complex eulaminate-II and -III cortices, anatomically, and the DMN, functionally. Previous research suggests that structural differentiation of the DMN from networks involved in sensory-perceptual processing⁴⁶ facilitates the maturation of cognitive functions requiring abstraction from the immediate environment^{57,58}. At the same time, DMN structure and functional connectivity are often implicated in psychiatric symptom domains, exposure to environmental adversity such as low socio-economic-status, but also to protective environmental factors such as positive parenting^{68–70}. A prominent explanation for the recurrent role of the DMN is its involvement in the generation of conceptual mental models of the self in the environment^{71–74}. Such self-in-context models include self-referential processing, emotional reappraisal, assigning meaning to external events and interpreting their causes in reference to one's own narrative. Maladaptive internal models and inaccurate attributions of causality fostering negative interpretations of experiences have been considered transdiagnostic risk factors for mental health impairments^{69,71}. Similarly, resilient or susceptible psychosocial trajectories may be tied to continuously evolving self-in-context representations. Here, ongoing refinement of the DMN may facilitate and stabilize beneficial self-referential mental narratives that influence adaptive strategies in the face of environmental stressors.

Lastly, investigating both an average myelin proxy (i.e., regional MT) and a more nuanced approximation of intra-cortical profiles

highlighted different facets of the associations between cortical maturation and change in resilient psychosocial functioning. Nevertheless, both perspectives support a beneficial role of myelin plasticity, as reflected in higher overall rates of (anterolateral prefrontal) myelin growth and, when considering depth-specific measures, higher levels of microstructural reorganization. Across present analyses, individuals who developed toward more susceptible outcomes showed maturational profiles more closely tied to patterns associated with earlier stages of adolescence. Conversely, microstructural maturation in individuals with increasingly resilient outcomes appeared less constrained by existing patterns, potentially highlighting the need for adaptive alterations to enhance selected cognitive circuits. Overall, it is likely that not only is the more the better, but that parallel refinement processes occur at multiple scales. Thus, the current findings demonstrate that adolescents exhibit marked intra-individual variability in resilient psychosocial functioning relative to environmental adversity that is reflected in both local and system-level brain maturation profiles.

Limitations, further considerations, & open questions

Our study takes a dimensional approach to environmental adversity exposure and psychosocial functioning. While differences exist in the brain correlates of both adversity type⁴⁰ and symptom domains⁴, we believe a dimensional approach enhances ecological validity as included forms of adversity are highly clustered together in the general population⁷⁵, have been shown to be associated with overlapping brain structural correlates (dice coefficients up to 0.54^{3,50}), and are transdiagnostic predictors of overall psychopathology^{48,49}. We acknowledge that our analyses of resilient psychosocial functioning are limited to the inclusion of only two timepoints. While this allows us to study longitudinal variation, we note that more timepoints per participant would be required to estimate trajectories with higher reliability⁷⁶. Future studies utilizing e.g., later release waves of the Adolescent Brain Cognitive Development (ABCD) cohort could track longitudinal trajectories over a longer period of time and further assess the question whether enhanced myelin maturation is also a predictor for adult mental health⁴⁹. Next, current evidence suggests that individual differences in myeloarchitectural maturation may be a potential neurobiological resilience factor, influencing adolescent adaptation to environmental risk factors. The exact mechanisms underlying a potential protective effect cannot be clearly elucidated in the current study due to its correlational nature but may involve increased structural stability to stress-induced remodeling and enhanced cognitive maturation. It is likely that resilient psychosocial development is closely coupled with the attainment of cognitive strategies that facilitate resilient outcomes⁷⁷. At the same time, environmental resilience factors such as social support facilitate resilient outcomes^{38,49,78}, and may in part exert their protective effect through an impact on brain maturational trajectories. Resilient outcomes are assumed to rely on a multi-modal and multi-faceted construct, acknowledging the environments we live in, but also other psychological variables beyond clinical symptomatology (such as positive affect, life satisfaction, personality traits). We cannot clearly disentangle the interaction of different intrinsic and extrinsic influences contributing to an individual's psychological well-being beyond resilience. While we estimated resilience/susceptibility by adjusting psychosocial well-being for adversity exposure - yielding a residualized psychosocial functioning score - we cannot rule out that derived resilience scores also reflect the influence of other genetic and environmental factors, as well as noise or measurement error to a certain degree (see Supplementary Information). For example, potential self-report/retrospectivity biases inherent to measures of well-being and adversity exposure⁷⁹ would persist in resilience scores, but are not caused by the residual approach to providing resilience scores. Our longitudinal approach allowed us to limit confounding effects of individual differences in genetic predispositions or environmental circumstances (such as family composition

or neighborhood) that are likely to contribute less variability to within-subject repeated measures than to between-subject cross-sectional data. Overall, our model (explaining 21% of the variance) controls for exposure to a similar extent as common resilience models (explaining 21–28% of the variance; see e.g., refs. 38,80,81). We also aimed to increase the robustness and generalizability of the model by implementing a nested cross-validation and a random forest regression robust to non-linear and non-parametric distributions of questionnaire data. Next, we observed a more skewed distribution of SES in the imaging sub-sample (Supplementary Fig. S2), suggesting a potential over-sampling of individuals from a comparatively more affluent background. Brain-behavior associations described here may thus be limited by the reduced variance in SES. This common issue in developmental neuroimaging research⁸² demands the study of resilience factors identified by the current study in specific sub-groups, such as cohorts facing specific economic difficulties, that were under-represented in the current sample. However, we also note that distributions in well-being, as well as other risk exposure assessments, did not differ between imaging and non-imaging sub-samples, implying that the over-representation of higher SES participants in the imaging sub-sample was not associated with a commensurate shift in the distributions of risk exposure measures that were weighted more strongly in the prediction of Res_{PSF}. We further acknowledge that this sample is of respectable but not massive size. The current sample size resulted from the inclusion of a sample for which adolescent, longitudinal, and multi-modal imaging including a myelin proxy, as well as in-depth phenotypic characterization, were available—rather than an a-priori power analysis. Overall, we found the reported results to be robust to model parameter manipulation and sub-sampling, and well in line with the existing literature, highlighting the central role of the PFC in stress adaptivity and vulnerability^{9,83}, as well as the role of association cortex maturation in psychiatric vulnerability^{1,21,22}. Moreover, individual differences in myelination rates were observed in regions that generally show the highest rates of myelination during adolescence (Fig. 1B). This supports a link to the protracted critical period of plasticity in the prefrontal cortex, extending well into early adulthood and associated with increased susceptibility to environmental risk factors²². We further observed convergence across imaging modalities, for example, effects on the maturation of prefrontal functional network that substantively corroborate the observed differences in rates of prefrontal myelination. However, recent reviews of the replicability of neuroimaging studies in the context of insufficient sample sizes⁸⁴ have cautioned against inflated effect sizes. Therefore, we emphasize that the current results should be interpreted with caution, pending replication in future studies with independent and larger samples, more representative of diverse cultural backgrounds and including individuals typically excluded from healthy samples, such as individuals with neurodevelopmental disorders, to assess the broader generalizability of neurobiological resilience factors identified here. Last, complementary to longitudinal approaches aimed at making prospective predictions of future mental health outcomes, our current work argues for tracking ongoing developmental trajectories to better understand of intra-individual variability in susceptibility to environmental risk factors at different time points in development.

To conclude, the transition to adulthood is considered a particularly susceptible period for the emergence of mental health symptoms. Consistent with prior research suggesting a central role of the protracted development of association cortices in susceptibility to psychiatric risk factors²¹, the current work suggests that intra-individual changes in psychosocial responses to environmental stressors are associated with the degree of myeloarchitectural plasticity and cortex-wide reorganization. The dynamic nature of myelin suggests a potential benefit of interventions that target aberrant trajectories in at-risk youth. These may include increased exposure to environmental resilience factors such as a supportive social

network^{38,49}, but also the facilitation of experience-dependent plasticity, such as has been demonstrated for e.g., social/mental training⁸⁵.

Methods

Study sample

This study included 2245 adolescents and young adults aged 14 to 26 years (54% females; mean age = 19.06 ± 3.02 y) from the NeuroScience in Psychiatry Network (NSPN⁸⁶). Participants were recruited in Cambridgeshire and north London in an accelerated longitudinal sampling design which balanced sex, ethnicity, and participant numbers in five age strata (14–15, 16–17, 18–19, 20–21, 22–25). All 2245 individuals were included in behavioral analyses (see Supplementary Fig. S10 for details on included sub-samples). Participants' sex was determined based on self-report. This study was conducted in accordance with U.K. National Health Service research governance standards and participants provided informed written consent during NSPN data acquisition, for which ethical approval was granted by the Cambridge East Research Ethics Committee under REC 12/EE/0250. Participants received monetary compensation for their participation.

Our neuroimaging analyses of group-level developmental principles were based on a subsample ($n = 199$; 416 sessions) of adolescents who were invited to undergo longitudinal functional and structural neuroimaging assessments at baseline and a 1 year follow up, with a subsample of 26 subjects invited for an intermediate six months scan. Neuroimaging analyses studying intra- and inter-individual differences with respect to adaptivity were restricted to participants who had at least two structural (MT) and functional scans after quality control, and completed all questionnaires included in this study at two or more timepoints ($n = 141$; 346 sessions; age stratification at baseline: $n = 34/34/22/37/14$; 50.3% female; inter-scan interval = 1.26 ± 0.33 y; Supplementary Fig. S10).

Generation of resilient psychosocial functioning (Res_{PSF}) scores

Res_{PSF} scores were generated in a three-step process (Fig. 1A): (1) Computation of a general distress score ($n = 1533$), (2) prediction of psychosocial distress from environmental adversity measures ($n = 712$), and (3) extractions of residuals from the model for participants with repeated MRI and behavioral data ($n = 141$). To avoid leakage, steps 1 and 2 were based on independent subsamples (Fig. 1A and Supplementary Fig. S10).

Psychosocial distress scores were based on self-report questionnaires spanning mental health domains for which emotional and behavioral symptoms tend to emerge during adolescence and are associated with commonly diagnosed mental disorders. Following previous work on latent mental health dimensions in NSPN³⁹, the following mental health domains and questionnaires were included: Depression (33-item Moods and Feelings Questionnaire; MFQ⁸⁷), generalized anxiety (including measures of social concerns, worry, physiological change; 28-item Revised Children's Manifest Anxiety Scale; RCMA⁸⁸), antisocial behaviors (11-item Antisocial Behavior Questionnaire; ABQ), obsessive compulsive behavior (11-item Revised Leyton Obsessional Inventory; r-LOI⁸⁹), self-esteem (10-item Rosenberg Self-Esteem Questionnaire; RSE⁹⁰), psychotic-like experiences (Schizotypal Personality Questionnaire; SPQ⁹¹), and mental well-being (14-item Warwick-Edinburgh Mental Well-Being Scale; WEMWBS⁹²). Please see Supplementary Information for details on the questionnaires. We applied a factor analysis (Matlab 2022b) aiming to derive one latent factor in 1533 individuals. This latent factor correlated highly ($r = 0.99$) with the general distress score derived from previously reported Bi-factor models that additionally include five sub-factors³⁹. In a separate subsample ($n = 712$), we then applied the derived item loadings to each individual's respective item scores. The sum of item scores multiplied by item loadings defined subject-level distress scores.

Conceptualizing relatively more resilient or susceptible outcomes as lower or higher than expected distress, respectively, given the

adversity faced, we then predicted distress scores from available adversity measures. These included: The Life Events Questionnaire (LEQ⁹³), Child Trauma Questionnaire (CTQ⁹⁴), Alabama Parenting Questionnaire (APQ⁹⁵), Measure of Parenting Style (MOPS⁹⁶), and socioeconomic status (as approximated by zip codes/IMD). See Supplementary Methods for details on included questionnaires. For the prediction, we used a random forest regression in a supervised machine learning approach implemented in sci-kit learn (v1.2.1, <https://scikit-learn.org>, in Python v3.10.9). We applied a nested cross-validation in which we left all sessions of one subject out in the outer scheme, i.e., 712 outer folds, and split the remaining data into five even groups for training, i.e., five inner folds, in each iteration. Performance was estimated based on mean absolute errors and parameter optimization was performed for the number of estimators (50, 100, 150, 200, 250, 300) and tree depth (5 to 15). We included a StandardScaler (z-scoring) to preprocess features within the cross-validation scheme.

Neuroimaging data acquisition

Magnetic Transfer (MT) data was acquired as a neuroimaging proxy of myelin content using a multi-parametric mapping (MPM) sequence²³ on three identical 3T Siemens MRI Scanners (Magnetom TIM Trio) in Cambridge (2) and London (1). A standard 32-channel radio-frequency (RF) receive head coil and RF body coil for transmission were used. Anatomical and functional data were acquired on the same day. Neuroimaging data acquisition and processing has also been described previously^{45,97}.

Myelin-sensitive MRI

MPM comprised three multi-echo 3D FLASH scans: predominant T1-weighting (repetition time (TR) = 18.7 ms, flip angle = 20°), and predominant proton density (PD) and MT-weighting (TR = 23.7 ms; flip angle = 6°). To achieve MT-weighting, an off-resonance Gaussian-shaped RF pulse (duration = 4 ms, nominal flip angle = 220°, frequency offset from water resonance = 2 kHz) was applied prior to the excitation. For MT weighted acquisition, several gradient echoes were recorded with alternate readout polarity at six equidistant echo durations (TE) between 2.2 and 14.7 ms. The longitudinal relaxation rate and MT signal are separated by the MT saturation parameter, creating a semi-quantitative measurement that is resistant to field inhomogeneities and relaxation times^{23,98}. Further acquisition parameters: 1 mm isotropic resolution, 176 sagittal partitions, field of view (FOV) = 256 × 240 mm, matrix = 256 × 240 × 176, parallel imaging using GRAPPA factor two in phase-encoding (PE) direction (AP), 6/8 partial Fourier in partition direction, non-selective RF excitation, readout bandwidth BW = 425 Hz/pixel, RF spoiling phase increment = 50°. The acquisition time was approx. 25 min, during which participants wore ear protection and were instructed not to move and rest. MPM further comprises a set of other contrasts, such as R2* sensitive to iron content, yielding complementary insights into different aspects of tissue micro-architecture in vivo^{49,99–101}. Here, we focused on MT, which is considered a particularly strong in vivo marker of myelin with a high spatial correspondence with myelin basic protein and other myelin-related molecules in the brain, as has been verified by several histological validation studies^{24–27}. MT has further been demonstrated to show high reliability¹⁰² suitable for the study of individual differences and brain-behavior associations^{5,16,100}.

Resting-state functional MRI

Resting-state functional MRI (fMRI) data were acquired using a multi-echo echo-planar imaging sequence (TR = 2.42 s; GRAPPA with acceleration factor = 2; flip angle = 90°; matrix size = 64 × 64 × 34; FOV = 240 × 240 mm; in plane resolution = 3.75 × 3.75 mm; slice thickness = 3.75 mm with 10% gap, sequential slice acquisition, 34 oblique slices; bandwidth, 2368 Hz/pixel; TE = 13, 30.55, and 48.1 ms).

Neuroimaging data preprocessing

Microstructure. T1w and MT images were visually inspected for motion artifacts (such as ringing, ghosting, smearing or blurring) by experts and scans were strictly excluded if motion artifacts were detected. Surface reconstruction was performed on T1w data using the FreeSurfer _recon-all_ command (v.5.3.0¹⁰³). Briefly, the pipeline performs non-uniformity correction, projection to Talairach space, intensity normalization, skull stripping, automatic tissue segmentation, and construction of the gray/white interface and the pial surface. Surface reconstructions/segmentations were edited by adding control points in FreeSurfer, re-processed, and then underwent quality control again. If further motion artifacts were detected in this process, the relevant scans were excluded. MT images were co-registered with reconstructed surfaces and 12 equivolumetric cortical surfaces were generated within the cortex (i.e., between the pial and white surface¹⁰⁴). The equivolumetric model takes cortical folding into account by manipulating the Euclidean distance (ρ) between intra-cortical surfaces, thereby preserving the fractional volume between pairs of surfaces (1):

$$\rho = \frac{1}{A(\text{out}) - A(\text{in})} \times (A(\text{in}) + \sqrt{\alpha A^2(\text{out}) + (1 - \alpha) A^2(\text{in})}) \quad (1)$$

α = a fraction of the total volume of the segment accounted for by the surface; $A(\text{out})$ and $A(\text{in})$ = the surface areas of outer and inner cortical surfaces, respectively.

The outer two surfaces were excluded to avoid potential partial volume effects (PVE) and MT intensities were extracted from 10 cortical depths at each vertex. In addition, depth-specific PVEs caused by cerebrospinal fluid (CSF) were corrected for using a mixed tissue class model¹⁰⁵. To this end, a linear model was fitted to each node at all 10 depths (2):

$$MT_{(n,s)} \sim b_0 + b_1 CSF_{(n,s)} \quad (2)$$

where n = node, s = surface. Derived CSF-corrected MT values reflect the sum of residuals (3):

$$MT_{c(n,s)} = T1_{(n,s)} - (b_0 + b_1 CSF_{(n,s)}) \quad (3)$$

and original group averaged MT.

Last, vertices were averaged within 360 bilateral cortical parcels using the Human Connectome Project (HCP) parcellation atlas that was mapped from standard fsaverage space to each participant's native space using surface-based registration^{104,106}.

Resting-state functional MRI

Multi-echo independent component analysis (ME-ICA^{107,108}) was applied to the fMRI data to isolate and remove variance caused by sources that do not scale linearly with the TR within the time series and are therefore assumed not to represent the blood oxygenation level dependent (BOLD) contrast. Variance in cerebrospinal fluid was estimated based on ventricular time series and regressed from parenchymal time series via Analysis of Functional NeuroImages (AFNI¹⁰⁹). Functional data were co-registered to R1 images, which were derived from the same MPM sequence as MT data, ensuring spatial alignment between functional and MT data. Volumes obtained within the 15-s steady-state equilibration were excluded. Anatomical-functional co-registration and motion correction parameters were computed using the middle TE data, and the base EPI image was the first volume following equilibration. Matrices for de-obliquing and six-parameter rigid body motion correction were computed. Using the LPC cost function with the EPI base image as the LPC weight mask, a 12-parameter affine anatomical-functional co-registration was computed. Matrices for de-obliquing, motion correction, and anatomical-functional co-registration were concatenated into a single alignment matrix using the AFNI

tool `align_epi_anat.py`. The dataset of each TE was then slice-time corrected and spatially aligned through repeated application of the alignment matrix. Data was parcellated into the same 360 bilateral HCP cortical regions applied to structural data within which regional time series were averaged across voxels of each respective parcel. Moreover, a band-pass-filter (range: 0.025 to 0.111 Hz¹⁰⁰) was applied to the regional time series using discrete wavelet transform. Following quality control, regional time series were z-scored and 30 regions, mainly in paralimbic areas, were excluded due to low z-scores ($Z < 1.96$) in at least one participant. A functional connectivity (FC) matrix was generated for each subject by computing Pearson's correlation coefficients between all 330 remaining parcels, yielding a 330×330 matrix. Correlation coefficients were then z-transformed by Fisher's transformation¹¹¹). Hence, FC units represent standard deviations of the normal distribution. Lastly, to avoid any residual effects of motion on FC, each edge/Z-score was regressed on each participant's mean frame-wise displacement. All further analyses were based on derived motion-corrected Z-scores (i.e., the residuals of this regression).

In total, 36 scans were excluded due to high in-scanner motion [mean framewise displacement (FD) > 0.3 mm or maximum FD > 1.3 mm], poor surface reconstructions, co-registration errors, and/or extensive fMRI dropout.

Intra-individual change

Intra-individual change in mean and layer-wise MT, as well as resting-state functional connectivity (FC), was assessed by calculating the Δ between first and last MRI sessions: $MT_{T2}-MT_{T1}$ or $FC_{T2}-FC_{T1}$ respectively, for each parcel. Δ s were winsorized to ± 3 SD to account for outliers.

Association between myeloarchitectural and intrinsic functional maturation and change in resilient psychosocial functioning

The association between change in ΔRes_{PSF} and ΔMT was assessed by applying a general linear model to each parcel (4):

$$\Delta MT(\text{parcel}) \sim 1 + \beta_{\Delta Res_{PSF}} * \Delta Res_{PSF} + \beta_{mean Res_{PSF}} * mean Res_{PSF} + \beta_{age} * age + \beta_{sex} * sex + \beta_{site} * site + \epsilon \quad (4)$$

Models were fitted in SurfStat¹¹² (Matlab 2022b) adjusting for mean age (i.e., $(Age_{baseline} + Age_{follow\ up})/2$) and mean Res_{PSF} (i.e., $(Res_{PSF\ at\ baseline} + Res_{PSF\ at\ follow\ up})/2$) across sessions, sex, and site. Before fitting the model, we adjusted ΔRes_{PSF} and ΔMT for inter-session-intervals, which varied between participants, by fitting linear regressions of Δage . This was done separately for imaging and behavioral data to adjust for the fact that behavioral and imaging data were mostly not collected on the same day. All statistical tests reported throughout this study comprised two-sided testing. Significance was assessed by non-linear permutation testing (10,000 permutations of Δ and mean Res_{PSF} and FDR correction of derived p -values at $\alpha < 0.05$). We then stratified the unthresholded t-map according to a cytoarchitectonic map defining six dominant cortical types²⁸, to reveal potential systematic links between cortical architecture and effects associated with changes in resilient psychosocial functioning.

We ran two post-hoc analyses based on the region of interest (ROI) defined by parcels that show a significant $\Delta Res_{PSF} * \Delta MT$ association. First, we tested whether significant associations between ΔRes_{PSF} and ΔMT were layer-specific by fitting the same linear model to MT values at each of the 10 surfaces, rather than the mean across surfaces. This was done to reveal a potential specificity of effects based on cortical depth, not to statistically confirm the observed association again. Next, we addressed the question of whether regions showing differences in ΔMT as a function of ΔRes_{PSF} also exhibit different functional connectivity. To this end, we computed global FC of the ROI as degree centrality (i.e., the sum of all connections) as well as a seed-

based FC analysis defining the ROI as a seed. As described for the ΔMT analysis, we regressed out the effects of inter-session intervals, fitted the same linear model as described above, and assessed significance of the seed-based analysis by non-linear permutation testing (10,000 permutations of Δ and mean Res_{PSF} + FDR correction of derived p -values at $\alpha < 0.05$). Last, we stratified the resulting t-map according to the Yeo 7 Network Atlas⁴⁷ to reveal systematic effects within specific intrinsic functional networks.

System-level maturation

We studied system-level maturation based on both myeloarchitectural and functional data. In order to assess the cortical topology of MT maturation, we computed a microstructural profile covariance (MPC) matrix and studied its change with age. MPC is based on myeloarchitectural profiles across cortical depths and is generated via partial correlations between nodal MT profiles of two given regions, corrected for the mean MT intensity across intra-cortical surfaces (Fig. 3A). An underlying assumption of this approach is that inter-regional similarity predicts axonal cortico-cortical connectivity^{29,33,113}. MPC has previously been shown to align well with post-mortem assessments of inter-regional microstructural similarity³⁰, and depth-dependent shifts in cytoarchitectonic features such as cell densities or myelin characteristics have been linked to architectural¹¹⁴ complexity and cortical hierarchy¹¹⁵.

First, we computed a microstructural and functional Maturation Index (MI), which has been shown to be a robust marker for adolescent modes of reorganization⁴⁵ sensitive to individual differences⁹⁷ in functional connectivity. To compute the MI, LMEs were fitted to each edge of the MPC and FC matrices, assessing effects of age and including sex, site, and repeated measures of the same individual in the model (5):

$$MRI(k,j) \sim 1 + \beta_{age} * age + \beta_{sex} * sex + \beta_{site} * site + \gamma_{subject} * (1|subject) + \epsilon \quad (5)$$

Where k and j are two nodes of the matrix. The MI captures the signed Spearman's correlation between predicted baseline patterns, at age 14, and rate of change, age 14–26, of all edges that connect a given node to all other nodes. Thus, it reflects a reorganization of network embedding.

Baseline values at age 14 for each group ($+ \Delta Res_{PSF}$ / $- \Delta Res_{PSF}$), $MRI_{14\ group}$, were extracted for MPC and FC matrices as follows (6):

$$MRI_{14} = 1 + \beta_{age} * 14 + \beta_{age} * 14 + \beta_{sex} * (1/2) + \beta_{site1} * (1/3) + \beta_{site2} * (1/3) \quad (6)$$

Whereas the rate of change MPC_{14-26} or FC_{14-26} simply reflects the β -coefficient of age (7):

$$MRI_{14-26}(k,j) = \beta_{age} \quad (7)$$

At each node, we then computed the row-wise Spearman's ρ between ranked extracted parameters reflecting baseline and change parameters of all edges (i.e., 360 for MPC, 330 for FC) of a specific node. A positive correlation indicates that a given region's edges that were already similar in either their myeloarchitectural or functional profile became more similar with development, this is termed 'conservative' development. Conversely, a negative correlation reflects reorganization, edges that were similar at baseline differentiate, or edges that were dissimilar at baseline integrate, which is termed 'disruptive' development. We computed normative MIs for MPC and FC across all participants ($n=199$) using all existing sessions (416 sessions). To probe convergence and divergence of structural compared to functional maturational modes, we further tested overlaps between regional MIs (individually thresholded at $pFDR < 0.05$).

Next, we contextualized the MI_{MPC} with a previously established measure of global organization of microstructural maturation: The MPC principal axis of age effects¹⁶. To this end, we applied the same LME as defined in Eq. 5 to each edge of the MPC matrix, assessing the main effect of age on inter-regional microstructural similarities. Diffusion map embedding was then applied to the matrix of t -values (thresholded at 90%), revealing a cortex-wide organizational axis of synchronized age effects. Regions with a similar loading on this axis are similarly embedded in a network of inter-regional synchronization of age effects, whereas regions at the apices of the axis show maximally different change patterns.

Group-level differences in system-level maturation

Last, we aimed to study differences in system-level maturation associated with intra-individual changes in adaptivity. Because the MI is computed from parameters extracted from group-level general linear models, it was required to split the sample into two groups. Thus, the sample was divided into adolescents who showed increasingly resilient outcomes ($+ΔRes_{PSF}$; $n = 81$, 193 sessions; 48% female, 18.93 ± 2.81 y at baseline) and adolescents who became more susceptible with age ($-ΔRes_{PSF}$; $n = 60$; 153 sessions; 53% female, 18.84 ± 2.87 y at baseline). MIs were computed separately for each group, and the resulting maps were subtracted from each other ($+ΔRes_{PSF} - (-ΔRes_{PSF})$). Significance was tested using two approaches that were combined for thresholding: (1) We first applied Z-tests testing for significant differences between the correlation coefficients, i.e., the difference between group MIs divided by the SE of the difference in MIs, as has been done previously⁹⁷ (8).

$$Z = \frac{MI_{+ΔRes_{PSF}} - MI_{-ΔRes_{PSF}}}{SE_{MI_{+ΔRes_{PSF}} - MI_{-ΔRes_{PSF}}}} = \frac{MI_{+ΔRes_{PSF}} - MI_{-ΔRes_{PSF}}}{\sqrt{SE_{MI_{+ΔRes_{PSF}}}^2 + SE_{MI_{-ΔRes_{PSF}}}^2}} \quad (8)$$

Derived p -values were FDR-corrected at $pFDR < 0.05$.

(2) Next, to control for the effects of sampling bias and potential effects of differences in group size or demographics, we performed non-parametric permutation testing, by shuffling group allocation 10,000 times while considering age and sex distributions as well as group size differences (see Supplementary Fig. S11). Finally, we depicted group differences as significant only if they were significant in both FDR-corrected p -values derived from Z-tests ($p < 0.05$), and non-parametric permutation testing ($p < 0.05$).

Reporting summary

Further information on research design is available in the Nature Portfolio Reporting Summary linked to this article.

Data availability

The behavioral resilience scores and microstructural profiles generated in this study have been deposited on Github and Zenodo under https://github.com/CNG-LAB/cngopen/tree/main/adolescent_resilience/ScrFun and <https://zenodo.org/records/11486553>. The item-level questionnaire data as well as unprocessed imaging data can be obtained from <https://portal.ide-cam.org.uk/overview/6/managed> or <https://www.repository.cam.ac.uk/handle/1810/264350>. The processed functional connectivity data are available at <https://zenodo.org/records/6390852>. The depicted data generated in this study are provided in the Supplementary Information/Source Data file. Source data are provided with this paper.

Code availability

Custom code generated for this project was made publicly available under https://github.com/CNG-LAB/cngopen/tree/main/adolescent_resilience/ScrFun and <https://zenodo.org/records/11486553>. Our analysis code makes use of open software: Gradient mapping analyses were carried out using BrainSpace (v. 0.1.2; <https://brainspace.readthedocs.io/en/latest/>) and surface visualizations were based on code from the

ENIGMA Toolbox (v.1.1.3; <https://enigma-toolbox.readthedocs.io/en/latest/>) in combination with ColorBrewer (v. 1.0.0; <https://github.com/scottclowe/cbrewer2>), and the Violin Plot Toolbox (Holger Hoffmann (2024); <https://www.mathworks.com/matlabcentral/fileexchange/45134-violin-plot>). Statistical analyses were carried out using SurfStat (<https://www.math.mcgill.ca/keith/surfstat/>). Equivolumetric surfaces were computed using code from: https://github.com/MICA-MNI/micaopen/tree/master/a_moment_of_change¹⁶. Z-tests were performed using the compare correlation coefficients function (Sisi Ma (2024). https://www.mathworks.com/matlabcentral/fileexchange/44658-compare_correlation_coefficients). Python: We made use of the following packages: scipy 1.10.1, sklearn 0.0.post1, matplotlib 3.7.1, numpy 1.24.2, pandas 1.5.3, seaborn 0.11.0.

References

- Paus, T., Keshavan, M. & Giedd, J. N. Why do many psychiatric disorders emerge during adolescence? *Nat. Rev. Neurosci.* **9**, 947–957 (2008).
- Parkes, L. et al. Transdiagnostic dimensions of psychopathology explain individuals' unique deviations from normative neurodevelopment in brain structure. *Transl. Psychiatry* **11**, 1–13 (2021).
- Holz, N. E. et al. A stable and replicable neural signature of lifespan adversity in the adult brain. *Nat. Neurosci.* Published online August 21:1–10. <https://doi.org/10.1038/s41593-023-01410-8> (2023).
- Yu, G. et al. Common and disorder-specific cortical thickness alterations in internalizing, externalizing and thought disorders during early adolescence: an Adolescent Brain and Cognitive Development study. *J. Psychiatry Neurosci.* **48**, E345–E356 (2023).
- Ziegler, G. et al. Compulsivity and impulsivity traits linked to attenuated developmental frontostriatal myelination trajectories. *Nat. Neurosci.* **22**, 992–999 (2019).
- Hoppen, T. H. & Morina, N. The prevalence of PTSD and major depression in the global population of adult war survivors: a meta-analytically informed estimate in absolute numbers. *Eur. J. Psychotraumatol.* **10**, 1578637 (2019).
- Kalisch, R. et al. The resilience framework as a strategy to combat stress-related disorders. *Nat. Hum. Behav.* **1**, 784–790 (2017).
- Kessler, R. C. et al. Trauma and PTSD in the WHO World Mental Health Surveys. *Eur. J. Psychotraumatol.* **8**, 1353383 (2017).
- Eaton, S., Cornwell, H., Hamilton-Giachritsis, C. & Fairchild, G. Resilience and young people's brain structure, function and connectivity: a systematic review. *Neurosci. Biobehav. Rev.* **132**, 936–956 (2022).
- van der Werff, S. J. A., van den Berg, S. M., Pannekoek, J. N., Elzinga, B. M. & van der Wee, N. J. A. Neuroimaging resilience to stress: a review. *Front Behav. Neurosci.* **7**, 39 (2013).
- Feder, A., Fred-Torres, S., Southwick, S. M. & Charney, D. S. The biology of human resilience: opportunities for enhancing resilience across the life span. *Biol. Psychiatry* **86**, 443–453 (2019).
- Malhi, G. S., Das, P., Bell, E., Mattingly, G. & Mannie, Z. Modelling resilience in adolescence and adversity: a novel framework to inform research and practice. *Transl. Psychiatry* **9**, 316 (2019).
- Stainton, A. et al. Resilience as a multimodal dynamic process. *Early Inter. Psychiatry* **13**, 725–732 (2019).
- Zemmar, A. et al. Oligodendrocyte- and neuron-specific nogo-A restrict dendritic branching and spine density in the adult mouse motor cortex. *Cereb. Cortex* **28**, 2109–2117 (2018).
- Giedd, J. N. et al. Brain development during childhood and adolescence: a longitudinal MRI study. *Nat. Neurosci.* **2**, 861–863 (1999).
- Paquola, C. et al. Shifts in myeloarchitecture characterise adolescent development of cortical gradients. *eLife* **8**. <https://doi.org/10.7554/elife.50482> (2019).
- Whitaker, K. J. et al. Adolescence is associated with genomically patterned consolidation of the hubs of the human brain connectome. *Proc. Natl. Acad. Sci.* **113**, 9105–9110 (2016).

18. Paus, T. Growth of white matter in the adolescent brain: myelin or axon? *Brain Cogn.* **72**, 26–35 (2010).
19. Mount, C. W. & Monje, M. Wrapped to adapt: experience-dependent myelination. *Neuron* **95**, 743–756 (2017).
20. Xin, W. & Chan, J. R. Myelin plasticity: sculpting circuits in learning and memory. *Nat. Rev. Neurosci.* **21**, 682–694 (2020).
21. Sydnor, V. J. et al. Neurodevelopment of the association cortices: Patterns, mechanisms, and implications for psychopathology. *Neuron* **109**, 2820–2846 (2021).
22. Larsen, B., Sydnor, V. J., Keller, A. S., Yeo, B. T. T., Satterthwaite, T. D. A critical period plasticity framework for the sensorimotor–association axis of cortical neurodevelopment. *Trends Neurosci.* <https://doi.org/10.1016/j.tins.2023.07.007> (2023).
23. Weiskopf, N. et al. Quantitative multi-parameter mapping of R1, PD*, MT, and R2* at 3T: a multi-center validation. *Front Neurosci.* **7**, <https://doi.org/10.3389/fnins.2013.00095> (2013).
24. Mancini, M. et al. An interactive meta-analysis of MRI biomarkers of myelin. *eLife* **9**, e61523 (2020).
25. Odrobina, E. E., Lam, T. Y. J., Pun, T., Midha, R. & Stanis, G. J. MR properties of excised neural tissue following experimentally induced demyelination. *NMR Biomed.* **18**, 277–284 (2005).
26. Paquola, C. & Hong, S. J. The potential of myelin-sensitive imaging: redefining spatiotemporal patterns of myeloarchitecture. *Biol. Psychiatry* **93**, 442–454 (2023).
27. Schmierer, K. et al. Quantitative magnetization transfer imaging in postmortem multiple sclerosis brain. *J. Magn. Reson Imaging* **26**, 41–51 (2007).
28. Garcia-Cabezas, M. Á., Zikopoulos, B. & Barbas, H. The Structural Model: a theory linking connections, plasticity, pathology, development and evolution of the cerebral cortex. *Brain Struct. Funct.* **224**, 985–1008 (2019).
29. Barbas, H. & Rempel-Clower, N. Cortical structure predicts the pattern of corticocortical connections. *Cereb. Cortex* **7**, 635–646 (1997).
30. Paquola, C. et al. Microstructural and functional gradients are increasingly dissociated in transmodal cortices. *PLOS Biol.* **17**, e3000284 (2019).
31. Valk, S. L. et al. Genetic and phylogenetic uncoupling of structure and function in human transmodal cortex. *Nat. Commun.* **13**, 2341 (2022).
32. Paquola, C. et al. The unique cytoarchitecture and wiring of the human default mode network. *Neuroscience* <https://doi.org/10.1101/2021.11.22.469533> (2021).
33. Saberi, A. et al. The regional variation of laminar thickness in the human isocortex is related to cortical hierarchy and interregional connectivity. *PLOS Biol.* **21**, e3002365 (2023).
34. Baum, G. L. et al. Development of structure–function coupling in human brain networks during youth. *Proc. Natl. Acad. Sci.* **117**, 771–778 (2020).
35. Paquola, C., Amunts, K., Evans, A., Smallwood, J. & Bernhardt, B. Closing the mechanistic gap: the value of microarchitecture in understanding cognitive networks. *Trends Cogn. Sci.* **26**, 873–886 (2022).
36. Di Martino, A. et al. Unraveling the miswired connectome: a developmental perspective. *Neuron* **83**, 1335–1353 (2014).
37. Hettwer, M. D. et al. Coordinated cortical thickness alterations across six neurodevelopmental and psychiatric disorders. *Nat. Commun.* **13**, 6851 (2022).
38. Van Harmelen, A. L. et al. Adolescent friendships predict later resilient functioning across psychosocial domains in a healthy community cohort. *Psychol. Med.* **47**, 2312–2322 (2017).
39. St Clair, M. C. et al. Characterising the latent structure and organisation of self-reported thoughts, feelings and behaviours in adolescents and young adults. *PLoS One* **12**, e0175381 (2017).
40. Bowes, L., Maughan, B., Caspi, A., Moffitt, T. E. & Arseneault, L. Families promote emotional and behavioural resilience to bullying: evidence of an environmental effect. *J. Child Psychol. Psychiatry* **51**, 809–817 (2010).
41. Collishaw, S. et al. Mental health resilience in the adolescent offspring of parents with depression: a prospective longitudinal study. *Lancet Psychiatry* **3**, 49–57 (2016).
42. Sapouna, M. & Wolke, D. Resilience to bullying victimization: the role of individual, family and peer characteristics. *Child Abuse. Negl.* **37**, 997–1006 (2013).
43. Miller-Lewis, L. R., Searle, A. K., Sawyer, M. G., Baghurst, P. A. & Hedley, D. Resource factors for mental health resilience in early childhood: an analysis with multiple methodologies. *Child Adolesc. Psychiatry Ment. Health* **7**, 6 (2013).
44. Garcia-Cabezas, M. Á., Joyce, M. K. P., John, Y. J., Zikopoulos, B. & Barbas, H. Mirror trends of plasticity and stability indicators in primate prefrontal cortex. *Eur. J. Neurosci.* **46**, 2392–2405 (2017).
45. Váša, F. et al. Conservative and disruptive modes of adolescent change in human brain functional connectivity. *Proc. Natl. Acad. Sci. USA* **117**, 3248–3253 (2020).
46. Park, B. et al. Adolescent development of multiscale structural wiring and functional interactions in the human connectome. *Proc. Natl. Acad. Sci. USA* **119**, e2116673119 (2022).
47. Yeo, B. T. et al. The organization of the human cerebral cortex estimated by intrinsic functional connectivity. *J. Neurophysiol.* Published online (2011).
48. Keyes, K. M. et al. Childhood maltreatment and the structure of common psychiatric disorders. *Br. J. Psychiatry J. Ment. Sci.* **200**, 107–115 (2012).
49. McLaughlin, K. A., Colich, N. L., Rodman, A. M. & Weissman, D. G. Mechanisms linking childhood trauma exposure and psychopathology: a transdiagnostic model of risk and resilience. *BMC Med.* **18**, 96 (2020).
50. Pollok, T. M. et al. Neurostructural traces of early life adversities: a meta-analysis exploring age- and adversity-specific effects. *Neurosci. Biobehav. Rev.* **135**, 104589 (2022).
51. Kalisch, R., Russo, S. J. & Müller, M. B. Neurobiology and systems biology of stress resilience. *Physiol. Rev.* **104**, 1205–1263 (2024).
52. Ford, M. C. et al. Tuning of Ranvier node and internode properties in myelinated axons to adjust action potential timing. *Nat. Commun.* **6**, 8073 (2015).
53. Kato, D. et al. Motor learning requires myelination to reduce asynchrony and spontaneity in neural activity. *Glia* **68**, 193–210 (2020).
54. Larson, V. A. et al. Oligodendrocytes control potassium accumulation in white matter and seizure susceptibility. *eLife* **7**, e34829 (2018).
55. Xin, W. et al. Oligodendrocytes support neuronal glutamatergic transmission via expression of glutamine synthetase. *Cell Rep.* **27**, 2262–2271.e5 (2019).
56. Wang, F. et al. Myelin degeneration and diminished myelin renewal contribute to age-related deficits in memory. *Nat. Neurosci.* **23**, 481–486 (2020).
57. Nelson, E. E. & Guyer, A. E. The development of the ventral prefrontal cortex and social flexibility. *Dev. Cogn. Neurosci.* **1**, 233–245 (2011).
58. Teffer, K., Semendeferi, K. Human prefrontal cortex. In: *Progress in Brain Research* Vol. 195, 191–218. <https://doi.org/10.1016/B978-0-444-53860-4.00009-X> (Elsevier, 2012).
59. Chini, M. & Hanganu-Opatz, I. L. Prefrontal cortex development in health and disease: lessons from rodents and humans. *Trends Neurosci.* **44**, 227–240 (2021).
60. Etkin, A., Gyurak, A. & O'Hara, R. A neurobiological approach to the cognitive deficits of psychiatric disorders. *Dialogues Clin. Neurosci.* **15**, 419 (2013).

61. Knowles, J. K., Batra, A., Xu, H. & Monje, M. Adaptive and maladaptive myelination in health and disease. *Nat. Rev. Neurol.* **18**, 735–746 (2022).
62. Maas, D. A. et al. Interneuron hypomyelination is associated with cognitive inflexibility in a rat model of schizophrenia. *Nat. Commun.* **11**, 2329 (2020).
63. McEwen, B. S. Physiology and neurobiology of stress and adaptation: central role of the brain. *Physiol. Rev.* Published online July 1. <https://doi.org/10.1152/physrev.00041.2006> (2007).
64. McEwen, B. S., Nasca, C. & Gray, J. D. Stress effects on neuronal structure: hippocampus, amygdala, and prefrontal cortex. *Neuropsychopharmacology* **41**, 3–23 (2016).
65. Lopez, K. C., Kandala, S., Marek, S. & Barch, D. M. Development of network topology and functional connectivity of the prefrontal cortex. *Cereb. Cortex* **30**, 2489–2505 (2020).
66. Sherman, L. E. et al. Development of the default mode and central executive networks across early adolescence: a longitudinal study. *Dev. Cogn. Neurosci.* **10**, 148–159 (2014).
67. Stevens, M. C., Pearson, G. D. & Calhoun, V. D. Changes in the interaction of resting-state neural networks from adolescence to adulthood. *Hum. Brain Mapp.* **30**, 2356–2366 (2009).
68. Whittle, S. et al. Role of positive parenting in the association between neighborhood social disadvantage and brain development across adolescence. *JAMA Psychiatry* **74**, 824–832 (2017).
69. Rebello, K., Moura, L. M., Pinaya, W. H. L., Rohde, L. A. & Sato, J. R. Default mode network maturation and environmental adversities during childhood. *Chronic Stress* **2**, 2470547018808295 (2018).
70. Doucet, G. E. et al. Transdiagnostic and disease-specific abnormalities in the default-mode network hubs in psychiatric disorders: A meta-analysis of resting-state functional imaging studies. *Eur. Psychiatry* **63**, e57 (2020).
71. Koban, L., Gianaros, P. J., Kober, H. & Wager, T. D. The self in context: brain systems linking mental and physical health. *Nat. Rev. Neurosci.* **22**, 309–322 (2021).
72. Seth, A. K. Interoceptive inference, emotion, and the embodied self. *Trends Cogn. Sci.* **17**, 565–573 (2013).
73. Friston, K. The free-energy principle: a unified brain theory? *Nat. Rev. Neurosci.* **11**, 127–138 (2010).
74. Barrett, L. F. The theory of constructed emotion: an active inference account of interoception and categorization. *Soc. Cogn. Affect Neurosci.* **12**, 1–23 (2017).
75. Green, J. G. et al. Childhood adversities and adult psychiatric disorders in the national comorbidity survey replication I: associations with first onset of DSM-IV disorders. *Arch. Gen. Psychiatry* **67**, 113–123 (2010).
76. Parsons, S. & McCormick, E. M. Limitations of two time point data for understanding individual differences in longitudinal modeling—what can difference reveal about change? *Dev. Cogn. Neurosci.* **66**, 101353 (2024).
77. Kjelkenes, R. et al. Mapping normative trajectories of cognitive function and its relation to psychopathology symptoms and genetic risk in youth. *Biol. Psychiatry Glob. Open Sci.* **3**, 255–263 (2023).
78. Reiter, A. M. F. et al. Preference uncertainty accounts for developmental effects on susceptibility to peer influence in adolescence. *Nat. Commun.* **12**, 3823 (2021).
79. Baldwin, J. R., Reuben, A., Newbury, J. B. & Danese, A. Agreement between prospective and retrospective measures of childhood maltreatment: a systematic review and meta-analysis. *JAMA Psychiatry* **76**, 584–593 (2019).
80. González-García, N. et al. Resilient functioning is associated with altered structural brain network topology in adolescents exposed to childhood adversity. *Dev. Psychopathol.* Published online July 26, 1–11. <https://doi.org/10.1017/S0954579423000901> (2023).
81. Veer, I. M. et al. Psycho-social factors associated with mental resilience in the Corona lockdown. *Transl. Psychiatry* **11**, 1–11 (2021).
82. Garcini, L. M. et al. Increasing diversity in developmental cognitive neuroscience: a roadmap for increasing representation in pediatric neuroimaging research. *Dev. Cogn. Neurosci.* **58**, 101167 (2022).
83. Luciana, M. & Collins, P. F. Neuroplasticity, the prefrontal cortex, and psychopathology-related deviations in cognitive control. *Annu. Rev. Clin. Psychol.* **18**, 443–469 (2022).
84. Marek, S. et al. Reproducible brain-wide association studies require thousands of individuals. *Nature* **603**, 654–660 (2022).
85. Valk, S. L. et al. Functional and microstructural plasticity following social and interoceptive mental training. Nord CL, Makin TR, Sui YV, Kim SG, eds. *eLife* **12**, e85188 (2023).
86. Kiddle, B. et al. Cohort profile: the NSPN 2400 cohort: a developmental sample supporting the wellcome trust neuroscience in psychiatry network. *Int. J. Epidemiol.* **47**, 18–19g (2018).
87. Costello, E. J. & Angold, A. Scales to assess child and adolescent depression: checklists, screens, and nets. *J. Am. Acad. Child Adolesc. Psychiatry* **27**, 726–737 (1988).
88. Reynolds, C. R. & Richmond, B. O. What I think and feel: a revised measure of children's manifest anxiety. *J. Abnorm. Child Psychol.* **6**, 271–280 (1978).
89. Bamber, D., Tamplin, A., Park, R. J., Kyte, Z. A. & Goodyer, I. M. Development of a short leyton obsessional inventory for children and adolescents. *J. Am. Acad. Child Adolesc. Psychiatry* **41**, 1246–1252 (2002).
90. Rosenberg, M. The measurement of self-esteem, Society and the adolescent self-image. *Princeton*. Published online 1965, 16–36.
91. Raine, A. The SPQ: a scale for the assessment of schizotypal personality based on DSM-III-R criteria. *Schizophr. Bull.* **17**, 555–564 (1991).
92. Tennant, R. et al. The Warwick-Edinburgh Mental Well-being Scale (WEMWBS): development and UK validation. *Health Qual. Life Outcomes* **5**, 63 (2007).
93. Goodyer, I. M., Herbert, J., Tamplin, A. & Altham, P. M. Recent life events, cortisol, dehydroepiandrosterone and the onset of major depression in high-risk adolescents. *Br. J. Psychiatry J. Ment. Sci.* **177**, 499–504 (2000).
94. Bernstein, D. P. et al. Development and validation of a brief screening version of the Childhood Trauma Questionnaire. *Child Abuse. Negl.* **27**, 169–190 (2003).
95. Elgar, F. J., Waschbusch, D. A., Dadds, M. R. & Sigvaldason, N. Development and validation of a short form of the Alabama parenting questionnaire. *J. Child Fam. Stud.* **16**, 243–259 (2007).
96. Parker, G. et al. The development of a refined measure of dysfunctional parenting and assessment of its relevance in patients with affective disorders. *Psychol. Med.* **27**, 1193–1203 (1997).
97. Dorfschmidt, L. et al. Sexually divergent development of depression-related brain networks during healthy human adolescence. *Sci. Adv.* **8**, eabm7825 (2022).
98. Hagiwara, A. et al. Myelin measurement: comparison between simultaneous tissue relaxometry, magnetization transfer saturation index, and T1w/T2w ratio methods. *Sci. Rep.* **8**, 10554 (2018).
99. Cler, G. J. et al. Elevated iron concentration in putamen and cortical speech motor network in developmental stuttering. *Brain* **144**, 2979–2984 (2021).
100. Krishnan, S. et al. Quantitative MRI reveals differences in striatal myelin in children with DLD. Griffiths TD, de Lange FP, Smith F, McMurray B, eds. *eLife* **11**, e74242 (2022).
101. Draganski, B. et al. Regional specificity of MRI contrast parameter changes in normal ageing revealed by voxel-based quantification (VBQ). *NeuroImage* **55**, 1423–1434 (2011).
102. Wenger, E. et al. Reliability of quantitative multiparameter maps is high for magnetization transfer and proton density but attenuated

- for R1 and R2* in healthy young adults. *Hum. Brain Mapp.* **43**, 3585–3603 (2022).
103. Fischl, B. FreeSurfer. *NeuroImage* **62**, 774–781 (2012).
 104. Wagstyl, K., Paquola, C., Bethlehem, R., Huth, A. kwagstyl/surface_tools: initial release of equivolumetric surfaces. Published online. <https://doi.org/10.5281/zenodo.1412054> (2018).
 105. Kim, J. S. et al. Automated 3-D extraction and evaluation of the inner and outer cortical surfaces using a Laplacian map and partial volume effect classification. *NeuroImage* **27**, 210–221 (2005).
 106. Glasser, M. F. et al. A multi-modal parcellation of human cerebral cortex. *Nature* **536**, 171–178 (2016).
 107. Kundu, P., Inati, S. J., Evans, J. W., Luh, W. M. & Bandettini, P. A. Differentiating BOLD and non-BOLD signals in fMRI time series using multi-echo EPI. *NeuroImage* **60**, 1759–1770 (2012).
 108. Kundu, P. et al. Integrated strategy for improving functional connectivity mapping using multiecho fMRI. *Proc. Natl. Acad. Sci.* **110**, 16187–16192 (2013).
 109. Cox, R. W. AFNI: software for analysis and visualization of functional magnetic resonance neuroimages. *Comput Biomed. Res.* **29**, 162–173 (1996).
 110. Bullmore, E. et al. Wavelets and functional magnetic resonance imaging of the human brain. *NeuroImage* **23**, S234–S249 (2004).
 111. Fisher, R. A. Frequency distribution of the values of the correlation coefficient in samples from an indefinitely large population. *Biometrika* **10**, 507–521 (1915).
 112. Worsley, K. et al. SurfStat: A Matlab toolbox for the statistical analysis of univariate and multivariate surface and volumetric data using linear mixed effects models and random field theory. *NeuroImage* **47**, S102 (2009).
 113. Huntenburg, J. M. et al. A systematic relationship between functional connectivity and intracortical myelin in the human cerebral cortex. *Cereb. Cortex* **27**, 981–997 (2017).
 114. Zilles, K. et al. Architectonics of the human cerebral cortex and transmitter receptor fingerprints: reconciling functional neuroanatomy and neurochemistry. *Eur. Neuropsychopharmacol.* **12**, 587–599 (2002).
 115. Mesulam, M. M. From sensation to cognition. *Brain* **121**, 1013–1052 (1998).
 116. Larivière, S. et al. The ENIGMA Toolbox: multiscale neural contextualization of multisite neuroimaging datasets. *Nat. Methods* **18**, 698–700 (2021).

Acknowledgements

Many scientists contributed to the NSPN consortium but did not take active part in the writing of this report. A full list of contributors to NSPN is available in the Supplementary Material. The authors would like to express their gratitude to the open science initiatives that made this work possible. MDH was funded by the German Federal Ministry of Education and Research (BMBF) and the Max Planck Society. L.D. was supported by a Gates Cambridge Scholarship. S.L.V. was supported by the Max Planck Society through the Otto Hahn Award and the Helmholtz International BigBrain Analytics and Learning Laboratory (Hiball). Data were curated and analysed using a computational facility funded by an MRC research infrastructure award (MR/M009041/1) to the School of Clinical Medicine, University of Cambridge and supported by the mental

health theme of the NIHR Cambridge Biomedical Research Center. The views expressed are those of the authors and not necessarily those of the NIH, NHS, the NIHR or the Department of Health and Social Care.

Author contributions

The authors confirm contribution to the paper as follows: Study conception and design: M.D.H. and S.L.V. Data collection: E.T.B. and NSPN. Analysis and interpretation of results: M.D.H., S.L.V., L.M.J., and L.D. Draft paper preparation: M.D.H. and S.L.V. Draft paper revision: M.D.H., S.L.V., S.B.E., L.D., L.P., L.M.J., C.P., R.A.B., and E.T.B. All authors reviewed the results and approved the final version of the paper.

Funding

Open Access funding enabled and organized by Projekt DEAL.

Competing interests

E.T.B. works in an advisory role for Sosei Heptares, Boehringer Ingelheim, GlaxoSmithKline, and Monument Therapeutics. E.T.B. is a stockholder and director of Centile Bioscience Ltd. RAB is a director of and hold equity in Centile Bioscience Ltd. The remaining authors declare no competing interests.

Additional information

Supplementary information The online version contains supplementary material available at <https://doi.org/10.1038/s41467-024-50292-2>.

Correspondence and requests for materials should be addressed to Meike D. Hettwer or Sofie L. Valk.

Peer review information *Nature Communications* thanks Maria Jalbrzikowski, Teresa Vargas and the other, anonymous, reviewer(s) for their contribution to the peer review of this work. A peer review file is available.

Reprints and permissions information is available at <http://www.nature.com/reprints>

Publisher's note Springer Nature remains neutral with regard to jurisdictional claims in published maps and institutional affiliations.

Open Access This article is licensed under a Creative Commons Attribution 4.0 International License, which permits use, sharing, adaptation, distribution and reproduction in any medium or format, as long as you give appropriate credit to the original author(s) and the source, provide a link to the Creative Commons licence, and indicate if changes were made. The images or other third party material in this article are included in the article's Creative Commons licence, unless indicated otherwise in a credit line to the material. If material is not included in the article's Creative Commons licence and your intended use is not permitted by statutory regulation or exceeds the permitted use, you will need to obtain permission directly from the copyright holder. To view a copy of this licence, visit <http://creativecommons.org/licenses/by/4.0/>.

© The Author(s) 2024

NSPN Consortium

Edward T. Bullmore⁵

A full list of members and their affiliations appears in the Supplementary Information.

6 Summary and Conclusion

6.1 Overall synopsis

The goal of this thesis was to reveal systems-level principles of cortical organization that may shape alteration patterns relevant to transdiagnostic psychopathology. I specifically aimed to characterize how cortical alterations co-occur across regions, integrating insights from cortical architecture and developmental susceptibility. To meet this objective, I leveraged systems-level and multiscale approaches in two complementary studies. *Study 1* proposes that CT alterations across six mental disorders are organized in a network-like fashion and along large-scale cortical axes that recapitulate the cortex's microstructural, transcriptomic, and functional diversity. These findings suggest that cortical regions with similar neurobiology share a common vulnerability across mental disorders, providing insights into the emergence of transdiagnostic alteration patterns. *Study 2* revealed that the efficacy with which adolescents can navigate psychosocial challenges varies within an individual and is associated with protracted cortical refinement processes at multiple scales. Specifically, individuals whose resilient functioning increased with age exhibited a higher rate of anterolateral prefrontal cortex (PFC) myelination, stabilization of its connectivity within the DMN, and stronger microstructural reorganization across widespread association cortices. Collectively, current findings support the notion that multiple neurobiological features and spatiotemporal organization schemes act in concert to constrain cortical alterations relevant to transdiagnostic psychopathology. While the two studies took different methodological approaches - one focused on global clinical cohorts, the other on developmental susceptibility - several key findings converge (**Figure 3**):

- 1) Both studies provide a systems-level understanding acknowledging how regional change, whether developmental or pathological, is connected to change in other regions with similar neurobiological properties or developmental trajectories. In the cross-disorder comparison, these co-alteration patterns were found to be intrinsically organized, like a biologically informed coordinate system. In the adolescent sample, variation in susceptibility/resilience was reflected in widely synchronized myeloarchitectural reorganization and functional network consolidation. Hence, current findings highlight coordinated processes in pathology and susceptibility, beyond regional effects.

- 2) Findings were concentrated in association cortices. Prefrontal and temporal regions exhibited the most distinct transdiagnostic co-alteration profiles and represented potential epicenters that may constrain structural alterations within their networks. Similarly, regions implicated in adolescent susceptibility/resilience were primarily located in late-maturing association cortices. These exhibited protracted consolidation through myelination and functional network refinement within DMN and frontoparietal networks. This prominent role of association cortices in dimensional psychopathology is in line with a large body of literature (e.g., Paus et al., 2008; Taylor et al., 2023).

3) Both studies link left anterolateral PFC connectivity to transdiagnostic vulnerability. CT co-alterations in patient samples mapped to the functional network of the left pars orbitalis, defining it as the strongest epicenter. At the same time, attenuated myelination and changes in anterolateral PFC connectivity already appeared to confer susceptibility during adolescence. This region's network embedding was thus associated with mental health variability across youth and clinical populations.

4) While *Study 2* specifically targeted developmental processes, transdiagnostic axes identified in *Study 1* may indirectly capture synchronized developmental aberrations as well, giving rise to similarities in co-alteration profiles. The frontotemporal axis aligned with transcriptomic patterns of developmentally enriched genes, and both axes combined differentiated functional networks that follow different developmental trajectories (e.g., sensory and cognitive control networks; Sydnor et al., 2021).

Overall, our findings demonstrate how integrative, multimodal approaches provide insight into spatiotemporal neurobiological features that may guide cortical alterations in mental illness.

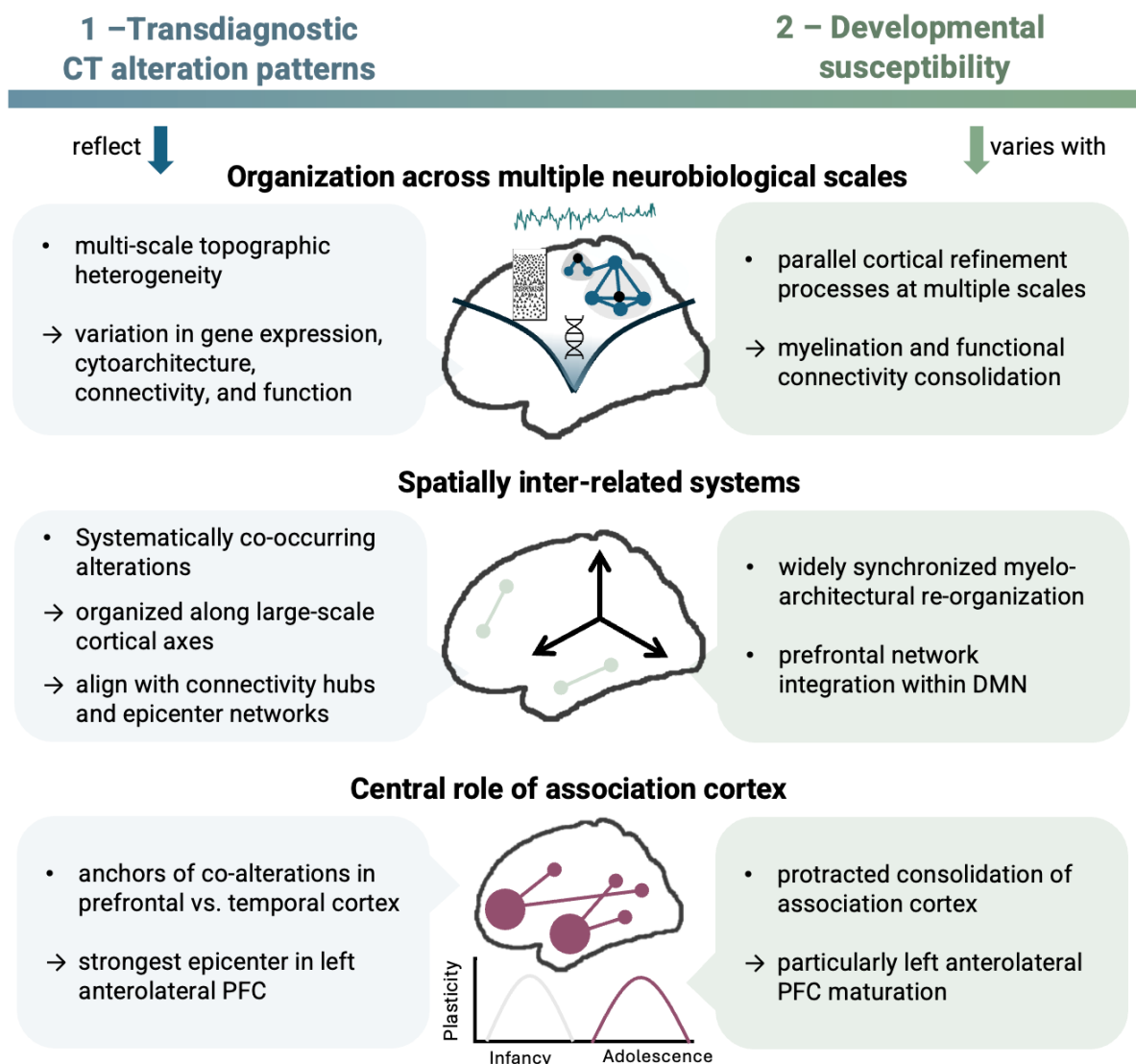


Figure 3. Integrative, multiscale approaches provide insights into spatiotemporal neurobiological features that may guide cortical alterations in dimensional mental health.

6.2 Integration with the literature

6.2.1 *Cortical alterations in mental disorders recapitulate cortical topography*

Current findings support the notion that spatial co-alteration patterns are systematically represented across mental disorders because they similarly recapitulate features of the underlying cortical architecture. This is independent of differences in the magnitude of CT alterations between disorders. Instead, it emphasizes whether any two regions are similarly (un)affected in one disorder, and whether this relationship, or co-alteration, is a consistent feature across disorders. In line with the assumption that pathological patterns are constrained by connectome organization and may recapitulate physiological stress on hubs (Fornito et al., 2015; Vanasse et al., 2021), regions that were topologically central to co-alteration networks were co-located with normative functional connectivity hubs. Moreover, systematic similarities in CT alterations aligned with cytoarchitectural, transcriptomic, and functional similarities, likely recapitulating their differential susceptibility.

During the work on this thesis, insights on the alignment between transdiagnostic patterns with underlying features of cortical architecture have been extended to further neurobiological layers. Adding to the cytoarchitectural and functional similarities we observed between similarly affected regions, Hansen et al. (2022b) reported that this similarity extends to neurotransmitter distribution and gene expression in a broader range of neuropsychiatric conditions. Their findings corroborate ours in that regions embedded within the same functional network are more likely to change in similar ways. However, they also identified molecular similarity to be more predictive of transdiagnostic vulnerability than connectomic markers. Stronger molecular influences were specifically found for MDD and ADHD, while SCZ, BD, and OCD showed a stronger role of connectomic predictors. This may explain why, in our findings, transdiagnostic epicenters mostly captured SCZ, BD, and OCD patterns. Park et al. (2022) and Patel et al. (2021) further describe a segregation of CT alterations in sensorimotor regions from transmodal/paralimbic regions, with paralimbic regions most frequently affected across disorders. In a collaborative study (Park et al. 2022), we report that this pattern was spatially aligned with microstructural differentiation and the distribution of serotonin and dopamine receptors. The axis also showed spatial convergence with gene expression patterns related to prenatal axon guidance and postnatal synaptic activity and plasticity (Patel et al., 2021). These findings converge with *Study 1*, which found that genes with spatial expression profiles resembling the frontotemporal co-alteration axis were overexpressed in the cortex during early/mid-fetal development and late childhood/adolescence. While we did not further annotate these genes, Patel et al. observed that psychiatric risk genes were primarily enriched in those expressed prenatally, whereas postnatal genes were linked to plasticity and susceptibility to environmental influences. The observed spatial axes may thus further reflect similarities in developmental susceptibility, such that synchronized developmental deviations are similarly embedded in co-alteration networks.

An intriguing convergence across analyses in *Study 1* is that epicenter likelihood was highest in prefrontal and temporal regions, which were also located at the apices of the principal co-alteration axis. This segregation suggests maximally different contributions to shaping cortex-wide patterns. It should, however, be noted that the term epicenters is adopted from neurological disorders, including neurodegenerative conditions, where epicenters denote origins of progressing structural change and might involve trans-synaptic spreading of pathogens (Zhou et al., 2012). In neurodevelopmental and psychiatric research, this concept rather refers to the suspicious accumulation of pathological alterations in the connectivity profile of specific regions. This notion aligns with observations that structural alterations in various mental disorders tend to be distributed yet coordinated within shared networks (Segal et al., 2023; Taylor et al., 2023). Correspondingly, prefrontal and temporal epicenters identified in *Study 1* capture co-occurrences of alterations within their networks. They may thus differentially shape pathological patterns but, from a methodological perspective, cannot inform about the origins of potential progression patterns. Intriguingly, a recent investigation of SCZ subtypes has identified such independent spatiotemporal progression patterns of grey matter alterations: one starting in the left inferior frontal gyrus (IFG) and spreading via broader fronto-insular regions, and one starting in the hippocampus, spreading via subcortical and temporal regions (Jiang et al., 2024). Despite the marked methodological differences, findings by Jiang et al. and ours show strikingly convergent evidence for differentiable epicenters in the left IFG and mediotemporal/limbic cortex in a psychiatric context. Jiang et al. further show that frontal and temporal progression patterns were associated with different symptom profiles, which we could not test in our group-level analysis.

Lastly, Hansen, et al. (2022b) defined transdiagnostic epicenters slightly differently, as hubs of networks of affected regions. This revealed partial overlaps with our co-alteration hubs and functional epicenters, e.g., in the angular gyrus and ventral temporal cortex. However, they also report a high epicenter likelihood in the motor cortex. Observed differences may be driven by the inclusion of epilepsy in their sample, for which sensorimotor epicenters have previously been described by Larivière et al. (2020). This further raises the question of the specificity of the observed epicenters, and their potentially different conceptual role in psychiatric compared to other brain pathologies. Overall, our findings converge with other integrative multiscale studies, suggesting that transdiagnostic cortical alteration patterns are constrained by the cortex's neurobiological organization.

6.2.2 *Adolescent susceptibility to adversity links to asynchronous cortical consolidation*

Our longitudinal study (*Study 2*) delineated the role of anterolateral PFC myelination, its network embedding, and the global myeloarchitectural reorganization of association cortices in adolescent resilience and susceptibility. This pertains particularly to myelin maturation in regions situated at the apex of a previously proposed maturational axis (Larsen et al., 2023; Norbom et al., 2021). This axis describes the spatiotemporal unfolding of plasticity windows and myelination towards the late-maturing

association cortices. From a neurobiological perspective, our findings thus align with the notion that cortical susceptibility peaks when exposure to risk factors temporally coincides with increased plasticity, particularly in areas involved in processing or reacting to risk factor exposure (Cooper & Mackey, 2016; Parkes et al., 2021; Paus et al., 2008). Accordingly, the increasing susceptibility levels we observed in individuals exhibiting attenuated myeloarchitectural consolidation may be explained by the extended time windows during which aberrations in network refinement can occur. It is, however, important to note that developmental consolidation through myelination does not solely imply a restriction of plasticity. Myelin is also adaptive and thus somewhat plastic in itself (Xin & Chan, 2020). This property facilitates cognitive refinement by modulating circuit efficiency and network dynamics to learn and respond to the ever-changing environment (Mount & Monje, 2017). Findings may thus not purely reflect variability in stability, e.g., to protect against stress-induced remodeling (McEwen et al., 2016). They may also imply adaptive change to environmental demands by enhancing beneficial circuits.

In addition to neurobiological susceptibility, biopsychosocial approaches propose that different types of adversity constitute transdiagnostic risk factors because they target cognitive functions implicated in several disorders (Etkin et al., 2013; McTeague et al., 2017). For instance, impaired executive functions are associated with multiple types of adversity, are a transdiagnostic predictor of psychopathology, and correlate with delayed development of left anterolateral PFC connectivity (Etkin et al., 2013; McTeague et al., 2017; Xie et al., 2023). The maturation of executive functions, such as cognitive flexibility and emotion regulation, has been linked in particular to prefrontal circuit refinement (Nelson & Guyer, 2011; Teffer & Semendeferi, 2012). However, more widespread association cortex reorganization, which involves its segregation from externally oriented networks, has also been implicated in the maturation of abstract cognitive functions (Baum et al., 2017). While *Study 2* does not measure changes in cognition, the attainment of potentially beneficial cognitive skills relies on similar maturational processes as those we found to be implicated in resilience/susceptibility. Likely, the two domains are closely intertwined, such that the maturation of adaptive and cognitive resources, including emotion regulation strategies and cognitive flexibility, may facilitate the successful navigation of psychosocial challenges. Taken together, our findings provide empirical and longitudinal evidence that regions maturing later in the spatiotemporal maturational hierarchy are implicated in the adaptation to transdiagnostic psychosocial risk factors in adolescence. The modulation of cortical plasticity/susceptibility and the facilitation of cognitive refinement are likely underlying mechanisms.

6.3 Broader implications, future directions, and further considerations

The growing burden of mental illness is a global phenomenon that increasingly affects youth populations (Arias et al., 2022; Kieling et al., 2024). Here, comorbidity is the rule rather than the exception, with about 50% of psychiatric patients meeting criteria for more than one mental disorder

(Caspi et al., 2020; Kessler et al., 2005). Fortunately, the increasing attention paid to transdiagnostic research coincides with the rise of open science, big data, and global collaborative initiatives. The current work is embedded in these initiatives, integrating data from international and more generalizable samples with multiscale analytical approaches.

6.3.1 *Integrating transdiagnostic perspectives and psychiatric variability*

Our efforts to elucidate transdiagnostic principles complement rather than contradict disorder-specific research. In *Study 1*, we observed that CT alterations in disorders with a typically earlier onset, such as ASD and ADHD (Solmi et al., 2022), aligned most strongly with transdiagnostic co-alteration axes. Conversely, transdiagnostic epicenters and hubs showed the strongest overlaps with those observed in SCZ, which is often considered a disconnection syndrome (Friston et al., 2016). We generally observed that disorders were clustered according to their alignment with transdiagnostic patterns. Thus, while we primarily investigated transdiagnostic phenomena, we also observed differences concerning which brain organizational features best recapitulated disorder-specific patterns. The coexistence of common organizational patterns and differential alignment of individual disorders with these patterns is consistent with existing transdiagnostic constructs that suggest the graded co-expression of disorder-specific features alongside generalized spectra (Caspi et al., 2014; Kotov et al., 2017).

Study 1 is primarily concerned with shared features *between* disorders, while transdiagnostic phenomena are arguably also driven by heterogeneity *within* disorders. Disentangling this heterogeneity using individual-level data was not possible in *Study 1*, as it leveraged well-powered but group-level meta-analytic effect size maps. While this approach hindered the study of demographic or clinical variation in observed patterns, it promoted global accessibility and representation, as participating institutions were not required to share sensitive or high-dimensional data. Yet, research focusing on single disorders has revealed marked variability and potential neurobiological subtypes within diagnostic categories (Jiang et al., 2024; Segal et al., 2023; Sun et al., 2023). Embracing and characterizing this variability may lead to the data-driven identification of dimensional transdiagnostic subtypes in line with RDoC principles (Insel et al., 2010; Segal et al., 2024). This calls for future research investigating between-disorder similarities and within-disorder heterogeneity in an integrated fashion. Semi-supervised clustering approaches yielding dimensional neuroimaging phenotypes (Yang et al., 2022) may serve this goal. If applied to large transdiagnostic samples, derived subtype probabilities could reveal neuroimaging patterns that simultaneously differentiate within and cut across diagnostic categories. Moreover, longitudinal and prospective studies may elucidate whether observed transdiagnostic co-alteration axes are in fact spatiotemporal (progression) axes. These efforts would further reveal whether cross-sectional co-alteration patterns reflect synchronized developmental aberrations. Lastly, it remains an open question how changes in symptom profiles across the lifespan (Caspi et al., 2020) may align with transdiagnostic patterns.

6.3.2 *Supporting youth mental health through neurodevelopmentally informed interventions*

Longitudinal analyses in *Study 2* were focused on adolescence and young adulthood, given the heightened vulnerability to the emergence of psychiatric symptoms during this period (Paus et al., 2008). The global increase in mental health challenges among adolescents and the impact of developmental deviations on long-term mental health underpin the urgent need to identify preventive mechanisms that target vulnerable developmental periods (Conradt et al., 2021; Kieling et al., 2024). Current findings link variation in susceptibility to psychosocial adversity to variation in nuanced and multiscale association cortex refinement – a process that may represent windows of both risk and opportunity (Larsen et al., 2023; Tooley et al., 2021). Crucially, this variation was observed longitudinally at the individual level, underpinning the dynamic nature of resilient functioning (Kalisch et al., 2017) and implying the potential for supportive interventions. Here, particularly social support, loving caregivers, and enriched environments have been shown to foster positive mental health outcomes amidst adversity exposure and facilitate normative development (McLaughlin et al., 2020; Van Harmelen et al., 2017; VanBronkhorst et al., 2024). Moreover, environmental enrichment in a social context, for instance, through accessible exercise interventions (Halperin & Healey, 2011), but also mindfulness training (Valk et al., 2023), and cognitive behavioral therapy (Yoshimura et al., 2017) have the potential to impact brain structure and function.

Interventions may be particularly effective when administered while the circuits involved in adaptive responses are still plastic. Thus, supporting resilient functioning during vulnerable developmental periods may be facilitated by acknowledging neurodevelopmentally informed models and the timing of adversity exposure. Such models may track malleable developmental stages at the individual level, for instance, through normative modeling (Marquand et al., 2024). Here, not only myelin measures could be useful indicators of cortical consolidation. Measures of intrinsic cortical activity have also been proposed to reflect consolidation through transitions from synchronized high-amplitude fluctuations to weaker and sparser signals (Martini et al., 2021; Sydnor et al., 2023). Capturing developmental stages at the individual level can inform when and where circuits are most malleable and potentially receptive to supportive actions and can be extended to other life phases. Lifespan approaches may highlight the relevance of different adaptive mechanisms in early childhood or adult neurodegeneration. These should also account for the different types of adversities most prevalent in different life phases, such as social isolation in aging. Ultimately, assessing resilience/susceptibility via deviations from predicted mental health scores is rooted in the continuous dose-response relationships between stressor exposure load and expected mental health impairment (Hamby et al., 2021; Kalisch et al., 2017). As such, it can similarly be applied to cohorts facing more pronounced adversity and clinical populations. That is, we identified maturational patterns that may promote beneficial responses to arguably more common types of adversities faced in a general

population sample. It remains a question for future research whether these are similarly beneficial in high-risk cohorts and help maintain general functioning in clinical samples.

In summary, current findings highlight the dynamic nature of resilience/susceptibility and how it is intertwined with the marked changes associated with adolescent cortical maturation. The pronounced role of late-maturing association cortex refinement encourages tailored interventions to address the asynchronous development and variability in the malleability of the cerebral cortex.

6.4 Conclusion

This thesis characterizes systematic cortical patterns associated with dimensional mental health impairments and embeds them in the context of cortical architecture and developmental trajectories. Based on large-scale cross-disorder comparisons and longitudinal developmental models, findings indicate that (1) spatially inter-related pathological alterations recapitulate the neurobiological similarity between regions as a transdiagnostic feature, and (2) ongoing myeloarchitectural refinement of association cortices during adolescence links to dynamic changes in resilient psychosocial functioning. Like an intrinsic cortical coordinate system, spatiotemporal constraints to transdiagnostic alterations may provide a framework that captures systematic cortical alteration patterns and allows for the integration of future psychiatric neuroimaging findings. Yet, open questions remain concerning the representation of within-disorder heterogeneity in transdiagnostic findings, potential temporal progressions of co-occurring brain structural alterations, and the generalizability of the role of association cortex consolidation in resilience/susceptibility across different cohorts. Meanwhile, global neuroscience continues to facilitate the collaborative aggregation of representative samples and multimodal analytical approaches. These efforts pave the way for nuanced and generalizable insights into the neurobiological underpinnings of mental health variability.

7 References

- Alexander-Bloch, A. F., Mathias, S. R., Fox, P. T., Olvera, R. L., Göring, H. H. H., Duggirala, R., Curran, J. E., Blangero, J., & Glahn, D. C. (2019). Human Cortical Thickness Organized into Genetically-determined Communities across Spatial Resolutions. *Cerebral Cortex*, 29(1), 106–118. <https://doi.org/10.1093/cercor/bhx309>
- Amunts, K., Mohlberg, H., Bludau, S., & Zilles, K. (2020). Julich-Brain: A 3D probabilistic atlas of the human brain's cytoarchitecture. *Science*, 369(6506), 988–992. <https://doi.org/10.1126/science.abb4588>
- Anttila, V., Bulik-Sullivan, B., Finucane, H. K., Walters, R. K., Bras, J., Duncan, L., Escott-Price, V., Falcone, G. J., Gormley, P., Malik, R., Patsopoulos, N. A., Ripke, S., Wei, Z., Yu, D., Lee, P. H., Turley, P., Grenier-Boley, B., Chouraki, V., Kamatani, Y., ... Neale, B. M. (2018). Analysis of shared heritability in common disorders of the brain. *Science*, 360(6395), eaap8757. <https://doi.org/10.1126/science.aap8757>
- Arias, D., Saxena, S., & Verguet, S. (2022). Quantifying the global burden of mental disorders and their economic value. *eClinicalMedicine*, 54. <https://doi.org/10.1016/j.eclinm.2022.101675>
- Barbas, H. (1995). Anatomic basis of cognitive-emotional interactions in the primate prefrontal cortex. *Neuroscience & Biobehavioral Reviews*, 19(3), 499–510. [https://doi.org/10.1016/0149-7634\(94\)00053-4](https://doi.org/10.1016/0149-7634(94)00053-4)
- Barch, D. M. (2017). The Neural Correlates of Transdiagnostic Dimensions of Psychopathology. *American Journal of Psychiatry*, 174(7), 613–615. <https://doi.org/10.1176/appi.ajp.2017.17030289>
- Baum, G. L., Ciric, R., Roalf, D. R., Betzel, R. F., Moore, T. M., Shinohara, R. T., Kahn, A. E., Vandekar, S. N., Rupert, P. E., Quarmley, M., Cook, P. A., Elliott, M. A., Ruparel, K., Gur, R. E., Gur, R. C., Bassett, D. S., & Satterthwaite, T. D. (2017). Modular Segregation of Structural Brain Networks Supports the Development of Executive Function in Youth. *Current Biology*, 27(11), 1561–1572.e8. <https://doi.org/10.1016/j.cub.2017.04.051>
- Biswal, B., Zerrin Yetkin, F., Haughton, V. M., & Hyde, J. S. (1995). Functional connectivity in the motor cortex of resting human brain using echo-planar mri. *Magnetic Resonance in Medicine*, 34(4), 537–541. <https://doi.org/10.1002/mrm.1910340409>
- Bourque, V.-R., Poulain, C., Proulx, C., Moreau, C. A., Joober, R., Forgeot d'Arc, B., Huguet, G., & Jacquemont, S. (2024). Genetic and phenotypic similarity across major psychiatric disorders: A systematic review and quantitative assessment. *Translational Psychiatry*, 14(1), 1–10. <https://doi.org/10.1038/s41398-024-02866-3>
- Briant, A. E., Sisk, L. M., & Gee, D. G. (2021). Associations among negative life events, changes in cortico-limbic connectivity, and psychopathology in the ABCD Study. *Developmental Cognitive Neuroscience*, 52, 101022. <https://doi.org/10.1016/j.dcn.2021.101022>
- Buckholtz, J. W., & Meyer-Lindenberg, A. (2012). Psychopathology and the Human Connectome: Toward a Transdiagnostic Model of Risk For Mental Illness. *Neuron*, 74(6), 990–1004. <https://doi.org/10.1016/j.neuron.2012.06.002>
- Carceller, H., Gramuntell, Y., Klimczak, P., & Nacher, J. (2023). Perineuronal Nets: Subtle Structures with Large Implications. *The Neuroscientist*, 29(5), 569–590. <https://doi.org/10.1177/10738584221106346>
- Caspi, A., Houts, R. M., Ambler, A., Danese, A., Elliott, M. L., Hariri, A., Harrington, H., Hogan, S., Poulton, R., Ramrakha, S., Rasmussen, L. J. H., Reuben, A., Richmond-Rakerd, L., Sugden, K., Wertz, J., Williams, B. S., & Moffitt, T. E. (2020). Longitudinal Assessment of Mental Health Disorders and Comorbidities Across 4 Decades Among Participants in the Dunedin Birth Cohort Study. *JAMA Network Open*, 3(4), e203221. <https://doi.org/10.1001/jamanetworkopen.2020.3221>
- Caspi, A., Houts, R. M., Belsky, D. W., Goldman-Mellor, S. J., Harrington, H., Israel, S., Meier, M. H., Ramrakha, S., Shalev, I., Poulton, R., & Moffitt, T. E. (2014). The p Factor: One General Psychopathology Factor in the Structure of Psychiatric Disorders? *Clinical Psychological Science*, 2(2), 119–137. <https://doi.org/10.1177/2167702613497473>

- Cauda, F., Nani, A., Manuello, J., Premi, E., Palermo, S., Tatu, K., Duca, S., Fox, P. T., & Costa, T. (2018). Brain structural alterations are distributed following functional, anatomic and genetic connectivity. *Brain*, *141*(11), 3211–3232. <https://doi.org/10.1093/brain/awy252>
- Cioli, C., Abdi, H., Beaton, D., Burnod, Y., & Mesmoudi, S. (2014). Differences in human cortical gene expression match the temporal properties of large-scale functional networks. *PloS one*, *9*(12), e115913. <https://doi.org/10.1371/journal.pone.0115913>
- Conradt, E., Crowell, S. E., & Cicchetti, D. (2021). Using development and psychopathology principles to inform the Research Domain Criteria (RDoC) framework. *Development and Psychopathology*, *33*(5), 1521–1525. <https://doi.org/10.1017/S0954579421000985>
- Cooper, E. A., & Mackey, A. P. (2016). Sensory and cognitive plasticity: Implications for academic interventions. *Current Opinion in Behavioral Sciences*, *10*, 21–27. <https://doi.org/10.1016/j.cobeha.2016.04.008>
- Copeland, W. E., Shanahan, L., Hinesley, J., Chan, R. F., Aberg, K. A., Fairbank, J. A., van den Oord, E. J. C. G., & Costello, E. J. (2018). Association of Childhood Trauma Exposure With Adult Psychiatric Disorders and Functional Outcomes. *JAMA Network Open*, *1*(7), e184493. <https://doi.org/10.1001/jamanetworkopen.2018.4493>
- Crossley, N. A., Mechelli, A., Scott, J., Carletti, F., Fox, P. T., McGuire, P., & Bullmore, E. T. (2014). The hubs of the human connectome are generally implicated in the anatomy of brain disorders. *Brain*, *137*(8), 2382–2395. <https://doi.org/10.1093/brain/awu132>
- Dell’Osso, L., Lorenzi, P., & Carpita, B. (2019). The neurodevelopmental continuum towards a neurodevelopmental gradient hypothesis. *Journal of Psychopathology*, *25*, 179–182.
- Di Biase, M. A., Cropley, V. L., Cocchi, L., Fornito, A., Calamante, F., Ganella, E. P., Pantelis, C., & Zalesky, A. (2019). Linking Cortical and Connectional Pathology in Schizophrenia. *Schizophrenia Bulletin*, *45*(4), 911–923. <https://doi.org/10.1093/schbul/sby121>
- Eaton, S., Cornwell, H., Hamilton-Giachritsis, C., & Fairchild, G. (2022). Resilience and young people’s brain structure, function and connectivity: A systematic review. *Neuroscience & Biobehavioral Reviews*, *132*, 936–956. <https://doi.org/10.1016/j.neubiorev.2021.11.001>
- Eickhoff, S. B., Constable, R. T., & Yeo, B. T. T. (2018). Topographic organization of the cerebral cortex and brain cartography. *NeuroImage*, *170*, 332–347. <https://doi.org/10.1016/j.neuroimage.2017.02.018>
- Eickhoff, S. B., Walters, N. B., Schleicher, A., Kril, J., Egan, G. F., Zilles, K., Watson, J. D. G., & Amunts, K. (2005). High-resolution MRI reflects myeloarchitecture and cytoarchitecture of human cerebral cortex. *Human Brain Mapping*, *24*(3), 206–215. <https://doi.org/10.1002/hbm.20082>
- Etkin, A., Gyurak, A., & O’Hara, R. (2013). A neurobiological approach to the cognitive deficits of psychiatric disorders. *Dialogues in clinical neuroscience*, *15*(4), 419. <https://doi.org/10.31887/DCNS.2013.15.4/aetkin>
- Fischl, B. (2012). FreeSurfer. *NeuroImage*, *62*(2), 774–781. <https://doi.org/10.1016/j.neuroimage.2012.01.021>
- Fornito, A., Zalesky, A., & Breakspear, M. (2015). The connectomics of brain disorders. *Nature Reviews Neuroscience*, *16*(3), 159–172. <https://doi.org/10.1038/nrn3901>
- Fortea, L., Ortuño, M., Prisco, M. D., Oliva, V., Albajes-Eizaguirre, A., Fortea, A., Madero, S., Solanes, A., Vilajosana, E., Yao, Y., Fabro, L. D., Galindo, E. S., Verdolini, N., Farré-Colomé, A., Serra-Blasco, M., Picó-Pérez, M., Lukito, S., Wise, T., Carlisi, C., ... Radua, J. (2024). Atlas of gray matter volume differences across psychiatric conditions: A systematic review with a novel meta-analysis that considers co-occurring disorders. *Biological Psychiatry*, *0*(0). <https://doi.org/10.1016/j.biopsych.2024.10.020>
- Friston, K., Brown, H. R., Siemerkus, J., & Stephan, K. E. (2016). The dysconnection hypothesis (2016). *Schizophrenia Research*, *176*(2), 83–94. <https://doi.org/10.1016/j.schres.2016.07.014>
- Fusar-Poli, P., Solmi, M., Brondino, N., Davies, C., Chae, C., Politi, P., Borgwardt, S., Lawrie, S. M., Parnas, J., & McGuire, P. (2019). Transdiagnostic psychiatry: A systematic review. *World Psychiatry*, *18*(2), 192–207. <https://doi.org/10.1002/wps.20631>
- Gandal, M. J., Zhang, P., Hadjimichael, E., Walker, R. L., Chen, C., Liu, S., Won, H., Van Bakel, H., Varghese, M., Wang, Y., Shieh, A. W., Haney, J., Parhami, S., Belmont, J., Kim, M., Moran Losada, P., Khan, Z., Mleczko, J., Xia, Y., ... Geschwind, D. H. (2018). Transcriptome-wide

- isoform-level dysregulation in ASD, schizophrenia, and bipolar disorder. *Science*, 362(6420), eaat8127. <https://doi.org/10.1126/science.aat8127>
- García-Cabezas, M. Á., Joyce, M. K. P., John, Y. J., Zikopoulos, B., & Barbas, H. (2017). Mirror trends of plasticity and stability indicators in primate prefrontal cortex. *European Journal of Neuroscience*, 46(8), 2392–2405. <https://doi.org/10.1111/ejn.13706>
- García-Cabezas, M. Á., Zikopoulos, B., & Barbas, H. (2019). The Structural Model: A theory linking connections, plasticity, pathology, development and evolution of the cerebral cortex. *Brain Structure and Function*, 224(3), 985–1008. <https://doi.org/10.1007/s00429-019-01841-9>
- Gell, M., Noble, S., Laumann, T. O., Nelson, S. M., & Tervo-Clemmens, B. (2024). Psychiatric neuroimaging designs for individualised, cohort, and population studies. *Neuropsychopharmacology*, 50, 1–8. <https://doi.org/10.1038/s41386-024-01918-y>
- Georgiadis, F., Larivière, S., Glahn, D., Hong, L. E., Kochunov, P., Mowry, B., Loughland, C., Pantelis, C., Henskens, F. A., Green, M. J., Cairns, M. J., Michie, P. T., Rasser, P. E., Catts, S., Tooney, P., Scott, R. J., Schall, U., Carr, V., Quidé, Y., ... Kirschner, M. (2024). Connectome architecture shapes large-scale cortical alterations in schizophrenia: A worldwide ENIGMA study. *Molecular Psychiatry*, 29, 1–13. <https://doi.org/10.1038/s41380-024-02442-7>
- Giedd, J. N., & Denker, A. H. (2015). The Adolescent Brain: Insights from Neuroimaging. In J.-P. Bourguignon, J.-C. Carel, & Y. Christen (Hrsg.), *Brain Crosstalk in Puberty and Adolescence* (p. 85–96). Springer International Publishing. https://doi.org/10.1007/978-3-319-09168-6_7
- Goodkind, M., Eickhoff, S. B., Oathes, D. J., Jiang, Y., Chang, A., Jones-Hagata, L. B., Ortega, B. N., Zaiko, Y. V., Roach, E. L., & Korgaonkar, M. S. (2015). Identification of a common neurobiological substrate for mental illness. *JAMA psychiatry*, 72(4). <https://doi.org/10.1001/jamapsychiatry.2014.2206>
- Gratton, C., Nelson, S. M., & Gordon, E. M. (2022). Brain-behavior correlations: Two paths toward reliability. *Neuron*, 110(9), 1446–1449. <https://doi.org/10.1016/j.neuron.2022.04.018>
- Green, J. G., McLaughlin, K. A., Berglund, P. A., Gruber, M. J., Sampson, N. A., Zaslavsky, A. M., & Kessler, R. C. (2010). Childhood Adversities and Adult Psychiatric Disorders in the National Comorbidity Survey Replication I: Associations With First Onset of DSM-IV Disorders. *Archives of General Psychiatry*, 67(2), 113–123. <https://doi.org/10.1001/archgenpsychiatry.2009.186>
- Halperin, J. M., & Healey, D. M. (2011). The influences of environmental enrichment, cognitive enhancement, and physical exercise on brain development: Can we alter the developmental trajectory of ADHD? *Neuroscience & Biobehavioral Reviews*, 35(3), 621–634. <https://doi.org/10.1016/j.neubiorev.2010.07.006>
- Hamby, S., Elm, J. H. L., Howell, K. H., & Merrick, M. T. (2021). Recognizing the cumulative burden of childhood adversities transforms science and practice for trauma and resilience. *American Psychologist*, 76(2), 230–242. <https://doi.org/10.1037/amp0000763>
- Hänisch, B., Hansen, J. Y., Bernhardt, B. C., Eickhoff, S. B., Dukart, J., Misić, B., & Valk, S. L. (2023). Cerebral chemoarchitecture shares organizational traits with brain structure and function. *eLife*, 12, e83843. <https://doi.org/10.7554/eLife.83843>
- Hankin, B. L., & Abela, J. R. Z. (2005). *Development of Psychopathology: A Vulnerability-Stress Perspective*. SAGE Publications. <https://doi.org/10.4135/9781452231655>
- Hansen, J. Y., Shafiei, G., Markello, R. D., Smart, K., Cox, S. M. L., Nørgaard, M., Beliveau, V., Wu, Y., Gallezot, J.-D., Aumont, É., Servaes, S., Scala, S. G., DuBois, J. M., Wainstein, G., Bezgin, G., Funck, T., Schmitz, T. W., Spreng, R. N., Galovic, M., ... Misić, B. (2022a). Mapping neurotransmitter systems to the structural and functional organization of the human neocortex. *Nature Neuroscience*, 25(11), 1569–1581. <https://doi.org/10.1038/s41593-022-01186-3>
- Hansen, J. Y., Shafiei, G., Vogel, J. W., Smart, K., Bearden, C. E., Hoogman, M., Franke, B., van Rooij, D., Buitelaar, J., McDonald, C. R., Sisodiya, S. M., Schmaal, L., Veltman, D. J., van den Heuvel, O. A., Stein, D. J., van Erp, T. G. M., Ching, C. R. K., Andreassen, O. A., Hajek, T., ... Misić, B. (2022b). Local molecular and global connectomic contributions to cross-disorder cortical abnormalities. *Nature Communications*, 13(1), 4682. <https://doi.org/10.1038/s41467-022-32420-y>
- Hansen, J. Y., Shafiei, G., Voigt, K., Liang, E. X., Cox, S. M. L., Leyton, M., Jamadar, S. D., & Misić, B. (2023). Integrating multimodal and multiscale connectivity blueprints of the human cerebral

- cortex in health and disease. *PLOS Biology*, 21(9), e3002314. <https://doi.org/10.1371/journal.pbio.3002314>
- Hawrylycz, M., Miller, J. A., Menon, V., Feng, D., Dolbeare, T., Guillozet-Bongaarts, A. L., Jegga, A. G., Aronow, B. J., Lee, C.-K., & Bernard, A. (2015). Canonical genetic signatures of the adult human brain. *Nature neuroscience*, 18(12), 1832.
- Hess, J. L., Barnett, E. J., Hou, J., Faraone, S. V., & Glatt, S. J. (2024). *Polygenic Resilience Scores are Associated with Lower Penetrance of Schizophrenia Risk Genes, Protection Against Psychiatric and Medical Disorders, and Enhanced Mental Well-Being and Cognition* (S. 2024.06.03.24308377). medRxiv. <https://doi.org/10.1101/2024.06.03.24308377>
- Hettwer, M. D., Dorfschmidt, L., Puhlmann, L. M. C., Jacob, L. M., Paquola, C., Bethlehem, R. A. I., Bullmore, E. T., Eickhoff, S. B., & Valk, S. L. (2024). Longitudinal variation in resilient psychosocial functioning is associated with ongoing cortical myelination and functional reorganization during adolescence. *Nature Communications*, 15(1), 6283. <https://doi.org/10.1038/s41467-024-50292-2>
- Hogg, B., Gardoki-Souto, I., Valiente-Gómez, A., Rosa, A. R., Fortea, L., Radua, J., Amann, B. L., & Moreno-Alcázar, A. (2023). Psychological trauma as a transdiagnostic risk factor for mental disorder: An umbrella meta-analysis. *European Archives of Psychiatry and Clinical Neuroscience*, 273(2), 397–410. <https://doi.org/10.1007/s00406-022-01495-5>
- Holz, N. E., Zabihi, M., Kia, S. M., Monninger, M., Aggensteiner, P.-M., Siehl, S., Floris, D. L., Bokde, A. L. W., Desrivieres, S., Flor, H., Grigis, A., Garavan, H., Gowland, P., Heinz, A., Brühl, R., Martinot, J.-L., Martinot, M.-L. P., Orfanos, D. P., Paus, T., ... Marquand, A. F. (2023). A stable and replicable neural signature of lifespan adversity in the adult brain. *Nature Neuroscience*, 1–10. <https://doi.org/10.1038/s41593-023-01410-8>
- Huntenburg, J. M., Bazin, P.-L., & Margulies, D. S. (2018). Large-Scale Gradients in Human Cortical Organization. *Trends in Cognitive Sciences*, 22(1), 21–31. <https://doi.org/10.1016/j.tics.2017.11.002>
- Hüttenrauch, M., Salinas, G., & Wirths, O. (2016). Effects of Long-Term Environmental Enrichment on Anxiety, Memory, Hippocampal Plasticity and Overall Brain Gene Expression in C57BL6 Mice. *Frontiers in Molecular Neuroscience*, 9, 62. <https://doi.org/10.3389/fnmol.2016.00062>
- Insel, T., Cuthbert, B., Garvey, M., Heinssen, R., Pine, D. S., Quinn, K., Sanislow, C., & Wang, P. (2010). Research Domain Criteria (RDoC): Toward a New Classification Framework for Research on Mental Disorders. *American Journal of Psychiatry*, 167(7). <https://doi.org/10.1176/appi.ajp.2010.09091379>
- Jiang, Y., Palaniyappan, L., Luo, C., Chang, X., Zhang, J., Tang, Y., Zhang, T., Li, C., Zhou, E., Yu, X., Li, W., An, D., Zhou, D., Huang, C.-C., Tsai, S.-J., Lin, C.-P., Cheng, J., Wang, J., Yao, D., ... the ZIB Consortium. (2024). Neuroimaging epicenters as potential sites of onset of the neuroanatomical pathology in schizophrenia. *Science Advances*, 10(24), eadk6063. <https://doi.org/10.1126/sciadv.adk6063>
- Kalisch, R., Baker, D. G., Basten, U., Boks, M. P., Bonanno, G. A., Brummelman, E., Chmitorz, A., Fernández, G., Fiebach, C. J., Galatzer-Levy, I., Geuze, E., Groppa, S., Helmreich, I., Hendler, T., Hermans, E. J., Jovanovic, T., Kubiak, T., Lieb, K., Lutz, B., ... Kleim, B. (2017). The resilience framework as a strategy to combat stress-related disorders. *Nature Human Behaviour*, 1(11), 784–790. <https://doi.org/10.1038/s41562-017-0200-8>
- Kalisch, R., Russo, S. J., & Müller, M. B. (2024). Neurobiology and systems biology of stress resilience. *Physiological Reviews*, 104(3), 1205–1263. <https://doi.org/10.1152/physrev.00042.2023>
- Keller, A. S., Moore, T. M., Luo, A., Visoki, E., Gataviņš, M. M., Shetty, A., Cui, Z., Fan, Y., Feczko, E., Houghton, A., Li, H., Mackey, A. P., Miranda-Dominguez, O., Pines, A., Shinohara, R. T., Sun, K. Y., Fair, D. A., Satterthwaite, T. D., & Barzilay, R. (2024). A general exposome factor explains individual differences in functional brain network topography and cognition in youth. *Developmental Cognitive Neuroscience*, 66, 101370. <https://doi.org/10.1016/j.dcn.2024.101370>
- Kessler, R. C., Berglund, P., Demler, O., Jin, R., Merikangas, K. R., & Walters, E. E. (2005). Lifetime prevalence and age-of-onset distributions of DSM-IV disorders in the National Comorbidity Survey Replication. *Archives of General Psychiatry*, 62(6), 593–602. <https://doi.org/10.1001/archpsyc.62.6.593>
- Keyes, K. M., Eaton, N. R., Krueger, R. F., McLaughlin, K. A., Wall, M. M., Grant, B. F., & Hasin, D.

- S. (2012). Childhood maltreatment and the structure of common psychiatric disorders. *The British Journal of Psychiatry: The Journal of Mental Science*, 200(2), 107–115. <https://doi.org/10.1192/bjp.bp.111.093062>
- Kieling, C., Buchweitz, C., Caye, A., Silvani, J., Ameis, S. H., Brunoni, A. R., Cost, K. T., Courtney, D. B., Georgiades, K., Merikangas, K. R., Henderson, J. L., Polanczyk, G. V., Rohde, L. A., Salum, G. A., & Szatmari, P. (2024). Worldwide Prevalence and Disability From Mental Disorders Across Childhood and Adolescence: Evidence From the Global Burden of Disease Study. *JAMA Psychiatry*, 81(4), 347–356. <https://doi.org/10.1001/jamapsychiatry.2023.5051>
- Kong, R., Li, J., Orban, C., Sabuncu, M. R., Liu, H., Schaefer, A., Sun, N., Zuo, X.-N., Holmes, A. J., Eickhoff, S. B., & Yeo, B. T. T. (2019). Spatial Topography of Individual-Specific Cortical Networks Predicts Human Cognition, Personality, and Emotion. *Cerebral Cortex*, 29(6), 2533–2551. <https://doi.org/10.1093/cercor/bhy123>
- Kotov, R., Krueger, R. F., Watson, D., Achenbach, T. M., Althoff, R. R., Bagby, R. M., Brown, T. A., Carpenter, W. T., Caspi, A., Clark, L. A., Eaton, N. R., Forbes, M. K., Forbush, K. T., Goldberg, D., Hasin, D., Hyman, S. E., Ivanova, M. Y., Lynam, D. R., Markon, K., ... Zimmerman, M. (2017). The Hierarchical Taxonomy of Psychopathology (HiTOP): A dimensional alternative to traditional nosologies. *Journal of Abnormal Psychology*, 126(4), 454–477. <https://doi.org/10.1037/abn0000258>
- Krug, A., Stein, F., David, F. S., Schmitt, S., Brosch, K., Pfarr, J.-K., Ringwald, K. G., Meller, T., Thomas-Odenthal, F., Meinert, S., Thiel, K., Winter, A., Waltemate, L., Lemke, H., Grotegerd, D., Opel, N., Repple, J., Hahn, T., Streit, F., ... Forstner, A. J. (2024). Factor analysis of lifetime psychopathology and its brain morphometric and genetic correlates in a transdiagnostic sample. *Translational Psychiatry*, 14(1), 1–10. <https://doi.org/10.1038/s41398-024-02936-6>
- Lahey, B. B., Applegate, B., Hakes, J. K., Zald, D. H., Hariri, A. R., & Rathouz, P. J. (2012). Is there a general factor of prevalent psychopathology during adulthood? *Journal of abnormal psychology*, 121(4), 971. <https://doi.org/10.1037/a0028355>
- Larivière, S., Paquola, C., Park, B., Royer, J., Wang, Y., Benkarim, O., Vos de Wael, R., Valk, S. L., Thomopoulos, S. I., Kirschner, M., Lewis, L. B., Evans, A. C., Sisodiya, S. M., McDonald, C. R., Thompson, P. M., & Bernhardt, B. C. (2021). The ENIGMA Toolbox: Multiscale neural contextualization of multisite neuroimaging datasets. *Nature Methods*, 18(7), 698–700. <https://doi.org/10.1038/s41592-021-01186-4>
- Larivière, S., Rodríguez-Cruces, R., Royer, J., Caligiuri, M. E., Gambardella, A., Concha, L., Keller, S. S., Cendes, F., Yasuda, C., Bonilha, L., Gleichgerricht, E., Focke, N. K., Domin, M., Von Podewills, F., Langner, S., Rummel, C., Wiest, R., Martin, P., Kotikalapudi, R., ... Bernhardt, B. C. (2020). Network-based atrophy modeling in the common epilepsies: A worldwide ENIGMA study. *Science Advances*, 6(47), eabc6457. <https://doi.org/10.1126/sciadv.abc6457>
- Larsen, B., Sydnor, V. J., Keller, A. S., Yeo, B. T. T., & Satterthwaite, T. D. (2023). A critical period plasticity framework for the sensorimotor–association axis of cortical neurodevelopment. *Trends in Neurosciences*, 0(0). <https://doi.org/10.1016/j.tins.2023.07.007>
- Lee, P. H., Anttila, V., Won, H., Feng, Y.-C. A., Rosenthal, J., Zhu, Z., Tucker-Drob, E. M., Nivard, M. G., Grotzinger, A. D., Posthuma, D., Wang, M. M.-J., Yu, D., Stahl, E. A., Walters, R. K., Anney, R. J. L., Duncan, L. E., Ge, T., Adolfsson, R., Banaschewski, T., ... Smoller, J. W. (2019). Genomic Relationships, Novel Loci, and Pleiotropic Mechanisms across Eight Psychiatric Disorders. *Cell*, 179(7). <https://doi.org/10.1016/j.cell.2019.11.020>
- Lerch, J. P., Worsley, K., Shaw, W. P., Greenstein, D. K., Lenroot, R. K., Giedd, J., & Evans, A. C. (2006). Mapping anatomical correlations across cerebral cortex (MACACC) using cortical thickness from MRI. *NeuroImage*, 31(3), 993–1003. <https://doi.org/10.1016/j.neuroimage.2006.01.042>
- Liang, X., Zou, Q., He, Y., & Yang, Y. (2013). Coupling of functional connectivity and regional cerebral blood flow reveals a physiological basis for network hubs of the human brain. *Proceedings of the National Academy of Sciences*, 110(5), 1929–1934. <https://doi.org/10.1073/pnas.1214900110>
- Liloia, D., Mancuso, L., Uddin, L. Q., Costa, T., Nani, A., Keller, R., Manuella, J., Duca, S., & Cauda, F. (2021). Gray matter abnormalities follow non-random patterns of co-alteration in autism: Meta-connectomic evidence. *NeuroImage: Clinical*, 30, 102583.

- <https://doi.org/10.1016/j.nicl.2021.102583>
- Lippard, E. T. C., & Nemeroff, C. B. (2020). The Devastating Clinical Consequences of Child Abuse and Neglect: Increased Disease Vulnerability and Poor Treatment Response in Mood Disorders. *The American journal of psychiatry*, 177(1), 20–36. <https://doi.org/10.1176/appi.ajp.2019.19010020>
- Luo, A., Sydnor, V. J., Pines, A., Larsen, B., Alexander-Bloch, A. F., Cieslak, M., Covitz, S., Chen, A., Esper, N. B., Feczko, E., Franco, A. R., Gur, R. E., Gur, R. C., Houghton, A., Hu, F., Keller, A. S., Kiar, G., Mehta, K., Salum, G. A., ... Satterthwaite, T. D. (2024). Functional Connectivity Development along the Sensorimotor-Association Axis Enhances the Cortical Hierarchy. *Nature Communications*, 15(1), 3511. doi: 10.1038/s41467-024-47748-w
- Lynch, S. J., Sunderland, M., Newton, N. C., & Chapman, C. (2021). A systematic review of transdiagnostic risk and protective factors for general and specific psychopathology in young people. *Clinical Psychology Review*, 87, 102036. <https://doi.org/10.1016/j.cpr.2021.102036>
- Mancini, M., Karakuzu, A., Cohen-Adad, J., Cercignani, M., Nichols, T. E., & Stikov, N. (2020). An interactive meta-analysis of MRI biomarkers of myelin. *eLife*, 9, e61523. <https://doi.org/10.7554/eLife.61523>
- Margulies, D. S., Ghosh, S. S., Goulas, A., Falkiewicz, M., Huntenburg, J. M., Langs, G., Bezgin, G., Eickhoff, S. B., Castellanos, F. X., Petrides, M., Jefferies, E., & Smallwood, J. (2016). Situating the default-mode network along a principal gradient of macroscale cortical organization. *Proceedings of the National Academy of Sciences*, 113(44), 12574–12579. <https://doi.org/10.1073/pnas.1608282113>
- Markello, R. D., Hansen, J. Y., Liu, Z.-Q., Bazinet, V., Shafiei, G., Suárez, L. E., Blostein, N., Seidlitz, J., Baillet, S., Satterthwaite, T. D., Chakravarty, M. M., Raznahan, A., & Misic, B. (2022). neuromaps: Structural and functional interpretation of brain maps. *Nature Methods*, 19(11), 1472–1479. <https://doi.org/10.1038/s41592-022-01625-w>
- Marquand, A., Rutherford, S., & Wolfers, T. (2024). Chapter 11—Normative modeling for clinical neuroscience. In K. Kay (Hrsg.), *Computational and Network Modeling of Neuroimaging Data* (S. 309–329). Academic Press. <https://doi.org/10.1016/B978-0-443-13480-7.00014-4>
- Martini, F. J., Guillamón-Vivancos, T., Moreno-Juan, V., Valdeolmillos, M., & López-Bendito, G. (2021). Spontaneous activity in developing thalamic and cortical sensory networks. *Neuron*, 109(16), 2519–2534. <https://doi.org/10.1016/j.neuron.2021.06.026>
- Masten, A. S., Lucke, C. M., Nelson, K. M., & Stallworthy, I. C. (2021). Resilience in Development and Psychopathology: Multisystem Perspectives. *Annual Review of Clinical Psychology*, 17, 521–549. <https://doi.org/10.1146/annurev-clinpsy-081219-120307>
- McEwen, B. S., Nasca, C., & Gray, J. D. (2016). Stress Effects on Neuronal Structure: Hippocampus, Amygdala, and Prefrontal Cortex. *Neuropsychopharmacology*, 41(1), 873–904. <https://doi.org/10.1038/npp.2015.171>
- McGee, A. W., Yang, Y., Fischer, Q. S., Daw, N. W., & Strittmatter, S. M. (2005). Experience-Driven Plasticity of Visual Cortex Limited by Myelin and Nogo Receptor. *Science*, 309(5744), 2222–2226. <https://doi.org/10.1126/science.1114362>
- McLaughlin, K. A., Colich, N. L., Rodman, A. M., & Weissman, D. G. (2020). Mechanisms linking childhood trauma exposure and psychopathology: A transdiagnostic model of risk and resilience. *BMC Medicine*, 18(1), 96. <https://doi.org/10.1186/s12916-020-01561-6>
- McLaughlin, K. A., Koenen, K. C., Hill, E. D., Petukhova, M., Sampson, N. A., Zaslavsky, A. M., & Kessler, R. C. (2013). Trauma Exposure and Posttraumatic Stress Disorder in a National Sample of Adolescents. *Journal of the American Academy of Child & Adolescent Psychiatry*, 52(8), 815–830.e14. <https://doi.org/10.1016/j.jaac.2013.05.011>
- McTeague, L. M., Huemer, J., Carreon, D. M., Jiang, Y., Eickhoff, S. B., & Etkin, A. (2017). Identification of Common Neural Circuit Disruptions in Cognitive Control Across Psychiatric Disorders. *American Journal of Psychiatry*, 174(7), 676–685. <https://doi.org/10.1176/appi.ajp.2017.16040400>
- Mesulam, M. M. (1998). From sensation to cognition. *Brain: A Journal of Neurology*, 121(6), 1013–1052. <https://doi.org/10.1093/brain/121.6.1013>
- Mount, C. W., & Monje, M. (2017). Wrapped to Adapt: Experience-Dependent Myelination. *Neuron*, 95(4), 743–756. <https://doi.org/10.1016/j.neuron.2017.07.009>

- Nelson, E. E., & Guyer, A. E. (2011). The development of the ventral prefrontal cortex and social flexibility. *Developmental Cognitive Neuroscience*, 1(3), 233–245. <https://doi.org/10.1016/j.dcn.2011.01.002>
- Newson, J. J., Pastukh, V., & Thiagarajan, T. C. (2021). Poor Separation of Clinical Symptom Profiles by DSM-5 Disorder Criteria. *Frontiers in Psychiatry*, 12. <https://doi.org/10.3389/fpsyt.2021.775762>
- Nieuwenhuys, R., & Broere, C. A. J. (2017). A map of the human neocortex showing the estimated overall myelin content of the individual architectonic areas based on the studies of Adolf Hopf. *Brain Structure and Function*, 222(1), 465–480. <https://doi.org/10.1007/s00429-016-1228-7>
- Norbom, L. B., Ferschmann, L., Parker, N., Agartz, I., Andreassen, O. A., Paus, T., Westlye, L. T., & Tamnes, C. K. (2021). New insights into the dynamic development of the cerebral cortex in childhood and adolescence: Integrating macro- and microstructural MRI findings. *Progress in Neurobiology*, 204, 102109. <https://doi.org/10.1016/j.pneurobio.2021.102109>
- Opel, N., Goltermann, J., Hermesdorf, M., Berger, K., Baune, B. T., & Dannlowski, U. (2020). Cross-Disorder Analysis of Brain Structural Abnormalities in Six Major Psychiatric Disorders: A Secondary Analysis of Mega- and Meta-analytical Findings From the ENIGMA Consortium. *Biological Psychiatry*, 88(9), 678–686. <https://doi.org/10.1016/j.biopsych.2020.04.027>
- Paquola, C., Bethlehem, R. A., Seidlitz, J., Wagstyl, K., Romero-Garcia, R., Whitaker, K. J., Vos De Wael, R., Williams, G. B., Vértes, P. E., Margulies, D. S., Bernhardt, B., & Bullmore, E. T. (2019a). Shifts in myeloarchitecture characterise adolescent development of cortical gradients. *eLife*, 8. <https://doi.org/10.7554/elife.50482>
- Paquola, C., Garber, M., Frässle, S., Royer, J., Zhou, Y., Tavakol, S., Rodriguez-Cruces, R., Cabalo, D. G., Valk, S., Eickhoff, S., Margulies, D. S., Evans, A., Amunts, K., Jefferies, E., Smallwood, J., & Bernhardt, B. C. (2024). *Architecture of the Human Default Mode Network: Cytoarchitecture, wiring and signal flow* (p. 2021.11.22.469533). bioRxiv. <https://doi.org/10.1101/2021.11.22.469533>
- Paquola, C., & Hong, S.-J. (2023). The Potential of Myelin-Sensitive Imaging: Redefining Spatiotemporal Patterns of Myeloarchitecture. *Biological Psychiatry*, 93(5), 442–454. <https://doi.org/10.1016/j.biopsych.2022.08.031>
- Paquola, C., Vos de Wael, R. V., Wagstyl, K., Bethlehem, R. A., Hong, S.-J., Seidlitz, J., Bullmore, E. T., Evans, A. C., Misic, B., & Margulies, D. S. (2019b). Microstructural and functional gradients are increasingly dissociated in transmodal cortices. *PLOS Biology*, 17(5), e3000284. <https://doi.org/10.1371/journal.pbio.3000284>
- Park, B., Kebets, V., Larivière, S., Hettwer, M. D., Paquola, C., van Rooij, D., Buitelaar, J., Franke, B., Hoogman, M., Schmaal, L., Veltman, D. J., van den Heuvel, O. A., Stein, D. J., Andreassen, O. A., Ching, C. R. K., Turner, J. A., van Erp, T. G. M., Evans, A. C., Dagher, A., ... Bernhardt, B. C. (2022). Multiscale neural gradients reflect transdiagnostic effects of major psychiatric conditions on cortical morphology. *Communications Biology*, 5(1), 1–14. <https://doi.org/10.1038/s42003-022-03963-z>
- Parkes, L., Moore, T. M., Calkins, M. E., Cook, P. A., Cieslak, M., Roalf, D. R., Wolf, D. H., Gur, R. C., Gur, R. E., Satterthwaite, T. D., & Bassett, D. S. (2021). Transdiagnostic dimensions of psychopathology explain individuals' unique deviations from normative neurodevelopment in brain structure. *Translational Psychiatry*, 11(1), 1–13. <https://doi.org/10.1038/s41398-021-01342-6>
- Patel, V., Saxena, S., Lund, C., Thornicroft, G., Baingana, F., Bolton, P., Chisholm, D., Collins, P. Y., Cooper, J. L., Eaton, J., Herrman, H., Herzallah, M. M., Huang, Y., Jordans, M. J. D., Kleinman, A., Medina-Mora, M. E., Morgan, E., Niaz, U., Omigbodun, O., ... Unützer, J. (2018). The Lancet Commission on global mental health and sustainable development. *The Lancet*, 392(10157), 1553–1598. [https://doi.org/10.1016/S0140-6736\(18\)31612-X](https://doi.org/10.1016/S0140-6736(18)31612-X)
- Patel, Y., Parker, N., Shin, J., Howard, D., French, L., Thomopoulos, S. I., Pozzi, E., Abe, Y., Abé, C., Anticevic, A., Alda, M., Aleman, A., Alloza, C., Alonso-Lana, S., Ameis, S. H., Anagnostou, E., McIntosh, A. A., Arango, C., Arnold, P. D., ... Paus, T. (2021). Virtual Histology of Cortical Thickness and Shared Neurobiology in 6 Psychiatric Disorders. *JAMA psychiatry*, 78(1), 47. <https://doi.org/10.1001/jamapsychiatry.2020.2694>
- Paus, T., Keshavan, M., & Giedd, J. N. (2008). Why do many psychiatric disorders emerge during

- adolescence? *Nature Reviews Neuroscience*, 9(12), 947–957. <https://doi.org/10.1038/nrn2513>
- Pierpaoli, C., Jezzard, P., Basser, P. J., Barnett, A., & Di Chiro, G. (1996). Diffusion tensor MR imaging of the human brain. *Radiology*, 201(3), 637–648. <https://doi.org/10.1148/radiology.201.3.8939209>
- Plana-Ripoll, O., Pedersen, C. B., Holtz, Y., Benros, M. E., Dalsgaard, S., De Jonge, P., Fan, C. C., Degenhardt, L., Ganna, A., & Greve, A. N. (2019). Exploring comorbidity within mental disorders among a Danish national population. *JAMA psychiatry*, 76(3), 259–270. <https://doi.org/0.1001/jamapsychiatry.2018.3658>
- Pollok, T. M., Kaiser, A., Kraaijenhanger, E. J., Monninger, M., Brandeis, D., Banaschewski, T., Eickhoff, S. B., & Holz, N. E. (2022). Neurostructural traces of early life adversities: A meta-analysis exploring age- and adversity-specific effects. *Neuroscience & Biobehavioral Reviews*, 135, 104589. <https://doi.org/10.1016/j.neubiorev.2022.104589>
- Radonjic, N. V., Hess, J. L., Rovira, P., Andreassen, O., Buitelaar, J. K., Ching, C. R. K., Franke, B., Hoogman, M., Jahanshad, N., McDonald, C., Schmaal, L., Sisodiya, S. M., Stein, D. J., van den Heuvel, O. A., van Erp, T. G. M., van Rooij, D., Veltman, D. J., Thompson, P., & Faraone, S. V. (2021). Structural brain imaging studies offer clues about the effects of the shared genetic etiology among neuropsychiatric disorders. *Mol Psychiatry*, (26), 2101–2110 <https://doi.org/10.1038/s41380-020-01002-z>
- Raznahan, A., Lerch, P., Lee, N., Greenstein, D., Wallace, L., Stockman, M., Clasen, L., Shaw, W., & Giedd, N. (2011). Patterns of Coordinated Anatomical Change in Human Cortical Development: A Longitudinal Neuroimaging Study of Maturational Coupling. *Neuron*, 72(5), 873–884. <https://doi.org/10.1016/j.neuron.2011.09.028>
- Repple, J., Gruber, M., Mauritz, M., de Lange, S. C., Winter, N. R., Opel, N., Goltermann, J., Meinert, S., Grotegerd, D., Leehr, E. J., Enneking, V., Borgers, T., Klug, M., Lemke, H., Waltemate, L., Thiel, K., Winter, A., Breuer, F., Grumbach, P., ... Dannlowski, U. (2023). Shared and Specific Patterns of Structural Brain Connectivity Across Affective and Psychotic Disorders. *Biological Psychiatry*, 93(2), 178–186. <https://doi.org/10.1016/j.biopsych.2022.05.031>
- Romer, A. L., Elliott, M. L., Knodt, A. R., Sison, M. L., Ireland, D., Houts, R., Ramrakha, S., Poulton, R., Keenan, R., Melzer, T. R., Moffitt, T. E., Caspi, A., & Hariri, A. R. (2021). Pervasively Thinner Neocortex as a Transdiagnostic Feature of General Psychopathology. *The American Journal of Psychiatry*, 178(2), 174–182. <https://doi.org/10.1176/appi.ajp.2020.19090934>
- Saberi, A., Paquola, C., Wagstyl, K., Hettwer, M. D., Bernhardt, B. C., Eickhoff, S. B., & Valk, S. L. (2023). The regional variation of laminar thickness in the human isocortex is related to cortical hierarchy and interregional connectivity. *PLOS Biology*, 21(11), e3002365. <https://doi.org/10.1371/journal.pbio.3002365>
- Schleicher, A., Amunts, K., Geyer, S., Morosan, P., & Zilles, K. (1999). Observer-Independent Method for Microstructural Parcellation of Cerebral Cortex: A Quantitative Approach to Cytoarchitectonics. *NeuroImage*, 9(1), 165–177. <https://doi.org/10.1006/nimg.1998.0385>
- Scrimin, S., Osler, G., Pozzoli, T., & Moscardino, U. (2018). Early adversities, family support, and child well-being: The moderating role of environmental sensitivity. *Child: Care, Health and Development*, 44(6), 885–891. <https://doi.org/10.1111/cch.12596>
- Segal, A., Parkes, L., Aquino, K., Kia, S. M., Wolfers, T., Franke, B., Hoogman, M., Beckmann, C. F., Westlye, L. T., Andreassen, O. A., Zalesky, A., Harrison, B. J., Davey, C. G., Soriano-Mas, C., Cardoner, N., Tiego, J., Yücel, M., Braganza, L., Suo, C., ... Fornito, A. (2023). Regional, circuit and network heterogeneity of brain abnormalities in psychiatric disorders. *Nature Neuroscience*, 26, 1–17. <https://doi.org/10.1038/s41593-023-01404-6>
- Segal, A., Tiego, J., Parkes, L., Holmes, A. J., Marquand, A. F., & Fornito, A. (2024). Embracing variability in the search for biological mechanisms of psychiatric illness. *Trends in Cognitive Sciences*, 0(0). <https://doi.org/10.1016/j.tics.2024.09.010>
- Sha, Z., van Rooij, D., Anagnostou, E., Arango, C., Auzias, G., Behrmann, M., Bernhardt, B., Bolte, S., Busatto, G. F., Calderoni, S., Calvo, R., Daly, E., Deruelle, C., Duan, M., Duran, F. L. S., Durston, S., Ecker, C., Ehrlich, S., Fair, D., ... Francks, C. (2022). Subtly altered topological asymmetry of brain structural covariance networks in autism spectrum disorder across 43 datasets from the ENIGMA consortium. *Molecular Psychiatry*, 27(4), 2114–2125. <https://doi.org/10.1038/s41380-022-01452-7>

- Shafiei, G., Markello, R. D., Makowski, C., Talpalaru, A., Kirschner, M., Devenyi, G. A., Guma, E., Hagmann, P., Cashman, N. R., Lepage, M., Chakravarty, M. M., Dagher, A., & Mišić, B. (2020). Spatial Patterning of Tissue Volume Loss in Schizophrenia Reflects Brain Network Architecture. *Biological Psychiatry*, 87(8), 727–735. <https://doi.org/10.1016/j.biopsych.2019.09.031>
- Sisk, L. M., & Gee, D. G. (2024). Developmental neuroplasticity and adversity-related risk for psychopathology. *Neuropsychopharmacology*, 50, 1–2. <https://doi.org/10.1038/s41386-024-01950-y>
- Sled, J. G. (2018). Modelling and interpretation of magnetization transfer imaging in the brain. *NeuroImage*, 182, 128–135. <https://doi.org/10.1016/j.neuroimage.2017.11.065>
- Solmi, M., Radua, J., Olivola, M., Croce, E., Soardo, L., Salazar de Pablo, G., Il Shin, J., Kirkbride, J. B., Jones, P., Kim, J. H., Kim, J. Y., Carvalho, A. F., Seeman, M. V., Correll, C. U., & Fusar-Poli, P. (2022). Age at onset of mental disorders worldwide: Large-scale meta-analysis of 192 epidemiological studies. *Molecular Psychiatry*, 27(1), 281–295. <https://doi.org/10.1038/s41380-021-01161-7>
- Sun, X., Sun, J., Lu, X., Dong, Q., Zhang, L., Wang, W., Liu, J., Ma, Q., Wang, X., Wei, D., Chen, Y., Liu, B., Huang, C.-C., Zheng, Y., Wu, Y., Chen, T., Cheng, Y., Xu, X., Gong, Q., ... Xia, M. (2023). Mapping Neurophysiological Subtypes of Major Depressive Disorder Using Normative Models of the Functional Connectome. *Biological Psychiatry*, 94(12), 936–947. <https://doi.org/10.1016/j.biopsych.2023.05.021>
- Sydnor, V. J., Larsen, B., Bassett, D. S., Alexander-Bloch, A., Fair, D. A., Liston, C., Mackey, A. P., Milham, M. P., Pines, A., Roalf, D. R., Seidlitz, J., Xu, T., Raznahan, A., & Satterthwaite, T. D. (2021). Neurodevelopment of the association cortices: Patterns, mechanisms, and implications for psychopathology. *Neuron*, 109(18), 2820–2846. <https://doi.org/10.1016/j.neuron.2021.06.016>
- Sydnor, V. J., Larsen, B., Seidlitz, J., Adebimpe, A., Alexander-Bloch, A. F., Bassett, D. S., Bertolero, M. A., Cieslak, M., Covitz, S., Fan, Y., Gur, R. E., Gur, R. C., Mackey, A. P., Moore, T. M., Roalf, D. R., Shinohara, R. T., & Satterthwaite, T. D. (2023). Intrinsic activity development unfolds along a sensorimotor–association cortical axis in youth. *Nature Neuroscience*, 26(4), 638–649. <https://doi.org/10.1038/s41593-023-01282-y>
- Takesian, A. E., & Hensch, T. K. (2013). Chapter 1—Balancing Plasticity/Stability Across Brain Development. In M. M. Merzenich, M. Nahum, & T. M. Van Vleet (Hrsg.), *Progress in Brain Research* (Bd. 207, S. 3–34). Elsevier. <https://doi.org/10.1016/B978-0-444-63327-9.00001-1>
- Taylor, J. J., Lin, C., Talmasov, D., Ferguson, M. A., Schaper, F. L. W. V. J., Jiang, J., Goodkind, M., Grafman, J., Etkin, A., Siddiqi, S. H., & Fox, M. D. (2023). A transdiagnostic network for psychiatric illness derived from atrophy and lesions. *Nature Human Behaviour*, 7(3), 420–429. <https://doi.org/10.1038/s41562-022-01501-9>
- Teffer, K., & Semendeferi, K. (2012). Human prefrontal cortex. In *Progress in Brain Research* (Bd. 195, pp. 191–218). Elsevier. <https://doi.org/10.1016/B978-0-444-53860-4.00009-X>
- Thompson, P. M., Stein, J. L., Medland, S. E., Hibar, D. P., Vasquez, A. A., Renteria, M. E., Toro, R., Jahanshad, N., Schumann, G., Franke, B., Wright, M. J., Martin, N. G., Agartz, I., Alda, M., Alhusaini, S., Almasy, L., Almeida, J., Alpert, K., Andreasen, N. C., ... Drevets, W. (2014). The ENIGMA Consortium: Large-scale collaborative analyses of neuroimaging and genetic data. *Brain Imaging and Behavior*, 8(2), 153–182. <https://doi.org/10.1007/s11682-013-9269-5>
- Tomasi, D., Wang, G.-J., & Volkow, N. D. (2013). Energetic cost of brain functional connectivity. *Proceedings of the National Academy of Sciences*, 110(33), 13642–13647. <https://doi.org/10.1073/pnas.1303346110>
- Tooley, U. A., Bassett, D. S., & Mackey, A. P. (2021). Environmental influences on the pace of brain development. *Nature Reviews Neuroscience*, 22(6), 372–384. <https://doi.org/10.1038/s41583-021-00457-5>
- Triarhou, L. C. (2007). The Economo-Koskinas Atlas Revisited: Cytoarchitectonics and Functional Context. *Stereotactic and functional neurosurgery*, 85(5), 195–203. <https://doi.org/10.1159/000103258>
- Valk, S. L., Kanske, P., Park, B., Hong, S.-J., Böckler, A., Trautwein, F.-M., Bernhardt, B. C., & Singer, T. (2023). Functional and microstructural plasticity following social and interoceptive mental training. *eLife*, 12, e85188. <https://doi.org/10.7554/eLife.85188>

- Valk, S. L., Xu, T., Margulies, D., Masouleh, S. K., Paquola, C., Goulas, A., Kochunov, P., Smallwood, J., Yeo, B. T. T., Bernhardt, B. C., & Eickhoff, S. B. (2020). Shaping brain structure: Genetic and phylogenetic axes of macroscale organization of cortical thickness. *Science Advances*, 6(39). <https://doi.org/DOI: 10.1126/sciadv.abb3417>
- van den Heuvel, M. P., Kahn, R. S., Goñi, J., & Sporns, O. (2012). High-cost, high-capacity backbone for global brain communication. *Proceedings of the National Academy of Sciences of the United States of America*, 109(28), 11372–7. <https://doi.org/10.1073/pnas.1203593109>
- van den Heuvel, M. P., & Sporns, O. (2013). Network hubs in the human brain. *Trends in cognitive sciences*, 17(12), 683–696.
- van der Meer, D., Shadrin, A. A., O’Connell, K., Bettella, F., Djurovic, S., Wolfers, T., Alnæs, D., Agartz, I., Smeland, O. B., Melle, I., Sánchez, J. M., Linden, D. E. J., Dale, A. M., Westlye, L. T., Andreassen, O. A., Frei, O., & Kaufmann, T. (2022). Boosting Schizophrenia Genetics by Utilizing Genetic Overlap With Brain Morphology. *Biological Psychiatry*, 92(4), 291–298. <https://doi.org/10.1016/j.biopsych.2021.12.007>
- van der Werff, S. J. A., van den Berg, S. M., Pannekoek, J. N., Elzinga, B. M., & van der Wee, N. J. A. (2013). Neuroimaging resilience to stress: A review. *Frontiers in Behavioral Neuroscience*, 7, 39. <https://doi.org/10.3389/fnbeh.2013.00039>
- Van Harmelen, A.-L., Kievit, R. A., Ioannidis, K., Neufeld, S., Jones, P. B., Bullmore, E., Dolan, R., The NSPN Consortium, Fonagy, P., & Goodyer, I. (2017). Adolescent friendships predict later resilient functioning across psychosocial domains in a healthy community cohort. *Psychological Medicine*, 47(13), 2312–2322. <https://doi.org/10.1017/S0033291717000836>
- Vanasse, T. J., Fox, P. T., Fox, P. M., Cauda, F., Costa, T., Smith, S. M., Eickhoff, S. B., & Lancaster, J. L. (2021). Brain pathology recapitulates physiology: A network meta-analysis. *Communications Biology*, 4(1), 301. <https://doi.org/10.1038/s42003-021-01832-9>
- VanBronkhorst, S. B., Abraham, E., Dambreville, R., Ramos-Olazagasti, M. A., Wall, M., Saunders, D. C., Monk, C., Alegria, M., Canino, G. J., Bird, H., & Duarte, C. S. (2024). Sociocultural Risk and Resilience in the Context of Adverse Childhood Experiences. *JAMA Psychiatry*, 81(4), 406–413. <https://doi.org/10.1001/jamapsychiatry.2023.4900>
- Vogt, C., & Vogt, O. (1919). *Allgemeine Ergebnisse unserer Hirnforschung*. J.A. Barth.
- Wannan, C. M. J., Croypley, V. L., Chakravarty, M. M., Bousman, C., Ganella, E. P., Bruggemann, J. M., Weickert, T. W., Weickert, C. S., Everall, I., McGorry, P., Velakoulis, D., Wood, S. J., Bartholomeusz, C. F., Pantelis, C., & Zalesky, A. (2019). Evidence for Network-Based Cortical Thickness Reductions in Schizophrenia. *American Journal of Psychiatry*, 176(7), 552–563. <https://doi.org/10.1176/appi.ajp.2019.18040380>
- Weiskopf, N., Edwards, L. J., Helms, G., Mohammadi, S., & Kirilina, E. (2021). Quantitative magnetic resonance imaging of brain anatomy and in vivo histology. *Nature Reviews Physics*, 3(8), 570–588. <https://doi.org/10.1038/s42254-021-00326-1>
- Whitaker, K. J., Vértes, P. E., Romero-Garcia, R., Váša, F., Moutoussis, M., Prabhu, G., Weiskopf, N., Callaghan, M. F., Wagstyl, K., Rittman, T., Tait, R., Ooi, C., Suckling, J., Inkster, B., Fonagy, P., Dolan, R. J., Jones, P. B., Goodyer, I. M., the NSPN Consortium, & Bullmore, E. T. (2016). Adolescence is associated with genomically patterned consolidation of the hubs of the human brain connectome. *Proceedings of the National Academy of Sciences*, 113(32), 9105–9110. <https://doi.org/10.1073/pnas.1601745113>
- WHO. (2022). *Mental disorders*. <https://www.who.int/news-room/fact-sheets/detail/mental-disorders>
- Xie, C., Xiang, S., Shen, C., Peng, X., Kang, J., Li, Y., Cheng, W., He, S., Bobou, M., Broulidakis, M. J., van Noort, B. M., Zhang, Z., Robinson, L., Vaidya, N., Winterer, J., Zhang, Y., King, S., Banaschewski, T., Barker, G. J., ... Feng, J. (2023). A shared neural basis underlying psychiatric comorbidity. *Nature Medicine*, 29(5), 1232–1242. <https://doi.org/10.1038/s41591-023-02317-4>
- Xin, W., & Chan, J. R. (2020). Myelin plasticity: Sculpting circuits in learning and memory. *Nature Reviews Neuroscience*, 21(12), 682–694. <https://doi.org/10.1038/s41583-020-00379-8>
- Xu, Z., Xia, M., Wang, X., Liao, X., Zhao, T., & He, Y. (2022). Meta-connectomic analysis maps consistent, reproducible, and transcriptionally relevant functional connectome hubs in the human brain. *Communications Biology*, 5(1), 1–17. <https://doi.org/10.1038/s42003-022-04028-x>
- Yang, Z., Wen, J., & Davatzikos, C. (2022). *Surreal-GAN: Semi-Supervised Representation Learning via GAN for uncovering heterogeneous disease-related imaging patterns* (arXiv:2205.04523).

- arXiv. <http://arxiv.org/abs/2205.04523>
- Yarkoni, T., Poldrack, R. A., Nichols, T. E., Van Essen, D. C., & Wager, T. D. (2011). Large-scale automated synthesis of human functional neuroimaging data. *Nature Methods*, 8(8), 665–670. <https://doi.org/10.1038/nmeth.1635>
- Yoshimura, S., Okamoto, Y., Matsunaga, M., Onoda, K., Okada, G., Kunisato, Y., Yoshino, A., Ueda, K., Suzuki, S., & Yamawaki, S. (2017). Cognitive behavioral therapy changes functional connectivity between medial prefrontal and anterior cingulate cortices. *Journal of Affective Disorders*, 208, 610–614. <https://doi.org/10.1016/j.jad.2016.10.017>
- Zhou, J., Gennatas, E. D., Kramer, J. H., Miller, B. L., & Seeley, W. W. (2012). Predicting Regional Neurodegeneration from the Healthy Brain Functional Connectome. *Neuron*, 73(6), 1216–1227. <https://doi.org/10.1016/j.neuron.2012.03.004>
- Ziegler, G., Hauser, T. U., Moutoussis, M., Bullmore, E. T., Goodyer, I. M., Fonagy, P., Jones, P. B., NSPN Consortium, Lindenberger, U., & Dolan, R. J. (2019). Compulsivity and impulsivity traits linked to attenuated developmental frontostriatal myelination trajectories. *Nature Neuroscience*, 22(6), 992–999. <https://doi.org/10.1038/s41593-019-0394-3>
- Zilles, K., & Amunts, K. (2015). Anatomical Basis for Functional Specialization. In K. Uludag, K. Ugurbil, & L. Berliner (Hrsg.), *fMRI: From Nuclear Spins to Brain Functions* (pp. 27–66). Springer US. https://doi.org/10.1007/978-1-4899-7591-1_4
- Zilles, K., Palomero-Gallagher, N., Grefkes, C., Scheperjans, F., Boy, C., Amunts, K., & Schleicher, A. (2002). Architectonics of the human cerebral cortex and transmitter receptor fingerprints: Reconciling functional neuroanatomy and neurochemistry. *European Neuropsychopharmacology*, 12(6), 587–599. [https://doi.org/10.1016/S0924-977X\(02\)00108-6](https://doi.org/10.1016/S0924-977X(02)00108-6)

8 Publications

Publications included in this thesis

Hettwer, M. D., Dorfschmidt, L., Puhlmann, L., ... Valk, S. L. (2024). Longitudinal variation in resilient psychosocial functioning is associated with ongoing cortical myelination and functional reorganization during adolescence. *Nature Communications*, 15(1), 6283.

Hettwer, M. D., Larivière, S., Park, B.-Y., van den Heuvel O. A., ... Eickhoff, S. B., Valk, S. L. (2022). Coordinated cortical thickness alterations across six neurodevelopmental and psychiatric disorders. *Nature Communications*, 13(1), 6851.

Peer-reviewed publications not subject to this thesis

Serio, B., **Hettwer, M. D.**, Wiersch, L. ... Valk, S. L. (2024) Sex differences in intrinsic functional cortical organization reflect differences in network topology rather than cortical morphometry. *Nature Communications*, 15(1), 7714.

Wan, B., Saberi, A., Paquola, C., Schaare, H. L., **Hettwer, M. D.**, Royer, J., ... & Valk, S. L. (2024). Microstructural asymmetry in the human cortex. *Nature Communications*, 15, 10124.

Saberi, A., Paquola, C., Wagstyl, K., **Hettwer, M. D.**, Bernhardt, B. C., Eickhoff, S. B., & Valk, S. L. (2023). The regional variation of laminar thickness in the human isocortex is related to cortical hierarchy and interregional connectivity. *PLoS biology*, 21(11), e3002365.

Hettwer, M. D., Lancaster, T. M., Raspor, E., Hahn, P. K., Mota, N. R., Singer, W., ... & Bittner, R. A. (2022). Evidence from imaging resilience genetics for a protective mechanism against schizophrenia in the ventral visual pathway. *Schizophrenia Bulletin*, 48(3), 551-562.

Park, B. Y., Kebets, V., Larivière, S., **Hettwer, M. D.**, Paquola, C., van Rooij, D., ... & Bernhardt, B. C. (2022). Multiscale neural gradients reflect transdiagnostic effects of major psychiatric conditions on cortical morphology. *Communications biology*, 5(1), 1-14.

Bayrak, Ş., de Wael, R. V., Schaare, H. L., **Hettwer, M. D.**, Caldairou, B., Bernasconi, A., ... & Valk, S. L. (2022). Heritability of hippocampal functional and microstructural organisation. *NeuroImage*, 264, 119656.

Sanfelici, R., Ruef, A., Antonucci, L. A., Penzel, N., Sotiras, A., Dong, M. S., ... **Hettwer, M. D.**, ...& PRONIA Consortium (2022). Novel Gyriification Networks Reveal Links with Psychiatric Risk Factors in Early Illness. *Cerebral Cortex*, 32(8), 1625-1636.

Preprints and commentaries

John, A., **Hettwer, M.D.**, Schaare, H.L., Saberi, A., Bayrak, S., Wan, B., Royer, J., Bernhardt, B.C., Valk, S.L. (2024). A Multimodal Characterization of Low-Dimensional Thalamocortical Structural Connectivity Patterns. *BioRxiv*.

Fan, Y.-S., Xu, Y., **Hettwer, M. D.**, Yang, P., Sheng, W., Wang, C., Yang, M., Kirschner, M., Valk, S. L., Chen, H. (2024). Neurodevelopmentally rooted epicenters in schizophrenia: sensorimotor-association spatial axis of cortical thickness alterations. *BioRxiv*.

Valk, S. & **Hettwer, M. D.** (2023). Commentary on ‘Reproducible brain-wide association studies require thousands of individuals’. *Aperture Neuro*, 1-2.

Hettwer, M. D., Saberi, A., Fan, Y. S., & Valk, S. L. (2022). Schizophrenia and Macroscale Brain Structure: Genes in Context. *Biological Psychiatry*, 92(4), 258-260.

9 Conference Contributions

Talk: Organization for Human Brain Mapping Conference (OHBM; Symposium: Non-specific neural P factor and multi-modal methods to obtaining disorder specific brain signatures), A cortical coordinate space of psychiatric vulnerability. Seoul, South Korea, 2024.

Talk: 49. Jahrestagung Psychologie und Gehirn (PuG; Symposium: Central nervous biomarkers of stress and resilience in the lab and in everyday life: What can be predicted and what needs to be considered?), Longitudinal trajectories of resilient psychosocial functioning link to ongoing cortical myelination and functional reorganization during adolescence. Hamburg, Germany, 2024.

Talk: Organization for Human Brain Mapping Conference (OHBM; Session: General Psychopathology and Psychosis), System-level cortical maturation links to adolescent resilience to adverse life events. Montreal, Canada, 2023.

- Merit Award Recipient

Talk: Organization for Human Brain Mapping Conference (OHBM; Session: Psychiatric Neuroimaging: Methods and Applications), Coordinated Cortical Thickness alterations across mental disorders: A transdiagnostic ENIGMA study. Glasgow, Scotland, 2022.

Talk: Gradients of Brain Organization Pre-OHBM Workshop (Session: Clinical and Cognitive Perspectives), Transdiagnostic gradients capture coordinated cortical thickness alterations across mental disorders. Cambridge, UK, 2022.

Poster: FLUX, Longitudinal trajectories of resilient psychosocial functioning link to ongoing cortical myelination and functional reorganization during adolescence. Baltimore, USA, 2024.

- Travel Award Recipient

Poster: Organization for Human Brain Mapping Conference (OHBM), System-level cortical maturation links to adolescent resilience to adverse life events. Montreal, Canada, 2023.

Poster: Gradients of Brain Organization Pre-OHBM Workshop, System-level cortical maturation links to adolescent resilience to adverse life events. Montreal, Canada, 2023.

Poster: Organization for Human Brain Mapping Conference (OHBM; Session: Psychiatric Neuroimaging: Methods and Applications), Coordinated Cortical Thickness alterations across mental disorders: A transdiagnostic ENIGMA study. Glasgow, Scotland, 2022.

10 Acknowledgements

I would like to thank the mentors, colleagues, family, and friends who supported me throughout this PhD journey!

My gratitude goes to:

My mentors, Dr. Sofie Valk and Prof. Dr. Simon Eickhoff. Thank you for welcoming me to the FZ Jülich / UKD / MPI-Leipzig world, for your continuous mentorship, and for giving me the freedom, trust and support to do the research I was interested in. Thanks for your confidence and brave ‘just do it’ mindsets that pushed me into (by me) uncharted territories and onto scarily big stages.

Prof. Dr. Tobias Kalenscher, who welcomed me into the Psychology Department and was always open for friendly and helpful discussions. I very much appreciate it!

The whole CNG lab! In particular Bianca, for our discussions and for being an amazing office mate, Lina, my inspiration and focus-aligner, Alex, my partner in crime for coffee breaks, Amin, my coding role model, Katerina, my Seoul travel buddy, Sarah, for our happy walks, and Neville, for the team spirit.

The Max Planck School of Cognition, in particular Cohort 2020. I loved going through this PhD journey together with a fun group of people! Thank you, Jenni, for being my first MPS-Cog friend and the friend who sat next to me in Max Planck’s Tegernsee apartment when I signed this thesis.

Meiner Familie und FreundInnen, für ihre liebevolle Unterstützung.

Meinem Vater Manni, der mein Studium immer aus voller Überzeugung unterstützt hat und mich in Münster, Frankfurt, München und Leipzig stets mit Fahrradflückzeug und Kuchen im Gepäck besucht hat. Meiner Mutter Uli, deren inspirierende Art, stets positiv gestimmt ihren Interessen zu folgen, ein großes Vorbild bleibt, und die sich sehr über diese PhD Reise gefreut hätte. Meiner Schwester Eva und ihrem Mann Justus, die immer ein offenes Ohr für die Hochs und Tiefs hatten, meine größten Cheerleader waren und jeden kleinen Meilenstein mit mir gefeiert haben. Der Rest meiner Familie, die sich stets über kurze Doktorarbeitsupdates, noch mehr aber über Fotos von Konferenzreisen gefreut hat.

Ariane, die durch unsere Freundschaft nicht nur den Kunstunterricht in Göttingen, sondern auch meine Zeit in Leipzig unschätzbar bereichert und geprägt hat. Danke für deine alternativen Denkanstöße, das gute italienische Essen und deine Leichtigkeit. Vera, ‘my fellow non-biologist’ im frankfurter Neuromaster und nun im PhD, der ich für stundenlange Telefonierspaziergänge durch Köln / Jülich / Leipzig / Philadelphia danke. FreundInnen aus verschiedensten Lebensabschnitten, ganz besonders Swenja, Vany, Eva, Yoko, Klara, Lina, Lioba und Malin.

I would also like to thank the open science initiatives that made this work possible.

11 Author Declaration

Ich versichere an Eides Statt, dass die Dissertation von mir selbständig und ohne unzulässige fremde Hilfe unter Beachtung der „Grundsätze zur Sicherung guter wissenschaftlicher Praxis an der Heinrich-Heine-Universität Düsseldorf“ erstellt worden ist.

Date: _____ Signature: _____

12 Appendix

Contains:

Supplementary information for Study 1

Supplementary information for Study 2

12.1 Supplementary Material for: Coordinated cortical thickness alterations across six neurodevelopmental and psychiatric disorders

Hettwer, M. D., Larivière, S., Park, B. Y., van den Heuvel, O. A., Schmaal, L., Andreassen, O. A., Ching, C. R. K., Hoogman, M., Buitelaar, J., van Rooij, D., Veltman, D. J., Stein, D. J., Franke, B., van Erp, T. G. M., ENIGMA ADHD Working Group, ENIGMA Autism Working Group, ENIGMA Bipolar Disorder Working Group, ENIGMA Major Depression Working Group, ENIGMA OCD Working Group, ENIGMA Schizophrenia Working Group, Jahanshad, N., Thompson, P. M., Thomopoulos, S. I., Bethlehem, R. A. I., Bernhardt, B. C., Eickhoff, S. B., Valk, S. L. (2022). Coordinated cortical thickness alterations across six neurodevelopmental and psychiatric disorders. *Nature communications*, 13(1), 6851. <https://doi.org/10.1038/s41467-022-34367-6>

Contains:

Supplementary Methods

Supplementary Results

Figures S1-S7

Tables S1-S3

References

Supplementary Methods

Population connectivity data

Population connectivity data was derived from a healthy young adult sample ($n=207$; 83 males, mean age \pm SD=28.73 \pm 3.73 years, range=22-36 years) from the Human Connectome Project (HCP; Van Essen et al., 2012). Resting-state functional data underwent distortion and motion corrections, intensity inhomogeneity corrections and intensity normalization, brain extraction, normalization to MNI152 space and projection onto the cortical surface. Pre-processing of diffusion MRI data included b0 intensity normalization as well as corrections for head motion, susceptibility distortion and eddy currents. Both functional and structural connectivity data was parcellated according to the Desikan-Killiany atlas (Desikan et al., 2006).

Subject-level functional connectivity matrices were generated by pair-wise correlations between time series of 68 cortical parcels and 12 sub-cortical structures. Z-scored subject-level data was accumulated to derive a group-average functional connectome (Larivière et al., 2021). Structural connectivity matrices included in the ENIGMA Toolbox (Larivière et al., 2021) are based on anatomically constrained tractography, where reconstructed streamlines were generated for 68 parcels and 12 sub-cortical structures. Using distance-dependent thresholding, a group-average structural connectome was derived and log-transformed.

Spin tests

Wherever possible, we implemented spin tests as included in the ENIGMA Toolbox to assess the significance of spatial similarities via permutations. Spatial permutation tests correct for auto-correlations between smooth spatial maps by generating null models of respective spatial overlaps. That is, coordinates of cortical data are inflated to a sphere and rotated 1000 times, matching phenotypic data to different parcels in every permutation (Alexander-Bloch et al., 2018; Larivière et al., 2021). This step is repeated for both maps. Significance is determined by testing initial correlation coefficients against the null distributions retrieved by correlating rotated spatial maps.

Supplementary Discussion

Association between co-alteration hubs, shared susceptibility, and epicenters

For a better understanding of what is reflected in transdiagnostic co-alteration hubs (**Supplementary Figure S1A**), we further examined their association with the topography of shared susceptibility and cortical thickness increases compared to decreases. First, we took the absolute Cohen's d maps for each disorder and rescaled each map between 0-1 to get the spatial patterns of illness effects independent from offsets in average effect between disorders. We then took the mean of the six resulting maps to receive a "hit map", where regions with values close to 6 (due to the number of included disorders) are most strongly and consistently affected across disorders (**Supplementary Figure S1B**). Second, we thresholded each Cohen's d map to get the top 20% percent of regions showing thickness decreases or increases, respectively. We then binarized and summed these maps to observe which regions most strongly and consistently show thickness increases or reductions across disorders (**Supplementary Figure S1C&D**). Last, we computed potential disease epicenters as described in the Main text using the "hit map" instead of co-alteration hubs to examine to which degree epicenters indeed relate to shared impact rather than coordinated impact (**Supplementary Figure S1E&F**).

Robustness of cross-disorder co-alteration network hubs

In order to assess stability of cross-disorder co-alteration hub maps, we recreated hub maps based on cross-disorder inter-regional correlation matrices thresholded at 90%, 70% and 50%. All three alternative hub maps correlated significantly with original co-alteration hubs (90% threshold: $r = 0.78$; 70% threshold: $r = 0.91$; 50% threshold: $r = 0.62$; all $p_{spin} < .0001$). Correcting the cross-disorder co-alteration matrix for sample sizes via a partial correlation did not impact resulting hubs (correlation of n -corrected co-alteration hub map with original co-alteration hub map: $r = 0.89$, $p_{spin} < .0001$; **Supplementary Figure S2A**).

Robustness of transdiagnostic gradients

To assess robustness of the first two transdiagnostic gradients, we compared them to gradients derived from manipulating analysis steps in the gradient computation and changing parameters in the BrainSpace Toolbox (Vos de Wael et al., 2020) (see **Supplementary Figure S2B**). First, since there were generalized differences in the strength of disease impact on cortical thickness across disorders, we mean-corrected the initial correlation matrix by using a partial correlation coefficient. Gradients computed based on this mean-corrected matrix correlated highly with original gradients (G1: $r = 0.94$; G2: $r = 0.87$; both $p_{spin} < .0001$). Second, original gradients correlated highly with gradients derived

using a different non-linear dimension reduction method (Laplacian eigenmap: G1: $r = 1$; G2: $r = 0.99$; both $p_{spin} < .0001$) or a linear dimension reduction method (principal component analysis: G1: $r = 1$; G2: $r = 0.99$; both $p_{spin} < .0001$). Third, even though data was normally distributed, it yielded relatively sparse data points for each inter-regional correlation. We therefore tested whether the use of Spearman's rho instead of Pearson's r in computing the initial correlation matrix influences gradient organization. Gradients based on Spearman's rho correlation coefficients correlated highly with the original gradients (Spearman: G1: $r = 0.94$; G2: $r = 0.84$). Fourth, gradients were not impacted by correcting for sample sizes of underlying disorder samples as tested by including sample sizes as covariates in the computation of the cross-disorder co-alteration matrix via partial correlation (G1: $r = 0.99$; G2: $r = 0.96$; both $p_{spin} < .0001$). Last, original gradients also correlated highly with gradients for which cut-off values (i.e. sparsity) of the correlation matrix was manipulated (sparsity of 90%: G1: $r = 0.97$; G2: $r = 0.92$; sparsity of 70%: G1: $r = 0.99$; G2: $r = 0.96$; sparsity of 50%: G1: $r = 0.94$; G2: $r = 0.80$; all $p_{spin} < .05$). Overall, original gradients were robust against multiple parameter manipulations.

Influence of individual disorders on gradient organization

To assess whether gradient organization was differentially impacted by individual disorders, we performed leave-one-disorder-out analyses and correlated resulting gradients with original gradients G1 and G2 (**Supplementary Figure S2B**). We observed that gradients were generally robust against leaving out single disorders (w/o ADHD: $r_{G1} = 0.95$; $r_{G2} = 0.77$; w/o BD: $r_{G1} = 0.99$; $r_{G2} = 0.86$; w/o SCZ: $r_{G1} = 0.98$; $r_{G2} = 0.94$; w/o OCD: $r_{G1} = 0.99$; $r_{G2} = 0.83$; w/o MDD: $r_{G1} = 0.99$; $r_{G2} = 0.97$; all $p_{spin} < .0001$). However, this was not the case for ASD (without ASD: $r_{G1} = 0.10$; $r_{G2} = 0.01$). Leaving out ASD in gradient computations appeared to lead to a switch in features to be reflected in principal and secondary gradients, as was observed in significant correlations of the principal gradient without ASD with the original G2 ($r = 0.86$, $p_{spin} < .001$) and of the secondary gradient without ASD with the original G2 ($r = 0.48$, $p_{spin} < 0.01$). This finding is not surprising, as cortical thickness alterations in ASD show a spatial pattern that is highly similar to G1 and thus likely strengthens the weight of features then represented in G1.

The third to eighth gradients of transdiagnostic co-alteration in cortical thickness

We additionally studied the third to eighth transdiagnostic gradients which are depicted in **Supplementary Figure S3**. The third gradient traversed from sensory-limbic to lateral temporal cortex, while the fourth segregated (para)limbic from lateral prefrontal regions. The fifth gradient had a bilateral axis in orbitofrontal and limbic cortex on the one hand, and superior parietal cortex on the other hand. The sixth gradient was characterized by hemispheric asymmetry, distinguishing entorhinal and superior temporal sulcus from the temporoparietal junction and paracentral lobule in the left hemisphere, but

lingual gyrus and cuneus from paracentral lobule and pars triangularis in the right hemisphere. Lastly, the seventh gradient captured a segregation between sensory-limbic and heteromodal cortices.

G1 captures segregation of functional disease epicenters

As we noticed that frontal and temporal disease epicenters appear to be segregated by G1 (see **Supplementary Figure S4**) suggesting differential impact on co-alteration network organization, we performed a follow up analysis to confirm this assumption. In order to evaluate whether whole-brain cross-disorder disease impact shows different covariance patterns for frontal and temporal epicenters, we i) extracted cross-disorder inter-regional correlations from the 68 x 68 correlation matrix (see **Figure 1C & 2A** of the main manuscript) for all frontal and temporal disease epicenters, respectively, and computed their degree centrality as the sum of all correlations of each epicenter parcel. ii) We extracted cross-disorder whole-brain structural covariance for two representative epicenters, the left *pars orbitalis* and entorhinal cortex, which emerged as the two strongest (functional) epicenters. Both approaches revealed that frontal epicenters show covariance of disease impact across wide-spread regions of the cortex, whereas temporal epicenters show highest regional correlations within temporal, and no correlations with frontal regions (see **Supplementary Figure S5**).

Distribution of NeuroSynth functional terms along gradient bins

In addition to the 2D space framed by the two transdiagnostic gradients within which cognitive terms were situated, see **Figure 2F** of the main manuscript, we also investigated the position of cognitive terms along each gradient separately. Following the same strategy and using the same 24 NeuroSynth cognitive terms, we binned each gradient into five-percentile bins. Regions of the same bin formed a region of interest (ROI), yielding 20 ROIs for each gradient. These ROIs were then tested for their overlap with meta-analytic ROIs associated with each of the 24 cognitive terms via z-statistics. The magnitude of an average z-value at a ROI (i.e., a position along the gradient) reflects the strength of its association with a certain functional task activation. We sorted the topic terms by their weighted mean position along both gradients, revealing systematic shifts in functional networks along transdiagnostic axes of co-alteration (**Figure S6**). While G1 segregated sensory ('auditory', 'multisensory') from higher order cognitive functions ('Cognitive control', 'inhibition'), G2 distinguished sensory ('auditory', 'multisensory') from perception/attention related functions ('visuospatial', 'attention').

Disorder-specific epicenters and their overlap with transdiagnostic epicenters

In order to investigate to which degree transdiagnostic epicenters are also observed in each disorder, we repeated the epicenter mapping approach using normative HCP connectivity data (rs-fMRI and DTI) in

combination with ENIGMA Cohen's d maps. For each disorder, we systematically correlated each parcel's normative functional or structural connectivity profile with the absolute Cohen's d map and identified parcel's at $p_{spin} < 0.05$ as potential disease epicenters. We then computed the overlap between disorder-specific and transdiagnostic epicenters in percent (See **Supplementary Figure S7**).

Supplementary Figures

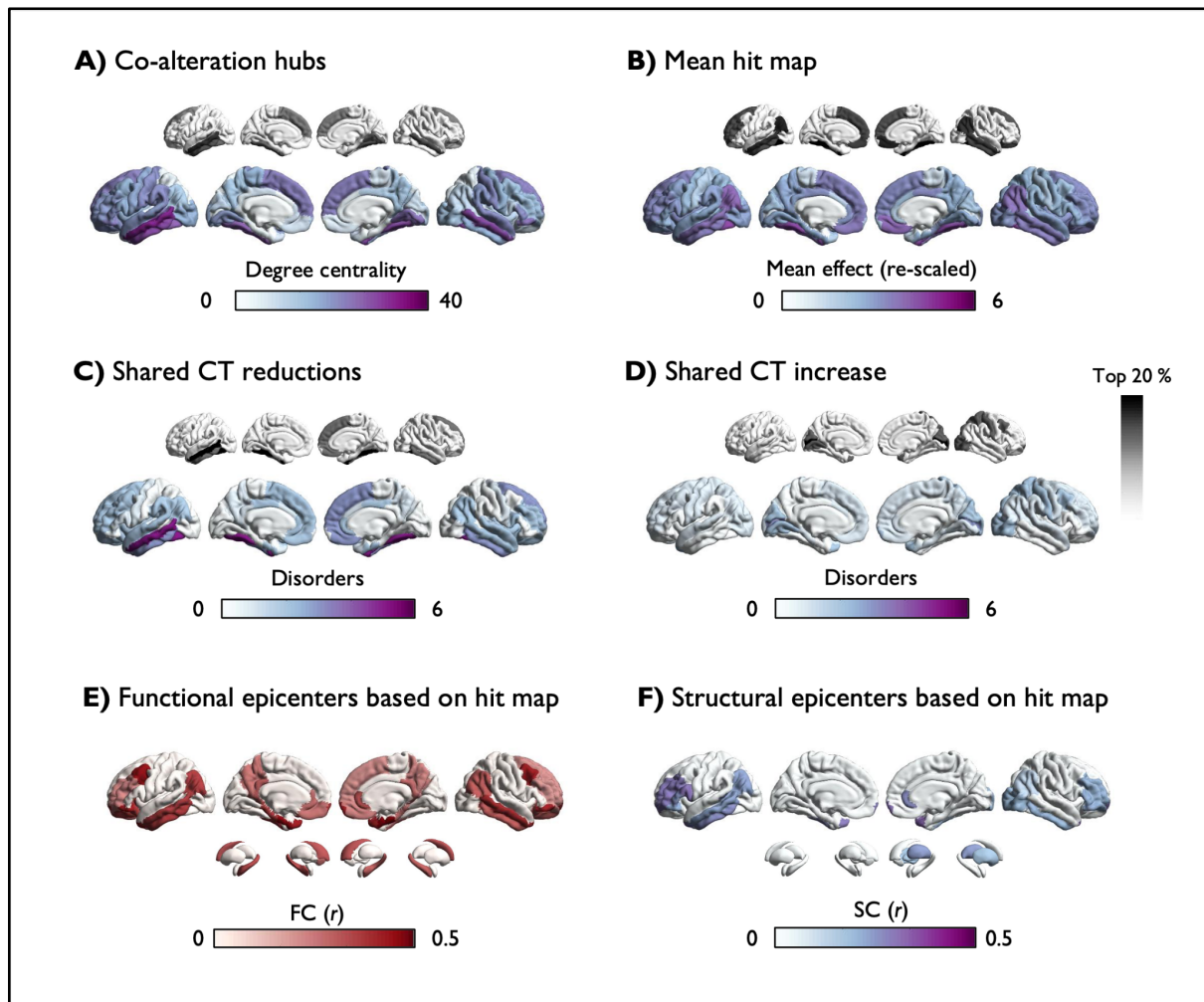


Figure S1. Correspondence between Co-alteration hubs, shared illness effects, and epicenters. **A)** Co-alteration hubs. **B)** Hit map based on average absolute Cohen's d values, rescaled between 0 and 1 within disorders. Overlaps in cortical thickness (CT) reductions (**C**) and increase (**D**). In subplots **A - D**), black and white brain images show a thresholded version (top 20%) of the brain image in the same subplot. **E)** and **F)** depict disease epicenters computed based on the hit map (**B**) for functional and structural connectivity, respectively.

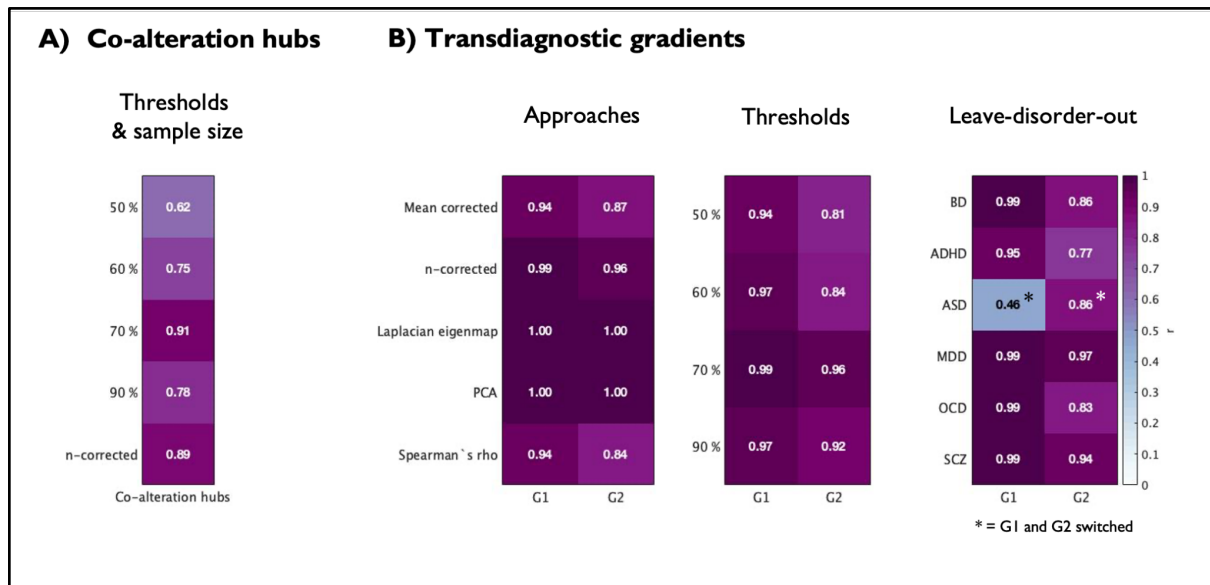


Figure S2. Robustness of co-alteration hubs and transdiagnostic gradients to parameter manipulations. Values indicate correlation with original hubs/gradients after parameter manipulation. **A)** Co-alteration hubs based on co-alteration matrix with different cut-offs or corrected for sample-size (n-corrected) per disorder. **B)** Left: Corrected for average illness effects and sample size, or Laplacian eigenmap or principal component analysis (PCA) as dimensionality reduction techniques, or co-alterations based on spearman's rho. Middle: Co-alteration matrix cut-offs. Right: Constructing gradients based on five disorders only, highlighting the contribution of single disorders. *G1 and G2 are switched for autism spectrum disorder (ASD). BD = Bipolar disorder, ADHD = Attention-deficit/hyperactivity disorder, MDD = Major depressive disorder, OCD = Obsessive compulsive disorder, SCZ = Schizophrenia spectrum disorder.

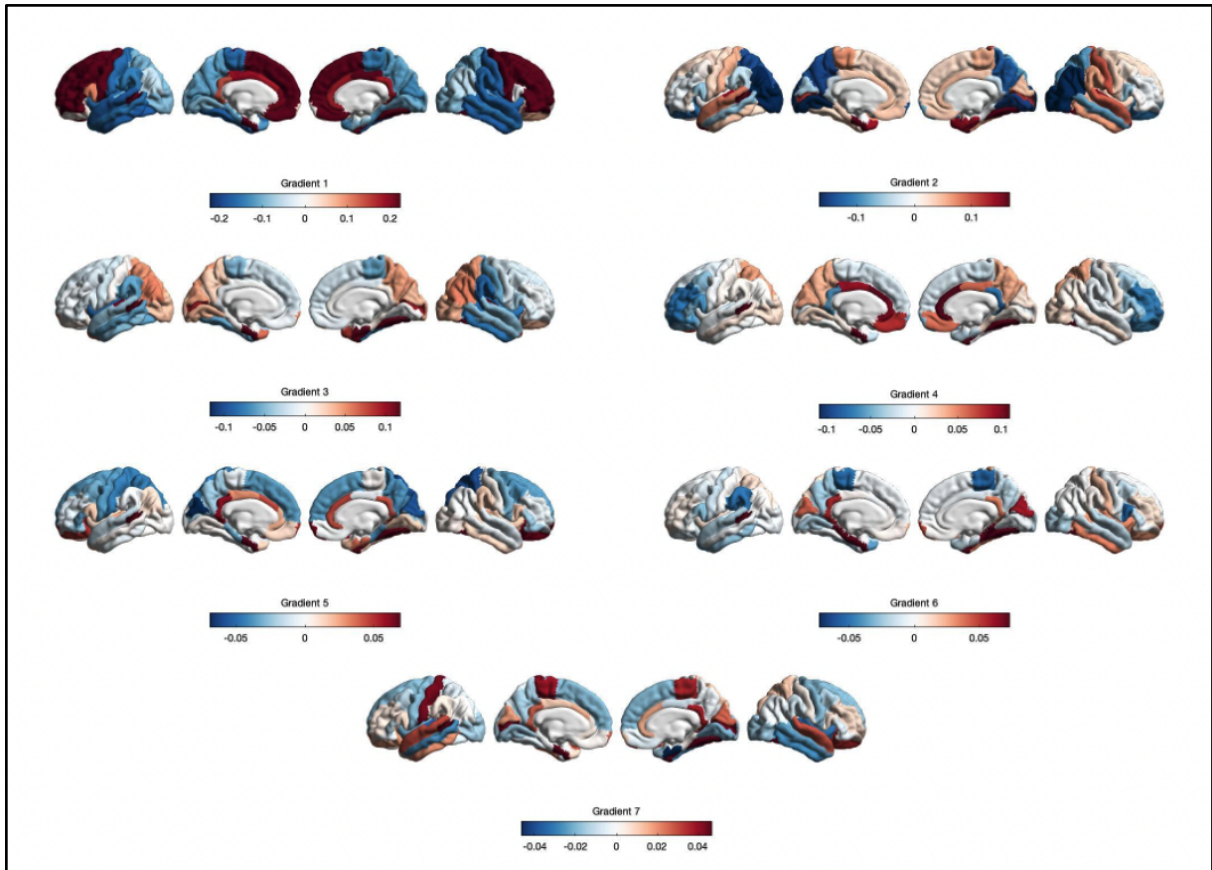


Figure S3. *Overview of all gradients computed from cross-disorder correlation matrix using diffusion embedding.*

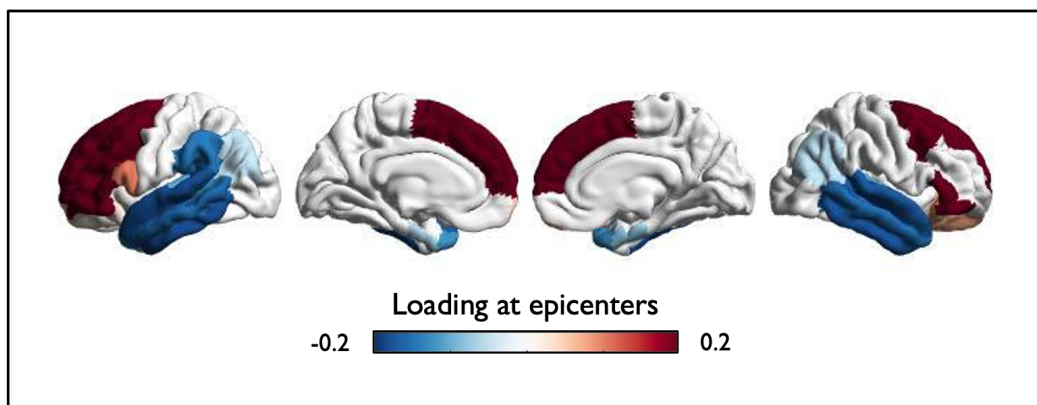


Figure S4. *Gradient loadings at epicenters.* Principal axis (G1) masked by significant functional epicenters, demonstrating that epicenters are strongly placed towards apices of the gradient. Red and blue colors indicate opposite apices of G1.

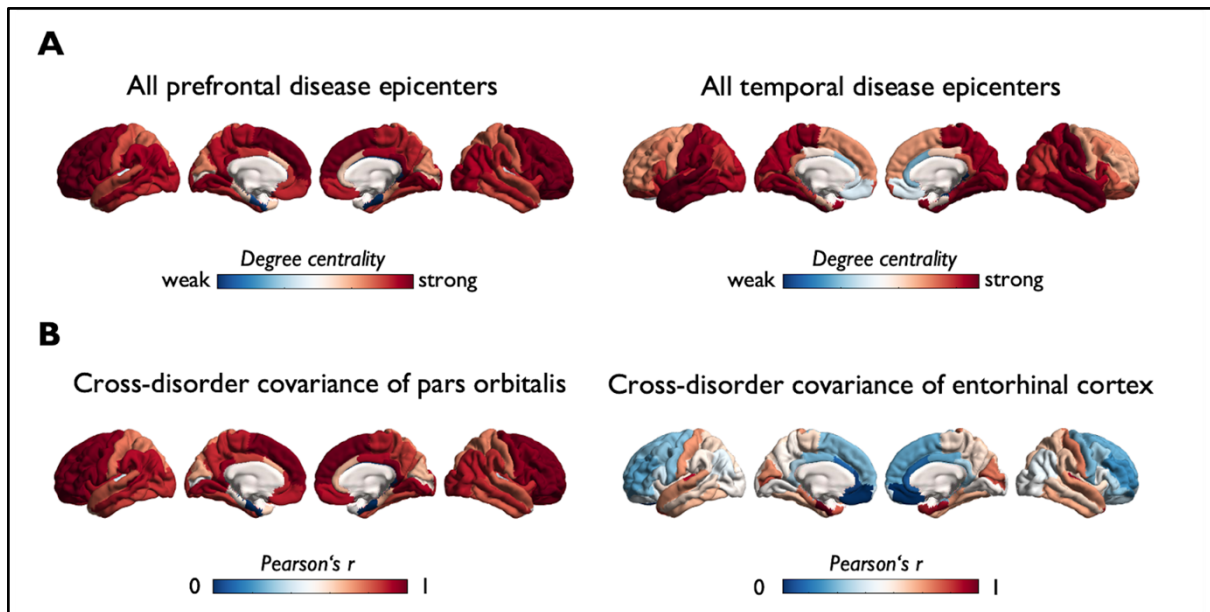


Figure S5. *G1* captures segregation of functional disease epicenters. **A)** Depicts degree centrality of frontal (left) and temporal (right) functional disease epicenters computed based on whole-brain covariance of cross-disorder disease impact for respective frontal and temporal parcels. **B)** Shows isolated covariance patterns for the two most likely disease epicenters representative for frontal and temporal structures.

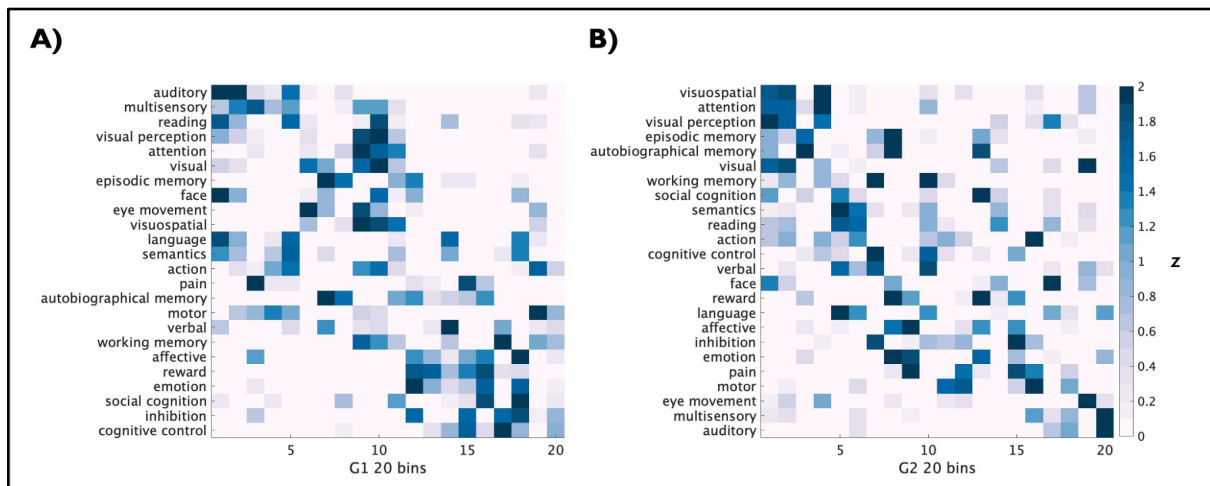


Figure S6. Meta-analysis for 24 cognitive terms obtained from NeuroSynth (Yarkoni et al., 2011) along the principal (*G1*) and secondary gradient (*G2*). We computed parcel-wise *z*-statistics, capturing node-function associations, and calculated the center of gravity of each function along 20 five-percentile bins of *G1* (**A**) and *G2* (**B**). Function terms are ordered by the weighted mean of their location along the gradients.

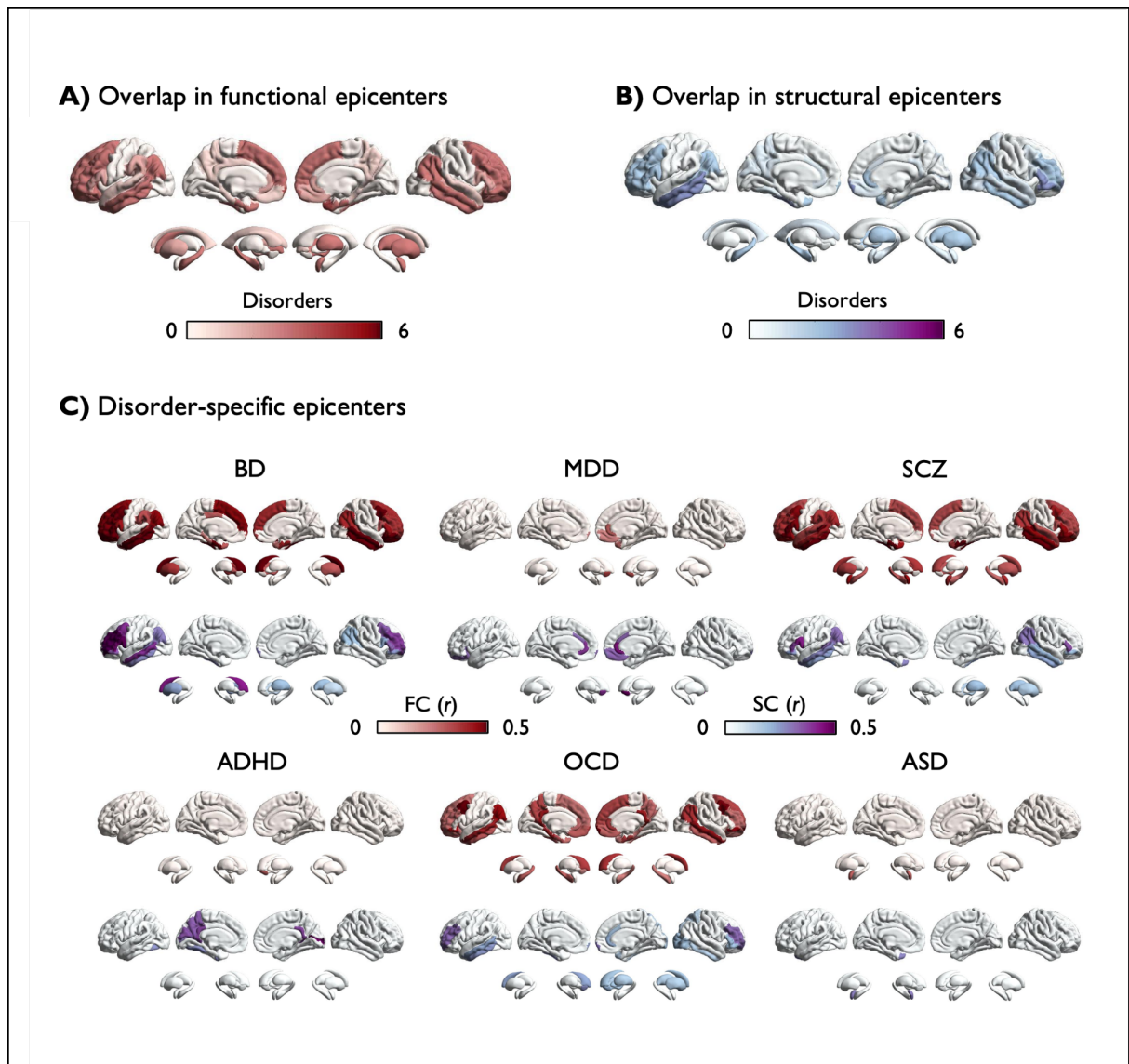


Figure S7. Overlaps in disorder-specific disease epicenters. In order to examine to which degree transdiagnostic epicenters also reflect individual disorder's epicenters, we quantified the overlap of functional (A) and structural (B) epicenters. Epicenter maps for each disorder were binarized, labeling a region as epicenter or no epicenter, and then summed, reflecting in how many disorders a region forms an epicenter. Epicenter maps for individual disorders are depicted in C).

Supplementary Tables

Table S1. Cohen's d values describing case-control differences in cortical thickness for 6 mental disorders used for transdiagnostic analyses.

ROI	ADHD	ASD	BD	MDD	OCD	SCZ
<i>L banks sts</i>	0.01	-0.07	-0.21	-0.06	-0.06	-0.35
<i>L caudal anterior cingulate</i>	-0.11	0.03	-0.10	-0.04	0.00	-0.12
<i>L caudal middle frontal</i>	-0.02	0.06	-0.27	-0.01	-0.09	-0.36
<i>L cuneus</i>	0.11	-0.06	-0.06	0.05	-0.04	-0.20
<i>L entorhinal</i>	-0.06	-0.24	-0.04	-0.04	-0.06	-0.20
<i>L fusiform</i>	-0.01	-0.19	-0.29	-0.12	-0.11	-0.49
<i>L inferior parietal</i>	0.08	-0.05	-0.27	-0.06	-0.14	-0.36
<i>L inferior temporal</i>	0.00	-0.16	-0.25	-0.05	-0.09	-0.45
<i>L isthmus cingulate</i>	0.04	0.05	-0.13	-0.10	-0.07	-0.31
<i>L lateral occipital</i>	0.14	-0.02	-0.16	-0.02	-0.07	-0.33
<i>L lateral orbitofrontal</i>	0.03	0.00	-0.22	-0.05	-0.10	-0.40
<i>L lingual</i>	0.11	-0.02	-0.21	0.01	-0.05	-0.35
<i>L medial orbitofrontal</i>	-0.08	0.08	-0.20	-0.13	-0.08	-0.23
<i>L middle temporal</i>	0.02	-0.12	-0.25	-0.09	-0.09	-0.44
<i>L parahippocampal</i>	0.10	-0.11	-0.02	-0.07	-0.06	-0.28
<i>L paracentral</i>	-0.01	-0.05	-0.14	0.00	-0.01	-0.25
<i>L pars opercularis</i>	-0.01	-0.03	-0.29	-0.06	-0.08	-0.38
<i>L pars orbitalis</i>	-0.01	0.04	-0.25	-0.07	-0.05	-0.32
<i>L pars triangularis</i>	-0.03	0.05	-0.27	-0.05	-0.03	-0.34
<i>L pericalcarine</i>	0.04	-0.01	0.02	0.09	0.01	-0.08
<i>L postcentral</i>	0.05	-0.07	-0.10	0.04	-0.02	-0.26
<i>L posterior cingulate</i>	-0.11	0.05	-0.11	-0.10	-0.07	-0.30
<i>L precentral</i>	-0.06	0.09	-0.21	-0.02	-0.02	-0.34
<i>L precuneus</i>	0.04	-0.08	-0.21	-0.02	-0.10	-0.30
<i>L rostral anterior cingulate</i>	-0.09	0.01	-0.15	-0.13	-0.07	-0.18
<i>L rostral middle frontal</i>	0.03	0.11	-0.28	-0.04	-0.10	-0.36
<i>L superior frontal</i>	-0.04	0.11	-0.23	-0.07	-0.07	-0.43
<i>L superior parietal</i>	0.10	-0.09	-0.16	-0.01	-0.06	-0.21
<i>L superior temporal</i>	0.04	-0.15	-0.21	0.01	-0.01	-0.44

Supplementary Material for Study 1

<i>L supramarginal</i>	0.02	-0.09	-0.25	-0.05	-0.05	-0.40
<i>L frontal pole</i>	0.08	0.04	-0.12	-0.01	-0.05	-0.21
<i>L temporal pole</i>	-0.02	-0.14	-0.12	0.01	0.03	-0.25
<i>L transverse temporal</i>	-0.02	-0.24	-0.12	-0.04	0.00	-0.25
<i>L insula</i>	-0.01	-0.09	-0.20	-0.11	-0.07	-0.41
<i>R bankssts</i>	0.01	-0.07	-0.13	-0.07	0.01	-0.36
<i>R caudal anterior cingulate</i>	-0.11	0.03	-0.06	-0.08	-0.04	-0.15
<i>R caudal middle frontal</i>	-0.02	0.06	-0.21	0.01	-0.08	-0.32
<i>R cuneus</i>	0.11	-0.06	-0.03	0.05	-0.03	-0.23
<i>R entorhinal</i>	-0.06	-0.24	-0.08	-0.06	0.01	-0.15
<i>R fusiform</i>	-0.01	-0.19	-0.27	-0.12	-0.09	-0.54
<i>R inferior parietal</i>	0.08	-0.05	-0.26	-0.04	-0.14	-0.35
<i>R inferior temporal</i>	0.00	-0.16	-0.19	-0.12	-0.06	-0.44
<i>R isthmus cingulate</i>	0.04	0.05	-0.18	-0.07	-0.05	-0.31
<i>R lateral occipital</i>	0.14	-0.02	-0.22	0.01	-0.07	-0.34
<i>R lateral orbitofrontal</i>	0.03	0.00	-0.21	-0.12	-0.11	-0.36
<i>R lingual</i>	0.11	-0.02	-0.20	-0.01	-0.04	-0.39
<i>R medial orbitofrontal</i>	-0.08	0.08	-0.23	-0.13	-0.10	-0.24
<i>R middle temporal</i>	0.02	-0.12	-0.22	-0.09	-0.10	-0.38
<i>R parahippocampal</i>	0.10	-0.11	-0.09	-0.06	-0.08	-0.29
<i>R paracentral</i>	-0.01	-0.05	-0.14	-0.01	0.01	-0.22
<i>R pars opercularis</i>	-0.01	-0.03	-0.25	-0.02	-0.06	-0.42
<i>R pars orbitalis</i>	-0.01	0.04	-0.24	-0.07	-0.07	-0.34
<i>R pars triangularis</i>	-0.03	0.05	-0.23	-0.03	-0.06	-0.37
<i>R pericalcarine</i>	0.04	-0.01	0.02	0.08	0.03	-0.09
<i>R postcentral</i>	0.05	-0.07	-0.08	0.03	0.04	-0.28
<i>R posterior cingulate</i>	-0.11	0.05	-0.17	-0.09	-0.06	-0.31
<i>R precentral</i>	-0.06	0.09	-0.18	-0.02	-0.04	-0.32
<i>R precuneus</i>	0.04	-0.08	-0.19	0.01	-0.10	-0.30
<i>R rostral anterior cingulate</i>	-0.09	0.01	-0.09	-0.10	0.01	-0.12
<i>R rostral middle frontal</i>	0.03	0.11	-0.26	-0.04	-0.09	-0.31
<i>R superior frontal</i>	-0.04	0.11	-0.26	-0.08	-0.04	-0.40
<i>R superior parietal</i>	0.10	-0.09	-0.16	0.03	-0.05	-0.22
<i>R superior temporal</i>	0.04	-0.15	-0.19	-0.03	0.01	-0.44

Supplementary Material for Study 1

<i>R supramarginal</i>	0.02	-0.09	-0.18	-0.05	0.00	-0.39
<i>R frontal pole</i>	0.08	0.04	-0.10	-0.06	0.02	-0.21
<i>R temporal pole</i>	-0.02	-0.14	-0.06	0.01	0.02	-0.24
<i>R transverse temporal</i>	-0.02	-0.24	-0.11	-0.05	-0.02	-0.26
<i>R insula</i>	-0.01	-0.09	-0.17	-0.12	-0.07	-0.41

Cohen's d values were accessed through the ENIGMA Toolbox (Larivière et al., 2021) and for adult samples (except for Autism spectrum disorder (ASD), for which data was only available for a pooled sample including younger subjects). Data was collected and analyzed by respective ENIGMA working groups (Attention-deficit/hyperactivity disorder (ADHD) (Hoogman et al., 2019), Autism spectrum disorder (ASD) (van Rooij et al., 2018), Bipolar disorder (BD) (Hibar et al., 2018), Major depressive disorder (MDD) (Schmaal et al., 2017), Obsessive compulsive disorder (OCD) (Boedhoe et al., 2018), Schizophrenia (SCZ) (van Erp et al., 2018)) and adjusted for different combinations of age, sex, scan site/scanner differences, intracranial volume, and intelligence quotient effects (see Supplementary **Table S2**). ROI = Region of interest.

Table S2. Sample Demographics.

Disorder	sites	Weighted mean age (cases)	Weighted mean age (controls)	<i>n</i>	Covariates
Schizophrenia spectrum (van Erp et al., 2018)	39	32.3 ^a	34.5 ^a	Cases: 4474 Controls: 5098 Total: 9572	age, sex, scan site
Attention deficit hyperactivity disorder (Hoogman et al., 2019)	36	32.97		Cases: 733 Controls: 539 Total: 1272	age, sex, scan site*
Autism spectrum disorder (van Rooij et al., 2018)	49	15.4	15.8	Cases: 1571 Controls: 1651 Total: 3222	age, sex, IQ, scan site*
Bipolar disorder (Hibar et al., 2018)	28	38.4 ^a	35.6 ^a	Cases: 1837 Controls: 2582 Total: 4419	age, sex, scan site*
Major depressive disorder (Schmaal et al., 2017)	20	44.8 ^a	54.6 ^a	Cases: 1911 Controls: 7663 Total: 9574	age, sex, scan site
Obsessive-compulsive disorder (Boedhoe et al., 2018)	27	32.1	30.5	Cases: 1498 Controls: 1436 Total: 2934	age, sex, scan site

Adapted from Radonjic et al. (2021). ^a = weighted mean computed by Radonjic et al. (2021). * = In this study, site was included as a random effect in a mixed-effect model and not as a covariate. IQ = Intelligence quotient.

Table S3. 232 Genes for which spatial transcription patterns correlated significantly with the principal transdiagnostic gradient ($P_{spin} < .01$).

<i>Gene symbol</i>	<i>r</i>	<i>P_{spin}</i>
<i>PRRX1</i>	0.8	0.002
<i>ZIC1</i>	0.74	0.001
<i>CTXN3</i>	0.71	0.001
<i>RPH3AL</i>	0.7	0.001
<i>CD6</i>	0.69	0.004
<i>LAMA2</i>	0.68	0.003
<i>HSPB8</i>	0.67	0.001
<i>KRT31</i>	0.67	0.001
<i>WNT10A</i>	0.67	0.002
<i>ACTC1</i>	0.67	0.002
<i>YBX2</i>	0.66	0
<i>GORAB</i>	0.65	0.003
<i>FOXF2</i>	0.65	0.009
<i>CCDC80</i>	0.64	0
<i>CD38</i>	0.64	0.005
<i>TCERG1L</i>	0.64	0.001
<i>TEX30</i>	0.64	0.003
<i>NRP1</i>	0.64	0.008
<i>CREB3L3</i>	0.63	0.002
<i>SPRY4</i>	0.63	0.001
<i>CBLN2</i>	0.62	0.004
<i>PCDH10</i>	0.62	0.001
<i>FAM213A</i>	0.62	0.003
<i>SULF1</i>	0.62	0.007
<i>HDAC9</i>	0.62	0.001
<i>ARHGAP25</i>	0.61	0.007
<i>RTP1</i>	0.6	0.004
<i>AEBP1</i>	0.6	0.002
<i>TSPAN33</i>	0.6	0.003
<i>PROCA1</i>	0.6	0.004
<i>TNFRSF14</i>	0.59	0.004
<i>RBPI</i>	0.59	0.001
<i>WFDC1</i>	0.59	0.006
<i>GALNT16</i>	0.59	0.005
<i>AZIN2</i>	0.58	0
<i>MRAP2</i>	0.58	0.006
<i>DBX2</i>	0.58	0.007
<i>ERICH1</i>	0.58	0
<i>OVOL2</i>	0.58	0.003

<i>ZC2HC1A</i>	0.58	0.006
<i>SCRG1</i>	0.58	0.001
<i>ITGA8</i>	0.58	0.005
<i>KCNN2</i>	0.58	0.001
<i>NT5DC2</i>	0.58	0.005
<i>HSPB3</i>	0.57	0.007
<i>CYP51A1</i>	0.57	0.008
<i>TMEM117</i>	0.57	0.007
<i>C6orf62</i>	0.57	0.002
<i>ATP2C2</i>	0.56	0.002
<i>CHRNA6</i>	0.56	0.002
<i>BAIAP2L2</i>	0.55	0.003
<i>TNC</i>	0.55	0.002
<i>RAB3C</i>	0.55	0.007
<i>VIT</i>	0.55	0.005
<i>NECTIN3</i>	0.55	0.001
<i>ZIC3</i>	0.55	0.001
<i>PPEF1</i>	0.55	0.003
<i>COL11A1</i>	0.55	0.007
<i>LINC02217</i>	0.55	0.003
<i>HRH3</i>	0.55	0.007
<i>GPR26</i>	0.55	0
<i>MEIS3P1</i>	0.55	0.003
<i>TMTC3</i>	0.54	0.001
<i>TGFB1</i>	0.54	0.008
<i>CCDC110</i>	0.54	0.008
<i>CMTM4</i>	0.54	0.005
<i>NANOS3</i>	0.54	0.001
<i>ASB6</i>	0.53	0.004
<i>MELTF</i>	0.53	0.001
<i>ASB2</i>	0.53	0.004
<i>FLJ30901</i>	0.53	0.006
<i>TRAF3</i>	0.53	0.008
<i>PLCH1</i>	0.52	0.009
<i>CLIC5</i>	0.52	0.005
<i>ADTRP</i>	0.51	0.008
<i>CASC10</i>	0.51	0.007
<i>BNIP3</i>	0.51	0.006
<i>MGAT4C</i>	0.51	0.009
<i>STBD1</i>	0.5	0.009
<i>PCDHB4</i>	0.5	0.006

Supplementary Material for Study 1

<i>CLU</i>	0.5	0.005
<i>CCNYL1</i>	0.5	0.001
<i>PCBP3</i>	0.49	0.009
<i>MPPED1</i>	0.49	0.003
<i>MPP6</i>	0.49	0.007
<i>SCYL3</i>	0.49	0.008
<i>GMPPB</i>	0.49	0.006
<i>GBAP1</i>	0.49	0.008
<i>SC5D</i>	0.49	0.004
<i>GULP1</i>	0.49	0
<i>SMPD1</i>	0.49	0.007
<i>GRM3</i>	0.49	0.007
<i>NMNAT3</i>	0.49	0.005
<i>PNPLA3</i>	0.48	0.008
<i>CAMK1G</i>	0.48	0.006
<i>GOLPH3L</i>	0.48	0.001
<i>ZNF704</i>	0.48	0.007
<i>GKAP1</i>	0.48	0.006
<i>TUBA4A</i>	0.47	0.008
<i>SORCS2</i>	0.47	0.003
<i>TFRC</i>	0.47	0.008
<i>DUSP6</i>	0.47	0.008
<i>CNIH3</i>	0.47	0.003
<i>LRRC4C</i>	0.47	0.008
<i>FREM3</i>	0.47	0.009
<i>ATP7A</i>	0.47	0.009
<i>RNF182</i>	0.47	0.007
<i>ITGB5</i>	0.46	0.007
<i>C2orf40</i>	0.46	0.001
<i>CCDC102B</i>	0.46	0.007
<i>DACT3</i>	0.46	0.005
<i>HACD1</i>	0.46	0.009
<i>COL23A1</i>	0.46	0.006
<i>PART1</i>	0.45	0.009
<i>DCUN1D3</i>	0.45	0.004
<i>SNORC</i>	0.45	0.004
<i>NXPH2</i>	0.45	0.009
<i>OSTN</i>	0.44	0.006
<i>ADCYAP1</i>	0.44	0.004
<i>DUSP3</i>	0.44	0.006
<i>RTP4</i>	0.42	0.009
<i>SLC6A13</i>	0.42	0.005
<i>PTPA</i>	0.42	0.007

<i>TAPT1</i>	0.42	0.009
<i>TUBA1B</i>	0.42	0.003
<i>TCIM</i>	0.41	0.005
<i>HCN3</i>	0.41	0.009
<i>PIK3CD</i>	0.41	0.009
<i>CNTNAP2</i>	0.4	0.008
<i>FAM234B</i>	0.4	0.003
<i>RRP8</i>	0.4	0.008
<i>OSCAR</i>	0.4	0.009
<i>KAT5</i>	0.4	0.006
<i>LOC108783654</i>	0.4	0.009
<i>SLC25A42</i>	0.4	0.009
<i>HDAC5</i>	0.39	0.006
<i>TRMT61A</i>	0.38	0.006
<i>NRSN1</i>	0.37	0.004
<i>GPR22</i>	0.37	0.008
<i>LRRC32</i>	0.37	0.003
<i>TRABD2A</i>	0.37	0.009
<i>PLK3</i>	0.37	0.008
<i>PRKX</i>	0.36	0.009
<i>KLF11</i>	0.35	0.007
<i>GNLY</i>	0.35	0.009
<i>TMEM232</i>	0.34	0.007
<i>PEX16</i>	-0.29	0.006
<i>FAM163B</i>	-0.3	0.008
<i>ZFYVE27</i>	-0.31	0.009
<i>IGFBPL1</i>	-0.33	0.009
<i>ALPK1</i>	-0.34	0.005
<i>LINC00167</i>	-0.34	0.004
<i>ANAPC13</i>	-0.35	0.004
<i>DUSP11</i>	-0.36	0.008
<i>VAMP5</i>	-0.37	0.009
<i>ZBTB49</i>	-0.37	0.003
<i>TBC1D17</i>	-0.38	0.005
<i>FAM118B</i>	-0.38	0.005
<i>MPPE1</i>	-0.38	0.009
<i>BCL2L11</i>	-0.39	0.008
<i>MAML3</i>	-0.4	0.002
<i>NELFA</i>	-0.4	0.009
<i>EXOSC2</i>	-0.4	0.005
<i>ZNF766</i>	-0.4	0.009
<i>ZNF594</i>	-0.41	0.006
<i>SRSF11</i>	-0.41	0.009

Supplementary Material for Study 1

PKP2	-0.41	0.009
SRSF4	-0.41	0.004
APIG2	-0.41	0.007
CCDC59	-0.42	0.008
ZNF781	-0.42	0.008
DDI2	-0.43	0.008
CXorf56	-0.44	0.007
HAUS4	-0.44	0.004
OLFML2A	-0.44	0.009
GPR83	-0.45	0.001
EPCAM	-0.45	0.007
SPEF1	-0.45	0.005
RNASEH1	-0.45	0.005
LDB1	-0.46	0.007
AGAP11	-0.46	0.005
LOC100130950	-0.46	0.009
TMEM19	-0.47	0.001
LOC100131289	-0.47	0.008
MRPL50	-0.47	0.003
MINPP1	-0.47	0.003
GPHN	-0.48	0.006
CRABP2	-0.48	0.003
LONRF3	-0.48	0.007
ALKBH5	-0.48	0.007
ACKR1	-0.49	0.006
STRIP2	-0.49	0.002
ITFG2	-0.49	0.007
WNT2B	-0.49	0.002
FBXO3	-0.49	0.007
ZFP37	-0.5	0.002
FGD1	-0.5	0.003
HEATR3	-0.5	0.007
GPR19	-0.5	0.007
TAP2	-0.5	0.003
HSD17B11	-0.5	0.008
BTBD3	-0.51	0.001
KRTCAP3	-0.51	0.006
PAM	-0.52	0.008
VCX	-0.52	0.007
ANKRD20A11P	-0.52	0.005
PATJ	-0.53	0.001
MTHFD2L	-0.54	0.007
FBXO11	-0.54	0.009

PLOD2	-0.54	0.005
RIPK1	-0.54	0.009
DPP6	-0.54	0.008
WNT3	-0.55	0.008
GREB1L	-0.55	0.005
SDHAF4	-0.56	0.008
MST1R	-0.56	0.008
PDGFD	-0.56	0.005
TENM4	-0.57	0.006
THSD7A	-0.57	0.007
SLFN11	-0.58	0.005
LAMP5	-0.58	0.002
ZNF662	-0.58	0.002
TPTE2P1	-0.59	0.005
CDH12	-0.61	0.007
DSP	-0.62	0.004
SLC17A6	-0.66	0.006
CPLX2	-0.67	0.001
ANKRD20A5P	-0.69	0.002
C15orf59	-0.69	0.003
COL27A1	-0.71	0.002
WDR97	-0.71	0.003
LXN	-0.73	0

Table S4. Link between principal (G1) and secondary (G2) transdiagnostic axes of pathological covariance and disease-specific Cohen's d maps.

	ADHD	ASD	BD	MDD	SCZ	OCD
G1	$r = -0.52,$ $p_{spin} = 0.002$	$r = 0.82,$ $p_{spin} = 0.001$	n.s.	n.s.	n.s.	$r = -0.20,$ $p_{spin} = 0.021$
G2	$r = -0.58,$ $p_{spin} < .0001$	$r = -0.26,$ $p_{spin} = 0.050$	$r = 0.42,$ $p_{spin} = 0.001$	n.s.	$r = 0.24,$ $p_{spin} = 0.041$	$r = 0.6,$ $p_{spin} = 0.001$

Supplementary References

- Alexander-Bloch, A. F., Shou, H., Liu, S., Satterthwaite, T. D., Glahn, D. C., Shinohara, R. T., Vandekar, S. N., & Raznahan, A. (2018). On testing for spatial correspondence between maps of human brain structure and function. *Neuroimage*, 178, 540–551. <https://doi.org/10.1016/j.neuroimage.2018.05.070>
- Boedhoe, P. S. W., Schmaal, L., Abe, Y., Alonso, P., Ameis, S. H., Anticevic, A., Arnold, P. D., Batistuzzo, M. C., Benedetti, F., Beucke, J. C., Bollettini, I., Bose, A., Brem, S., Calvo, A., Calvo, R., Cheng, Y., Cho, K. I. K., Ciullo, V., Dallspezia, S., ... Enigma Ocd Working Group. (2018). Cortical Abnormalities Associated With Pediatric and Adult Obsessive-Compulsive Disorder: Findings From the ENIGMA Obsessive-Compulsive Disorder Working Group. *Am J Psychiatry*, 175(5), 453–462. <https://doi.org/10.1176/appi.ajp.2017.17050485>
- Desikan, R. S., Ségonne, F., Fischl, B., Quinn, B. T., Dickerson, B. C., Blacker, D., Buckner, R. L., Dale, A. M., Maguire, R. P., & Hyman, B. T. (2006). An automated labeling system for subdividing the human cerebral cortex on MRI scans into gyral based regions of interest. *Neuroimage*, 31(3), 968–980.
- Hibar, D. P., Westlye, L. T., Doan, N. T., Jahanshad, N., Cheung, J. W., Ching, C. R. K., Versace, A., Bilderbeck, A. C., Uhlmann, A., Mwangi, B., Kramer, B., Overs, B., Hartberg, C. B., Abe, C., Dima, D., Grotegerd, D., Sprooten, E., Boen, E., Jimenez, E., ... Andreassen, O. A. (2018). Cortical abnormalities in bipolar disorder: An MRI analysis of 6503 individuals from the ENIGMA Bipolar Disorder Working Group. *Mol Psychiatry*, 23(4), 932–942. <https://doi.org/10.1038/mp.2017.73>
- Hoogman, M., Muetzel, R., Guimaraes, J. P., Shumskaya, E., Mennes, M., Zwiers, M. P., Jahanshad, N., Sudre, G., Wolfers, T., Earl, E. A., Soliva Vila, J. C., Vives-Gilabert, Y., Khadka, S., Novotny, S. E., Hartman, C. A., Heslenfeld, D. J., Schweren, L. J. S., Ambrosino, S., Oranje, B., ... Franke, B. (2019). Brain Imaging of the Cortex in ADHD: A Coordinated Analysis of Large-Scale Clinical and Population-Based Samples. *Am J Psychiatry*, 176(7), 531–542. <https://doi.org/10.1176/appi.ajp.2019.18091033>
- Larivière, S., Paquola, C., Park, B., Royer, J., Wang, Y., Benkarim, O., Vos de Wael, R., Valk, S. L., Thomopoulos, S. I., Kirschner, M., Lewis, L. B., Evans, A. C., Sisodiya, S. M., McDonald, C. R., Thompson, P. M., & Bernhardt, B. C. (2021). The ENIGMA Toolbox: Multiscale neural contextualization of multisite neuroimaging datasets. *Nature Methods*, 18(7), 698–700. <https://doi.org/10.1038/s41592-021-01186-4>
- Radonjic, N. V., Hess, J. L., Rovira, P., Andreassen, O., Buitelaar, J. K., Ching, C. R. K., Franke, B., Hoogman, M., Jahanshad, N., McDonald, C., Schmaal, L., Sisodiya, S. M., Stein, D. J., van den Heuvel, O. A., van Erp, T. G. M., van Rooij, D., Veltman, D. J., Thompson, P., & Faraone, S. V. (2021). Structural brain imaging studies offer clues about the effects of the shared genetic etiology among neuropsychiatric disorders. *Mol Psychiatry*, 26, 2101–2110. <https://doi.org/10.1038/s41380-020-01002-z>
- Schmaal, L., Hibar, D. P., Samann, P. G., Hall, G. B., Baune, B. T., Jahanshad, N., Cheung, J. W., van Erp, T. G. M., Bos, D., Ikram, M. A., Vernooij, M. W., Niessen, W. J., Tiemeier, H., Hofman, A., Wittfeld, K., Grabe, H. J., Janowitz, D., Bulow, R., Selonke, M., ... Veltman, D. J. (2017). Cortical abnormalities in adults and adolescents with major depression based on brain scans from 20 cohorts worldwide in the ENIGMA Major Depressive Disorder Working Group. *Mol Psychiatry*, 22(6), 900–909. <https://doi.org/10.1038/mp.2016.60>
- van Erp, T. G. M., Walton, E., Hibar, D. P., Schmaal, L., Jiang, W., Glahn, D. C., Pearlson, G. D., Yao, N., Fukunaga, M., Hashimoto, R., Okada, N., Yamamori, H., Bustillo, J. R., Clark, V. P., Agartz, I., Mueller, B. A., Cahn, W., de Zwarte, S. M. C., Hulshoff Pol, H. E., ... Turner, J. A. (2018). Cortical Brain Abnormalities in 4474 Individuals With Schizophrenia and 5098 Control Subjects via the Enhancing Neuro Imaging Genetics Through Meta Analysis (ENIGMA) Consortium. *Biol Psychiatry*, 84(9), 644–654. <https://doi.org/10.1016/j.biopsych.2018.04.023>
- Van Essen, D. C., Ugurbil, K., Auerbach, E., Barch, D., Behrens, T. E. J., Bucholz, R., Chang, A., Chen, L., Corbetta, M., Curtiss, S. W., Della Penna, S., Feinberg, D., Glasser, M. F., Harel, N., Heath, A. C., Larson-Prior, L., Marcus, D., Michalareas, G., Moeller, S., ... Yacoub, E. (2012). The Human Connectome Project: A data acquisition perspective. *Neuroimage*, 62(4), 2222–2231. <https://doi.org/10.1016/j.neuroimage.2012.02.018>
- van Rooij, D., Anagnostou, E., Arango, C., Auzias, G., Behrmann, M., Busatto, G. F., Calderoni, S., Daly, E., Deruelle, C., Di Martino, A., Dinstein, I., Duran, F. L. S., Durston, S., Ecker, C., Fair, D., Fedor, J., Fitzgerald, J., Freitag, C. M., Gallagher, L., ... Buitelaar, J. K. (2018). Cortical and Subcortical Brain Morphometry Differences Between Patients With Autism Spectrum Disorder and Healthy Individuals

- Across the Lifespan: Results From the ENIGMA ASD Working Group. *Am J Psychiatry*, 175(4), 359-369.
<https://doi.org/10.1176/appi.ajp.2017.17010100>
- Vos de Wael, R., Benkarim, O., Paquola, C., Lariviere, S., Royer, J., Tavakol, S., Xu, T., Hong, S. J., Langs, G., Valk, S., Misic, B., Milham, M., Margulies, D., Smallwood, J., & Bernhardt, B. C. (2020). BrainSpace: A toolbox for the analysis of macroscale gradients in neuroimaging and connectomics datasets. *Commun Biol*, 3(1), 103.. <https://doi.org/10.1038/s42003-020-0794-7>
- Yarkoni, T., Poldrack, R. A., Nichols, T. E., Van Essen, D. C., & Wager, T. D. (2011). Large-scale automated synthesis of human functional neuroimaging data. *Nature Methods*, 8(8), 665-670.
<https://doi.org/10.1038/nmeth.1635>

12.2 Supplementary Material for: Longitudinal variation in resilient psychosocial functioning is associated with ongoing cortical myelination and functional reorganization during adolescence

Hettwer, M. D., Dorfschmidt, L., Puhlmann, L., Jacob, L. M., Paquola, C., Bethlehem, R. A., NSPN Consortium, Bullmore, E. T., Eickhoff, S. B., Valk, S. L. (2024). Longitudinal variation in resilient psychosocial functioning is associated with ongoing cortical myelination and functional reorganization during adolescence. *Nature Communications*, 15(1), 1-15.

Contains:

Supplementary Results
Supplementary Methods
Supplementary Table S1-S3
Supplementary Figures S1-S11
NSPN Consortium author list
Supplementary References

Supplementary Results

Distribution of distress scores and resilient psychosocial functioning with respect to demographics

Having derived distress scores (see Supplementary **Table S1** for loadings) and resilient psychosocial functioning (Res_{PSF}) scores and their intra-individual rates of change (Δ), we tested whether scores differed between self-reported sexes or as an effect of age (see Supplementary **Table S2** for statistics). In the larger sample of 712 individuals, we observed significantly higher Res_{PSF} and lower distress levels in males than in females. This sex difference was not significant in the smaller sample ($n = 141$) included in the imaging analyses. Neither Res_{PSF} nor distress scores were significantly associated with age. Intra-individual change in Res_{PSF} and distress showed no sex or age effects in neither sub-sample. As change in Res_{PSF} was the main behavioral variable of interest in the current study and did not show a significant sex difference, we did not perform further sex-stratified analyses.

Table S1. Factor loadings of questionnaires included for the computation of a general distress factor.

<i>Item</i>	<i>Loading</i>		
ypq 84 no good at all	0.803	ypq 53 hurt fussed	0.649
ypq 89 useless	0.783	ypq 42 others dislike way	0.647
ypq 92 failure	0.782	ypq 24 bad person	0.644
ypq 51 others happier	0.769	ypq 66 bad nothing wrong	0.643
ypq 23 hated myself	0.769	ypq 72 unsure right things	0.642
ypq 08 no good any more	0.767	ypq 60 against me	0.639
ypq 45 alone with people	0.755	ypq 09 blame myself	0.637
ypq 30 never as good	0.739	ypq 54 did things wrong	0.636
ypq 31 everything wrong	0.725	ypq 56 worried night	0.635
ypq 38 worried lots	0.725	ypq 20 not see friends	0.622
ypq 50 worried happen	0.725	ypq 01 miserable	0.613
ypq 59 worried	0.724	ypq 17 dying	0.608
ypq 88 not proud	0.716	ypq 02 not enjoy	0.595
ypq 39 afraid lots	0.712	ypq 18 family better off	0.584
ypq 36 others do easily	0.708	ypq 19 kill myself	0.581
ypq 27 lonely	0.705	ypq 29 no fun	0.576
ypq 15 no good future	0.702	ypq 49 tired a lot	0.575
ypq 16 not worth living	0.691	ypq 40 angry easily	0.571
ypq 28 nobody loved me	0.689	ypq 91 more respect	0.565
ypq 44 what others think	0.681	ypq 12 talk less	0.563
ypq 22 bad things happen	0.68	ypq 11 grumpy	0.558
ypq 61 worried bad	0.675	ypq 46 often sick	0.557
ypq 35 things went wrong	0.674	ypq 41 worry parents say	0.549
ypq 21 hard to think	0.67	ypq 34 trouble making mind	0.545
ypq 25 looked ugly	0.654	ypq 69 something wrong	0.541
		ypq 14 cried	0.524

Supplementary Material for Study 2

ypq 43 hard to sleep	0.517	ypq 65 special number	0.255
ypq 32 sleep badly	0.504	spq 40 saw invisible	0.245
ypq 52 bad dreams	0.486	ypq 77 skived	0.244
ypq 55 wake scared	0.48	spq 28 special sign	0.231
ypq 05 tired	0.479	ypq 79 ran away	0.231
spq 09 talked about	0.467	ypq 76 hurt someone	0.218
ypq 63 over and over	0.455	ypq 74 stole	0.21
ypq 06 moving slowly	0.451	ypq 75 damage property	0.163
ypq 58 wiggled seat	0.436	ypq 83 hurt animal	0.133
ypq 07 restless	0.435	wemwbs 05 energy	-0.418
ypq 62 certain things	0.433	wemwbs 13 interested	-0.454
spq 60 others watching	0.42	wemwbs 09 feel close	-0.507
spq 63 people talk	0.413	wemwbs 11 make mind	-0.549
ypq 13 talk slowly	0.412	wemwbs 12 loved	-0.553
ypq 67 clean enough	0.397	wemwbs 01 optimistic	-0.559
ypq 26 aches pains	0.396	ypq 90 as good	-0.574
ypq 37 getting breath	0.392	ypq 86 good qualities	-0.575
spq 64 hear thoughts	0.374	wemwbs 02 useful	-0.581
spq 61 distract sounds	0.349	wemwbs 03 relaxed	-0.582
ypq 64 hated dirt	0.318	wemwbs 06 problems	-0.598
ypq 73 broke rules	0.315	ypq 87 do things well	-0.608
spq 04 mistake objects	0.304	ypq 85 satisfied	-0.61
ypq 78 cheated	0.303	ypq 93 positive	-0.64
spq 13 force around you	0.291	wemwbs 07 think clear	-0.645
ypq 68 special way	0.285	wemwbs 10 confident	-0.669
ypq 70 hands clean	0.281	wemwbs 14 cheerful	-0.702
ypq 71 special words	0.28	wemwbs 08 feel good	-0.713
spq 31 thoughts aloud	0.264		

Ypg = Young person's questionnaire (containing: Moods and Feelings Questionnaire, Revised Children's Manifest Anxiety Scales, Leyton Obsessional Inventory, The Behaviours Checklist, Rosenberg Self-Esteem Scale); spq = Schizotypal Personality Questionnaire; wemwbs = Warwick-Edinburgh Mental Wellbeing Scale.

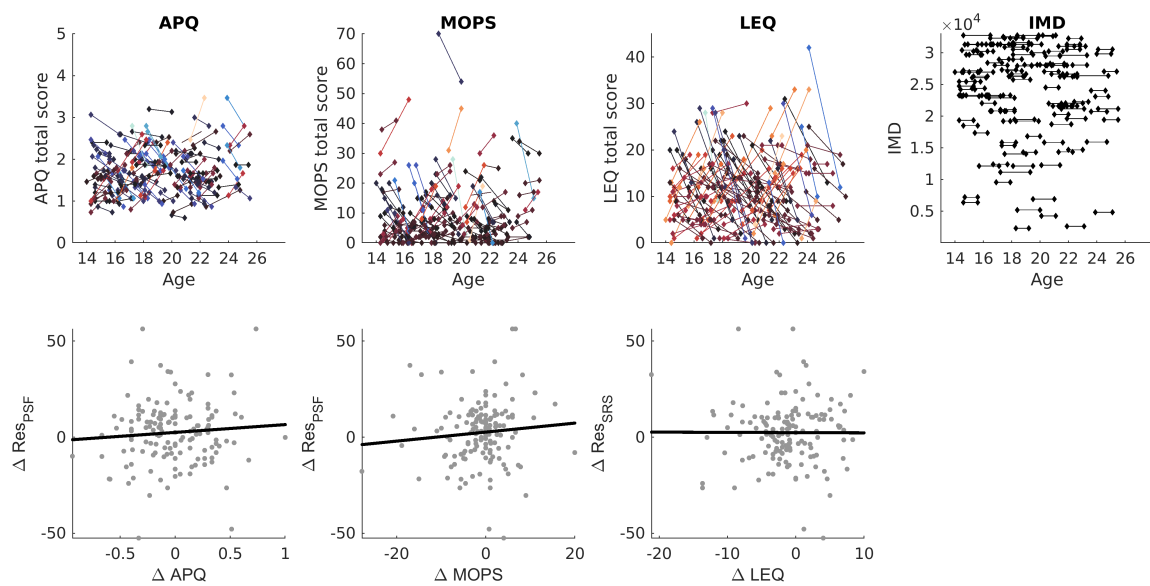
Table S2. Distribution of distress and resilient psychosocial functioning (Res_{PSF}) scores with respect to sex (mean +/- SD) and age in the prediction sample (i.e., 712 individuals included for the computation of Res_{PSF}; 455 with repeated measures) and the imaging sample (i.e., 141 individuals for which both imaging and behavioral data was available for two time points).

	Prediction sample (<i>n</i> = 712)	Imaging sub-sample (<i>n</i> = 141)
<i>Mean Res_{PSF}</i>	Male: 2.46 ± 16.93 Female: -2.74 ± 19.36 <i>t</i> (710) = -3.81, <i>p</i> = 0.0001, [-7.89, -2.52] Correlation with age: <i>r</i> = 0.04, <i>p</i> = 0.22	Male: 3.59 ± 17.08 Female: 0.83 ± 16.16 <i>t</i> (139) = -0.99, <i>p</i> = 0.32, CI = [-8.3 2.77] Correlation with age: <i>r</i> = 0.08, <i>p</i> = 0.32
<i>ΔRes_{PSF}</i>	Male: 0.60 ± 15.84 Female: 1.97 ± 10.84 <i>t</i> (453) = 0.81, <i>p</i> = 0.42, CI = [-1.98, 4.73] Correlation with age: <i>r</i> = -0.06, <i>p</i> = 0.20	Male: 2.62 ± 15.83 Female: 2.18 ± 16.96 <i>t</i> (139) = -0.16, <i>p</i> = 0.88, CI = [-5.9, 5.02] Correlation with age: <i>r</i> = -0.01, <i>p</i> = 0.9
<i>Mean distress</i>	Male: -6.39 ± 20.07 Female: -1.43 ± 21.43 <i>t</i> (710) = 3.15, <i>p</i> = 0.002, CI = [1.85, 7.97] Correlation with age: <i>r</i> = 0.08, <i>p</i> = 0.04	Male: -8.70 ± 20.70 Female: -5.91 ± 18.14 <i>t</i> (139) = 0.85, <i>p</i> = 0.39, CI = [-3.67, 9.27] Correlation with age: <i>r</i> = 0.01, <i>p</i> = 0.86
<i>Δdistress</i>	Male: -3.15 ± 16.03 Female: -5.12 ± 20.44 <i>t</i> (453) = -0.90, <i>p</i> = 0.37, CI = [-5.01, 1.87] Correlation with age: <i>r</i> = 0.03, <i>p</i> = 0.57	Male: -0.91 ± 16.77 Female: 2.15 ± 17.64 <i>t</i> (139) = 1.06, <i>p</i> = 0.29, CI = [-2.67, 8.80] Correlation with age: <i>r</i> = 0.05, <i>p</i> = 0.22

Res_{PSF} = Resilient psychosocial functioning scores. Bold = significant at *p* < 0.05.

Potential links between changes in Res_{PSF} and changes in adversity exposure

Given that Res_{PSF} were computed separately for each time point by predicting distress levels based on adversity levels measured at each time point, our approach inherently adjusts for changes in adversity exposure between measurement time points. We still wanted to confirm that changes in Res_{PSF} were not simply a correlate of increasing or decreasing adversity levels. Correlating Δ Res_{PSF} with Δ s of individual risk assessment scores revealed no significant associations between Δ Res_{PSF} and Δ -scores from the MOPS ($r = 0.10$), APQ ($r = 0.10$), LEQ ($r = -0.02$; all $p > 0.05$), or SES (remained unchanged for most individuals; Supplementary Figure S1). Changes in adversity exposure were further not associated with changes in myelin-sensitive MT (all $p > 0.05$).



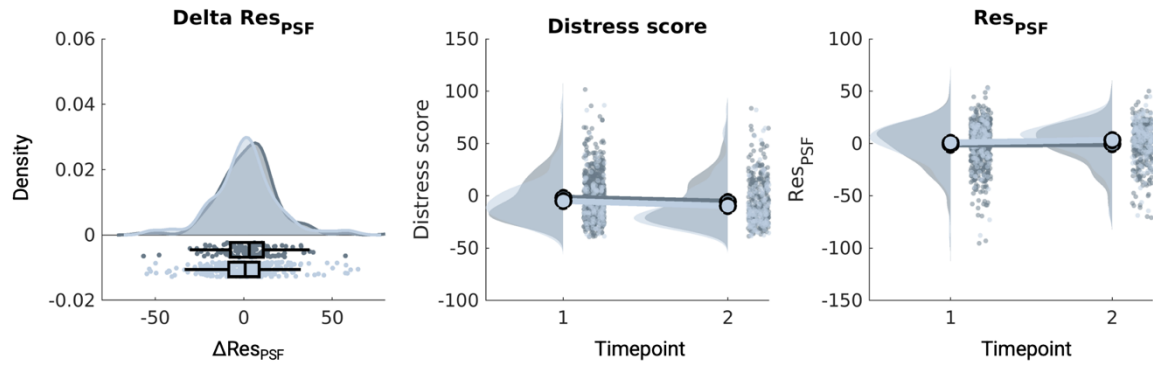
Supplementary Figure S1. Changes in adversity exposure between measurement timepoints. The upper row depicts intra-individual changes in adversity measures ($n = 141$ individuals). The lower row depicts respective Pearson's correlations between changes in adversity measures and changes in resilient psychosocial functioning (Δ Res_{PSF}; $n=141$). No significant association with Δ Res_{PSF} was observed for change in adversity exposure as captured by the Measure of Parenting Style (MOPS; $r = 0.10$, $p = 0.24$), the Alabama parenting questionnaire (APQ; $r = 0.10$, $p = 0.21$), or the Life events questionnaire (LEQ; $r = -0.02$, $p = 0.79$). IMD = Index of mean deprivation.

Representativeness of the MRI subsample

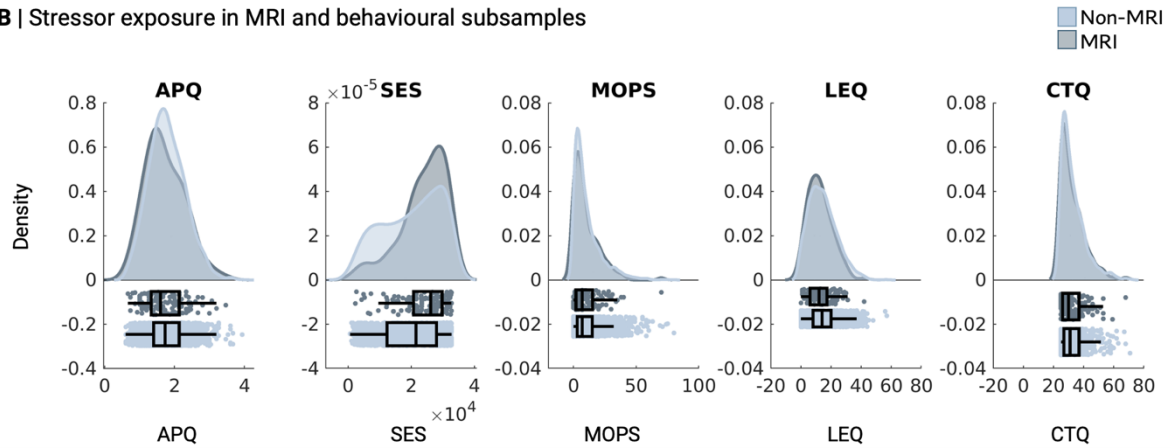
To address concerns that developmental neuroimaging studies may not be representative of the general developmental population (Garcini et al., 2022), we descriptively compared the distributions of levels of environmental risk exposures as well as behavioral outcome measures in $n = 144$ individuals included in neuroimaging analyses (the imaging subsample) and the larger sample of individuals included in behavioral analyses only (the non-imaging subsample; **Supplementary Figure S2**). We generally observed strongly overlapping distributions for distress and resilient psychosocial functioning (Res_{PSF}) scores, as well as for APQ, MOPS, LEQ and CTQ questionnaires, between the two sub-samples. For SES, considered here as an index of mean deprivation (IMD), we observed a comparable range but a relatively higher proportion of higher SES in the imaging sub-sample (i.e., a more left-skewed distribution). This suggests a potential oversampling of individuals from higher socioeconomic backgrounds for the neuroimaging analysis. At the same time, it should be noted that the behavioral outcome measure (Res_{PSF}) was computed in the full sample, including more individuals with lower SES, and also that SES was weighted with the lowest feature importance by the model used to predict Res_{PSF} (**Figure 1A**).

We also note that the NSPN sample is a locally collected sample from London and Cambridgeshire in the UK. 75% of the total sample and 84% of the imaging sub-sample were white. Moreover, the sample is predominantly healthy, thereby excluding individuals with, for example, neurodevelopmental disorders who are part of the general population. It will be important to test the replicability of the current results in more socio-economically and ethnically representative samples of the general population. The efficacy of potential resilience factors implied by the current study in a largely white, relatively affluent and healthy sample requires further validation in ethnically, socio-economically and clinically defined groups that are underrepresented in this sample.

A | Distress and Stressor resilience scores in MRI and behavioural subsamples



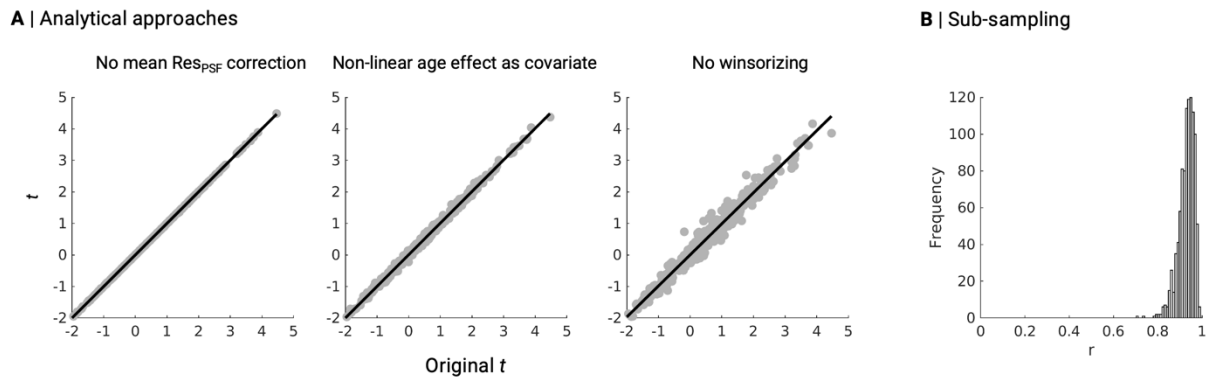
B | Stressor exposure in MRI and behavioural subsamples



Supplementary Figure S2. Representativeness of the MRI subsample. The MRI subsample comprises the $n = 141$ individuals included in the main analyses linking changes in resilient psychosocial functioning (Res_{PSF}) scores to myeloarchitectonic and functional maturation. The Non-MRI sample comprises all other individuals that were included in behavioral analyses only and for whom respective behavioral data were available: In A), the non-MRI sub-sample includes $n = 314$ individuals with longitudinal $\Delta\text{Res}_{\text{PSF}}$ scores and $n=885$ individuals with distress scores. In B), the non-MRI sub-sample comprises $n = 1457$ individuals with all risk exposure assessments completed. Distributions show density plots. APQ = Alabama Parenting Questionnaire; MOPS = Measure of Parenting Style; LEQ = Life Events Questionnaire; IMD = Index of Mean Deprivation.

*Sensitivity tests for $\Delta Res_{PSF} * \Delta MT$ effects*

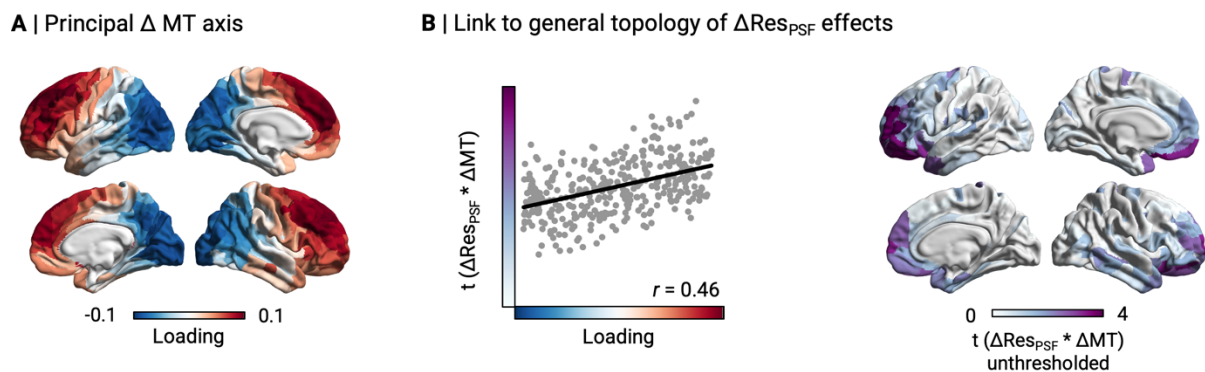
We tested whether the observed association between ΔRes_{PSF} and ΔMT was robust to analytical choices by spatially correlating (Pearson's r) the original unthresholded t-map with t-maps derived from alternative analytical approaches (Supplementary Figure S3A). We observed virtually unchanged results when 1) not including mean Res_{PSF} as a covariate in the general model ($r = 1$ with the original map), 2) including a quadratic age term to control for non-linear age effects ($r = 0.998$ with the original map), and 3) not winsorizing the input data (correlation of $r = 0.987$ with the original map). Next, we tested whether the observed prefrontal effect was present in different sub-samples. For this purpose, we drew 1000 sub-samples each containing 80% of the individuals and repeated the analysis 1000 times. The average correlation between the original t-map and the t-maps derived from the sub-samples was $r = 0.929$ (Supplementary Figure S3B).



Supplementary Figure S3. Sensitivity tests for $\Delta Res_{PSF} * \Delta MT$ effects. A) Pearson's correlation between original the t-map (x-axis) presented in the main manuscript and t-maps derived from alternative analytical approaches ($n = 141$ individuals, all $p < 0.001$). B) Histogram depicting Pearson's correlations between the original t-map and t-maps computed based on 1000 randomly drawn sub-samples (80% of data).

Organizational axis of developmental change in MT

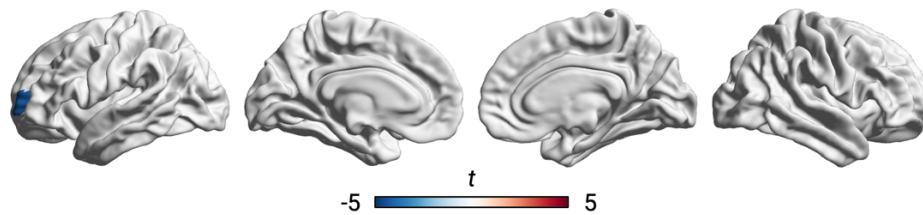
To assess whether ΔMT occurred in a synchronized manner across the cortex, we further observed that inter-regional covariance of ΔMT was organized along an anterior to posterior pattern (**Figure S4**). We then examined whether the topological distribution of ΔRes_{PSF} effects on ΔMT aligns with general organizational principles of intra-individual MT development and observed a positive correlation between the t-map and the previously identified principal axis of ΔMT ($r = 0.46$, $p_{spin} = 0.016$, $CI = [0.36, 0.53]$). Significance was assessed by a spin test (10000 permutations) correcting for spatial auto-correlations between cortical maps (Alexander-Bloch et al., 2018). Thus, the association between change in resilient psychosocial functioning and MT maturation follows general organizational principles of MT development. This suggests that differences in the cortex-wide embedding of developmental change in anterior vs. posterior regions are reflected in the degree to which both apexes play a role in the development of resilient psychosocial functioning. The observed axis likely reflects differences in the timeline on which regions are most developmentally active with respect to myelination, and thus have differential relevance for adolescent resilience.



Supplementary Figure S4. Principal axis of synchronized MT change. **A)** Structural covariance of intra-individual deltas of Magnetic Transfer (ΔMT) was organized along an anterior-posterior cortical axis ($n = 141$ individuals). **B)** The unthresholded effect map reflecting the association between change in resilient psychosocial functioning (ΔRes_{PSF}) and ΔMT presented in the main manuscript was spatially correlated with the principal axis of MT development, as tested via a Pearson's correlation and significant after spin tests using 1000 rotations to control for spatial auto-correlation ($p_{spin} = 0.016$).

Cross-sectional effects of Res_{PSF} and ΔRes_{PSF}

We observed no cross-sectional association between baseline MT and baseline Res_{PSF} . However, we observed a negative effect of ΔRes_{PSF} on baseline MT in a parcel in the left middle frontal gyrus (L_p10p; $t = -4.16$, $p_{10,000 \text{ permutations} + FDR} < 0.05$). Thus, individuals who had lower Res_{PSF} at baseline compared to the follow-up time point also had cross-sectionally lower levels of MT in this region (**Figure S5**).

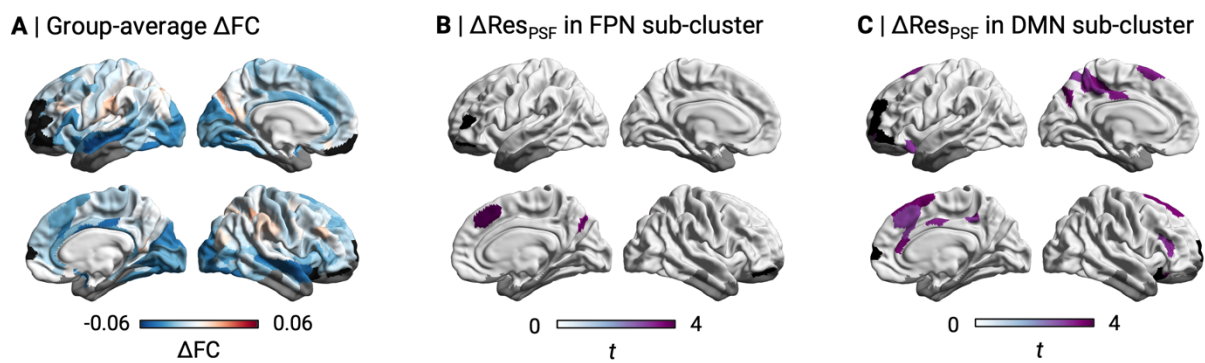


Supplementary Figure S5. Effects of change in resilient psychosocial functioning scores on baseline Magnetic Transfer (MT). P-values were corrected by 10.000 non-parametric permutations and FDR ($p < 0.05$; $n = 141$ individuals).

PFC sub-clusters in ΔFC analyses

Using functional connectivity data, we investigated whether regions that show differences in ΔMT as a function of ΔRes_{PSF} also exhibit different functional embedding. For this analysis, presented in the main manuscript, connectivity profiles were averaged across parcels that are part of the prefrontal ROI within each participant. As the mask/ROI includes large parts of the PFC and thus a nexus of different functional profiles, we further subdivided the cluster based on parcels' assignment to functional communities (Yeo et al., 2011). The ROI spanned sub-regions of frontoparietal, default mode, and limbic networks. Because large parts of the limbic network were excluded in FC analyses in this study due to low signal-to-noise ratios (see Methods), we tested associations between ΔRes_{PSF} and ΔFC only for frontoparietal and default mode sub-regions.

The prefrontal cluster showed predominantly negative change in FC across large parts of the frontal, temporal, and occipital cortex, as well as the insula and anterior cingulate cortex (**Supplementary Figure S6A**). Studying the association between ΔRes_{PSF} and ΔFC in sub-parts of the prefrontal cluster, it appeared that positive associations were largely driven by sub-regions that are part of the default mode network. That is, when defining sub-regions that are part of the frontoparietal network as seed, two regions (right medial PFC and PCC; **Supplementary Figure S6B**) showed significant effects after 10,000 permutations and FDR ($\alpha = 0.05$). In contrast, defining sub-regions that are part of the default mode network as seed revealed positive associations between ΔRes_{PSF} and ΔFC in 21 regions, spanning medial and lateral PFC, posterior cingulate cortex, and parts of unimodal sensorimotor cortices (**Supplementary Figure S6C**).



Supplementary Figure S6. Effects of change in resilient psychosocial functioning (ΔRes_{PSF}) scores on change in functional connectivity (FC) of sub-parts of the prefrontal region-of-interest presented in the main analysis ($n=141$ individuals). A) Group-average pattern of change in FC (ΔFC) for the total prefrontal region of interest (ROI). B) We observed no significant association between ΔRes_{PSF} and ΔFC in the ROI sub-regions that are part of the frontoparietal network (FPN). C) Associations between ΔRes_{PSF} and ΔFC in ROI sub-regions that are part of the default mode network (DMN). B and C include age, sex, site, and mean Res_{PSF} as covariates. The respective ROIs are masked in black. Regions excluded due to low signal-to-noise ratio are masked in dark grey.

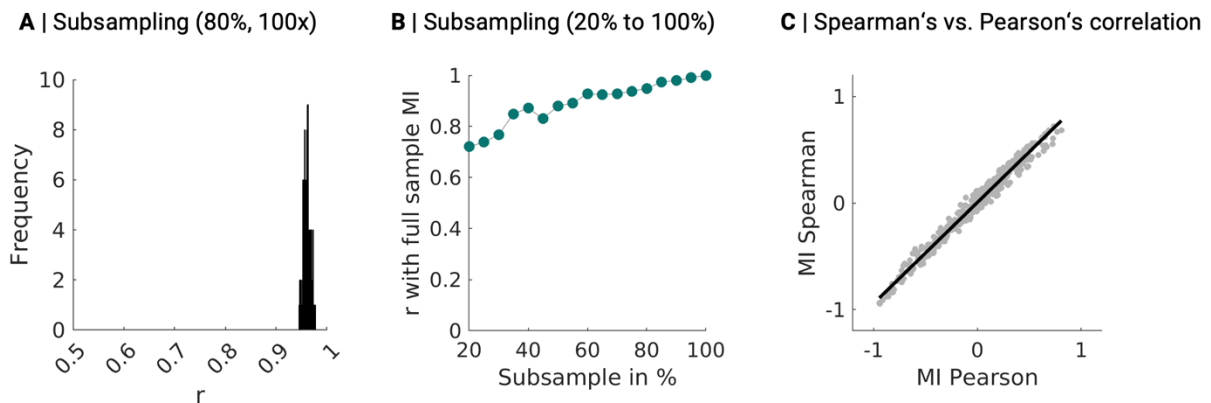
Robustness, estimated maturational processes, and future utility of the MPC maturational index

The maturational index based on microstructural profile similarity (MI_{MPC}) is a structural extension of the previously established functional connectivity maturational index, capturing conservative (i.e. strengthening of existing connections) and disruptive maturational modes (i.e., a reorganization of existing connectivity patterns (Váša et al., 2020)). While the functional maturational index identifies increasing levels of reorganization from unimodal (little reorganization) to transmodal cortex (more reorganization), the microstructural maturational index mirrors insights gained from a previously established cortical topology of synchronized age effects on microstructural profile covariance (Paquola et al., 2019). In the MI_{MPC} , we observe the strongest re-organization in frontoparietal heteromodal cortex, whereas a “frame” of ventral/paralimbic and dorsal/somatosensory cortex shows mostly an age-related strengthening of existing MPC patterns (i.e., little re-organization). This is consistent with what Paquola & Bethlehem et al. reported: association cortical areas, in which overall intra-cortical myelin content increases, develop towards a more “sensory” architecture, whereas regions in which preferably mid-to-deeper layers show increases in myelin develop towards a more “paralimbic” architecture. This differentiation process is reflected in the ‘disruptive re-organization’ captured by the MI_{MPC} , and mirrors the modular segregation observed in tractography-based adolescent data (Baum et al., 2017). At the same time, paralimbic-temporal/ventral and somatosensory/dorsal regions show ‘conservative development’ (i.e., little re-organization) in the MI_{MPC} , suggesting that MPC patterns are well-defined prior to adolescence (Grydeland et al., 2019; Paquola et al., 2019). Overall, the MI_{MPC} pattern meaningfully captures synchronized microstructural maturation and re-organization, consistent with previous observations.

To probe the robustness of the MI derived from microstructural data, we repeated the computation of the MI_{MPC} based on different subsamples. First, we drew 100 sub-samples, each containing 80% of the individuals per NSPN age bin and repeated the analysis 100 times. The average correlation between the MI_{MPC} map based on all individuals for whom MT data was available ($n = 295$ subjects, 512 sessions/datapoints) and MI_{MPC} maps derived from 80%-sub-samples was $r = 0.96$ (Supplementary Figure S7A). Next, we assessed whether the MI_{MPC} map can be observed with smaller sample sizes. To this end, we again drew sub-samples per age bin, but this time the size of the subsamples ranged between 20% and 100% (in steps of 5%) of individuals (see Supplementary Figure S7B). Last, results stayed consistent when computing the MI_{MPC} – which reflects the correlation between baseline and age-related change patterns – based on Spearman’s or Pearson’s correlation ($r = 0.99$; $p_{spin} < .0001$) (Supplementary Figure S7C).

The maturational index based on microstructural profile covariance adds to our understanding of inter-regionally synchronized cortical maturation, capturing adolescent re-organization (integration and segregation) of primarily frontoparietal association cortex. That is, emerging work highlights integrated multi-scale approaches to elucidate biological risk factors associated with neuropsychiatric

conditions. It is increasingly recognized that pathological functional perturbations are coupled with microstructural perturbations (Lariviere et al., 2019; B.-Y. Park et al., 2021; Yang et al., 2016; Zheng et al., 2019). Moreover, taking a nuanced approach to studying intracortical myeloarchitectural profiles, beyond mean myelin content, has revealed parallel maturational processes at different scales and topologies (Paquola et al., 2019; Whitaker et al., 2016; Ziegler et al., 2019). The use of the MI_{MPC} in future studies may mirror the current use of similar, already established measures such as the main axis of MPC age effects and the maturational index for functional connectivity. That is, the main axis of MPC age effects has already been linked to the cortical topology from microstructural profiles and histology (Paquola et al., 2019), which in turn has been combined with other measures of ‘cortical wiring’ in adolescence (B. Park et al., 2022). Assessing the topology of synchronized structural maturation based on intra-cortical profiles further extends classical structural covariance approaches, assessing e.g. cortical thickness covariance (Raznahan et al., 2011), towards a more nuanced myeloarchitecture. Last, similar to our study, the previously established maturational index of functional connectivity (Váša et al., 2020) has been demonstrated to robustly capture sex differences in adolescent functional network maturation (Dorfschmidt et al., 2022). In summary, the MI_{MPC} may be of interest for future studies of adolescent cortical maturation.



Supplementary Figure S7. Robustness of the MPC maturational index. A) Histogram depicting correlations between the microstructural profile covariance maturational index (MI_{MPC}) derived from all $n = 295$ individuals (512 sessions) and the MI_{MPC} based on 100 sub-samples (80% of data). B) Correlations between the MI_{MPC} derived from all 295 individuals (512 sessions) and the MI_{MPC} based on subsamples of different sizes, ranging from 25-100% in steps of 5%. C) The MI is computed as the correlation between baseline and change patterns. Here, we applied both Spearman's and Pearson's correlation to compute the MI and correlated the MI pattern resulting from either method via a Pearson's correlation ($r = 0.99$, $p_{spin} < .0001$).

Conservative vs. disruptive trends MI_{MPC} Group differences

We tested for differences in the maturational index (MI) between groups of individuals who showed increasingly resilient vs. susceptible outcomes. **Table S3** summarizes all 43 parcels displaying significant group differences in MI_{MPC} (as determined both via z-tests and non-parametric permutation testing). Trends were determined with respect to the full sample MI_{MPC} presented in **Figure 2**. For example, a positive ΔMI_{MPC} in a region labeled ‘conservative’ in the full sample MI_{MPC} is interpreted as ‘+ ΔRes_{PSF} more conservative’, whereas a positive ΔMI_{MPC} in a region labeled ‘disruptive’ in the full sample is interpreted as ‘+ Res_{PSF} less disruptive’. Regions that show a significant group difference but neither a clear conservative nor disruptive pattern in the full sample are labeled as ‘tipping points’.

Table S3. ROIs with significant group differences in MI_{MPC} and their trends. Group differences were derived from z-tests and adjusted for multiple comparisons by thresholding at $pFDR < 0.05$ as well as non-parametric permutation testing using 10,000 permutations. Tests were two-sided.

ROI	ΔMI_{MPC}	z	Trend
L_RSC	-0.507	-7.09	tipping points
L_31pv	-0.565	-9.51	+ ΔRes_{PSF} more disruptive
L_7AL	-0.28	-3.79	+ ΔRes_{PSF} less conservative
L_7PL	-0.619	-8.63	tipping points
L_9p	-0.37	-5	tipping points
L_10d	-0.564	-8.41	+ ΔRes_{PSF} more disruptive
L_IFSa	-0.579	-13	+ ΔRes_{PSF} more disruptive
L_PoI2	-0.262	-3.52	+ ΔRes_{PSF} less conservative
L_TE2a	-0.352	-4.82	+ ΔRes_{PSF} less conservative
L_TF	-0.388	-5.49	+ ΔRes_{PSF} less conservative
L_IP1	-0.694	-9.92	+ ΔRes_{PSF} less conservative
L_PGi	-0.938	-15.1	+ ΔRes_{PSF} more disruptive
L_V6A	-1.044	-16.8	+ ΔRes_{PSF} less conservative
L_s32	-0.617	-8.53	+ ΔRes_{PSF} less conservative
L_Ig	-0.54	-12.1	+ ΔRes_{PSF} more disruptive
L_p10p	0.525	9.98	+ ΔRes_{PSF} less disruptive
R_RSC	-0.468	-6.38	+ ΔRes_{PSF} less conservative
R_FFC	-0.553	-8.01	+ ΔRes_{PSF} less conservative
R_SFL	-0.225	-3.02	+ ΔRes_{PSF} less conservative
R_PCV	-0.426	-7.07	+ ΔRes_{PSF} more disruptive
R_7Pm	-0.694	-13.1	tipping points
R_v23ab	-1.021	-15.1	tipping points
R_24dv	1.003	17.3	+ ΔRes_{PSF} less disruptive
R_7Am	-0.802	-11.3	+ ΔRes_{PSF} less conservative

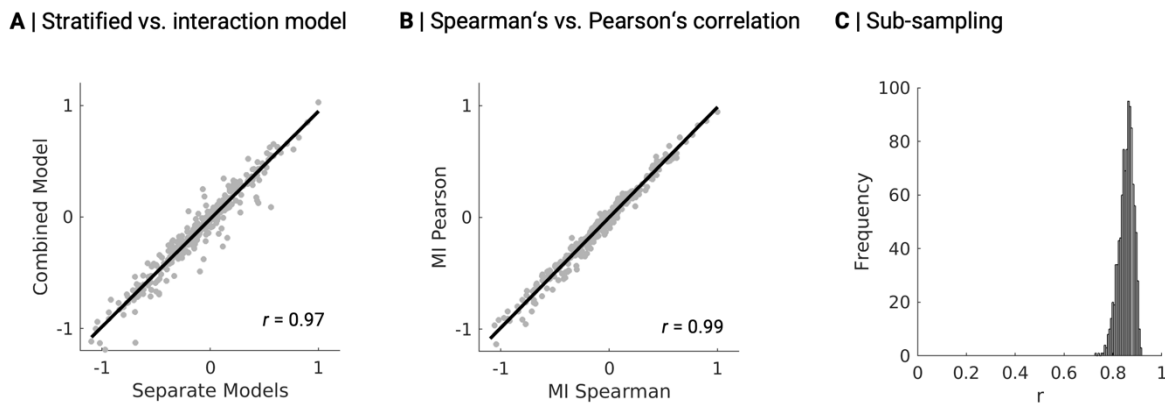
Supplementary Material for Study 2

R_7PL	-0.713	-10.2	+ΔRes _{PSF} less conservative
R_p32	-0.543	-7.52	+ΔRes _{PSF} less conservative
R_10r	-0.935	-13.6	+ΔRes _{PSF} less conservative
R_47m	-0.549	-8.42	+ΔRes _{PSF} more disruptive
R_OFC	-0.618	-8.67	+ΔRes _{PSF} less conservative
R_6a	0.625	16.1	+ΔRes _{PSF} less disruptive
R_PFCm	-0.846	-13.7	tipping points
R_FOP4	-0.707	-9.88	+ΔRes _{PSF} less conservative
R_A5	-0.621	-9.15	+ΔRes _{PSF} less conservative
R_STSda	-0.839	-12	+ΔRes _{PSF} less conservative
R_TE1a	-0.667	-9.27	+ΔRes _{PSF} less conservative
R_TE2a	-0.552	-7.72	+ΔRes _{PSF} less conservative
R_TPOJ1	-0.76	-11	+ΔRes _{PSF} more disruptive
R_V6A	-1.098	-18.5	tipping points
R_VMV1	-0.97	-15.7	+ΔRes _{PSF} less conservative
R_pOFC	-0.186	-2.65	+ΔRes _{PSF} less conservative
R_FOP5	-0.483	-6.59	+ΔRes _{PSF} less conservative
R_LBelt	-0.312	-4.35	+ΔRes _{PSF} less conservative
R_TE1m	-0.404	-5.5	+ΔRes _{PSF} less conservative

+Δ ResPSF = Increasingly resilient psychosocial functioning with age. ROI labels refer to the HCP parcellation (Glasser et al., 2016)

Testing group differences in MI_{MPC} via alternative modeling approaches

To test the robustness of the observed group differences in MI_{MPC} to an alternative modeling approach, we also combined the groups in a joint interaction model (see Supplementary Methods). We observed a high correlation between group-difference maps derived from the original, group-stratified analysis compared to the alternative analysis based on a fixed term for the group-by-age interaction ($r = 0.97$; **Supplementary Figure S8A**). Thus, we concluded that the results were independent from the modeling approach, however, we consider the group-stratified approach more intuitive. Furthermore, the results remained consistent when computing the MI_{MPC} – which reflects the correlation between baseline and age-related change patterns – based on Spearman's or Pearson's correlation ($r = 0.99$; **Supplementary Figure S8B**). Next, we tested whether the observed topology of group differences in MI_{MPC} stay consistent in sub-samples. To this end, we drew 1000 sub-samples each containing 80% of the individuals and repeated the analysis 1000 times. The average correlation between the group difference map based on 141 individuals and the group difference maps derived from sub-samples was $r = 0.85$ (**Supplementary Figure S8C**).

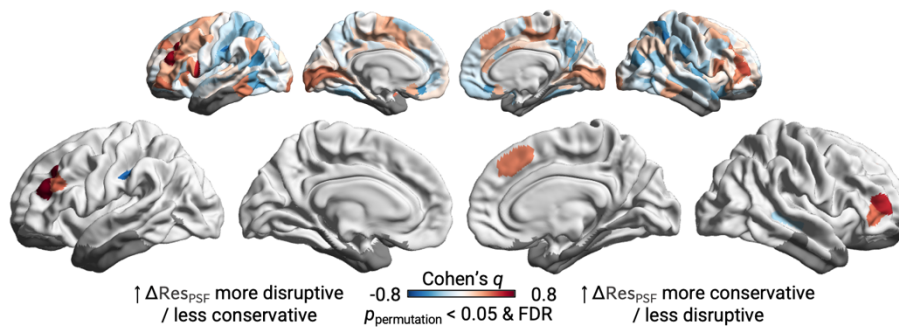


Supplementary Figure S8. Group differences in the maturational index (MI_{MPC}) based on alternative modeling approaches. A) Pearson's correlation between group differences in MI_{MPC} modeled in separate models compared to a joint interaction model ($n = 141$ individuals; $p_{spin} < .0001$). B) The MI is computed as the correlation between baseline and change patterns. Here, we applied both Spearman's and Pearson's correlation to compute the MI per group and correlated the group difference pattern resulting from either method using a Pearson's correlation ($p_{spin} < .0001$). C) Histogram depicting Pearson's correlations between the group difference map based on all 141 individuals and group difference maps computed based on 1000 randomly drawn sub-samples (80% of data).

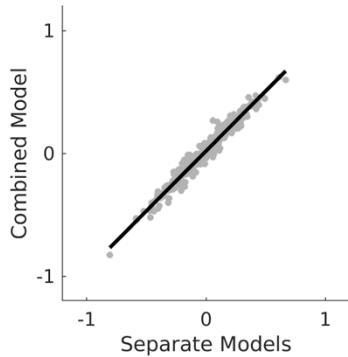
FC Maturational index in increasingly resilient vs. increasingly susceptible psychosocial functioning

We observed a decoupling of microstructural and functional connectivity MIs in large parts of the heteromodal cortex (see **Figure 3G**). For completeness, we therefore also tested for group differences in MI_{FC} between individuals who developed towards more resilient vs. more susceptible outcomes as well, following the same analytical steps as described for MI_{MPC} . We observed significant but more subtle group differences in 8 limited, primarily prefrontal regions (Supplementary **Figure S9A**). The results were robust to alternative modeling approaches (Supplementary **Figure S9B-D**).

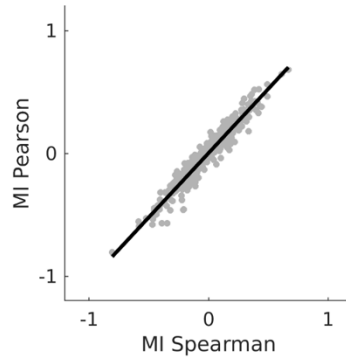
A | FC Maturational index in increasingly resilient vs. susceptible outcomes



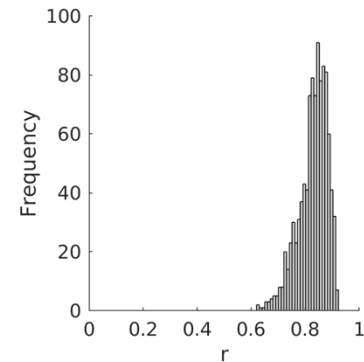
B | Stratified vs. interaction model



C | Spearman's vs. Pearson's correlation



D | Sub-sampling



Supplementary Figure S9. Regionally less disruptive development of functional connectivity networks with increasingly resilient psychosocial functioning. A) Group differences in the functional connectivity Maturational Index (MI_{FC} ; $n = 141$ individuals). In this visualization, the MI_{FC} of the group of individuals becoming more susceptible with age was subtracted from the MI_{FC} of the group of individuals becoming more resilient with age ($\uparrow \Delta Res_{PSF}$), and thresholded at $p < 0.05$ (FDR & 10,000 permutations). The smaller brain plot on top depicts the unthresholded group difference map. Parcels masked in dark grey were excluded due to low signal-to-noise ratios. B-D) depict sensitivity checks using alternative modeling approaches and sub-sampling. B) Pearson's correlation between group differences in MI_{FC} modeled in separate models (stratified approach) compared to a joint interaction model ($r = 0.98$, $p < 0.0001$). C) The MI is computed as the correlation between baseline and change patterns. Here, we applied both Spearman's and Pearson's correlation to compute the MI_{FC} per group and correlated the resulting group difference patterns ($r = 0.96$, $p < 0.0001$). D) Histogram depicting correlations between the group difference map based on all 141 individuals and group difference maps computed based on 1000 randomly drawn sub-samples (80% of data; average Pearson's correlation: 0.83).

Supplementary Discussion

Insights gained and potential sources of noise related to using residuals as resilience scores

Assessing resilient/susceptible outcomes based on the deviation of observed from expected levels of well-being given a certain adversity exposure is a well-established approach in the resilience literature (Bowes et al., 2010; Collishaw et al., 2016; Kalisch et al., 2017; Miller-Lewis et al., 2013; Sapouna & Wolke, 2013; Van Harmelen et al., 2017). It addresses the issue that simple quantification of mental health variables can provide only limited insights into resilience or susceptibility, as they are heavily conflated with individual differences in adversity exposure (Kalisch et al., 2021). Leveraging residuals to quantify better or worse well-being than predicted by adversity exposure thus provides a corrected well-being score that is adjusted for individual differences in stressor exposure and thus allows comparing resilience scores of individuals with differing exposure levels. That is, ‘residuals’ in the resilience use case are interpreted as ‘residual variance in mental health problems’ that is not explained by the normative response to exposure, and therefore indicate individually weaker response (resilience) or a stronger response (susceptibility). It is thus analogous to the process of correcting a dependent variable for potential confounders such as age or sex.

While the basic assumption of this approach is that residualized mental health outcomes reflect degrees of resilience/susceptibility, there are other potential influences such as 1) measurement error and noise related to the questionnaires used, 2) noise related to the performance of our prediction model, and 3) confounding influences of other environmental influences.

- 1) Self-report / retrospectivity biases may pose one source of measurement error, e.g. for the reporting of childhood maltreatment (Baldwin et al., 2019), despite the relatively short reporting time windows of the current study. It should be noted, however, that such sources of measurement error are not unique to / caused by the residual approach, but rather persist from the original measures of psychosocial well-being. The resilience scores should therefore not contain more measurement error than the original measures of psychosocial well-being. In the current study, our longitudinal approach may further mitigate some aspects of measurement error if it is linked to e.g., self-report bias. That is, an individual systematically self-reporting his/her well-being as a bit better than it is will receive higher resilience scores at all time points. However, as our study investigates intra-individual change, such a general offset in resilience scores would not affect change scores, whereas it would affect cross-sectional analyses more strongly.
- 2) Another question is how well our prediction model controls for differences in adversity exposure in order to reveal resilient / susceptible responses – and to what extent influence is still uncontrolled for, thus causing noise in in our measure of individual resilience. The amount of variance explained by our model (approx. 21%) is comparable with previous work reporting 24% of variance explained for the prediction of psychosocial functioning from family experiences in longitudinal settings (Van

Harmelen et al., 2017); 21% when predicting internalizing symptoms from general life stressors during the covid pandemic (Veer et al., 2021); or 28% when predicting psychosocial functioning from childhood adversity (González-García et al., 2023). We thus conclude that our model controls for exposure to a comparable degree as common resilience models.

- 3) Capturing meaningful variation in psychological outcomes is complicated by the complex influence of a multitude of interacting factors, which likely contribute to the variance not explained by our model. Such factors may include genetic predispositions, other environmental risk or protective factors not measured here, but likely also sources of noise we cannot quantify. For instance, an individual with a genetic predisposition for mental illness may systematically show lower psychological well-being, which cannot fully be explained by adversity exposure and would thus create a bias in that individuals' derived resilience scores. Similar to 1), if general offsets in resilience scores exist due to e.g., a genetic predisposition, studying longitudinal change helps us to account for such an offset.

Overall, our results using resilient psychosocial functioning scores suggest a central role for multi-modal prefrontal maturation and more wide-spread re-organization of association cortices for resilience and susceptibility during adolescence, tested against null models by non-parametric permutation. This observation is well in line with previous reports of structural and functional involvement of these brain regions in stress responses and susceptibility/resilience (Eaton et al., 2022; Larsen et al., 2023; Luciana & Collins, o. J.; Paus et al., 2008; Sydnor et al., 2021). We believe the fact that observed associations of residuals / resilience scores with multi-modal measures of cortical maturation survived non-parametric permutation tests, and were found in regions previously suggested by the literature, argues for a dominance of meaningful variance reflected in the scores used.

Supplementary Methods

Sample

The NeuroScience in Psychiatry (NSPN; (Kiddle et al., 2018)) Cohort was recruited via NHS primary care services, schools, colleges, and direct advertisement for five sex and ethnicity-balanced age bins (14-15, 16-17, 18-19, 20-21, and >22). This ‘NSPN 2K Cohort’ completed demographic and medical, as well as mental health related assessments via home questionnaire packs. A ‘U-change’ MRI cohort (n = 318) subsample completed structural and functional scanning in either London or Cambridge, UK. All participants aged 16 years and over gave informed consent. Participants younger than 16 years gave informed assent, and consent was provided by their parent or guardian. Demographics of different subsamples used in this study are presented in **Supplementary Figure S10**. Although neuroimaging was only conducted in a sub-set of individuals, we performed behavioral analyses on the entire NSPN sample to maximize training data for Res_{PSF} computation.

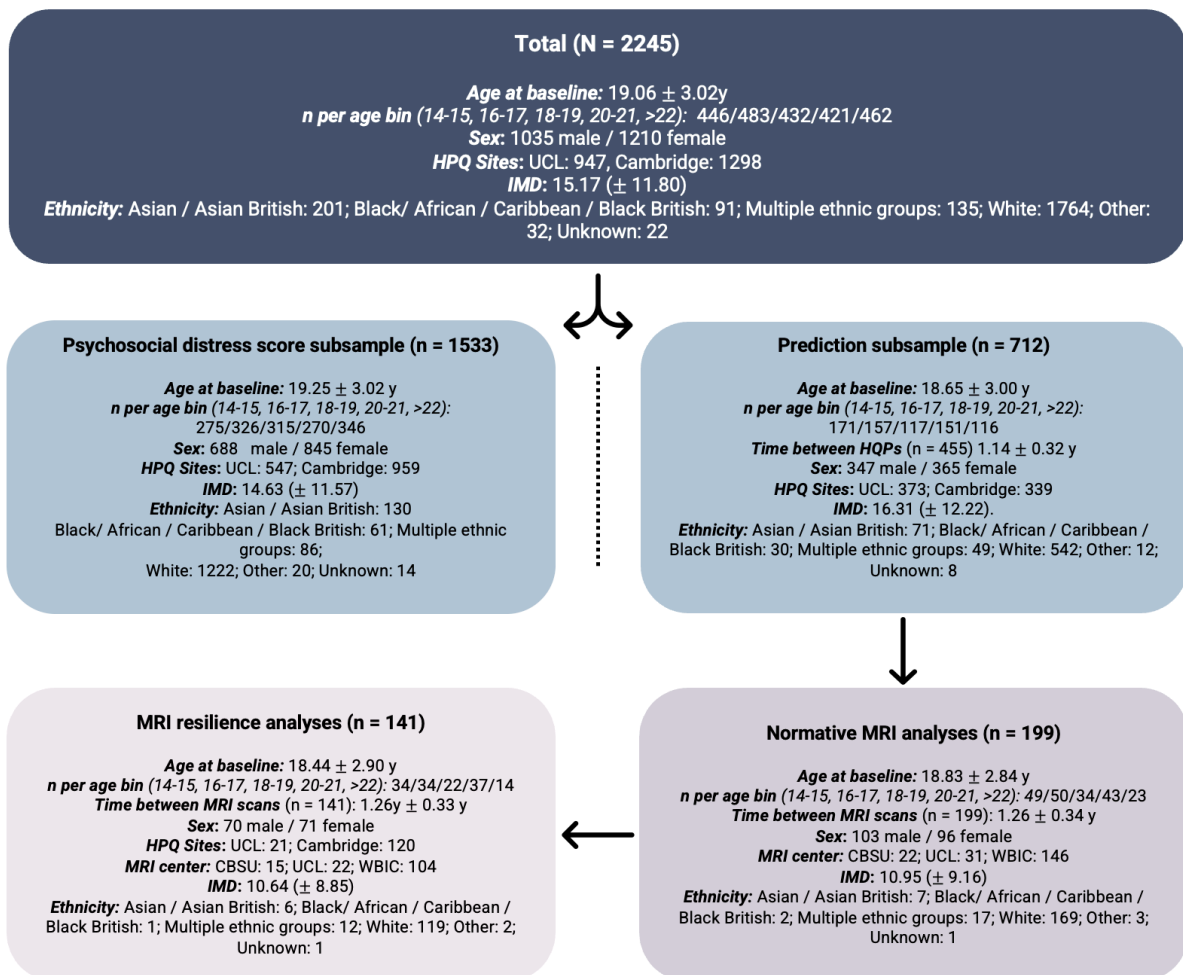


Figure S10. Demographic information for different subsamples included in presented analyses. HPQ = Home Questionnaire Pack; UCL = University College London; IMD = Indices of multiple deprivation; WBIC: Wolfson Brain Imaging Centre, Cambridge; CBSU: MRC Cognition and Brain Sciences Unit, Cambridge; UCL: University College London, London

*Sensitivity tests for ΔRes_{PSF} * ΔMT association*

We tested whether the observed association between ΔRes_{PSF} and ΔMT was robust to analytical choices. Alternative models assessed were:

1. not including mean Res_{PSF} as a covariate in the general model (1):

(1)

$$\Delta MT(\text{parcel}) \sim 1 + \beta_{\Delta Res_PSF} * \Delta Res_{PSF} + \beta_{age} * age + \beta_{sex*sex} + \beta_{site*site},$$

2. Including a quadratic age term to control for non-linear effects (2):

(2)

$$\Delta MT(\text{parcel}) \sim 1 + \beta_{\Delta Res_PSF} * \Delta Res_{PSF} + \beta_{mean Res_PSF} * mean Res_{PSF} + \beta_{age} * age + \beta_{age^2} * age^2 + \beta_{sex*sex} + \beta_{site*site},$$

3. Not winsorizing the input data.

Main axis of ΔMT development

For a system-level understanding of how MT change is synchronized across the cortex, we derived a principal axis of microstructural group-level covariance. To this end, we first computed pairwise correlations between ΔMT values between all pairs of regions, across individuals. This served as an indicator of the degree to which the slopes of ΔMT are similar between any two regions. Next, we applied diffusion map embedding, a nonlinear dimensionality reduction technique (Coifman & Lafon, 2006), to the derived matrix, to capture the spatial topography of synchronized MT change on a unidimensional axis. Regions at the peaks of the derived axis reflect maximally different embeddings of MT change, whereas regions closer together on this axis change in a similar manner, across individuals.

In order to assess whether associations between ΔRes_{PSF} and ΔMT follow the overall organizational axis of ΔMT , we correlated the unthresholded t-map with the principal axis. Significance of this correlation was assessed via spin-tests which correct for spatial auto-correlations (10,000 spins; (Alexander-Bloch et al., 2018)).

Psychosocial distress score questionnaire information

Following scoring procedures described in St Clair et al. (St Clair et al., 2017), we used the following response system: RSE, ABQ, r-LOI, and RCMAS (Bamber et al., 2002; Reynolds & Richmond, 1978; Rosenberg, 1965) were scored in a four-level response system ('never', 'sometimes', 'mostly', and 'always') in which individuals indicated how frequently the emotion or behavior described by an item

applied to them within the previous two weeks. All but five RSE items were negatively worded, but they were not reversed for the factor analysis. For the ABQ, the large majority of individuals did not ever select the ‘mostly’ and ‘always’ categories, which is why responses were binarized to ‘never’ and ‘sometimes/mostly/always’.

The Warwick-Edinburgh Mental Wellbeing Scale (WEMWBS; (Tennant et al., 2007)) is a 14-item questionnaire that measures mental well-being in a positively worded fashion. Participants were asked to respond on a 5-point Likert scale (‘none of the time’, ‘rarely’, ‘some of the time’, ‘often’, ‘all of the time’) to which degree statements described their experiences in the last two weeks. Example items are ‘I’ve been feeling good about myself’, ‘I’ve been feeling useful’, ‘I’ve been feeling close to other people’. A sum score was used for present analyses.

The Schizotypal Personality Questionnaire (SPQ; (Raine, 1991)) originally includes 74 binary (‘present’ or ‘absent’) self-report items designed to capture symptoms associated with the DSM-III definition of Schizotypal Personality disorder, such as psychotic-like experiences. We included only items that have previously been tested to be significantly associated and showing medium to high effect sizes with psychotic-like experiences as measured by the semi-structured PLIKS interview (PLIKSi; total score, hallucinations, delusions, and perceptual abnormalities; (Horwood et al., 2008; St Clair et al., 2017). Items retained based on this face validity include: SPQ 4, 9, 13, 28, 31, 40, 55, 60, 61, 63 and 64.

Adversity questionnaires information

The Life Events Questionnaire (LEQ; (Goodyer et al., 2000) asks individuals about significant life events that have occurred within the previous 18 months. Such significant life events include changing schools / college / jobs, moving, changes in family composition like death or divorce, disasters at home (e.g. fire), serious illness and/or hospitalization of self or someone in the close network of family and friends, deaths, loss of family pet, problems with or end of friendships, and others. Participants were instructed to focus on the most impactful event if they experienced multiple situations captured by the same category. Moreover, participants rated how (un)pleasant the event was (‘very pleasant’, ‘pleasant’, ‘neither’, ‘quite unpleasant’, ‘very unpleasant’) and whether it impacted them for more than 2 weeks. For our analyses, we used the LEQ sum score capturing how many adverse life events (i.e., events scored as ‘quite unpleasant’ or ‘very unpleasant’) an individual faced within the given time period.

The Child Trauma Questionnaire (CTQ; (Bernstein et al., 2003)) measures abuse and neglect up to age 18 years on a five-point Likert scale (‘never’ to ‘always’) in five overarching categories: emotional abuse (e.g., ‘family members called me stupid, lazy, or ugly’), physical abuse (e.g., ‘someone from my family hit me so hard that I had to see a doctor or go to the hospital’), sexual abuse (e.g., ‘someone tried to touch me in a sexual way or made me touch him/her in a sexual way’), emotional neglect (e.g., ‘I felt loved’), physical neglect (e.g., ‘someone took me to the doctor when it was

necessary'). Each category contains five items. Items 2,5,7,13,19,26, and 28 were reversed before taking the sum score for current analyses. If data was missing for one time point but was available for other timepoints, the missing datapoint was imputed for that subject based on the average of the remaining time points. Imputation was done within the five categories separately (sessions / % per category: emotional abuse: 15/0.0054, physical abuse: 4/0.0014, sexual abuse: 4/0.0014, emotional neglect: 17/0.0061, physical neglect: 19/0.0068). Moreover, the CTQ was part of the questionnaires given only to participants of the U-change cohort, meaning that the measurement time point did not match that of other questionnaires. As CTQ items are also less timepoint specific compared to e.g., the LEQ, we used the average CTQ rating across sessions for our analyses.

The Alabama Parenting Questionnaire (APQ) as included in the NSPN study contains 15 items asking about parenting styles. These 15 items are a combination of 9 items from the original version of the APQ (Elgar et al., 2007), the Corporal Punishment scale (3 items), and the Involvement scale (3 items). Participants rated the frequency of occurrences of certain parenting styles in their family on a five-point scale ('never' to 'always'), asking about positive parenting (3 items), inconsistent discipline (3), poor supervision (3 items), involvement (3 items), and corporal punishment (3 items). We reversed the 'positive parenting' and 'involvement' items so that higher scores reflect more adverse parenting styles. Imputation was performed in the same way as described for the CTQ. Imputed sessions/% per category: positive parenting: 30/0.0054, inconsistent parenting: 51/0.0062, poor supervision: 48/0.0086, involvement: 50/0.0090, corporal punishment: 12/0.0022.

The Measure of Parenting Style (MOPS; (Parker et al., 1997)) measures dysfunctional parenting practices in 30 items, 15 for each parent. The questionnaire covers indifference/neglect (6 items, e.g., 'Was uninterested in me'), over-control (4 items, e.g., 'Sought to make me feel guilty'), and abuse (5 items, e.g. 'Physically violent or abusive of me '). Higher scores reflect more dysfunctional parenting styles in all sub-scales. Scores were first summed within categories and then across categories for the current analyses.

Socioeconomic status was indirectly derived from the Index of Multiple Deprivation (IDM) associated with the area a participant lived in. The MDI is based on regional income, employment rate, education, health and health service, crime rates, barriers to housing and serviced, living environment and others. IDMs were imputed based on the mean if missing (15 sessions = 0.01%).

Cross-sectional effects of Res_{PSF} and ΔRes_{PSF} on MT

In order to assess whether the observed positive association between ΔRes_{PSF} and ΔMT in the prefrontal cortex co-occurs with 1) pre-existing hypo- or hypermyelination, or 2) cross-sectional differences in baseline MT as a correlate of Res_{PSF} , we applied two general linear models to baseline MT data:

(3)

$$MT_{baseline}(\text{parcel}) \sim 1 + \beta_{\Delta Res_{PSF}} * \Delta Res_{PSF} + \beta_{Res_{PSF_mean}} * Res_{PSF_mean} + \beta_{age} * age + \beta_{sex} * sex + \beta_{site} * site,$$

and

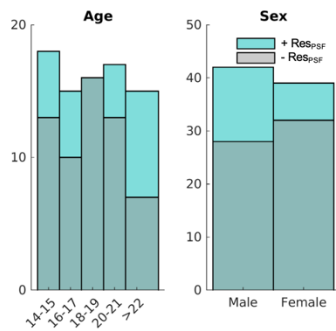
(4)

$$MT_{baseline}(\text{parcel}) \sim 1 + \beta_{Res_{PSF_baseline}} * Res_{PSF_baseline} + \beta_{age} * age + \beta_{sex} * sex + \beta_{site} * site,$$

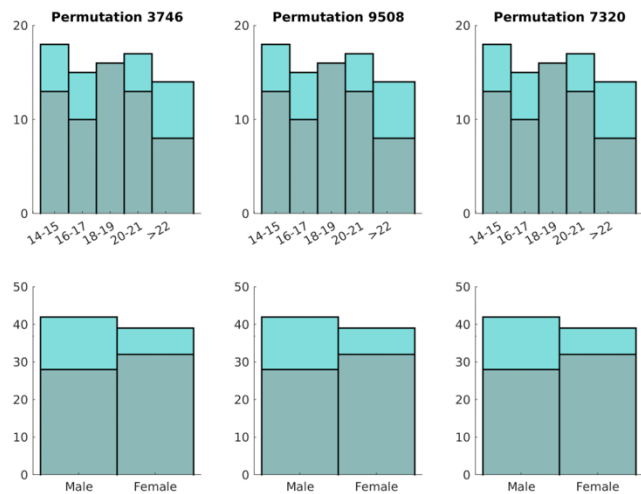
Non-parametric permutations for +/- ΔRes_{PSF} group allocations

Comparing maturational index (MI) patterns between individuals with increasingly resilient vs. vulnerable outcomes, the sample had to be divided into two groups. We followed previously published procedures comparing regional MI patterns between two groups via z-tests (Dorfschmidt et al., 2022). To further control for sampling bias, we tested differences in MI against 10,000 null-models derived by shuffling participant group allocations 10,000 times. In each permutation, repeated sessions of the same individual were allocated together, group size imbalances and distributions were controlled to resemble the original groups, and permutations were performed within age groups to maintain the stratified design of the NSPN cohort upright (see **Supplementary Figure S10**).

A | Group demographics



B | Demographics of permuted groups



Supplementary Figure S11. Age and sex distributions per group in the original (A) and example permuted (B) data (n=141 individuals).

Maturational index group differences via interaction model

To test the robustness of the observed group differences in the MI_{MPC} between $+\Delta$ vs. $-\Delta$ Res_{PSF} groups to an alternative modeling strategy, we also analyzed the main effects of age and Δ Res_{PSF} group, and the age-by- ΔRes_{PSF} group interaction, in the full data (i.e., both groups combined) using a linear mixed effects model at each edge:

(5)

$$MPC(k,j) \sim 1 + \beta_{\Delta Res_PSF_group} * \Delta Res_{PSF_group} + \beta_{age} * age + \beta_{age * \Delta Res_PSF_group} * age * \Delta Res_PSF_group + \beta_{sex * sex} + \beta_{site} * site + \gamma_{subject} * (1|subject) + \epsilon$$

where $MPC(k,j)$ refers to the MPC at edge level, β refers to coefficients for the fixed effects, $\gamma_{subject}$ refers to coefficients for random effects and ϵ represents the residual error.

We then estimated MPC_{14} for $+\Delta Res_{PSF}$ and $-\Delta Res_{PSF}$ groups as follows:

(6)

$$MPC_{14 \ +\Delta Res_PSF} = 1 + \beta_{\Delta Res_PSF_group} * 1 + \beta_{age} * 14 + \beta_{age * \Delta Res_PSF_group} * 14 * 1 + \beta_{sex} * (1/2) + \beta_{site1} * (1/3) + \beta_{site2} * (1/3)$$

(7)

$$MPC_{14 \ -\Delta Res_PSF} = 1 + \beta_{\Delta Res_PSF_group} * 0 + \beta_{age} * 14 + \beta_{age * \Delta Res_PSF_group} * 14 * 0 + \beta_{sex} * (1/2) + \beta_{site1} * (1/3) + \beta_{site2} * (1/3)$$

And then estimated MPC_{14-26} for the $+\Delta Res_{PSF}$ and $-\Delta Res_{PSF}$ groups:

(8)

$$MPC_{14-26 \ +\Delta Res_PSF_group} = \beta_{age} + \beta_{age * \Delta Res_PSF_group} * 1$$

(9)

$$MPC_{14-26 \ -\Delta Res_PSF_group} = \beta_{age} + \beta_{age * \Delta Res_PSF_group} * 0$$

Finally, like in the main analysis, we computed row-wise Spearman's correlations between extracted MPC_{14} and MPC_{14-26} data for each group separately.

NSPN Consortium Member List

Principal investigators:

Edward Bullmore (CI from 01/01/2017)
Raymond Dolan
Ian Goodyer (CI until 01/01/2017)
Peter Fonagy
Peter Jones

NSPN (funded) staff:

Michael Moutoussis
Tobias Hauser
Sharon Neufeld
Rafael Romero-García
Michelle St Clair
Petra Vértes
Kirstie Whitaker
Becky Inkster
Gita Prabhu
Cinly Ooi
Umar Toseeb
Barry Widmer
Junaaid Bhatti
Laura Willis
Ayesha Alrumaithi
Sarah Birt
Aislinn Bowler
Kalia Cleridou
Hina Dadabhoy
Emma Davies
Ashlyn Firkins
Sian Granville
Elizabeth Harding
Alexandra Hopkins
Daniel Isaacs
Janchai King
Danae Kokorikou
Christina Maurice
Cleo McIntosh
Jessica Memarzia
Harriet Mills
Ciara O'Donnell
Sara Pantaleone
Jenny Scott

Affiliated scientists:

Pasco Fearon
John Suckling
Anne-Laura van Harmelen

References

- Alexander-Bloch, A. F., Shou, H., Liu, S., Satterthwaite, T. D., Glahn, D. C., Shinohara, R. T., Vandekar, S. N., & Raznahan, A. (2018). On testing for spatial correspondence between maps of human brain structure and function. *Neuroimage*, 178, 540–551. <https://doi.org/10.1016/j.neuroimage.2018.05.070>
- Baldwin, J. R., Reuben, A., Newbury, J. B., & Danese, A. (2019). Agreement Between Prospective and Retrospective Measures of Childhood Maltreatment: A Systematic Review and Meta-analysis. *JAMA Psychiatry*, 76(6), 584–593. <https://doi.org/10.1001/jamapsychiatry.2019.0097>
- Bamber, D., Tamplin, A., Park, R. J., Kyte, Z. A., & Goodyer, I. M. (2002). Development of a short leyton obsessional inventory for children and adolescents. *Journal of the American Academy of Child and Adolescent Psychiatry*, 41(10), 1246–1252. <https://doi.org/10.1097/00004583-200210000-00015>
- Baum, G. L., Ciric, R., Roalf, D. R., Betzel, R. F., Moore, T. M., Shinohara, R. T., Kahn, A. E., Vandekar, S. N., Rupert, P. E., Quarmley, M., Cook, P. A., Elliott, M. A., Ruparel, K., Gur, R. E., Gur, R. C., Bassett, D. S., & Satterthwaite, T. D. (2017). Modular Segregation of Structural Brain Networks Supports the Development of Executive Function in Youth. *Current Biology*, 27(11), 1561–1572.e8. <https://doi.org/10.1016/j.cub.2017.04.051>
- Bernstein, D. P., Stein, J. A., Newcomb, M. D., Walker, E., Pogge, D., Ahluvalia, T., Stokes, J., Handelsman, L., Medrano, M., Desmond, D., & Zule, W. (2003). Development and validation of a brief screening version of the Childhood Trauma Questionnaire. *Child Abuse & Neglect*, 27(2), 169–190. [https://doi.org/10.1016/S0145-2134\(02\)00541-0](https://doi.org/10.1016/S0145-2134(02)00541-0)
- Bowes, L., Maughan, B., Caspi, A., Moffitt, T. E., & Arseneault, L. (2010). Families promote emotional and behavioural resilience to bullying: Evidence of an environmental effect. *Journal of Child Psychology and Psychiatry, and Allied Disciplines*, 51(7), 809–817. <https://doi.org/10.1111/j.1469-7610.2010.02216.x>
- Coifman, R. R., & Lafon, S. (2006). Diffusion maps. *Applied and computational harmonic analysis*, 21(1), 5–30. <https://doi.org/10.1016/j.acha.2006.04.006>
- Collishaw, S., Hammerton, G., Mahedy, L., Sellers, R., Owen, M. J., Craddock, N., Thapar, A. K., Harold, G. T., Rice, F., & Thapar, A. (2016). Mental health resilience in the adolescent offspring of parents with depression: A prospective longitudinal study. *The Lancet. Psychiatry*, 3(1), 49–57. [https://doi.org/10.1016/S2215-0366\(15\)00358-2](https://doi.org/10.1016/S2215-0366(15)00358-2)
- Dorfschmidt, L., Bethlehem, R. A., Seidlitz, J., Váša, F., White, S. R., Romero-García, R., Kitzbichler, M. G., Aruldas, A. R., Morgan, S. E., Goodyer, I. M., Fonagy, P., Jones, P. B., Dolan, R. J., NSPN Consortium, Harrison, N. A., Vértes, P. E., & Bullmore, E. T. (2022). Sexually divergent development of depression-related brain networks during healthy human adolescence. *Science Advances*, 8(21), eabm7825. <https://doi.org/10.1126/sciadv.abm7825>
- Eaton, S., Cornwell, H., Hamilton-Giachritsis, C., & Fairchild, G. (2022). Resilience and young people's brain structure, function and connectivity: A systematic review. *Neuroscience & Biobehavioral Reviews*, 132, 936–956. <https://doi.org/10.1016/j.neubiorev.2021.11.001>
- Elgar, F. J., Waschbusch, D. A., Dadds, M. R., & Sigvaldason, N. (2007). Development and Validation of a Short Form of the Alabama Parenting Questionnaire. *Journal of Child and Family Studies*, 16(2), 243–259. <https://doi.org/10.1007/s10826-006-9082-5>
- Garcini, L. M., Arredondo, M. M., Berry, O., Church, J. A., Fryberg, S., Thomason, M. E., & McLaughlin, K. A. (2022). Increasing diversity in developmental cognitive neuroscience: A roadmap for increasing representation in pediatric neuroimaging research. *Developmental Cognitive Neuroscience*, 58, 101167. <https://doi.org/10.1016/j.dcn.2022.101167>
- Glasser, M. F., Coalson, T. S., Robinson, E. C., Hacker, C. D., Harwell, J., Yacoub, E., Ugurbil, K., Andersson, J., Beckmann, C. F., Jenkinson, M., Smith, S. M., & Van Essen, D. C. (2016). A multi-modal parcellation of human cerebral cortex. *Nature*, 536(7615), 171–178. <https://doi.org/10.1038/nature18933>
- González-García, N., Buimer, E. E. L., Moreno-López, L., Sallie, S. N., Váša, F., Lim, S., Romero-Garcia, R., Scheuplein, M., Whitaker, K. J., Jones, P. B., Dolan, R. J., Consortium, N., Fonagy, P., Goodyer, I., Bullmore, E. T., & Harmelen, A.-L. van. (2023). Resilient functioning is associated with altered structural brain network topology in adolescents exposed to childhood adversity. *Development and Psychopathology*, 35(5), 1–11. <https://doi.org/10.1017/S0954579423000901>

- Goodyer, I. M., Herbert, J., Tamplin, A., & Altham, P. M. (2000). Recent life events, cortisol, dehydroepiandrosterone and the onset of major depression in high-risk adolescents. *The British Journal of Psychiatry: The Journal of Mental Science*, 177, 499–504. <https://doi.org/10.1192/bjp.177.6.499>
- Grydeland, H., Vértés, P. E., Váša, F., Romero-Garcia, R., Whitaker, K., Alexander-Bloch, A. F., Bjørnerud, A., Patel, A. X., Sederevicius, D., Tamnes, C. K., Westlye, L. T., White, S. R., Walhovd, K. B., Fjell, A. M., & Bullmore, E. T. (2019). Waves of Maturation and Senescence in Micro-structural MRI Markers of Human Cortical Myelination over the Lifespan. *Cerebral Cortex*, 29(3), 1369–1381. <https://doi.org/10.1093/cercor/bhy330>
- Horwood, J., Salvi, G., Thomas, K., Duffy, L., Gunnell, D., Hollis, C., Lewis, G., Menezes, P., Thompson, A., Wolke, D., Zammit, S., & Harrison, G. (2008). IQ and non-clinical psychotic symptoms in 12-year-olds: Results from the ALSPAC birth cohort. *The British Journal of Psychiatry: The Journal of Mental Science*, 193(3), 185–191. <https://doi.org/10.1192/bjp.bp.108.051904>
- Kalisch, R., Baker, D. G., Basten, U., Boks, M. P., Bonanno, G. A., Brummelman, E., Chmitorz, A., Fernández, G., Fiebach, C. J., Galatzer-Levy, I., Geuze, E., Groppa, S., Helmreich, I., Hendler, T., Hermans, E. J., Jovanovic, T., Kubiak, T., Lieb, K., Lutz, B., ... Kleim, B. (2017). The resilience framework as a strategy to combat stress-related disorders. *Nature Human Behaviour*, 1(11), 784–790. <https://doi.org/10.1038/s41562-017-0200-8>
- Kalisch, R., Köber, G., Binder, H., Ahrens, K. F., Basten, U., Chmitorz, A., Choi, K. W., Fiebach, C. J., Goldbach, N., Neumann, R. J., Kampa, M., Kollmann, B., Lieb, K., Plichta, M. M., Reif, A., Schick, A., Sebastian, A., Walter, H., Wessa, M., ... Engen, H. (2021). The Frequent Stressor and Mental Health Monitoring-Paradigm: A Proposal for the Operationalization and Measurement of Resilience and the Identification of Resilience Processes in Longitudinal Observational Studies. *Frontiers in Psychology*, 12. <https://www.frontiersin.org/articles/10.3389/fpsyg.2021.710493>
- Kiddle, B., Inkster, B., Prabhu, G., Moutoussis, M., Whitaker, K. J., Bullmore, E. T., Dolan, R. J., Fonagy, P., Goodyer, I. M., & Jones, P. B. (2018). Cohort Profile: The NSPN 2400 Cohort: a developmental sample supporting the Wellcome Trust Neuroscience in Psychiatry Network. *International Journal of Epidemiology*, 47(1), 18–19g. <https://doi.org/10.1093/ije/dyx117>
- Larivière, S., Vos de Wael, R., Paquola, C., Hong, S. J., Misic, B., Bernasconi, N., Bernasconi, A., Bonilha, L., & Bernhardt, B. C. (2019). Microstructure-Informed Connectomics: Enriching Large-Scale Descriptions of Healthy and Diseased Brains. *Brain Connect*, 9(2), 113–127. <https://doi.org/10.1089/brain.2018.0587>
- Larsen, B., Sydnor, V. J., Keller, A. S., Yeo, B. T. T., & Satterthwaite, T. D. (2023). A critical period plasticity framework for the sensorimotor–association axis of cortical neurodevelopment. *Trends in Neurosciences*, 0(0). <https://doi.org/10.1016/j.tins.2023.07.007>
- Luciana, M., & Collins, P. F. (2022). Neuroplasticity, the Prefrontal Cortex, and Psychopathology-Related Deviations in Cognitive Control. *Annual Review of Clinical Psychology*, 18, 443–469
- Miller-Lewis, L. R., Searle, A. K., Sawyer, M. G., Baghurst, P. A., & Hedley, D. (2013). Resource factors for mental health resilience in early childhood: An analysis with multiple methodologies. *Child and Adolescent Psychiatry and Mental Health*, 7(1), 6. <https://doi.org/10.1186/1753-2000-7-6>
- Paquola, C., Bethlehem, R. A., Seidlitz, J., Wagstyl, K., Romero-Garcia, R., Whitaker, K. J., Vos De Wael, R., Williams, G. B., Vértés, P. E., Margulies, D. S., Bernhardt, B., & Bullmore, E. T. (2019). Shifts in myeloarchitecture characterise adolescent development of cortical gradients. *eLife*, 8. e50482. <https://doi.org/10.7554/elife.50482>
- Park, B., Paquola, C., Bethlehem, R. A. I., Benkarim, O., Neuroscience in Psychiatry Network (NSPN) Consortium, Mišić, B., Smallwood, J., Bullmore, E. T., & Bernhardt, B. C. (2022). Adolescent development of multiscale structural wiring and functional interactions in the human connectome. *Proceedings of the National Academy of Sciences*, 119(27), e2116673119. <https://doi.org/10.1073/pnas.2116673119>
- Park, B.-Y., Hong, S.-J., Valk, S. L., Paquola, C., Benkarim, O., Bethlehem, R. A. I., Di Martino, A., Milham, M. P., Gozzi, A., Yeo, B. T. T., Smallwood, J., & Bernhardt, B. C. (2021). Differences in subcortico-cortical interactions identified from connectome and microcircuit models in autism. *Nature Communications*, 12(1), 2225. <https://doi.org/10.1038/s41467-021-21732-0>
- Parker, G., Roussos, J., Hadzi-Pavlovic, D., Mitchell, P., Wilhelm, K., & Austin, M.-P. (1997). The development of a refined measure of dysfunctional parenting and assessment of its relevance in patients with affective disorders. *Psychological Medicine*, 27(5), 1193–1203. <https://doi.org/10.1017/S003329179700545X>

- Paus, T., Keshavan, M., & Giedd, J. N. (2008). Why do many psychiatric disorders emerge during adolescence? *Nature Reviews Neuroscience*, 9(12), 947-957. <https://doi.org/10.1038/nrn2513>
- Raine, A. (1991). The SPQ: A scale for the assessment of schizotypal personality based on DSM-III-R criteria. *Schizophrenia Bulletin*, 17(4), 555–564. <https://doi.org/10.1093/schbul/17.4.555>
- Raznahan, A., Lerch, P., Lee, N., Greenstein, D., Wallace, L., Stockman, M., Clasen, L., Shaw, W., & Giedd, N. (2011). Patterns of Coordinated Anatomical Change in Human Cortical Development: A Longitudinal Neuroimaging Study of Maturational Coupling. *Neuron*, 72(5), 873–884. <https://doi.org/10.1016/j.neuron.2011.09.028>
- Reynolds, C. R., & Richmond, B. O. (1978). What I think and feel: A revised measure of children’s manifest anxiety. *Journal of Abnormal Child Psychology*, 6(2), 271–280. <https://doi.org/10.1007/BF00919131>
- Rosenberg, M. (1965). The measurement of self-esteem, Society and the adolescent self-image. Princeton, 16–36.
- Sapouna, M., & Wolke, D. (2013). Resilience to bullying victimization: The role of individual, family and peer characteristics. *Child Abuse & Neglect*, 37(11), 997–1006. <https://doi.org/10.1016/j.chiabu.2013.05.009>
- St Clair, M. C., Neufeld, S., Jones, P. B., Fonagy, P., Bullmore, E. T., Dolan, R. J., Moutoussis, M., Toseeb, U., & Goodyer, I. M. (2017). Characterising the latent structure and organisation of self-reported thoughts, feelings and behaviours in adolescents and young adults. *PLOS ONE*, 12(4), e0175381. <https://doi.org/10.1371/journal.pone.0175381>
- Sydnor, V. J., Larsen, B., Bassett, D. S., Alexander-Bloch, A., Fair, D. A., Liston, C., Mackey, A. P., Milham, M. P., Pines, A., Roalf, D. R., Seidlitz, J., Xu, T., Raznahan, A., & Satterthwaite, T. D. (2021). Neurodevelopment of the association cortices: Patterns, mechanisms, and implications for psychopathology. *Neuron*, 109(18), 2820–2846. <https://doi.org/10.1016/j.neuron.2021.06.016>
- Tennant, R., Hiller, L., Fishwick, R., Platt, S., Joseph, S., Weich, S., Parkinson, J., Secker, J., & Stewart-Brown, S. (2007). The Warwick-Edinburgh Mental Well-being Scale (WEMWBS): Development and UK validation. *Health and Quality of Life Outcomes*, 5, 63. <https://doi.org/10.1186/1477-7525-5-63>
- Van Harmelen, A.-L., Kievit, R. A., Ioannidis, K., Neufeld, S., Jones, P. B., Bullmore, E., Dolan, R., The NSPN Consortium, Fonagy, P., & Goodyer, I. (2017). Adolescent friendships predict later resilient functioning across psychosocial domains in a healthy community cohort. *Psychological Medicine*, 47(13), 2312–2322. <https://doi.org/10.1017/S0033291717000836>
- Váša, F., Romero-Garcia, R., Kitzbichler, M. G., Seidlitz, J., Whitaker, K. J., Vaghi, M. M., Kundu, P., Patel, A. X., Fonagy, P., Dolan, R. J., Jones, P. B., Goodyer, I. M., the NSPN Consortium, Vértés, P. E., & Bullmore, E. T. (2020). Conservative and disruptive modes of adolescent change in human brain functional connectivity. *Proceedings of the National Academy of Sciences*, 117(6), 3248–3253. <https://doi.org/10.1073/pnas.1906144117>
- Veer, I. M., Riepenhausen, A., Zerban, M., Wackerhagen, C., Puhlmann, L. M. C., Engen, H., Köber, G., Bögemann, S. A., Weermeijer, J., Uściłko, A., Mor, N., Marciniak, M. A., Askelund, A. D., Al-Kamel, A., Ayash, S., Barsuola, G., Bartkute-Norkuniene, V., Battaglia, S., Bobko, Y., ... Kalisch, R. (2021). Psycho-social factors associated with mental resilience in the Corona lockdown. *Translational Psychiatry*, 11(1), 1–11. <https://doi.org/10.1038/s41398-020-01150-4>
- Whitaker, K. J., Vértés, P. E., Romero-Garcia, R., Váša, F., Moutoussis, M., Prabhu, G., Weiskopf, N., Callaghan, M. F., Wagstyl, K., Rittman, T., Tait, R., Ooi, C., Suckling, J., Inkster, B., Fonagy, P., Dolan, R. J., Jones, P. B., Goodyer, I. M., the NSPN Consortium, & Bullmore, E. T. (2016). Adolescence is associated with genomically patterned consolidation of the hubs of the human brain connectome. *Proceedings of the National Academy of Sciences*, 113(32), 9105–9110. <https://doi.org/10.1073/pnas.1601745113>
- Yang, G. J., Murray, J. D., Wang, X.-J., Glahn, D. C., Pearlson, G. D., Repovs, G., Krystal, J. H., & Anticevic, A. (2016). Functional hierarchy underlies preferential connectivity disturbances in schizophrenia. *Proceedings of the National Academy of Sciences*, 113(2), E219–E228. <https://doi.org/10.1073/pnas.1508436113>
- Yeo, B. T., Krienen, F. M., Sepulcre, J., Sabuncu, M. R., Lashkari, D., Hollinshead, M., Roffman, J. L., Smoller, J. W., Zöllei, L., & Polimeni, J. R. (2011). The organization of the human cerebral cortex estimated by intrinsic functional connectivity. *Journal of neurophysiology*, 106(3), 1125-65. doi: 10.1152/jn.00338.2011.
- Zheng, Y.-Q., Zhang, Y., Yau, Y., Zeighami, Y., Larcher, K., Misic, B., & Dagher, A. (2019). Local vulnerability and global connectivity jointly shape neurodegenerative disease propagation. *PLOS Biology*, 17(11), e3000495. <https://doi.org/10.1371/journal.pbio.3000495>

Ziegler, G., Hauser, T. U., Moutoussis, M., Bullmore, E. T., Goodyer, I. M., Fonagy, P., Jones, P. B., NSPN Consortium, Lindenberger, U., & Dolan, R. J. (2019). Compulsivity and impulsivity traits linked to attenuated developmental frontostriatal myelination trajectories. *Nature Neuroscience*, 22(6), 992–999. <https://doi.org/10.1038/s41593-019-0394-3>